NEURAL SUBSTRATES OF COGNITIVE PROCESSING ARCHITECTURES

By

Kaleb A. Lowe

Doctoral Dissertation

Submitted to the Faculty of the

Graduate School of Vanderbilt University

in partial fulfillment of the requirements

for the degree of

DOCTOR OF PHILOSOPHY

In

Psychology

August 31, 2020

Nashville, Tennessee

Professor Jeffrey D. Schall, advisor

Professor Stefan Everling

Professor Gordon D. Logan

Associate Professor Thilo Womelsdorf

ACKNOWLEDGEMENTS

First and foremost, I must thank my family (born and chosen) for their continual and lasting support. I thank my mom for always believing in me and pushing me to do my best. I thank my wife for encouraging and supporting me through these final and most stressful stages of my training, and for always reminding me what's important.

I thank Ford Ebner for introducing me to systems neuroscience and the Vanderbilt University Department of Psychology; I began my graduate training in June of 2015, but my introduction to the department was in the spring of 2012 in his course on the cerebral cortex. Thanks to his teaching and encouragement to pursue research, I may not have found myself here now. I thank Alex Maier for allowing me to join his laboratory as an undergraduate, and for his continuing intellectual support upon my return to Vanderbilt. I thank Kacie Dougherty and especially Michele Cox for welcoming and guiding me then. I thank Vivien Casagrande and Jeff Schall for serving on my honors committee at that time and encouraging me to consider science as a career.

Of course, I must further thank Jeff Schall for allowing me to join his laboratory, for guiding me in research at both broad and fine scales, for introducing me to fascinating research questions, and for giving me new perspectives on balance. I thank the members of Jeff's laboratory: I thank Joshua Cosman and Wolf Zinke for training me in neurophysiology and collecting data, I thank Jacob Westerberg and Steven Errington for being stimulating office mates and being partners in project discussions, I thank Amir Sajad for project discussions, and of course I thank Thomas Reppert for sharing the load of data collection, analysis, and interpretation. I thank Chrissy Suell and especially Micala Maddox for assistance and training in animal care. I thank Michelle Schall for

keeping the laboratory running smoothly and interfacing with administration, allowing me to give my all to the research.

Outside the lab, I thank Gordon Logan for teaching me the history of cognitive psychology, as well as serving on my committee and asking stimulating questions and providing continual and thorough encouragement. I thank Thilo Womelsdorf as well for serving on my committee and providing complementary and contemporary perspectives on my work. I also thank Stefan Everling for serving on my committee and providing valuable feedback even while being in a different department and indeed in a different country. I thank the remainder of the faculty of the Psychology Department for their support, for giving stimulating talks and for providing thoughtful commentary on mine.

I thank everyone in the Division of Animal Care, Vanderbilt Vision Research Center, Center for Integrative and Cognitive Neuroscience, and the staff of the Psychology Department (specifically Luanne Toy, Mary Fuertado, Bruce Williams, Roger Williams, Jeremy Parker, Kate Shuster, Sergey Motorny, Chenchal Subraveti, Isaac Haniff, Pat Henry, Angel Gaither, Beth Clark, Cris Zerface, and Dan Stewart) for exceptional support throughout the years.

Finally, I thank the monkeys Cajal, Darwin, Gauss, Helmholtz, and Leonardo. Without them and those before and after them, none of this would be possible.

The efforts of this dissertation were supported by the National Institutes of Health (R01-EY-08890, P30-EY-008126, T32-EY-007135), Vanderbilt University (U54-HD-083211), and Robin and Richard Patton through the E. Bronson Ingram Chair in Neuroscience.

TABLE OF CONTENTS

LIST OF TABLES

LIST OF FIGURES

CHAPTER 1: BACKGROUND

One perspective of the goal of neuroscience is to unite the understanding of biology and psychology; to understand how the physical world underlies the mental world. Such an appreciation of a link between these two realms was noted as early as 1865 when Ernst Mach wrote, “To every psychical there corresponds a physical, and conversely. Like psychical processes correspond to like physical, unlike to unlike. If a psychical process can be resolved, in a purely psychological manner, into a multiplicity of qualities, a, b, c, then to these there correspond an equal number of different physical processes, α, β, γ. Particulars of the physical correspond to all the particulars of the psychic.” (Boring, 1942). We now aim to identify psychical and physical processes involved in cognition by recording neural activity during behavior. Ultimately, the goal is to explain the psychical processes by way of understanding the physical processes.

The central theme of my dissertation is one specific slice of this question: what are the physical entities that instantiate the psychological phenomena observed in visual search? For reasons that will become clear, these studies will be targeted at the *frontal eye field (FEF)*, an area of the brain intimately involved in the control of eye movements in both humans (Tehovnik et al., 2000; Vernet et al., 2014) and monkeys (Bisley, 2011; Schall, 2015; Tehovnik et al., 2000; Thompson & Bichot, 2005; Wardak et al., 2011). As progress is made, more sophisticated mechanisms of understanding both types of processes become available, at the expense of revealing additional complexities. Below, I will outline the approach I have taken to address additional complexities revealed by previous work by making this goal experimentally tangible. But first, I address the current status of the components of this approach.

Below, I will discuss the psychological foundations of this work by exploring the history of the study of stages of processing and response times. I will also briefly discuss the origins of psychology as a tangible science partially motivated by the appreciation of the link between neurophysiology and mental phenomena and partially by the discovery of mathematical regularities in subjective experience. Next, I will discuss several examples of neurophysiological breakthroughs motivated by psychological constructs. Then, I will discuss the necessity of appreciating neural diversity for understanding the mechanistic basis of cognition, and how a lack of such appreciation leads to shortcomings in current models. Finally, I will provide an overview of the experiments contained in the body of this dissertation.

1.1 Stages of Processing

Behavior occurs through time. More difficult behaviors take longer amounts of time to perform. These two ideas were essential to an early instance of studying the speed of mental processes: Donders first attempted to identify the time needed to make a perceptual choice by comparing *response times (RTs)* for a simple detection task to the RTs for a choice task (Donders, 1868). As expected, the choice task took longer. The extra time was taken to be the time needed to make a decision. Further, a discrimination task was performed in which responses should be made to only some stimuli, and this task also took longer. This additional time was taken to be the time necessary to form a conception, or idea of the world. This sparked the field of *mental chronometry*, or the study of the timing of mental events. In addition to demonstrating the utility of RTs for studying the mind, this study makes the explicit assumption of the

presence of *processing stages*. Processing stages are, in essence, conceptualized as the units or modules of mental function.

One central assumption of Donders' RT work is the presence of such discrete stages or *operations*. This has been highly contested throughout the years. The presence of discrete operations and approaches to identifying them were addressed by Sternberg's *selective influence* or additive factors method (Sternberg, 1969, 2001). The technique posits that discrete operations can be identified if independent manipulations selectively influence RTs in a task. That is, assuming operations A and B are independently influenced by factors F and G, then the RTs and RT variance of factors F and G in tandem are the arithmetic sum of the durations of operations A and B when F and G are manipulated in isolation. This allows the reverse inference whereby additive influence of F and G implies the existence of independent operations A and B.

Shortly thereafter, Eriksen provided evidence for *continuous flow* (Eriksen & Eriksen, 1974; Eriksen & Schultz, 1979). In this conception, rather than information being processed first by operation A and then by operation B, information flow through the system is continuous and is not limited by discrete operations. More complex models containing elements of both discrete operations and continuous flow arose from these ideas, e.g. cascade, in which operations are arranged serially with continuous information transfer between them (McClelland, 1979), and asynchronous discrete flow, in which components of information processing are accomplished discretely and in parallel but with different finishing times (Miller, 1982, 1988). Importantly, Miller (1988) detailed the distinction between information representation, transformation, and

transmission (i.e., encoding, processing, and output) and noted that discrete or continuous information processing relies on the *packet size*, or unit of processing, and can differ between the three types.

As with much of this research, behavioral models of these phenomena are prone to *model mimicry*, in which multiple models can produce identical behaviors. Sternberg's additive factor method is a concrete way of resolving this mimicry by identifying potential independent operations. However, this method is severely limited by its assumption of a serial architecture with an exhaustive stopping rule. It is certainly possible that independent operations, when arranged in parallel, do not produce additivity (Fig. 1.1). As can be seen, the presence or absence of discrete operations and the manner in which these operations are organized is critical for full understanding of cognition. That is, one must understand the *cognitive architecture*.

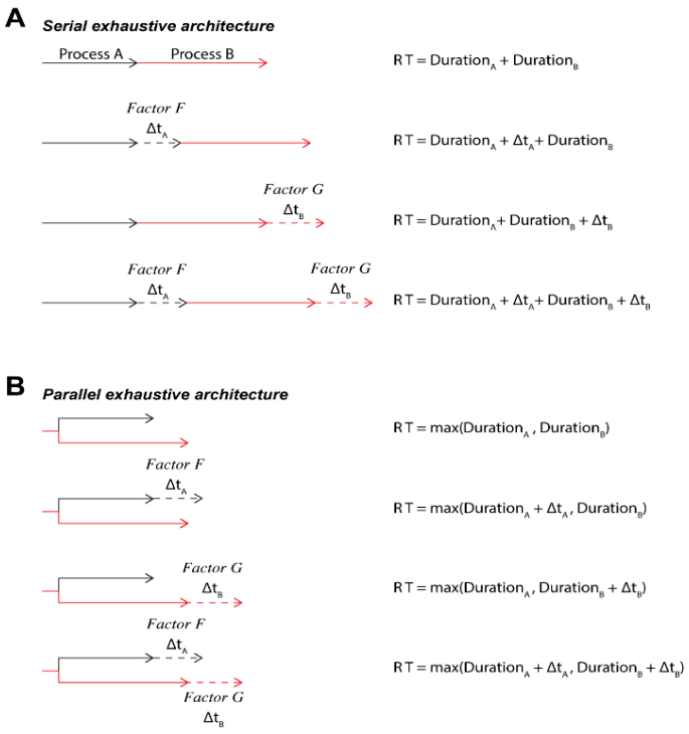

Figure 1.1: Non-additive influence of independent manipulations. (A) In a serial exhaustive architecture, if two processes A and B are independently influenced by factors F and G, the resulting response time when both factors are manipulated is the sum of the durations of A and B when factors F and G are manipulated in isolation. (B) In a parallel exhaustive architecture, independence of manipulations results in under-additive response times even though the factors are fully isolated to separate discrete stages. From Lowe et al., 2019.

1.2 Response Times and Cognitive Architectures.

In the nearly two centuries since Donders' study, RTs have proven to be indispensable in cognitive psychology literature. However, as studies become more powerful the

questions that are raised become more complex. Specifically, by making the assumption that the time required to make a decision is a simple subtraction of RTs between choice and detection conditions, he demonstrated the assumption that such processes are *serial*, or taking place in an orderly, non-simultaneous fashion. This is in contrast with *parallel* processing, in which mental sub-processes have some simultaneity in their execution. Because the word “stage” may suggest a serial temporal ordering, I will use the term *operation* to refer to the same concept but without assuming the organization of multiple operations.

In visual search, whether processing multiple stimuli occurs in a serial or parallel manner is a crucial but heretofore unanswered question. In a seminal 1980 study, Treisman & Gelade proposed that visual search can be performed in either a serial or parallel manner depending on the nature of the stimuli (Fig. 1.2A). If the search target can be identified by a single, salient feature, then search can be performed in parallel. If the search target cannot be identified by a single, salient feature, then the search must be performed serially. The diagnostic criterion for serial or parallel processing, here, was the *set-size curve*, or the change in RTs for different numbers of stimuli in the array, or set size. If this curve is flat, or RT does not depend on the size of the array, then all items must have been processed in parallel because additional stimuli do not interfere with processing. However, if the set size curve was not flat, then the items must have been processed in serial because each additional stimulus affected RT.

This perspective of the distinction between serial and parallel search is certainly elegant and was supported by the empirical results of the time, but it quickly faced challenges. Most specifically, parallel processing can mimic serial set size curves

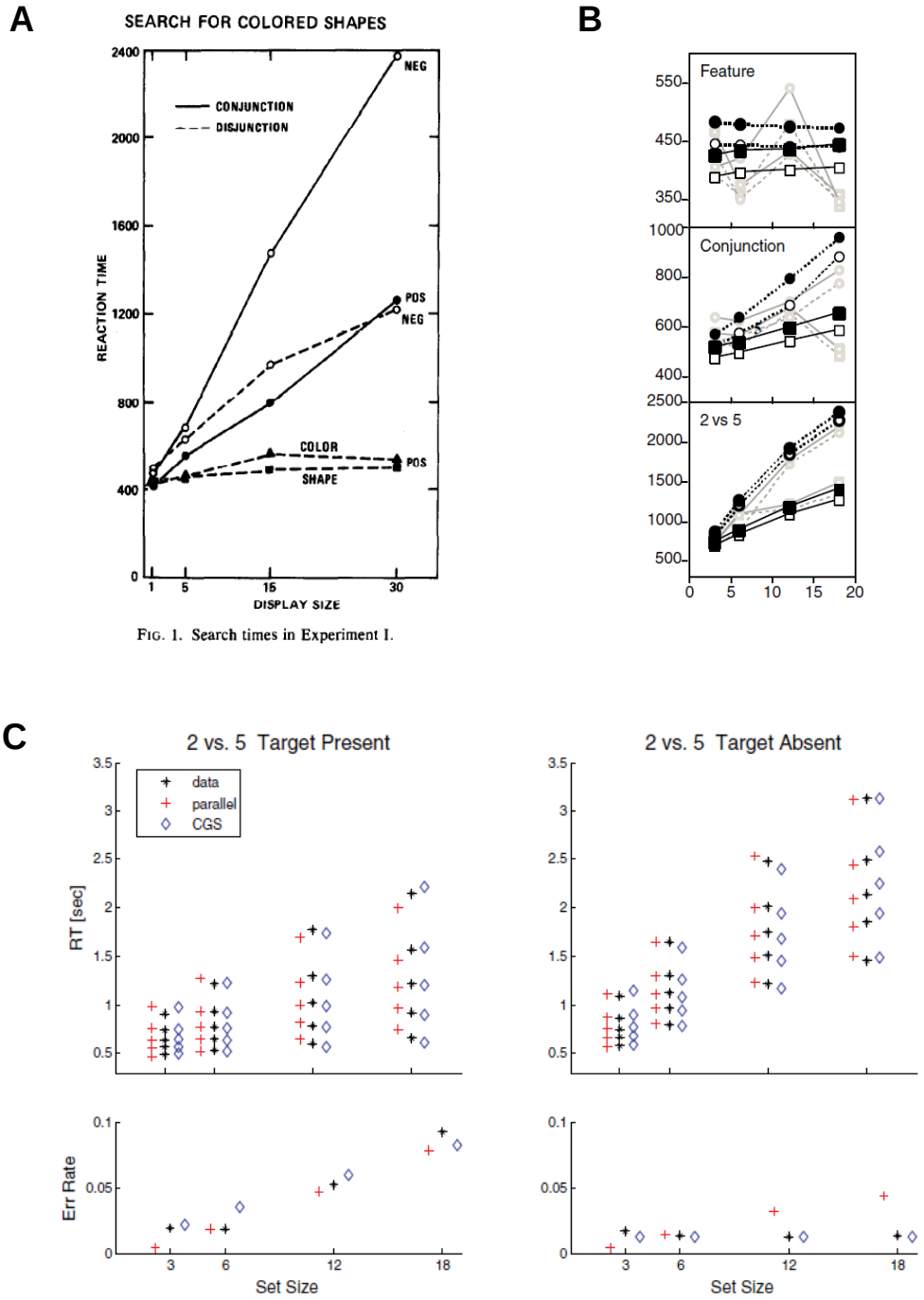

FIG. 1. Search times in Experiment I.

Figure 1.2: Set size curves from different models. (A) Feature search produces response times that are invariant with respect to set size whereas searches for conjunctions produce response times with positive slopes with respect to set size. These set size curves were taken to indicate parallel and serial processing, respectively. From Treisman & Gelade, 1980. (B) Feature search and conjunction search set size curves are recapitulated using a mixed serial and parallel model, Guided Search, mimicking the results from strictly serial and parallel conceptions in (A). From Wolfe, 2007. (C) Positive slopes in set size curves were accomplished with a model assuming strictly parallel processing (red crosses), matching both the data (blue crosses) and serial-only (CGS, blue diamonds) models. From Moran et al., 2016. These three subplots highlight the problem of model micry, where different models produce indistinguishable behavioral results.

(Moran et al., 2016; Townsend, 1972, 1990; Fig. 1.2B,C). Other models that can explain

set size curves include both serial and parallel components, where an initial parallel search is performed followed by a serial search if a target is not initially identified (Wolfe et al., 2015; Wolfe 1994, 2007). Again we see the problem of model mimicry. Thus, behavioral research is often limited by model mimicry as identical behaviors cannot resolve the different architectures. Of course, much research since has been performed to resolve these issues, but at present it is sufficient to note that this is far from a solved problem.

It is also important to note that the understanding of visual search has been sought in a variety of ways, such as by adding a conspicuous non-target item (Bacon & Egeth, 1994; Theeuwes, 1994), repeating target locations (Klein, 2000; Posner & Cohen, 1984) or target feature (Maljkovic & Nakayama, 1994), or adding arbitrary stimulus-response mappings (Katnani & Gandhi, 2013; Sato & Schall, 2003). These manipulations are effective in manipulating search and have continued to be used for psychological research. It should be noted that the efficacy of these manipulations is defined by changes in RT. This further indicates that RTs and visual search are prime candidates for studying the neurobiological underpinnings of mental chronometry.

1.3 Psychology as a Tangible Science

While many of the above studies take the quantitative study of psychological phenomena as a given, this was not always the case. For some time, philosophers considered the study of the mind to be intangible. For example, Kant argued that because psychological phenomena are not mathematically expressible, psychology cannot be an exact science, and that the mind cannot be studied because it is not

possible to isolate different thoughts (Kitcher, 1990). However, with the benefit of hindsight we see that neither of these preclusions hold.

First, the argument that psychological phenomena are not mathematically expressible has been shown to be incorrect. As described above and elaborated in the next section, current cognitive models of RTs are frequently and most impactfully quantitative; they are expressed as sets of mathematical expressions. And this is not a contemporary phenomenon; an early example from the work of Weber and Fechner shows that the intensity of a perception is proportional to the intensity of a stimulus but, importantly, this relationship is non-linear with a constant ratio between stimulus strength and the additional stimulus strength necessary to change perception (Fechner, 1860). The notion that the mapping of experienced intensity and physical intensity is exponential is *Weber's Law*, and it is indeed a mathematical expression in terms of stimulus strength.

Second, the argument that it is not possible to isolate different thoughts remains potentially valid. However, as the lasting influence of Wundt shows, experimental rigor and the presentation of stimuli such that a repeatable perception is achieved allows one to study a single thought, defined by that repeated perception. More broadly, Sternberg articulates the method of selective influence and additive factors; now, his equations serve as a set of test statistics by which selective influence can be evaluated, but his identification of behavioral tasks exhibiting selective influence demonstrate that thoughts, operationalized as cognitive operations, can be isolated by virtue of their behavioral additivity (Sternberg, 1969, 2001).

While the appreciation of cognitive phenomena as studiable emerged through their mathematical descriptions, their relationship to the physical needed definition. In order to do so, the philosophy of science needed to shift away from Kantian ideas. This occurred briefly in German philosophy when *Naturphilosophie*, the philosophy of nature, became a prominent movement. Whereas its origins were Kantian in essence with respect to the necessity of experimentally validating conjectures about the world, it disagreed with Kant's limited scope and posited a unity of natural forces, including the spiritual (e.g., Shanahan, 1989; Stauffer, 1953). *Naturphilosophie* was quickly rejected again due to its perceived lack of experimental rigor, but nevertheless its ideas inspired scientists to look more broadly at the implications and scope of their findings. For example, Ørsted discovered electromagnetism through seeking unity of chemical and electrical forces (Dibner, 1963). This discovery has been alternately attributed to *Naturphilosophie* (Friedman, 2007; Stauffer, 1953; Williams, 1980) or as a rejection of it (Shanahan, 1989), but the idea of seeking unity of natural forces is distinctly reminiscent of *Naturphilosophie*.

In the realm of physiology, Johannes Müller was similarly inspired by *Naturphilosophie* (Müller, 1824), though he took a data-driven approach to it (Finger & Wade, 2002; Rheinberger, 1998). The notion of unity found in *Naturphilosophie* echoes in Müller's law of specific nerve energies, which suggests that perception is governed by the qualities of the signals in nerves as opposed to being governed directly by the qualities of external stimuli (Müller, 1835). The electrical nature of these signals in nerves, or nerve impulses, was discovered by Galvani (McComas, 2011). Müller neither accepted nor denied this electrical nature due to insensitivity of instruments at the time

(Finger & Wade, 2002; Müller, 1840). However, his student Emil du Bois-Reymond measured the nerve current (Finkelstein, 2015) and another student Hermann von Helmholtz developed more precise instruments and measured the conduction velocity of the nerve impulse (Helmholtz, 1850). As this velocity is finite, and not instantaneous, this conduction of the nerve impulse has been used to explain RT differences (De Jaager, 1865; Donders, 1868). Notably, even in describing his detection task Donders includes the conduction delay as one of many stages between stimulus and response. Thus, even in 19th century conceptualizations of behavior one can appreciate the contribution of physical sciences. This contribution was further strengthened when nerve impulses generating movements were demonstrated to be reliant on the ionic nature of neural signals (Huxley & Stämpfli, 1949), and that the frequency of nerve impulses in sensory neurons encode stimulus strength via a rate code (Adrian & Zotterman, 1926).

Interestingly, the ionic nature of neural signals is reminiscent of Øersted's demonstration of the unity of chemical and electrical forces. Further, the demonstration that light is electromagnetic by Faraday, Maxwell, Hertz, and others relies on the discovery of electromagnetism motivated in part by *Naturphilosophie*. Thus, vision science's pursuit of the mental interpretation of light owes itself largely to such philosophical advances (and as an additional historical connection, the first to use *c* to represent the speed of light and the namesake of the unit of magnetic flux, Wilhelm Edouard Weber, was the brother of Ernst Heinrich Weber, the namesake of Weber's law described above). To the German Naturphilosph, if Denken (thought) and Sein (being) are the same, then the same laws governing the physical world govern the

spiritual as well (Shanahan, 1989). To the French rationalist, this idea is familiar, formulated as Descartes' famous statement "je pense, donc je suis." This identity of the psychical and physical, allowed by philosophical advancements, now allows us to appreciate the tangibility of psychological research.

1.4 Application of Psychological Constructs to Neuroscience

As much as an appreciation of psychology was motivated by the ability to map the nerve impulse to behavior, the influence has now become bidirectional. Next, I discuss a number of constructs defined in the psychology literature that have extended our understanding of the underlying neurobiology.

1.4.1 Choice Theory

One early set of mathematical relationship concerning behavior was *Luce's Choice axioms* (Luce, 1959). In short, these axioms describe the probability of selecting some response as a function of the strength of a stimulus that cues that response and a stimulus-independent *response bias* for that response, normalized by identical calculations for all options in a response set. That is, the probability of a response is the product of stimulus strength and response bias divisively normalized by the sum of such products for all responses. This concept has been applied broadly in the psychological literature (Luce & Marley, 1997). One specific application is in the context of attentional selection, Bundesen's theory of visual attention (TVA; Bundesen, 1990). In this framework, responses are selected as a two stage process, each incorporating choice probabilities; response probabilities are a function of responses biases and attentional

weights of objects, and those attentional weights of objects are a function of feature priorities and stimulus strength of those feature dimensions.

These concepts have also been incorporated into the neuroscientific literature. For example, the neural theory of visual attention relates known neurophysiological findings to the equations proposed in TVA and find that TVA can account for a variety of attentional effects observed in single neuron recordings (Bundesen et al., 2005). Further, the concept of biases for certain responses or stimulus features is fundamental to the biased competition theory of attentional selection (Desimone & Duncan, 1995), and the concept of divisive normalization to generate a response probability is readily seen in the normalization model of attention (Reynolds & Heeger, 2009). Finally, while TVA is generally concerned with choice probability and thereby response accuracy, it has recently been expanded to account for RTs (Blurton et al., 2020). This expansion rests on a framework of *sequential sampling models*, specifically random walks, which I discuss next.

1.4.2 Sequential Sampling Models

Naturally, given Donders' interest in decision tasks compared to detection tasks, most computational models which seek neurobiological counterparts involve decision tasks. These generally invoke a family of models for decision tasks known as sequential sampling models. These include ballistic *accumulator models* formulated from counter models (Audley & Pike, 1965; Vickers, 1970) and *drift diffusion models* developed from Brownian motion models and random walks (Ratcliff, 1978; Ratcliff & McKoon, 2008; Stone, 1960; Fig. 1.3).

The latter models are most prominent in the work of Shadlen and colleagues which seeks to identify neurobiological counterparts to the computational models. A particularly striking example of such a link is work in the middle temporal area MT and the lateral intraparietal area LIP. Neurons in LIP had response dynamics that ramped in a manner that matched computational models of drift diffusion and peaked at a common threshold, at which point a response was generated (Shadlen & Newsome, 1996, 2001). The interpretations of these studies were that LIP was instantiating drift diffusion, being supplied evidence by MT (see below, section 1.4.4). These findings have come under scrutiny (e.g., Latimer et al., 2015; Law & Gold, 2008), but still they provide strong evidence that (1) computational models used in cognitive psychology research can be mapped to neural responses and (2) accuracy and RTs can be dictated by neurobiological processes. However, the random dot motion task is a simple decision, in that the response is based only on one feature dimension, and the drift diffusion model makes assumptions regarding cognitive operations and their cognitive architectures that may not apply to more complex decisions. These considerations will be described in more detail in section 1.6.

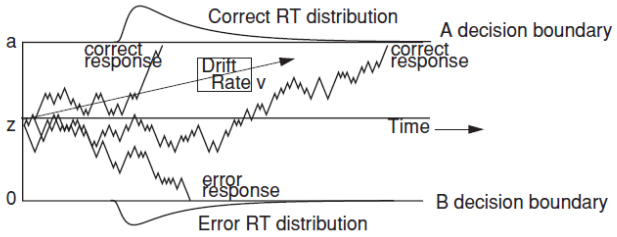

Figure 1.3: Drift Diffusion Parameterization. Three trials of a diffusion model are depicted as the jagged lines. Correct reaction time distributions are shown above the top line and error reaction times are shown below the bottom line. Parameters that define the model are shown as starting point (z), boundary separation (a), and drift rate (v). Non-decision time is not depicted but corresponds to the constant time added to the RT distributions. From Ratcliff and McKoon, 2008.

Accumulator models have enjoyed similar success in generating linking propositions between neurobiology and behavior. Hanes & Schall (1995, 1996) recorded neural activity from FEF during the *countermanding* or *stop-signal* task. This

task, a GO signal is delivered instructing a response toward some stimulus. On some trials, a STOP signal instructs the withholding of the programmed response (Logan & Cowan, 1984). This again shares similarity with Donders' method, in that he assessed in the difference in time necessary to make a response and to decide whether a response should be made as opposed to being withheld. The behavior of this task has proven amenable to accumulator models. This is true in monkeys as demonstrated by Boucher and colleagues (2007), and the responses of FEF mirror the accumulator dynamics. This includes a ramping of response toward a fixed threshold at which point a response is made (Hanes & Schall, 1996). Here, we see that FEF instantiates cognitive models of behavioral tasks. However, it shares the pitfalls of the drift diffusion model for random dot motion tasks by assuming a particular cognitive architecture.

FEF responses have also been explored in visual search, and these responses also closely mirror the dynamics of an accumulator model (Purcell et al., 2010, 2012b; Fig. 1.4). In the gated accumulator model, responses of FEF visual neurons are used as input to an accumulator framework and precisely reproduce the activity of FEF motor neurons. These two subtypes of neurons have repeatedly been found within FEF (Bruce & Goldberg, 1985; Lowe & Schall, 2018; Schall, 1991) and are considered to be distinct subpopulations with different patterns of connectivity to other brain regions (Segraves & Goldberg, 1987; c.f., Sommer & Wurtz, 2000). This model explicitly assumes the transfer of information between neuron types, which can be identified as separate operations, which will be discussed in sections 1.5 and 1.6 (see also Scerra et al., 2019, Costello et al., 2013). Further, it explicitly compared multiple models that predicted identical behavior, thus resolving model mimicry by identifying the one model consistent

with the underlying neurobiology. However, it still is limited to a relatively simple singleton search paradigm and doesn't necessarily extend to more complex behavior. Nevertheless, it further demonstrates the ability of neurobiology to explain cognitive psychological constructs.

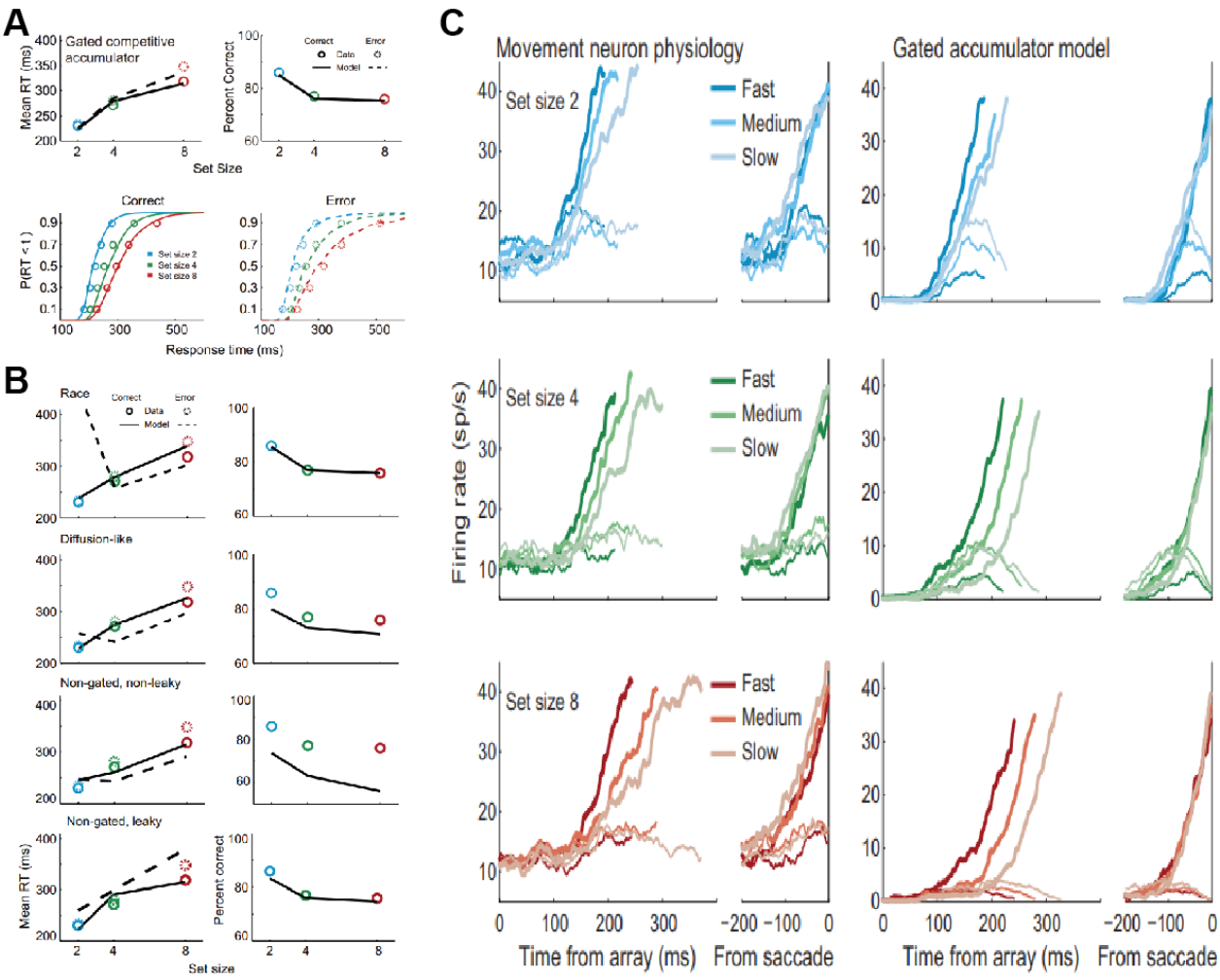

Figure 1.4: Gated Accumulator Model. (A) The gated accumulator model accurately reproduces behavior in four monkeys, including set size curves and full response time distributions. (B) Alternative models produce qualitatively, but not quantitatively, similar behavioral patterns. (C) The gated accumulator model outputs, generated from visual neuron inputs, accurately reproduce movement neuron responses in FEF. All subplots reproduced from and details are available in Purcell et al., 2012b.

1.4.3 Differentiating Neural Responses Through Memory Tasks.

In some cases, psychological constructs have been used to differentiate between responses of neurons that seem superficially similar. For example, the inactivation of

both prefrontal cortex and inferotemporal cortex cause deficits in working memory tasks (Bauer & Fuster, 1976; Fuster et al., 1981). Neurons in both areas are selective for specific complex images (Fuster et al., 1982; Fuster & Jervey, 1981). On the surface, these two areas seem to perform the same function with respect to object identification. However, by looking more closely at the activity of these neurons during the delay period of the memory task, Miller, Desimone and colleagues demonstrated an important functional difference. They found that while neurons in IT were selective for particular stimuli and were modulated dependent on whether a stimulus matched or did not match a sample stimulus, they did not maintain information about the sample during the delay period (Miller et al., 1991, 1993). Neurons in prefrontal cortex, on the other hand, did maintain such representations through the delay (Miller et al., 1996).

These studies were inspired by Baddeley's model of working memory (Miller & Desimone, 1994), which contains multiple components as opposed to one single construct (Baddeley, 1986). These separate components that pass information between themselves can explain the high similarity of neural activity in the two brain areas, with the prefrontal cortex resembling Baddeley's central executive and inferotemporal cortex resembling his visuo-spatial sketchpad. Without this psychological grounding, the phenomena would likely have been observed but may have missed strong theoretical implications.

This is not, of course, to say that the neural basis of memory is fully understood. In the above physiological studies, neural responses were averaged over trials and demonstrated sustained delay period activity. However, averaging across trials can be misleading and demonstrate dynamics that are not present at the individual trial level,

such as ramping or stepping dynamics in accumulator models (Latimer et al., 2015). In working memory tasks, both individual neuron spiking activity (Shafi et al., 2007) and activity pooled across multiple neurons, the *local field potential, LFP,* (Lundqvist et al., 2016), demonstrate delay period dynamics inconsistent with persistent elevation in activity. This has been taken as evidence that it is not single neurons maintaining elevated activity that hold information in memory, but instead the dynamics among pools of neurons during the delay (Lundqvist et al., 2018). Others maintain that memory is best understood through single neuron activity (Constantinidis et al., 2018; Riley & Constantinidis, 2016), and that non-spiking influences such as potentiation explain the apparent dynamics (Murray et al., 2017; Wimmer et al., 2014). Thus, the precise mechanisms of memory maintenance are still debated.

The debate between persistent or dynamic activity underlying working memory demonstrates that the neural mechanisms of memory are still not understood. However, the granularity of these differences reinforces the utility of psychology for motivating neuroscientific research; specifically that there are levels of explanation for psychological phenomena. I discuss this in more detail in Chapter 8, but a summary is warranted here. David Marr defines three levels of analysis: the *computational*, the *algorithmic*, and the *implementational* (Marr & Poggio, 1976; Marr, 1982). These levels correspond to what computations are performed, which algorithms are used to perform them, and the physical manifestation of the algorithms. It seems here that the persistent or dynamic activity debate is concerned with the physical manifestation of working memory, the implementational level. However, there seems to be less disagreement regarding the computations that are being performed; that is, the computational level is

settled (to a degree sufficient for the present discussion). Baddeley's models formed a basis for understanding what is being done by the brain, and current research is concerned with how these functions are carried out by neural activity. Thus, psychology is able to constrain physical models by identifying the computational level of analysis.

1.4.4 Signal Detection Theory

I have described the connections between psychology and biology as critical to the goals of neuroscience, and this is certainly the case. However, it is similarly important to acknowledge the impact of disparate fields and the tools that may be applicable across disciplines. One such example that has greatly impacted psychology, and thus, as we will see, neuroscience, is the formulation of *signal detection theory* (Green & Swets,

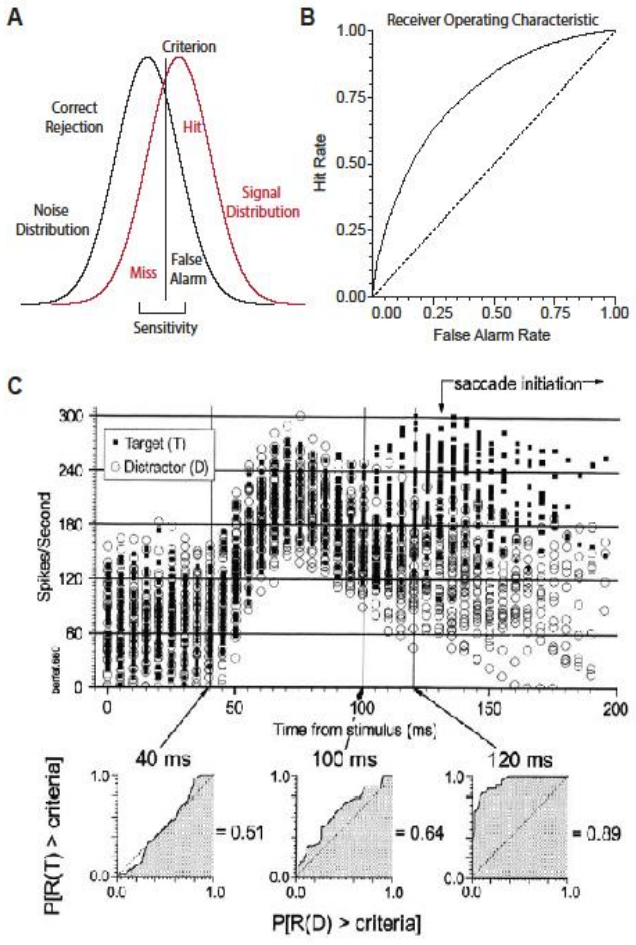

Figure 1.5: Signal Detection Theory. (A) Two distributions are shown, one representing signal strength when no true signal is present (black), and one representing signal strength when a stimulus is present (red). The separation between the centers of these distributions is the sensitivity of the system. The criterion, shown as a vertical line, sets the threshold for responding that a signal is present. The area under the signal distribution to the right of the criterion represents the hit rate. The area under the noise distribution to the left of the criterion represents the correct rejection rate. Errors can be misses, signals that were present but reported absent, the area under the signal distribution to the left of the criterion, and false alarms, erroneous reports that a signal was present when it was not. The position of the criterion represents the bias toward responding one way or the other. (B) Receiver operating characteristic curve. By changing the criterion, false alarm rates and hit rates for different levels of bias can be obtained. Plotting these against one another demonstrates the sensitivity of the system. The diagonal, where hit rate and false alarm rate are equal, represents inseparable distributions. (C) The use of receiver operating characteristic curves to identify target selection time in an example FEF neuron. From Thompson et al., 1996.

1966; Marcum, 1947). Originally, signal detection theory was developed to address the problems faced by radar technicians: Is this a real incoming missile, or is this a goose? This is a hypothetical example, here, but the concept is: is the incoming radar signal indicative of a real threat, or is it incidental? Consider being a radar technician tasked with reporting some incident to a workplace superior. Reporting that there is a disturbance may result in the elimination of a flock of geese, but the failure to report a serious threat may miss incoming missiles that would cost thousands of lives. In this case, one might have a low *bias*, in that any potential signal, regardless of mitigating factors, should be reported to the superior. On the other hand, consider that you are that superior. In this case, failure to launch a counterattack may maintain international relations, because some geese are simply trying to migrate, but a counterattack may initiate an international incident by sparking the powder keg. Though the same signal is received by both the worker and the superior, the consequences are pertinent.

Ultimately, as inaccessible as the phrase *signal detection theory* may seem on the surface, within psychological literature it has condensed to the two more basic concepts of *sensitivity* and *bias*. In simple terms, sensitivity is just how discriminable two signals are, or how discriminable a signal is from background noise. Bias is just a representation of how willing one is to respond positively or negatively (Fig. 1.5). If the consequences of missing some signal are severe but the consequences of falsely identifying that signal are mild, then one may have a bias toward responding that a signal is present. Conversely, when the consequences for falsely identifying a signal are severe, one may have a bias toward responding that the signal is absent. For example, if a doctor suspects that a patient may have a brain tumor they may have a bias for

recommending a follow up screening or MRI as those procedures are minimally burdensome, but may also be hesitant to recommend a highly invasive brain surgery. But independent of the bias, if the symptoms are severe or the tumor is large, or if the doctor or equipment are highly sensitive to such changes, even a high-stakes choice can be made confidently. Interestingly, an alternate but mathematically equivalent approach can be formulated using Choice theory (Luce, 1959; Treisman & Faulkner, 1985). As discussed above, the probability of choosing that a tumor is present is proportional to a response bias for its presence and the strength of the evidence that it is present (normalized by identical calculations for all response options).

Within neuroscience, signal detection theory has been used to characterize neuronal responses. For example, signal detection theory has been used in the study of area MT to determine the reliability of motion signals. In a random dot motion task, one in which a patch of moving dots of varying coherence (0% coherence being when each dot moved in a random direction, 100% coherence being when all dots moved in identical directions), monkeys were required to report the overall direction of motion in the display. Neurons in area MT, known to respond to motion in a particular direction (Dubner & Zeki, 1971), were found to discriminate the motion of the dot patch with accuracy that matched the behavior (Britten et al., 1992, 1993; Shadlen et al., 1996). These inferences were made by constructing *receiver operating characteristic* curves, which are fundamentally intertwined with signal detection theory, and determined the sensitivity of neural activity irrespective of behavioral choice.

Similar analyses have been performed in MST (Celebrini & Newsome, 1994), superior colliculus (Kim & Basso, 2008), prefrontal cortex (Lennert & Martinez-Trujillo,

2013; Wimmer et al., 2016), and other areas (see Crapse & Basso, 2015 for review). Even within FEF physiology research, early reports of *target selection*, or responses of neurons when a search target is within as compared to outside that neuron's receptive field, have been fundamentally driven by signal detection theory (Thompson et al., 1996; Fig. 1.5), using receiver operating characteristics to identify the time at which the signal emerges.

So, we now see that signal detection theory is a term that, to the unfamiliar, may sound imposing and inaccessible. But this is not the case. Instead, the concepts underlying and applications of signal detection theory are quite approachable. The relatively simple notions of sensitivity and bias have been used by psychology and neuroscience researchers for some time now and have been fruitful in understanding neural signaling.

1.5 The Importance of Accounting for Neural Diversity

The above section describes the applications of psychological constructs to advancing understanding in neuroscience. It is notable, though, that many of the studies different tasks were used and different brain regions were studied. Thus, there was an implicit assumption in the above section, which I will now make explicit: that different brain regions have different functions. The history of localization of function within the brain is long and complicated, but the existence of localization of function is an intrinsic assumption of contemporary neuroscience (for a relevant early example in the eye movement domain, in which stimulating different parts of the cerebral cortex resulted in different types of movements see Ferrier, 1875). In general, brain regions, or sets of brain regions, are considered as separate neurobiological systems.

While the localization of function among brain regions is assumed, one must also understand the heterogeneity of function within a brain region. That is, in order to identify how a system works, it is necessary to first identify the components of that system. Take three examples from neurobiology: First, how does the brain convert light from the world into an interpretable image? This is, initially at least, solved by the retina. The retina contains photosensitive neurons, rods and cones, whose signaling states are dependent on the location and chromaticity of light entering the pupil. These neurons send signals to bipolar cells, which in turn send signals to retinal ganglion cells. These synapses are modulated by horizontal cells and amacrine cells. The organization of these different neuron types has been used to explain phenomena like center-surround receptive field organization and color opponency (see Demb & Singer, 2015 for review). Critically, this mechanistic understanding of the retina would be impossible without accounting for the variety of neuron types comprising it.

Second: how does the brainstem initiate saccades? This behavior has been explained at a fine level of mechanistic detail through the study of the brainstem saccade generator (e.g., Scudder et al., 2002; Fig. 1.6). Long lead burst neurons begin increasing their activity some considerable time before the saccade. Omnipause neurons tonically fire to maintain fixation. The long lead burst neurons latch the omnipause neurons, inhibiting them when a saccade is eminent. Short lead burst neurons rapidly increase their activity just before the saccade. The details of this circuitry can be found elsewhere, and are shown in Fig. 1.6, but nonetheless the understanding of this circuit is only accomplishable by understanding the functional diversity of saccade related neurons in the oculomotor brainstem.

Third, studies in primary visual cortex by Hubel and Wiesel serve such a cataloguing of functional neuron types in the cat (Hubel & Wiesel, 1959, 1962) and monkey (Hubel & Wiesel, 1968). Individual neurons were reported to have orientation selectivity, or a preference for a line at a particular angle, and a preferred eye, or preference for a signal coming from either the left or right eye. Later, they characterized simple, complex, and hypercomplex cells based on the spatial characteristics of their receptive fields. Together, these findings have been integrated into the concept of a *hypercolumn*, or a set of neurons with members responding to all orientations and both

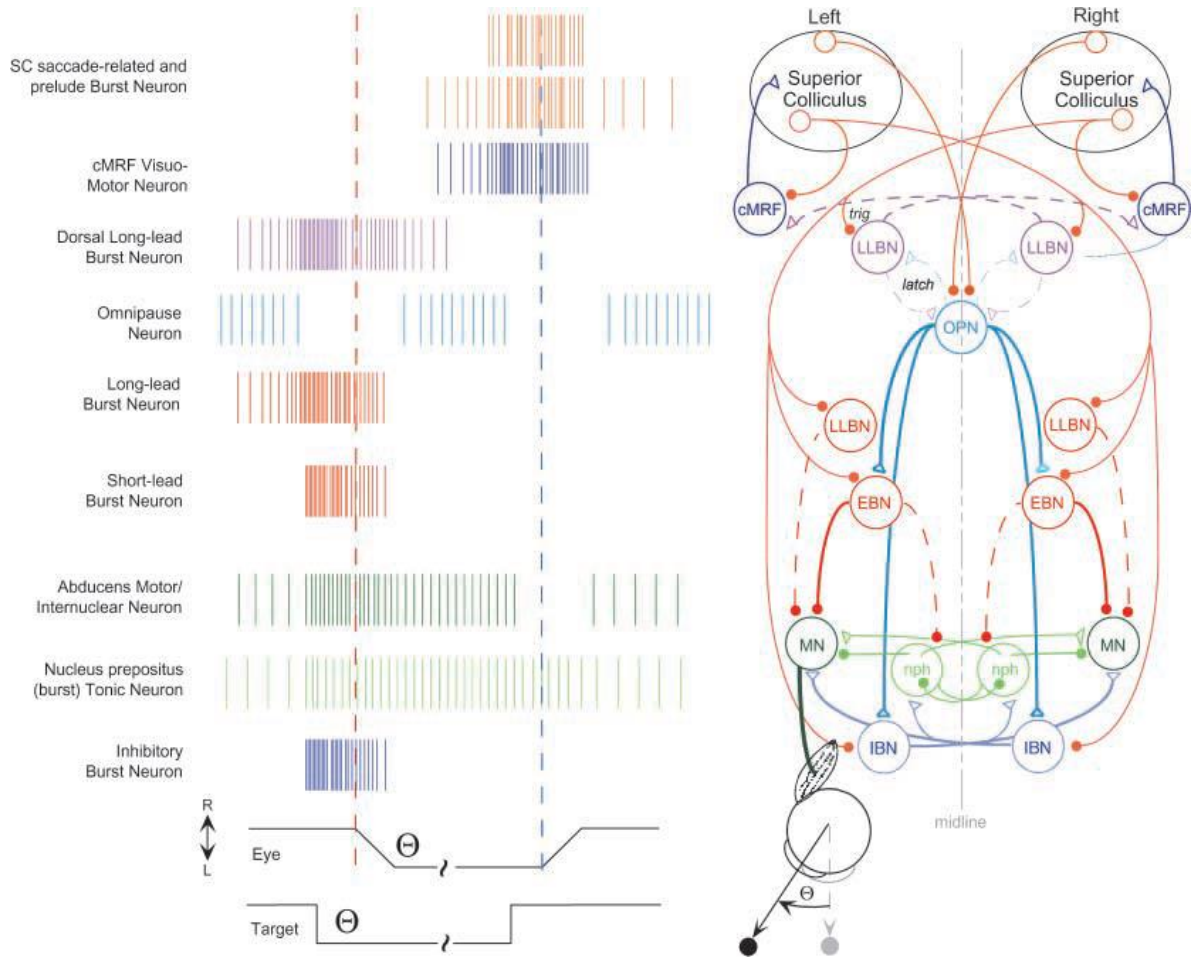

Figure 1.6: Oculomotor saccade generator circuitry. Midbrain circuitry for saccade generation comprises multiple distinct neuron types whose circuitry (right) and response profiles (left) have been used to mechanistically describe the generation of saccades. Of note is the variety of functional neuron types (left) which illustrate the importance of understanding response diversity for a mechanistic understanding of eye movement behavior. From Scudder et al., 2002.

eyes, which constitutes a complete representation of an area of the visual field (Hubel & Wiesel, 1974). These ideas have had a profound effect on the understanding of cortical structure, refined models of columnar structure (e.g., Douglas & Martin, 1991), increased understanding of cortical processing, and have even earned a Nobel prize.

These three examples demonstrate that a powerful and detailed mechanistic understanding of neural functions and their relation to phenomenology and behaviors is accomplishable, but only when the component neurons are identified and individually understood.

Additional studies of the cerebral cortex have taken a similar, though less complete, approach to understanding neuronal diversity and the way this diversity contributes to cortical function. Most approaches to cortical function rely on the idea of *segregation of function*, or the idea that different parts of the brain serve different functions. Of course, that sensory cortices are spatially distinct and preferentially respond to one modality (i.e., visual cortex responds to light, auditory cortex responds to sounds, etc.) is taken as given. But this train of thought can be and has been extended. Early lesion studies in macaque monkeys selectively ablated areas in either the temporal or parietal lobes, and found deficits in object identification or location, respectively (Mishkin et al., 1983; Ungerleider & Mishkin, 1982). They coined the phrases *ventral stream* and *dorsal stream* to identify streams of information related to these two functions, respectively, or rather the *what* and *where* pathways. This perspective was reimagined as a distinction between *perception* and *action* (Goodale & Milner, 1992), but nevertheless the critical assignment of different brain areas to different functions holds and motivates particular tasks for particular areas since.

In FEF, the appreciation of the diversity of neural responses has been apparent for decades. In 1970, Bizzi and Schiller described two types of neurons, those that responded during saccadic eye movements and those that responded during smooth pursuit. In 1985, Bruce and Goldberg reported a variety of neuron types, including visually responsive, movement-related, and visuomovement neurons. Schall (1991) also identified visually responsive, movement-related, and visuomovement neurons. Among the diversity of neurons reported from both studies, these three categories have become a canonical tripartite division guiding much FEF research since. However, such a classification has been shown to be insufficient for fully describing or predicting neural responses in more complex tasks (e.g. Type I and Type II neurons of Sato & Schall, 2003). Clearly, respecting the heterogeneity of functional properties of neurons is crucial for a mechanistic understanding of mental function. But equally clearly, there is still much work to be done to fully catalogue the sets of neuron types in a way that allows such an understanding.

1.6 Shortcomings in Current Models

Now that the importance of appreciating neural diversity, and the applications of psychological constructs in neuroscience, including the importance and utility of RTs and approaches toward identifying the presence and architecture of cognitive operations, have been described, we can now turn to the shortcomings of current neurobiological models. Specifically, that these models limit themselves to single operations, or at least single operations relevant to RT variability.

Take for example the prominence of the drift diffusion model in the modeling of responses of LIP. This approach to LIP function was introduced above, but also

includes more recent work with similar approaches (for review, see Shadlen & Kiani, 2013). While this work has come under scrutiny from a neurobiological perspective, e.g. that the apparent ramping of activity in LIP on average may be the result of state changes that occur at different points in time (Latimer et al., 2015), there have been fewer if any criticisms of the assumption that the RT variability in the random dot motion task used comes from a single decision encoding process. In fact, the drift diffusion model used as a mathematical basis for the linking proposition that LIP encodes the decision has frequently been used to study the Eriksen flanker task (e.g., White et al., 2011) which mirrors Eriksen's viewpoint that information is processed in a continuous flow. Additional complexity has since been superimposed upon the flanker task, as well as the related Simon task, but modeling has still been restricted largely to drift diffusion based frameworks (e.g., White et al., 2018). It should be noted that whereas these frameworks may recognize distinct operations, only the decision formation operation is seen as relevant to RT differences, not stimulus encoding or response preparation. Instead, the stages of visual encoding and response preparation and execution are lumped together as a single *non-decision time* parameter. Thus, even though additional complexity may be introduced, the mechanisms by which information sources are combined are ignored and are thus unable to address the issue of model mimicry.

The gated accumulator model assesses different issues, but is similar in that its output is an accumulation of evidence toward a decision threshold. It makes a stark improvement by separating input from visual neurons and output from movement neurons, explicitly acknowledging the difference in functional neuron types and at least implicitly acknowledging the difference between a stimulus encoding operation and a

decision output operation. The distinction between visual and motor activity in FEF neurons has been shown in several previous studies of FEF function that differentiate visual and motor stages by either requiring stimulus-response rule mapping (Lowe & Schall, 2019; Sato & Schall, 2003) or compelling responses with incomplete stimulus information (Costello et al., 2013; Scerra et al., 2019; Stanford et al., 2010). However, the gated accumulator model has not yet been tested when additional levels of complexity, e.g. a mapping of stimulus-response rules or temporally offsetting streams of information. Thus, to achieve full generalizability it requires additional refinement by adding modules that correspond to rules in a different dimension than what the search *per se* requires.

1.7 Overview of Experiments

So far, I have demonstrated that (1) RTs are critical for understanding both behavior and the neurobiological control of such behavior, particularly for visual search paradigms, (2) understanding neural diversity is critical for a mechanistic understanding of a neural system, (3) current RT models of behavior, while elegant for the particular problems they aim to solve, are insufficient or not yet generalizable for explaining more complex rules, and (4) such shortcomings are due, in no small part, to explicit and implicit assumptions regarding cognitive architectures and the existence, or lack thereof, of distinct processing operations. To that end, the next generation of models must include an account of heterogeneity of neural responses as well as some index of the cognitive architecture involved in any task. Further, to fully understand the performance of any task, multidimensional tasks must be used to aid in the expansion and generalization of current models.

In Chapter 2, I develop a method for categorizing functional response properties in FEF neurons in a manner beyond the traditional visual, motor, and visuomotor tripartite division. Importantly, such a technique should be developed such that it can identify functional response variability in tasks more complicated than traditional memory-guided saccades. In Chapter 3, I extend this method to allow for additional task conditions to contribute to categorization and to allow comparisons of functional categories across brain regions.

In Chapter 4, I introduce a specifically designed 2x2 factorial visual search task, the GO/NO-GO search task. This task involves the manipulation of the ease of performing the search *per se* and importantly, it imposes a stimulus-response rule association to that search. These two factors, ease of search and stimulus-response rule, satisfy the multidimensional nature of tasks needed for more general models. Further, this factorial design allows the application of *systems factorial technology (SFT)*, an approach developed by Townsend and colleagues (Townsend & Nozawa, 1995), to identify cognitive architecture. As imposing a phrase as *systems factorial technology (SFT)* is, we find considerable parallels with signal detection theory. Neither is necessarily organized for use in neuroscientific research, but the latter has enjoyed considerable success, as described above. With SFT, cognitive architectures can be identified. Cognitive architectures, as a phrase, can itself be seen as unnecessarily complex. However, similarly to signal detection theory, it can provide tangible, accessible metrics relevant to neuroscience. Put simply, cognitive architectures that can be differentiated by SFT imply whether one or two operations are occurring, whether they occur simultaneously, and whether behavior is initiated when one or both

operations are completed. Taken this way, SFT can provide interpretable information that can guide hypotheses regarding neural function, just as signal detection theory has.

In Chapter 5, I identify several neurometric indices of cognitive processing in a related visual search task. Specifically, I identify distinctions between stimulus-related and saccade endpoint-related selection operations. We have reported that, given particular stimulus array configurations and stimulus-response rule combinations, FEF neurons both select salient objects in a search array, then select a saccade endpoint at a later time (Lowe & Schall, 2019). We take this as clear evidence that search is comprised of multiple distinct operations and that visually responsive FEF neurons represent both. Finally, in Chapter 6 I use these neurometric indices and cognitive architectures to assess the neural substrates of the cognitive architectures involved during the GO/NO-GO search task.

1.8 Summary

The aim of the dissertation, at large, is as follows: given that (A) a task must be solved by some cognitive architecture, (B) a multitude of functional neuron types exist in the brain, (C) cognitive architectures can be identified, and (D) neurobiology must underlie behavior, then it must be the case that if the cognitive architecture and responses of the underlying neurons are known, then the architectures by which certain behaviors are performed must be explainable by the responses of the various underlying functional neuron types. I seek to identify those cognitive architectures, identify the functional neuron types in FEF, and explain visual search behavior by mapping neuron types to the processes enabling the cognitive strategies.

CHAPTER 2: FUNCTIONAL CATEGORIES OF VISUOMOTOR NEURONS IN MACAQUE FRONTAL EYE FIELD

2.0 SUMMARY

In the Introduction, section 1.5, I described the utility of appreciating diversity in anatomical and functional neuron types, and how understanding the set of functional neuron types in an area or task allows for a detailed mechanistic understanding of neural information processing. The examples in which this understanding has allowed the most complete characterizations are in relatively low-level processes such as retinal processing, saccade generation, and ocular and orientation preferences in primary visual cortex.

The set of neural responses contributing to complex cognitive behaviors are far less well understood. Thus, to understand the neural instantiation of cognitive architectures, one must understand both the architecture itself as well as the characteristics of the neurons contributing to the behavior. To address this problem of categorizing possible neural responses, I developed a method by which functional categories are defined from a population of neurons. This method of *consensus clustering* improves traditional categorization by minimizing assumptions used in the categorization and using several different clustering methods to enforce consistency of categorization across sets of assumptions that cannot be avoided.

In the remainder of this chapter, I describe this method as applied to neurons recorded from FEF during a memory-guided saccade task which has traditionally been used to categorize these neurons. I show that there are sub-categories of neurons that are not detected by traditional categorization schemes that could reflect important

differences regarding their contribution to the underlying neural circuitry. This chapter has been published as Lowe & Schall (2018).

In Chapter 3, I apply this method to an additional dataset that includes an additional, more complex task and includes neurons from the dorsal premotor cortex. This extension of the consensus clustering method demonstrates its utility in complex tasks and with additional trial conditions, as well as an approach by which the diversity of responses in multiple brain regions can be compared. Chapter 3 is in preparation for submission.

2.1 INTRODUCTION

Like all cortical areas, frontal eye field (FEF) is comprised of neurons distinguished by morphology, neurochemistry, biophysics, layer, and connectivity. Biophysical distinctions can be made via action potential waveforms (Cohen et al., 2009d; Ding & Gold, 2012; McCormick et al., 1985; Mitchell et al., 2007; Thiele et al., 2016), calcium binding proteins (Pouget et al., 2009), and neuromodulatory receptors (Noudoost & Moore, 2011; Soltani et al., 2013). Neurons with distinct biophysical characteristics must play different roles in the cortical microcircuit (DeFelipe, 1997; Lund & Lewis, 1993; Pouget et al., 2009; Zaitsev et al., 2012). Connectivity studies find FEF connected with at least 80 cortical areas (e.g., Huerta et al., 1986, 1987; Markov et al., 2014; Schall et al., 1993, 1995a; Stanton et al., 1993, 1995), and most pyramidal neurons do not project to more than one cortical area (Markov et al., 2014; Ninomiya et al., 2012; Pouget et al., 2009). Numerous functional distinctions among FEF neurons have been reported, beginning with the traditional sorting into visual, visuomovement, and movement plus fixation and postsaccadic categories (e.g., Bruce & Goldberg, 1985;

Schall, 1991). Subsequently, FEF neurons have been implicated in numerous functions including visual search (Costello et al., 2016; Fernandes et al., 2014; Lee & Keller, 2008; Purcell et al., 2012b; Schall et al., 1995a; Thompson et al., 1996; Zhou & Desimone, 2011), saccade preparation and inhibition (Boucher et al., 2007; Hanes et al., 1998; Ray et al., 2009), perceptual choice (Ding & Gold, 2012), visual attention (Bichot et al., 1996; Bichot & Schall, 2002; Gregoriou et al., 2009; Khayat et al., 2009; Noudoost et al., 2014; Schafer & Moore, 2011; Thiele et al., 2016; Zhou & Desimone, 2011), visual working memory (Clark et al., 2012; Reinhart et al., 2012), transsaccadic stability (Chen et al., 2018; Crapse & Sommer, 2008, 2012; Joiner et al., 2013; Shin & Sommer, 2012), planning saccade sequences (Phillips & Segraves, 2010), eye-head coordination (Elsley et al., 2007; Izawa & Suzuki, 2018; Knight, 2012; Sajad et al., 2015), and anticipating reward (Glaser et al., 2016; Roesch & Olson, 2003). Can so many functions be accomplished by so few neuron categories?

The problem of classification is neither new to science nor unique to neurophysiology. Cluster analysis is a powerful statistical tool, developed to find self-segregating categories in gene expression (Sharp et al., 1986), psychiatric diagnostics (Lochner et al., 2005), linguistics (Gries & Stefanowitsch, 2010), and Scotch whisky (Lapointe & Legendre, 1994). It has also been used to describe the biophysical diversity of cortical neurons (Ardid et al., 2015; Druckmann et al., 2013; Nowak et al., 2003), expanding the *in vivo* description of putative excitatory and inhibitory cells. Cluster analysis should be similarly powerful for assessing the functional diversity that must parallel anatomical diversity and should reproduce the functional categories known to exist in FEF.

Cluster analysis requires strategic decisions about the method of grouping observations and how to calculate pair-wise distance, which lacks rigorous specification for clustering functional characteristics of neurons. Therefore, we applied multiple pre-processing pipelines to a large sample of FEF neurons then applied an agglomerative clustering algorithm to discover functional categories. Because *a priori* endorsement of any particular pre-processing pipeline is impossible, and each result is unique, the results of an individual clustering procedure are difficult to interpret. However, second-order clustering procedures known as consensus clustering combine outcomes from different pipelines (Strehl & Ghosh, 2003). Distinct consensus clustering procedures use different theoretical motivations and computational efficiencies (Goder & Filkov, 2008). We applied a procedure that operates on the median pairwise similarity across all pre-processing pipelines because it is tractable and efficient. This consensus clustering procedure identified ten robust functional categories of FEF neurons, which elaborate conventional functional classifications.

2.2 METHODS

2.2.1 Subjects and Behavioral Task

Three male macaque monkeys (*M. radiata*) participated in this study. All procedures were in accordance with the National Institutes of Health Guide for the Care and Use of Laboratory Animals and approved by the Vanderbilt Institutional Animal Care and Use Committee. Monkeys were trained to perform a memory guided saccade task (C. J. Bruce & Goldberg, 1985). Trials began when a central fixation point appeared. After fixating this point for 500 ms, a peripheral target was presented for one screen refresh (16.7 ms at 60 Hz refresh rate) at 8° eccentricity at one of 8 locations

separated by 45°. After a variable delay between 300 and 800 ms the fixation point was extinguished, and the monkey was required to shift gaze to and maintain fixation on the location of the peripheral stimulus. The peripheral stimulus was re-illuminated after the saccade to provide a fixation stimulus. Fluid reward was delivered if the monkey maintained fixation on the peripheral, now reilluminated, stimulus for 500 ms. If the monkey broke fixation, made a saccade to an incorrect location, or made a saccade before the fixation point was extinguished, a 5,000 ms time-out delay occurred.

2.2.2 Recording Techniques

MRI compatible headposts and recording chambers were placed over the arcuate sulcus. Surgery was conducted under aseptic conditions with animals under isoflurane anesthesia. Antibiotics and analgesics were administered postoperatively. Details have been described previously (Cohen et al., 2009b; Sato et al., 2001; Schall et al., 1995a). Data were streamed to a data acquisition system: MNAP (40 kHz, Plexon, Dallas, TX - monkeys Da, Ga, and He) or TDT System 3 (25 kHz, Tucker Davis Technologies – monkey Da; Fig. 2.1a). Eye position was collected using EyeLink 1000 (SR Research). Eye position was calibrated daily and streamed to the data acquisition system and stored at 1 kHz. Electrophysiological data was obtained from linear electrode arrays, either a 24-channel Plexon Uprobe (monkeys Ga, He) or a 32-channel Neuronexus Vector Array (monkey Da). Both probes had a 150 μm recording contact spacing. Single units were identified online using a window discriminator (Plexon) or principal component analysis (TDT). Units recorded from the TDT system were sorted offline using Kilosort (Pachitariu et al., 2016).

Unit isolation was assessed by measuring waveform signal-to-noise ratio, interspike interval distributions, and baseline firing rate. Signal to noise ratio (SNR) was calculated by dividing the voltage difference between the peak and trough of the mean action potential waveform by the standard deviation of concatenated waveform residuals (Joshua et al., 2007). A minimum SNR criterion was set for each recording system. Units with more than 10% of interspike intervals less than 2 ms were excluded. Units with a mean baseline discharge rate of less than five spikes per second were excluded. Of 1864 potential single units, 963 were excluded based on SNR; 22 were excluded based on interspike interval distribution, and 439 were excluded based on baseline firing rate. All together, these criteria excluded 1383 potential units, leaving 481 for analysis. An additional 15 units were excluded for lacking non-zero values in either the visual or perisaccadic epochs of their spike density function (SDF). These very conservative criteria resulted in only 25% of potential units being included in the categorization, which indicates that they were well-isolated single units (Fig. 2.1b).

2.2.3 Neuron Classification

SDFs were calculated by convolving the spike trains with a function that resembles the postsynaptic influence of each spike (Thompson et al., 1996). SDFs were calculated only for correct trials on which the visual stimulus was presented in the visual receptive field and the saccade was made into the movement field. The number of trials contributing to characterizing each neuron ranged from as few as four to as many as 317 (median 34), with trials with fewer than five spikes excluded. If the spike density function was not a stable estimate, we did not include the neuron. A sequence of classification procedures was employed. The first was based on the traditional criteria of

Bruce & Goldberg (1985). A unit was considered to have visual activity if the firing rate between 50 and 150 ms after stimulus presentation was elevated more than six standard deviations above the baseline mean. A unit was considered to have movement activity if the firing rate in the 100 ms preceding the saccade was more than six standard deviations above the baseline mean and the SDF showed a positive correlation over time in the 20 ms preceding saccade. This prevents elevated delay activity with no pre-saccadic ramping from being considered movement-related activity. Visual units had visual responses with no movement activity, movement units had movement activity with no visual responses, and visuomovement units had both. Other units were considered uncategorized; we did not test for fixation or postsaccadic activity in this categorization.

Units were categorized via agglomerative hierarchical cluster analyses (Everitt et al., 2011; Sokal & Michener, 1958). These analyses iteratively combine units, or groups of units, based on the weighted average similarity of units. In each case the analysis algorithm was identical, though the method for determining similarity differed due to the scaling of discharge rates across units (Fig. 2.1c), measurement of the units' response (Fig. 2.1d), or the similarity metric (Fig. 2.1e). The agglomerative cluster analysis was performed as follows: First, the sample was considered as *n* groups, each with one member. Then, the two groups with the smallest pairwise distance were combined into one group, leaving (*n*-1) groups, one of which with two members. The distances of this group to the other groups were determined by the weighted mean of the distances of the individuals in each group:

$$D'(I,J) = \frac{\sum_{x\in I}\sum_{y\in J} D(x,y) + \sum_{y\in J}\sum_{x\in I} D(x,y)}{2 * \left(n_I + n_J\right)}$$

where *I* is the first group in consideration and *J* is the second, *x* are the members of group *I*, *y* are the members of group *J*, and n_I and n_J are the number of members in groups *I* and *J*, respectively. The value of 2 in the denominator is required because the distances are symmetrical and thus represented twice in the numerator of the equation. More simply, this averages the pairwise distances of the members of *I* and *J* such that the similarity of two groups will not be skewed by uneven group sizes.

This procedure was repeated until all observations were agglomerated into a single group. Then, category identifications were made for a range of number of categories, *k,* by finding the most recent step in the algorithm at which *k* categories with a minimum of *x* members were present. For example, for a *k* of five, the most recent set with five categories of at least *x* members was assigned as the final classification. Category membership for *k* was assessed between 1 and 20. The value of *x* was set to 10; only categories with 10 or more members were considered to assure robust results.

Category membership was assessed for six scaling procedures, four measurements of the response, and two similarity metrics (Fig. 2.1c-e). The mean skewness across time points was used to assess the quality of scaling for cross-unit comparisons. We refer to each combination of scaling procedure, SDF measurement, and similarity metric as a pre-processing pipeline. We evaluated categories derived from each pipeline but will show outcomes for only three.

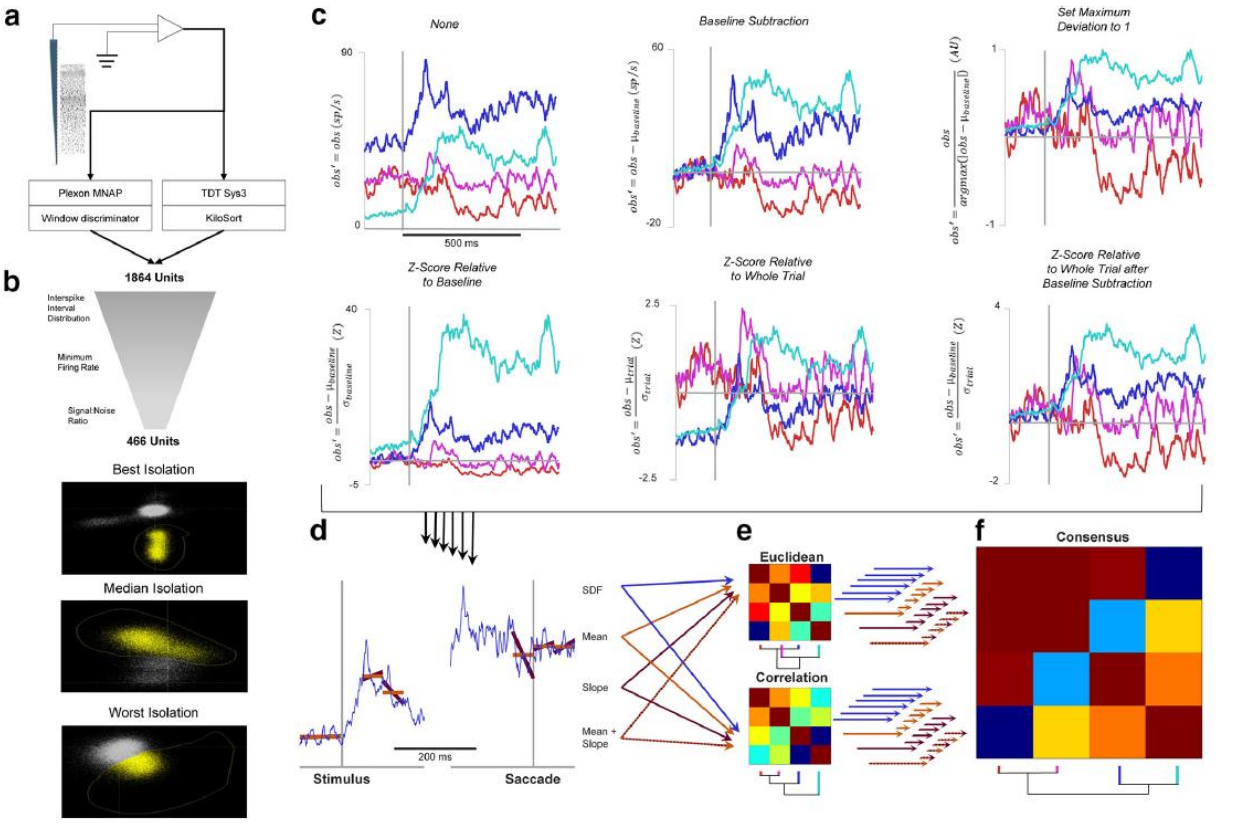

Figure 2.1. Analysis pipeline. ***a***, Potential neurons were recorded from FEF using multicontact electrode arrays. These recordings were performed either in the Plexon MNAP or the Tucker-Davis Technologies System 3. Potential units from the Plexon MNAP were sorted on-line with a window discriminator, whereas potential units from TDT Sys3 were sorted off-line using KiloSort (Pachitariu et al., 2016). A total of 1884 potential units were recorded. ***b***, The 1884 potential units were subjected to several criteria to ensure that only single units were analyzed further. These criteria include interspike interval distributions, a minimum baseline firing rate, and a signal-tonoise ratio of sorted action potential waveforms. The quality of isolation is illustrated, where the PCA space of off-line sorting is shown for the units with the best, median, and worst signal-to-noise ratio that still meet the criterion. ***c***, Six methods of scaling spike density functions were applied for normalization. Four units were selected to illustrate the effects of these different scaling methods. The colors of each unit were assigned arbitrarily. The equations for each scaling method are shown on the ordinates. Zero points in scaling and time are shown in light gray. ***d***, After each scaling method, features for inclusion in the clustering algorithm are measured. Four ways of measurement were used and are demonstrated on one of the example units from above: the full SDF (blue), the mean of the SDF during epochs of interest (orange), the slope of the SDF during epochs of interest (purple), and the combination of mean and slope. Each of these four measurements, for each of the six scaling methods, were clustered individually. ***e***, Clustering on the feature vectors generated from the scaling and measurement techniques can be performed using either Euclidean or correlation distance. Euclidean distance measures whether pairs of units have similar values of the measurements, regardless of the patterns of modulation, whereas correlation distance measures the similarity of modulation patterns regardless of absolute similarity. An example clustering dendrogram and distance matrix for each distance metric is shown as applied to the four example units, and it can be seen that these two clustering methods produce different categorizations. ***f***, Because there is no a priori way to select which scaling method, measurement, or distance metric is most appropriate, and each may produce different categorizations, the final categorization was selected by applying consensus clustering. The distance matrices for each scaling method, measurement, and distance metric (48 total combinations) were normalized and combined to create a consensus distance matrix. The same clustering algorithm was applied to this consensus distance matrix. The consensus distance matrix and corresponding final dendrogram for the four example units is shown. Final categories were determined by applying additional criteria (minimum category membership and maximum number of uncategorized neurons).

Modulation of discharge rates was measured according to the following approaches. Three (mean, slope, mean and slope) account for the firing rates during epochs: -200 to -100 ms before stimulus onset, 50 to 100 ms post-stimulus, 100 to 150 ms post-stimulus, -100 to -50ms before saccade, -50 to 0ms before saccade, and 50-

100 ms post-saccade. “Mean” measurement was based on the mean firing rates in these epochs, “slope” measurement was based on the slope of the firing rate changes in these epochs (i.e., the difference in mean firing rate at the beginning and end of the epoch), and “mean and slopes” were based on the concatenation of mean firing rate and slope. “SDF” measurement did not parse the responses into epochs, and was instead based on the values of the SDF aligned on stimulus onset (-200 to 300 ms) or saccade (-300 to 200 ms) at each time point to millisecond resolution. To emphasize equally all epochs, means, and slopes, each measurement value was individually converted to a z-score across the sample.

Pairwise distance was measured two ways: Euclidean distance and correlation. Euclidean distance can be conceptualized as the physical distance between two points in multidimensional space while disregarding which dimensions contribute to this distance. Correlation assesses the relationships between the dimensions while disregarding the particular values of those dimensions. The different emphases of these two distance metrics can and often does assign two units to the same category via one metric but not the other.

Euclidean distance*.* Based on the firing rate each unit was placed in a multi-dimensional space. This multi-dimensional space had either 6 (for mean measurement and slope measurement), 12 (for mean and slope measurement), or 1002 (for SDF measurement). The Euclidean distance between the units in this space:

$$D(x, y) = \sqrt{\sum_{i}^{e} (x_i - y_i)^2}$$

defines a pairwise distance matrix, where *e* is the number of epochs (or milliseconds).

Correlation. Based on the firing rate each unit was defined a 6-, 12-, or 1002-element vector, depending on measurement method, and the correlation between two vectors:

$$D(x, y) = 1 - \rho(x, y)$$

measures the similarity of the modulation patterns of two units while disregarding absolute differences in firing rates.

All of these pre-processing pipelines were tested, and all produced unique results. Some pipelines produced categories that were subjectively easy to endorse, while others produced subjectively poor categories. The results of three representative pipelines are presented, two that produced poor categorizations, for different reasons, and one that produced good categorizations. The first combination scales by z-scoring relative to baseline, mean measurement, and uses Euclidean distance. The second does not scale the data before measurement, uses mean measurement, and uses correlation distance. The third scales by z-scoring relative to the whole trial, and mean and slope measurement.

2.2.4 Consensus Clustering

No *a priori* reason endorses the categories yielded by a particular SDF scaling procedure, summary of response modulation, or distance measurement. Therefore, we employed a novel strategy of combining the results of multiple clustering pipelines. This algorithm considers the pairwise distance between units for each individual pre-processing pipeline tested by creating a composite distance matrix. Each individual distance matrix was z-scored internally to correct for the absolute scale differences between different scaling procedures and distance measurements. Then, the median for

each pair was selected to prevent skewing by non-optimal pipelines. Thus, if the pairwise distance between two units was consistently small, then this composite measure was also small, whereas if the pairwise distance between two units was small in some parameter sets but was generally larger, then the composite distance metric reflected the trend toward differences but accounted for the isolated cases of similarity. After creating this composite distance matrix, the same agglomerative algorithm used for each individual pipeline was applied to identify categories (Fig. 2.1f). Intuitively, this method was intended to distinguish units that were clustered together regardless of pre-processing pipeline from units that were members of different clusters regardless of pre-processing pipeline.

In essence, this procedure performs a clustering that operates on a distance matrix whose entries represent robustness of categorization across a number of individual procedures, or a “consensus clustering” problem (Goder & Filkov, 2008). Indeed, consensus clustering has been used to identify biophysical classes of neurons (Ardid et al., 2015). However, while conceptually similar, the previous “meta-clustering” and the present consensus clustering differ operationally in both the algorithm used for performing clustering and the pre-processing of input data. Ardid and colleagues performed K-means clustering, which does not provide a unique clustering solution and is highly sensitive to starting points (Bradley & Fayyad, 1998; Celebi et al., 2013; Peña et al., 1999), so their meta-clustering involved multiple iterations of the K-means procedure using the same input data and then assigning clusters via robust co-membership across each iteration. Unlike Ardid and colleagues, we used agglomerative clustering, which delivers unique solutions because no optimization steps are involved.

However, we found that clustering outcomes were sensitive to the pre-processing pipeline, varying with discharge rate scaling procedure, measurement, and distance metric. Hence, our consensus clustering approach was conceived to assess cluster assignment consistency over pre-processing steps, not local solutions to clustering one set of pre-processed data.

2.2.5 Assessing Number of Categories

The number of categories in individual clustering procedures was selected using a lenient version of Tibshirani's gap procedure (Tibshirani et al., 2001), which assesses the reduction in intra-cluster distance with respect to randomized null sets created with no intrinsic clustering. Valid splitting of clusters should have a greater than chance reduction in intra-cluster distance, assessed by the standard deviations of the intra-cluster distance in the null sets, whereas excessive splitting should have a reduction in intra-cluster distance within the standard deviation of the null set. The strict version selects *k* categories as the first number of categories meeting this criterion. In the lenient version of this test, each occasion on which the above criterion is met was treated as potentially valid, and visual inspection was used to determine whether categorizations were either insufficient or excessive. In some cases, due to the difficulty in creating a reasonable null-set from physiological data, categories were selected based on the properties of the gap curve. When a reasonable null-set could not be determined, an inflection in the gap-curve was identified. This inflection identified the number of categories at which the reduction of intra-cluster distance was markedly less than that of the previous sequence of clusters.

For consensus categories and the composite distance matrix, the means of creating a null set in order to use Tibshirani's gap procedure is unclear. Therefore, in such cases a pair of criteria for determining the maximum number of categories was set: no more than 10% of units were allowed to remain un-categorized, and each category required at least 10 members. The maximum number of categories that met both criteria was selected.

2.2.6 Comparing Categorization Schemes

The quality of alternative categorization schemes was assessed by calculating an index of member variability through the ratio of variances of the spike density values. Specifically, for each time point in the spike density functions, the within-category variance at that time point was divided by the variance of the category mean across time points. For each category, the average ratio was calculated, and then the grand average was taken. Because this ratio will decrease by definition as more categories are formed, a penalty for over-splitting was imposed by multiplying the grand average ratio by the square root of the number of categories. That is, for a given category the modulation strength was calculated as:

$$MS_c = \frac{\sum_t (\overline{X}_{c,t} - \overline{X}_{c,\cdot})^2}{N_t}$$

where *c* indexes category and *t*, time. Then, for each time point a ratio of variances (*RoV*) was calculated:

$$RoV_{c,t} = \frac{\sum_{i \in c} (X_{i,t} - \overline{X}_{c,t})^2 \Big/ N_i}{MS_c}$$

These are then combined by averaging the values for each category over time, then across categories, then applying a penalty for over-clustering proportional to the square root of the number of categories identified:

$$RoV = \sqrt{N_c}\frac{\sum_c \frac{\sum_t RoV_{c,t}}{N_t}}{N_c}$$

Small *RoV* values can be obtained either through large group-wise modulations over time or a lack of variability among the categories' constituent members, whereas large *RoV* values are obtained through weak category-wise modulations or large variability. That is, smaller *RoV* values indicate better categorization, and vice versa. No benchmarks have been established for this index, so we interpret relative values in comparing the quality of two categorization schemes.

The similarity of two categorization schemes was assessed by the Adjusted Rand Index (*ARI*) (Hubert and Arabie, 1985):

$$ARI = \frac{\sum_i \sum_j \binom{n_{ij}}{2} - \left[\sum_i \binom{a_i}{2} \sum_j \binom{b_j}{2}\right] / \binom{n}{2}}{\frac{1}{2}\left[\sum_i \binom{a_i}{2} + \sum_j \binom{b_j}{2}\right] - \left[\sum_i \binom{a_i}{2} \sum_j \binom{b_j}{2}\right] / \binom{n}{2}}$$

Where a_i and b_j are the counts of category *i* or *j* in categorization procedure *a* or *b*, respectively, and $n_{i,j}$ is the number of observations in both category *i* in categorization scheme *a* and in category *j* in categorization scheme *b*. This quantity measures similarity of two data categorizations and is adjusted by chance co-categorization produced through the two schemes. To assess significance, each categorization was randomly shuffled separately, destroying internal structure between the two schemes, and *ARI* was recalculated. This was repeated 1000 times and *p* was the proportion of shuffled *ARI* that exceeded the non-shuffled *ARI*.

To visualize the overlap, for each pairwise categorization combination a *signed* χ^2 was calculated:

$$Signed\ \chi^2{}_{i,j} = \frac{n_{ij} - n(\frac{n_i}{n} * \frac{n_j}{n})}{n(\frac{n_i}{n} * \frac{n_j}{n})}$$

That is, the difference between the observed pairwise count and the count expected by the marginal probabilities of each individual categorization scheme was calculated, then normalized by that expected value. Each category assignment was shuffled separately 1000 times and the signed χ^2 was recomputed for each combination and iteration. A bootstrapped z-score was then calculated for each category combination.

2.2.7 Biophysical Characteristics

Several biophysical characteristics were calculated for each neuron to assess the identification of consensus categories with measurements that were not included in the clustering process. Spike width of the average waveform of each neuron was calculated as the time between the initial trough of the action potential and the following peak, or the time between the initial peak and following trough for spikes with positive deflections. Coefficient of variation (Cv), which measures firing rate variability, and local coefficient of variation (Cv2), which measures Cv across smaller time periods, were calculated as described previously (Holt et al., 1996). Local variation (Lv), which is another metric of local firing rate variability, and revised local variation (LvR), which accounts for a 5 ms refractory period, were also calculated as previously (Shinomoto et al., 2003, 2009). Fano factor was calculated by computing spike counts in 100 ms bins, then dividing the spike count variance by the mean spike count (Purcell et al., 2012a).

Response field characteristics (maximum response, preferred location, and tuning width) were calculated by fitting a unimodal Gaussian function to the mean responses to the eight target locations. Response field characteristics were calculated separately for visual (50-150 ms after target presentation) and movement epochs (50 ms preceding saccade initiation). Response field values were excluded from analysis if the Gaussian tuning function wIas unable to fit well ($r^2 < 0.5$).

2.2.8 Cross Validation

To verify the accuracy of the consensus clustering algorithm, a leave-one-out classification procedure was used. An SVD classifier with a linear kernel was trained. To preserve the consensus metrics, the basis for the classifier training set was the composite pairwise distance matrix. However, this matrix was under-specified, so principal components of the pairwise distance matrix were calculated. The classifier was trained for the first principal component, the first and second components, the first through third components, etc. for the first 100 principal components. The cumulative variance explained ranged from 43.4% to 93.4%. Due to the possible presence of groups with few members, this classifier was trained on all units but one, and the remaining unit was tested. No explicit regularization was performed when training the classifier. Only units that were assigned a category by the consensus clustering algorithm were included (n = 422/466, 90.6%).

2.3 RESULTS

This analysis is based on 466 units sampled in FEF from three macaque monkeys performing memory guided saccades in pursuit of other research aims.

2.3.1 Traditional Response Categorization

First, units were categorized based on traditional criteria (Bruce & Goldberg, 1985; Schall, 1991) and the canonical visual, movement, and visuomovement units were identified (Fig. 2.2). Of 466 neurons sampled, 210 (45.1% of sampled neurons, 70.2% of presaccadic modulated neurons) were identified as visual, 16 (5.4%, 5.4%) were movement related, and 73 (15.7%, 24.4%) were visuomovement. The remainder exhibited other patterns of modulation. Earlier studies using different tasks than we used here reported more diversity among the three major groups. We will consider this in the Discussion. For now, this simpler categorization facilitates the motivation of this approach.

While the average discharge rates of these categories were as expected, the SDF of the individual units categorized into each type exhibited considerable variation. For reference with subsequent analyses, the *RoV* value was 50.89. Thus, while the traditional categorization methods captured general trends in the modulation patterns of FEF neurons, additional variation was present but unaccounted for.

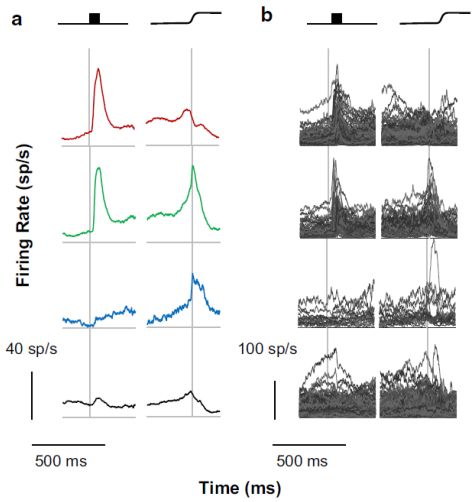

Figure 2.2. Traditional classification. The current sample was classified according to traditional criteria. ***a***, Group mean SDFs for visual, visuomovement, movement, and unclassified neurons are depicted from top to bottom, with left panels aligned on stimulus onset and right panels aligned on saccade. Here and in subsequent figures, the categories of neurons are arranged on a visual-to-motor axis, and colors are assigned such that red indicates visual activity and no movement activity, green indicates both visual and movement activity, and blue indicates movement activity without visual activity. Black indicates unclassified neurons. Scale bars for response magnitude and time are shown at the bottom left. ***b***, Individual spike density functions comprising each category. Scale bars for response magnitude and time are shown at the bottom left.

2.3.2 Cluster Pipeline 1: Z-Score Relative to Baseline, Mean Measurement, Euclidean Distance

To begin accounting for this excessive variability, a cluster analysis was performed on the SDFs that were z-scored based on the mean and standard deviation of the baseline firing rate. This captured the definition of visual and movement activity used above. However, the data-driven clustering procedure revealed functional categories that are similar in their firing rate modulations in more than just two epochs. Based on the mean firing rate in the six specific task epochs described in Methods, each unit was represented as a six-element vector. Based on Euclidean distance measures of pairwise distances eight categories of units, numbered 1_a-8_a to distinguish this set of results, were found (Fig. 2.3). Unlike the traditional categorization scheme, two categories of visual units were identified, identified as categories 1_a and 4_a (17/466 (3.7%) and 11/466 (2.4%) respectively). Both categories had modest visual responses and no perisaccadic activity. They were differentiated by the presence or absence of anticipatory activity before the target appeared and by delay period activity. An additional category, category 5_a (37/466 (7.9%)), had a robust visual response with weak presaccadic ramping. Four categories of units had both visual and presaccadic responses. Two of these categories had robust visual responses and intermediate presaccadic ramping: categories 2_a and 7_a (40/466 (5.2%) and 112/466 (24.0%) respectively). These categories were differentiated by the return to baseline after the saccade: category 7_a had a typical slow return to baseline whereas category 2_a returned to baseline almost immediately. The other two categories, 6_a and 8_a (135/466 (29.0%) and 16/466 (3.4%) respectively), had only modest firing rate modulation in both epochs and were distinguished by the presence (8_a) or absence (6_a) of anticipatory activity. The

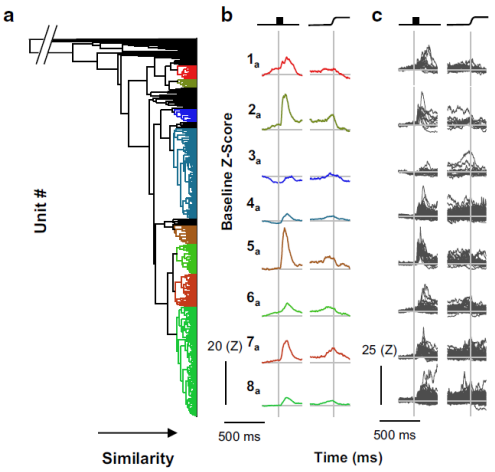

Figure 2.3. Cluster pipeline 1. Neurons were categorized via cluster analysis scaling by the *z* score relative to the baseline, mean measurement, and Euclidean distance. ***a***, The dendrogram resulting from cluster pipeline 1 shows the eight identified categories. Horizontal distance indicates pairwise similarity, with individual neurons on the right and full agglomeration on the left. Colors indicate categories and are arbitrarily assigned on a visual-to-motor axis as in Figure 3. The break at the top left indicates that the final agglomeration takes place at a point that prevents the visibility of categories. ***b***, Category means are plotted aligned on stimulus onset and saccade. Each category was given an arbitrary numerical identifier for convenience and are ordered according to their position in the dendrogram. Scale bars are shown at the lower left. ***c***, Individual neurons comprising each category aligned on stimulus and saccade. Scale bars are shown at the lower left.

final category, 3_a (24/466 (5.2 %)), did not show firing rate modulation during the trial. This demonstrates that additional diversity is present in FEF firing patterns that has been unaccounted for in the traditional scheme. However, this clustering approach failed to identify purely movement neurons or post-saccadic neurons.

The eight categories did not match the three traditional categories in FEF that should have been recovered through cluster analysis. However, similar to the traditional categorization scheme, these category means captured some general trends of the individual units comprising the categories. Variation was reduced (*RoV* = 18.36 relative to 50.89 for the traditional classification), but considerable variation was still evident. This was particularly pronounced in categories 4_a and 8_a which were also much larger categories than the other six. Thus, these categories seem to be “catch-all” categories. Other categories seem to be nearly identical, though are clearly seen as different groups in the dendrogram (e.g., 2_a and 5_a). The dendrogram in Fig. 2.3a also shows that units did not exhibit clear clustering. Instead, it appears as though small groups or individual units are progressively grouped together such that, at the clustering step when eight categories meet the membership criterion, 74 of 466 (16%) of units were still uncategorized. That is, for the number of categories identified via Tibshirani’s

gap procedure, 16% of neurons were so dissimilar to each other and the eight categories that they could not be placed in any of the eight categories, or form a ninth separately. This may be so because the variation of the SDF of the identified units was high (mean skewness = 1.35). Taken together, these considerations indicate that this clustering procedure is insufficient.

2.3.3 Cluster Pipeline 2: Non-scaled SDF, Mean Measurement, Correlation Distance

To account for more of the excessive variability, a cluster analysis using a correlation distance measurement was performed on the non-normalized data. This approach captures relative rather than absolute changes in firing rate. That is, if two units were similarly modulated but have different firing rates, this procedure treated them as members of the same category. In other words, this approach emphasized the pattern of modulation of FEF neurons rather than the absolute discharge rate.

This procedure identified six categories, 1_b-6_b (Fig. 2.4). These categories did not match the three traditional categories; movement neurons are missing. Instead, each of the six identified categories demonstrated modulation following visual stimulation to different degrees. Two of these categories, 1_b (123/466) and 6_b (122/466), showed visual modulation only, and were differentiated by the baseline firing rate and degree of visual modulation. Three categories had both visual and movement-related activity: 2_b (28/466), 4_b (44/466), and 5_b (24/466). Category 2_b had modest visual modulation and no delay activity;

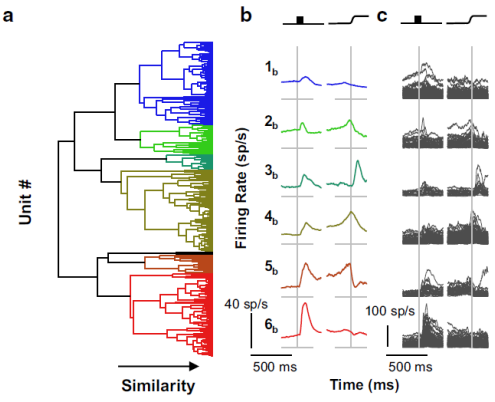

Figure 2.4. Cluster pipeline 2. Neurons were categorized via cluster pipeline using no scaling procedure, mean measurement, and correlation distance. Conventions for ***a*** through ***c*** are as in Figure 2.3.

category 4_b had modest visual activity and some delay activity, and category 5_b had robust visual modulation, prominent delay activity and presaccadic ramping, but its activity fell off dramatically at the time of the saccade. The final category, 3_b (121/466), had modest visual modulation and a sharp post-saccadic transient. Four of 466 neurons were placed in no category.

Considerable variability within categories remained and in fact increased relative to cluster analysis 1 (*RoV* = 29.70 as opposed to 18.36), though the category means did capture category trends. This variability may be due to the skewed firing rates (mean skewness: 2.09), which allowed few units in one category to drive the modulations apparent in the category means. For example, the inclusion of some units with large visual responses and high firing rates in category 2_b was a driving factor in the modest visual activity seen in the category mean. Thus, both the z-score relative to baseline and un-scaled firing rates may be ineffective for comparing across units, even though they are useful for assessing within-unit modulation. However, the appearance of the dendrogram for this clustering outcome should be noted (Fig. 2.4a). Unlike that from pipeline 1, a more sensible structure is apparent when this combination of clustering parameters was used; fewer neurons are non-classified and the categories visibly self-segregate.

2.3.4 Cluster Pipeline 3: Z-Score Relative to Whole Trial, Mean and Slope Measurement, Correlation Distance

To account for more of the variability in modulation patterns, a different scaling procedure was used: Z-scoring across the entire trial and measuring the SDF with both the means of the SDF and the slopes during the relevant epochs were considered. The

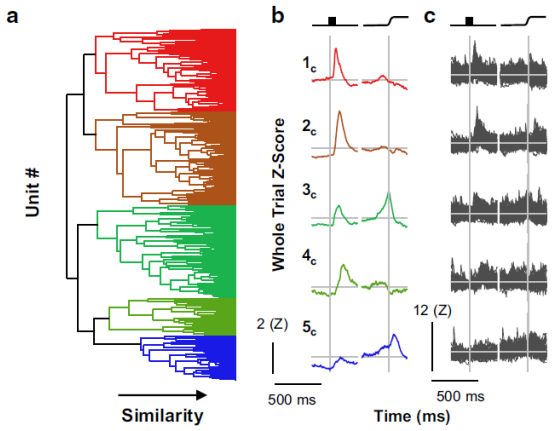

Figure 2.5. Cluster pipeline 3. Neurons were categorized via cluster analysis scaling by the *z* score relative to the whole trial, mean and slope measurement, and correlation distance. Conventions for ***a*** through ***c*** as in Figure 2.3.

agglomerative clustering algorithm identified five categories, 1_c-5_c (Fig. 2.5). Three of these categories had visual activity only: 1_c (110/466), 2_c (124/466), and 4_c (124/466). Category 4_c had pronounced delay activity. The other two were distinguished by the time of peak visual response, with the visual activity of category 1_c peaking earlier and that of category 2_c, later. Category 3_c (50/466) had robust visual and presaccadic modulation but did not have delay activity. The final category 5_c (58/466) showed robust presaccadic ramping and only modest, if any, visual activity. It should be noted that the presaccadic ramping activity in category 5_c peaked after the saccade and showed a slow reduction of firing rate back to baseline, whereas the category with both visual and saccadic responses had a peak perisaccadic activity at the time of the saccade followed by a sharp return to baseline, but this sharp return is not as pronounced as the “clipped” movement neurons in category 5_b. This indicates that the additional diversity evident in visual inspection of discharge rate modulation patterns is tangible and identifiable. Further, of the three cluster pipelines, pipeline 3 produced the classification most similar to the traditional. Visual and visuomovement categories were identified as well as a putative pure movement group (category 5_c).

The range of values through this scaling was smaller and is less skewed (mean skewness: 0.73), suggesting that this scaling method provided a more equitable cross-unit comparison. As with analysis 2, these categories are apparent in the dendrogram

structure, though some additional heterogeneity can be observed, particularly among categories 1_c and 2_c. This may explain, in their particular cases, the seeming similarity between the two; it could be that splitting further would reveal additional heterogeneity, and in the case of the category 3_c, further splitting could reveal a second visuomovement group without "clipped" activity as well as a pure movement category. However it should be noted that unlike cluster analyses 1 and 2, the category means were much more representative of the members (*RoV* = 5.19 as opposed to 18.36 and 29.70 for cluster pipelines 1 and 2, respectively).

2.3.5 Consensus Clustering

We now address the problem of individual units being members of different categories following different analysis paths (Fig. 2.6). This occurs because different pre-processing pipelines resulted in different distance matrices upon which the agglomerative clustering algorithm operates. Consequently, a given pair of units could be members of the same category following one pipeline but members of different categories following another pipeline. For example, all four individual units shown in Fig. 2.6 belong to category 2_c, but only three belong to category 6_b; the unit on the top-right belongs instead to category 1_b. With no cluster pipeline being more confidently motivated or more certainly correct than another, should all four units be considered members of the same category or not? Nevertheless, assuming the existence of ground-truth categories, consistent with anatomical constraints, units that are actually members of the same ground-truth category should have small pair-wise distances regardless of scaling or clustering procedure. Likewise, units that are members of

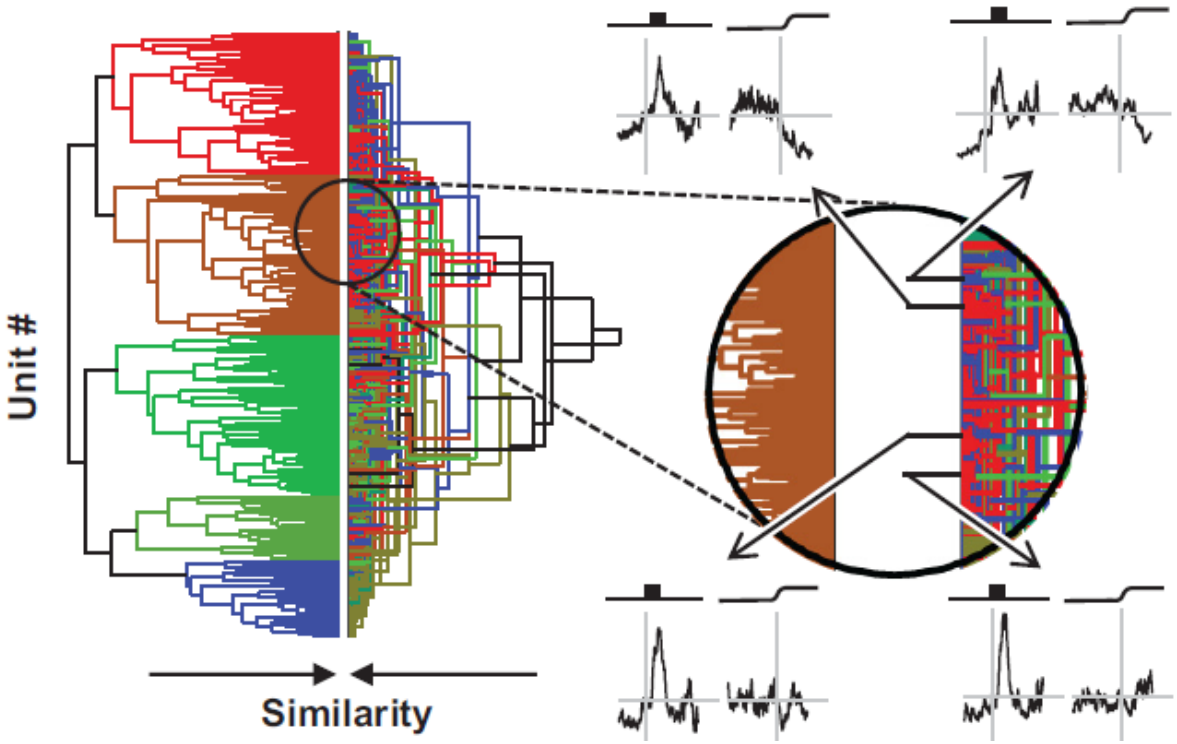

Figure 2.6. Comparison of analysis pipelines. Left: Dendrograms from cluster pipelines 2 (right) and 3 (left). They are shown side-by-side to highlight the similarities and differences in the respect categories. The dendrogram for cluster pipeline 3 is identical to the dendrogram in this figure. The dendrogram for cluster pipeline 2 shows the same results as in Figure 5; however, the vertical arrangement was reordered so that common units are horizontally aligned in both dendrograms. Where common colors are horizontally aligned, units were assigned to the same category. Where different colors are horizontally aligned, units were assigned to different categories. Although horizontal alignment of some dendrogram elements is evident, the disagreement between the two dendrograms is more prominent. The extent and nature of this disagreement is illustrated in the expanded view of the dendrogram on the right. SDFs of four representative units are shown. Through analysis of pipeline 3, all four units were placed in category 2c, which characterized by a pronounced visual response and weak perisaccadic suppression (left dendrogram). Through analysis of pipeline 2, three of the units were placed in category 6b, which is characterized by a pronounced visual response and weak perisaccadic suppression (red, right dendrogram), whereas the unit shown at the upper right was placed in category 1b, which is characterized by a weak visual response and no perisaccadic modulation (blue, right dendrogram). Thus, the two analysis pipelines provide overlapping, but far from identical, categorizations. Which categorization is correct is uncertain.

different ground-truth categories would have small pair-wise distances only as an artifact of particular measurement parameters and clustering algorithm.

To address this fundamental problem, we employed a second-order clustering procedure known as “consensus clustering” (Goder & Filkov, 2008; Strehl & Ghosh, 2003). We created a composite distance matrix by z-scoring individual distance matrices from all of the pre-processing pipelines (Fig. 2.1f) and then calculated the median distance across all pre-processing pipelines. This composite distance metric was used to identify units that were consistently similar to one another across pre-processing pipelines and clustering algorithms. The agglomerative clustering algorithm

was applied to this distance matrix to identify robust categories of units superordinate to any individual cluster analysis. Clusters were continually split until either of two membership criteria were no longer satisfied: (1) minimum number of units per cluster and (2) maximum proportion of unclustered units.

Consensus clustering identified 10 categories, clearly distinguished in the dendrogram and evident in the distance matrix (Fig. 2.7). Of 466 neurons 43 (9.2%) were not placed in any category. These categories were robust and consistent (*RoV*: 3.91). Even with the penalty for over-clustering in the *RoV* metric, consensus clusters account for more of the variability in the neural data than the classification produced by the best individual classification.

Categories with visual responses only. We identified two categories of neurons that had visual, but not saccade-related, activity. These categories, 1_{con} (74/466) and 2_{con} (105/466), showed flat baseline activity and a sharp visual transient. The time of peak firing rate differentiated these two categories, with mean peak latencies of 74 ms (1_{con}) and 136 ms (2_{con}). Also, category 2_{con} had persistent delay activity until the saccade.

Categories with visual and saccade-related facilitation. We identified five categories of neurons with both visual and pre-saccadic increases in firing rate. Two of these categories, 3_{con} (21/466) and 4_{con} (25/466), showed marked increases in firing rates following visual stimulation and were distinguished by the time of peak visual activity (mean values of 70 ms and 161 ms respectively). They were also distinguished by the time and character of the pre-saccadic ramping. The firing rate of category 3_{con} neurons peaked at the time of the saccade and quickly returned to baseline, whereas

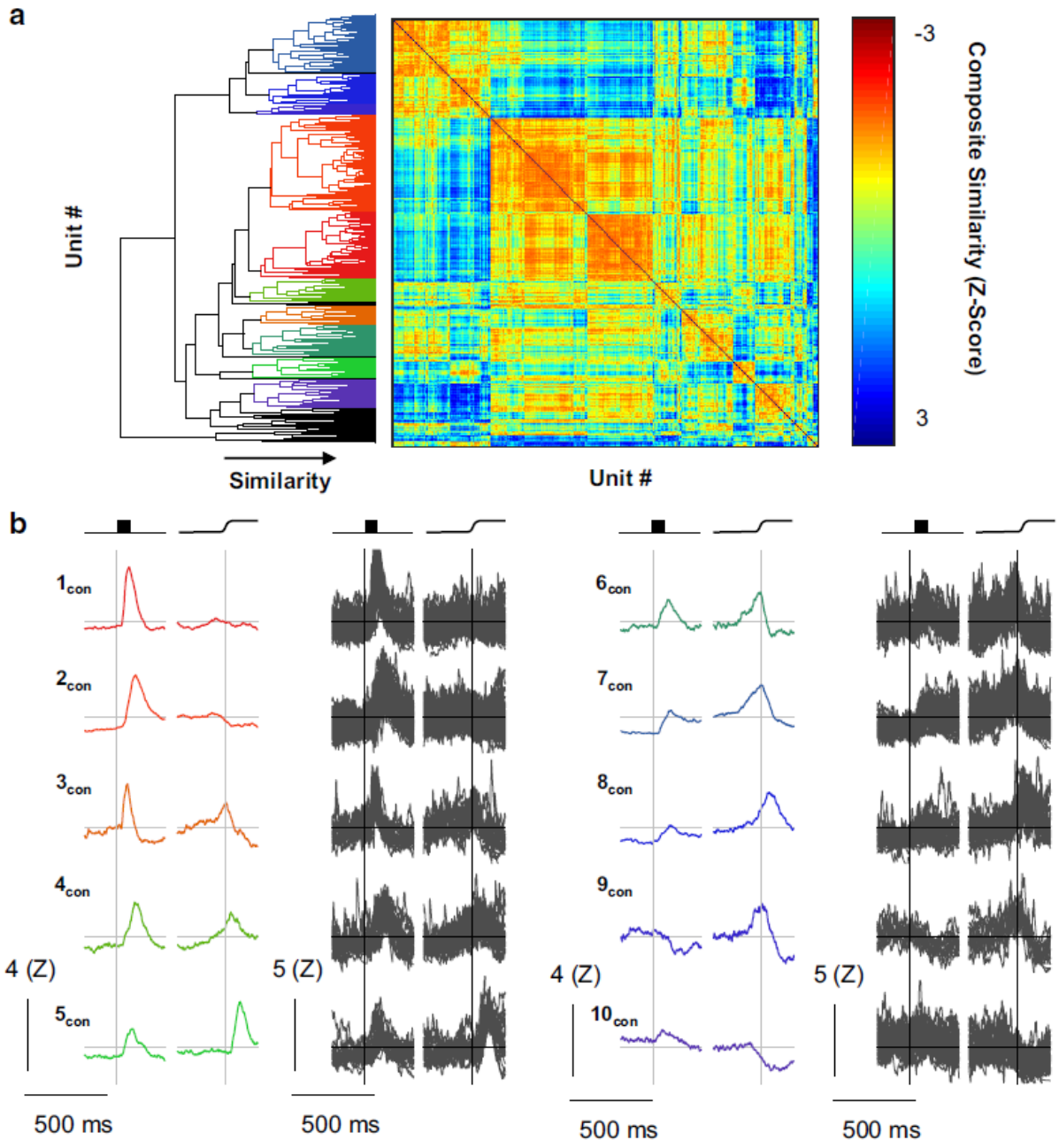

Figure 2.7. Consensus clusters. Consensus clusters were identified by creating a composite distance matrix and applying the agglomerative clustering procedure to this matrix. ***a***, The resulting dendrogram is shown abutting the composite distance matrix. Colors in the dendrogram are assigned as in Figures 3–6. Color in the distance matrix is indicative of composite similarity. Warm colors (low composite *z* score) indicate consistently similar units, whereas cool colors indicate consistently different units (high composite *z* score). ***b***, The category mean SDFs (columns 1 and 3) and the individual SDFs (columns 2 and 4) comprising them are shown aligned on stimulus onset (left) and saccade (right). Scale bars are shown at the lower left of each column. Arbitrary category labels were assigned for convenience.

the firing rate of category 4_{con} peaked after the saccade and returned to baseline more slowly. Two of the three remaining categories, 6_{con} (35/466) and 7_{con} (64/466), also had clipped movement activity with late, weak visual responses. These two categories are

differentiated by the absence (6_{con}) or presence (7_{con}) of delay period activity. The final category, having both visual and movement activity, 8_{con} (33/466), showed only modest visual activity and may be more accurately described as a pure movement category. In either case, the movement-related activity peaked just after the saccade but returned slowly to baseline. An additional category, 5_{con} (23/466), was not movement-related *per se*, but exhibited a strong post-saccadic transient with a modest, early visual response.

Categories with response attenuation. Two categories of units showed distinct decreases in firing rate. The first of these, 9_{con} (11/466), was unique in having an "off" response to visual stimulation, but it also showed clipped presaccadic ramping that peaked just before the saccade. This provides a fruitful contrast with the final visuomovement category, 8_{con}, which showed only a modest increase in firing rate but robust, un-clipped perisaccadic ramping. This distinction may be a useful criterion in future studies examining the differences in stimulus-driven or goal-directed saccades. The second category with an off response, 10_{con} (31/466), showed little or no visual modulation, but was sharply inhibited around the time of the saccade, characteristic of fixation neurons.

Relation to other functional characteristics. To preclude that these categories are accidental and arbitrary, we quantified several other characteristics of each neuron. These included typical measures such as response field size and center location, baseline discharge rate, and maximal response for both the visual and motor periods of modulation. These were supplemented by the following discharge variability metrics: Fano factor, coefficient of variation (CV), local coefficient of variation (CV_2), local

variation (LV), and revised local variation accounting for a 5 ms refractory period (LVR). Finally, spike width was also measured.

First, omnibus Kruskal-Wallis tests were performed for each of these factors. Factors with significant differences include visual response field width ($\chi^2(9,274) = 18.300$; $p = 0.032$), maximum visual response ($\chi^2(9,267) = 20.881$; $p = 0.013$), and baseline firing rate ($\chi^2(9,401) = 28.600$; $p = 0.001$).

Second, to take a more targeted approach, categories 1_{con} and 2_{con} were considered visual; categories 3_{con}, 4_{con}, 6_{con}, and 7_{con} were considered visuomovement; and categories 8_{con} and 9_{con} were considered movement-related. The analyses were repeated separately for these sets of consensus categories. Among the visual categories, receptive field width was significantly larger for category 2_{con} ($60.6^o \pm 31$) than for category 1_{con} ($52.4^o \pm 34.8$) ($\chi^2(1,136) = 4.568$; $p = 0.033$). For movement-related categories, category 8_{con} had a significantly wider spikes (266.0 μs ± 122.5) than category 9_{con} (173.6 μs ± 67.2) ($\chi^2(1,42) = 5.625$; $p = 0.018$). No significant differences or trends were identified among the visuomotor categories. Thus, these consensus clusters identify differences in neuron types, even when the factors for which differences were identified were not included as parameters for clustering.

2.3.6 Cross-validation Analysis

Clustering analyses can be problematic because the algorithms involved will yield as many categories as are requested from any data sample, regardless of the underlying category structure. The use of a minimum membership criterion and a maximum uncategorized percentage criterion aim to mitigate this, but the contribution of these criteria to eliminating the problem of over-splitting the categories cannot be

directly quantified. Instead, to quantitatively assess the quality of the categorization, a classification analysis was used. This analysis uses a leave-one-out cross-validation approach in which a classifier is trained on the consensus category membership of all recorded units except one, then assigns that remaining unit to one of the consensus categories. To prevent under-specifying the classifier, principal components of the composite consensus matrix were used (see Methods). Classification accuracy is assessed by the percentage of units that, when left out of the training set, are assigned to the same category as that specified by the full consensus clustering algorithm.

Peak accuracy was 86.7%, which was achieved when the

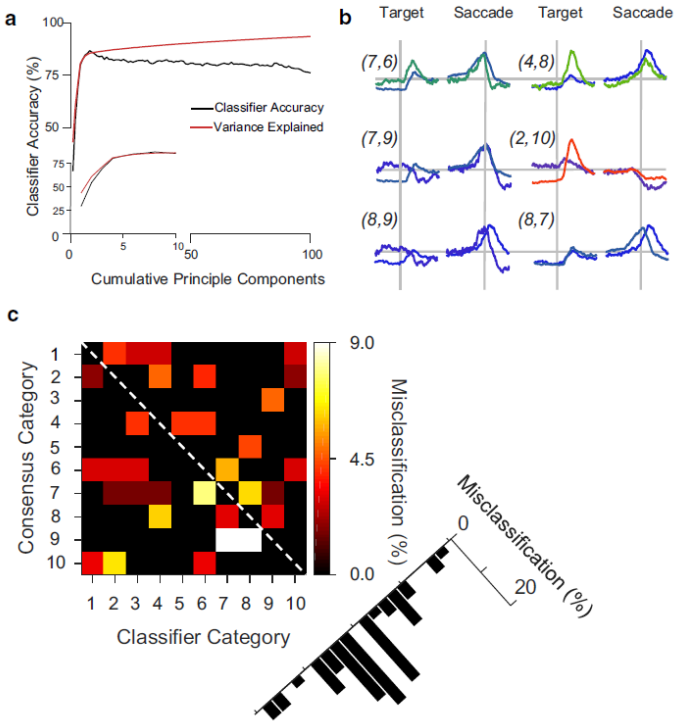

Figure 2.8. Cross-validation analysis. Leave-one-out cross-validation was performed separately for 1 through 100 principal components of the composite distance matrix. A singular value decomposition classifier (SVD) classifier with a linear kernel was trained on the principal components of all but one neuron, and that remaining neuron was categorized. ***a***, Classifier accuracy as a function of cumulative principal components, plotted up to 100 principal components (main plot) and for first 10 (inset). Peak accuracy (86.7%; chance accuracy was 10%) was achieved using eight principal components, which corresponds to a plateau of variance explained by additional components. ***b***, Superimposed mean SDFs for pairs of categories that were most frequently misclassified, labeled as (classifier category, consensus category). Although the category SDFs clearly differ, the source of misclassification is apparent through particular common features between pairs. ***c***, Matrix showing the incidence and nature of misclassifications. Matrix rows distinguish the consensus algorithm categories; numbers correspond to consensus cluster spike density functions. Matrix columns distinguish the classifier categories. If the classifier were perfectly accurate, then the matrix would be entirely black, indicating no misclassification. The black cells along the unity diagonal (classifier column C _ consensus category row R, indicated by dashed line) are the 86.7% of neurons for which the classifier correctly identified the consensus algorithm category; they are not misclassified. Black cells off of the unity diagonal (C _ R) indicate that the classifier did not misclassify neurons in row R as belonging to column C. Colored cells off of the unity diagonal indicate that the classifier misclassified neurons in row R as belonging to column C. The color map shows percentages of misclassified neurons relative to the count of consensus category R. Misclassified neurons can be identified, for example, as an adjacent category (C_ R _ 1) or two categories away (C _ R _ 2). The percentage of total misclassifications that were assigned to C _ R _ *n* are shown to the lower right. Misclassifications are most common for adjacent categories (C _ R _ 1) and are generally progressively less common with greater category separation.

classifier was trained with eight principal components after which cumulative variance explained remained on a plateau (Fig. 2.8a). The units misclassified by the classifier were identified. The percentage of units from each consensus category (Fig. 2.8b) misclassified in each classifier category is depicted as a matrix of consensus categories rows and classifier prediction columns (Fig. 2.8c). Generally, mis-classified units were found in adjacent categories, with misclassifications becoming less frequent as the categories become further apart. Given the purposeful ordering of these units on a visual-motor spectrum, this is not surprising. The highest percentage of mis-classified units (9.1%) was in category 9_{con}, which also has the fewest members according to the consensus clustering algorithm.

Category pairs with frequent misclassifications are superimposed in Fig. 2.8e. Categories 6_{con} and 7_{con} both show robust movement activity and similar visual activity. Categories 7_{con} and 8_{con} both have weak visual activity as well as robust movement activity, although with different timing. Categories 4_{con} and 8_{con} have nearly identical late-peaking movement activity. Categories 7_{con} and 9_{con} also have highly similar movement-related activity. Categories 8_{con} and 9_{con} are the two categories of nearly pure movement activity. Finally, categories 2_{con} and 10_{con} both have suppressed responses at the time of saccade. Overall, though there are differences between these pairs of categories, there are features that explain why misclassifications could be made between these pairs.

To confirm that the peak classification accuracy was indeed greater than the nominal chance value of 10%, the above procedure was used with the category assignments randomly shuffled. For these shuffled assignments, the first eight principal

components were used to train the classifier because this corresponds to the peak in classifier accuracy. Including additional components decreases accuracy, most likely due to over-fitting. Shuffling was performed 1000 times. No randomized classification accuracy exceeded the empirical classification accuracy (mean = 8.2%, SD = 3.7%, range = 1.0% - 21.6%). This indicates that the consensus clustering algorithm categorizes neurons in a highly internally-consistent manner. The robust re-classification of the original set also allows for new data to be categorized according to the present consensus categories.

2.4 DISCUSSION

We applied a consensus clustering technique and identified ten robust functional categories in FEF based on modulation of discharge rates alone. This categorization includes but exceeds the traditional categories. We will discuss the relationship of the new functional categories to the traditional categorization and possible functional and anatomical implications of these consensus clusters. We will conclude by considering the limitations and extensions of these consensus clustering techniques.

2.4.1 Correspondence with Traditional Functional Categories

To compare the traditional and this new categorization, we assessed their overlap by calculating the proportion of consensus clusters identified as visual, movement, visuomovement, or unclassified. The traditional scheme and our new consensus clustering procedure show significant overlap (Fig. 2.9; *ARI* = 0.0931, $p < 0.001$). Thus, our procedure complements the traditional categorization. In fact, although not sought specifically, both post-saccadic and fixation neurons were identified

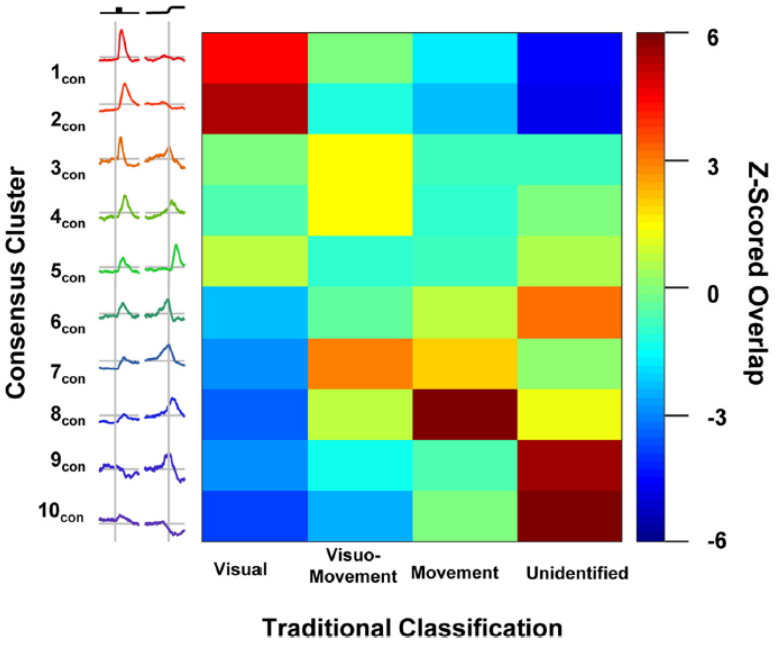

Figure 2.9. Relation to traditional classification. The consensus cluster assignments were compared with traditional classifications. The consensus clusters are depicted on the vertical axis, and traditional classification is depicted on the horizontal axis. The color in the heat map indicates the prevalence of neurons being classified in a given combination. For a given cell in the matrix, a warm color indicates that more neurons were assigned to both that consensus cluster and that traditional classification than expected by chance, green indicates that the expected number of neurons were assigned to both categories, and a cool color indicates that fewer than expected neurons were assigned to both categories. Cluster 1_{con} and 2_{con} neurons were more often identified as visual cells and were rarely uncategorized. Cluster 3_{con}, 4_{con}, and 7_{con} neurons were often identified as visuomovement cells. Cluster 8_{con} neurons were more often identified as movement cells and not visual cells. Cluster 9_{con} and 10_{con} neurons were generally not categorized, but when they were they were not classified as visual cells.

via consensus clustering. This unsupervised discovery increases confidence that consensus clustering identifies natural neural categories.

We now compare the proportions of different categories to previous surveys. Bruce and Goldberg (1985) identified 40% of their sample as visually related, 40% visuomovement, and 20% movement only, not including post-saccadic and fixation neurons. Post-saccadic and fixation neurons account for 17% and 7% of their total sample, respectively. Schall (1991) identified 17% of the sample as visual, 41% as visuomovement, 22% movement, and 13% post-saccadic. When using the traditional categorization, 45% of the current sample were visual, 16% were visuomovement, and only 3% were movement. This proportion of visual neurons with respect to the whole sample is consistent with Bruce and Goldberg (1985) but not with Schall (1991). The proportions of neurons are more similar to earlier descriptions when consensus categories are considered with 38% visual, 31% visuomovement, 9% movement, 7% fixation, and 5% post-saccadic. Still, visuomovement, movement, and post-saccadic

neurons are still underrepresented in the current relative to previous studies. This under-representation of movement-related neurons seems curious, for these are thought to be large pyramidal neurons in layer 5 (Fries, 1984; Segraves & Goldberg, 1987; Sommer & Wurtz, 2000), which should be easier to isolate. Similarly, fixation neurons are also layer 5 pyramidal cells (Izawa & Suzuki, 2014), but are instead found in the same proportion as Bruce and Goldberg (1985). Perhaps the linear electrode array failed to sample layer 5 neurons. Future reconstructions of the recording sites will determine whether laminar differences can explain the differences in proportions of neurons.

Another possible explanation for differences in category proportions concerns the nature of the electrodes. The neural spiking analyzed for this study was obtained with linear electrode arrays (Plexon U-probe and Neuronexus vector probe). The studies cited above sampled neurons with a variety of sharp electrodes including glass-coated platinum-iridium and tungsten. The differential sampling characteristics of various electrodes in FEF requires further investigation.

A third possibility involves the eccentricity represented by the neuron samples across studies. The central visual field is represented laterally and peripheral field medially in FEF and rostrally adjacent cortex (Suzuki & Azuma, 1983), and RF size increases with eccentricity (Mayo et al., 2015). Lateral and medial FEF have qualitatively and quantitatively different patterns of connectivity (Babapoor-Farrokhran et al., 2013; Markov et al., 2014; Schall et al., 1995b). Convergence from the dorsal and ventral processing streams occurs in lateral but not in medial FEF. Lateral FEF, which is responsible for generating short saccades, receives visual afferents from the foveal

representation in retinotopically organized areas, from areas that represent central vision in inferotemporal cortex and from other areas having no retinotopic order. In contrast, medial FEF, which is responsible for generating longer saccades, is innervated by the peripheral representation of retinotopically organized areas, from areas that emphasize peripheral vision or are multimodal and from other areas that have no retinotopic order or are auditory. Hence, neural spiking samples from lateral and medial FEF are likely to differ in a variety of as yet uncertain ways. Here, all stimuli were placed at 8º eccentricity, whereas Bruce and Goldberg (1985) tested locations ranging from 5º and 45º, and Schall (1991) used 15º horizontal and 8º vertical. Systematic mapping across eccentricities is needed to resolve this question.

A fourth possibility involves the nature of tasks and reward contingencies. As noted above, the particular memory-guided saccade task used here is not identical to tasks used in previous studies. Factors like stimulus luminance, chromaticity and contrast will need to be explored systematically (Krock & Moore, 2016). Moreover, FEF neurons are sensitive to reward contingency (Roesch & Olson, 2003) and other cognitive processes (Ferrera et al., 2009; Middlebrooks & Sommer, 2012; Teichert et al., 2014).

Functional differences can arise from structural differences in connectivity (Markov et al., 2014; Schall et al., 1995b), in morphology (e.g., Lund & Lewis, 1993), and in biophysical properties (e.g., Casale et al., 2015; Connors & Gutnick, 1990; Krimer et al., 2005; McCormick et al., 1985; Rocco et al., 2016; Vigneswaran et al., 2011), although the relative contributions of these factors are unknown in FEF. Indeed, using a related consensus clustering approach on physiological measures from monkey

prefrontal cortex, Ardid et al. (2015) reported four broad spiking, putative pyramidal cell classes and three narrow spiking, putative inhibitory cell classes, which were distinguished by sparse, bursting, or regular spike trains. Using a related agglomerative clustering approach, Zaitsev et al. (2012) also reported four classes of neurons visually identified as pyramidal cells *in vitro* that were also distinguished by sparse, bursting, or regular spike trains. These authors also identified three classes of inhibitory interneurons identified morphologically *in vitro* that were distinguished by firing rate variability measures, and these classes were each associated with calcium binding proteins parvalbumin, calbindin, or calretinin.

In this sample we found no significant differences in measures of firing rate variability across the consensus categories. However, spike width differed between the two movement-related categories, indicating some differences in biophysical characteristics. Curiously, spike width did not differ between consensus clusters identified as visual, movement-related, and visuomovement, which is at odds with previous studies (e.g., Cohen et al., 2009d; Ding & Gold, 2012; Thiele et al., 2016). Further investigation is necessary to determine the reason for this difference. To that end, the consensus clustering method can be extended to incorporate biophysical characteristics such as spike polarity and phase (Gold et al., 2009), spike width (Cohen et al., 2009d; Vigneswaran et al., 2011), spike timing patterns (Cohen et al., 2009b; Holt et al., 1996; Nawrot et al., 2008; Shinomoto et al., 2009), and Fano factor (Purcell, Heitz, et al., 2012b).

2.4.2 Possible Functional Implications

Most of the consensus categories where characterized by pronounced peri-saccadic activity. Many such neurons also had pronounced visual responses (3_{con}, 4_{con}, 5_{con}, 6_{con}, 7_{con}) and will be discussed below. Categories 8_{con} and 9_{con} were distinguished by (a) weaker modulation of opposite signs after the target appeared, (b) time of peak saccade-related activity, (c) duration of activity after the saccade, and (d) spike width. Both patterns of modulation have been reported previously in FEF (e.g., Bruce & Goldberg, 1985; Everling & Munoz, 2000; Hanes & Schall, 1996; Lawrence et al., 2005; Sommer & Wurtz, 2000). The peak activity of category 9_{con} neurons coincides with saccade initiation, and discharge rate is reset by saccade termination. Such clipped neurons have been reported in FEF by one study (Hanes et al., 1995) but not another (Segraves & Park, 1993). Clipped movement neurons have been associated with saccade dynamics in superior colliculus (Waitzman et al., 1991). Confirming the presence of clipped movement neurons in FEF would substantiate the hypothesis that FEF contributes to the dynamics of saccade production (e.g., Dias & Segraves, 1999; Peel et al., 2014; Schiller et al., 1987). The activity of category 8_{con} has a more sluggish relationship to saccade timing, peaking after the saccade and resetting well after saccade termination. These properties are inconsistent with a direct role in saccade production. Further investigation with other task conditions is necessary. For example, another approach to determining whether individual neurons are involved in controlling saccade initiation involves testing with the saccade countermanding task (Hanes et al., 1998; cf. Costello et al., 2013; Murthy et al., 2009). Alternatively, distinct functions may be revealed when planning of saccade sequences (Phillips & Segraves, 2010).

Relative to category 8_{con}, category 9_{con} neurons had significantly narrower spike widths. This does not entail, necessarily, that 9_{con} neurons are inhibitory interneurons. In primary motor cortex some identified corticospinal pyramidal neurons have narrow spike widths (Vigneswaran et al., 2011), presumably because these neurons have a fast potassium channel Kv3.1b subunit (Ichinohe et al., 2004). If corticotectal and corticopontine neurons are analogous to corticospinal, then spike width may be misleading in identification of projection neurons. However, whether layer 5 neurons in FEF stain positively for fast potassium channels is unknown.

The analysis also identified a consensus cluster with characteristics of fixation neurons (10_{con}). These neurons seem involved in the active maintenance of fixation and may release inhibition on presaccadic movement neurons to produce saccades (Hanes et al., 1998; Segraves & Goldberg, 1987). The cluster exhibited a modest visual response. If these neurons do indeed inhibit presaccadic movement neurons, then this could be the origin of the brief reduction of discharge rate characteristic of the movement neuron consensus cluster 9_{con}. Greater diversity of this category may be found if tested with pursuit eye movements (Izawa & Suzuki, 2014).

Most of the consensus categories where characterized by pronounced visual responses. This is consistent with previous descriptions of FEF neural properties (e.g., Bruce & Goldberg, 1985; Mohler et al., 1973; Schall, 1991). Two consensus clusters were distinguished by strong visual responses and no modulation associated with saccades (1_{con} and 2_{con}). Category 1_{con} had an earlier peak response and no delay activity whereas category 2_{con} had a later peak response and clear activity during the memory delay. The receptive fields of Category 1_{con} were narrower than those of

category 2_{con}. Diversity of FEF visual responses along multiple dimensions is well known in the early visual pathway. For example, the well-known distinction of transient and phasic visual responses (Cleland et al., 1971) is evident in FEF (e.g., Sato et al., 2001). Diversity of visual responses likely arises principally from diversity of connectivity. As noted above, FEF is reciprocally connected with an unusually large number of extrastriate visual cortical areas, and pronounced differences in connectivity distinguish medial and lateral FEF (Babapoor-Farrokhran et al., 2013; Markov et al., 2014; Schall et al., 1995b). Subcortical afferents can also influence visual responses; neurons in FEF that are activated orthodromically by SC stimulation have visual and saccade-related responses (Sommer & Wurtz, 1998). The extent to which visual response properties vary with cortical and subcortical connectivity is unresolved. The diversity of visual responses in FEF also relates to the variety of cortical areas in which FEF axons terminate. For example, V4 is influenced by visual neurons in L2/3 of FEF (Gregoriou et al., 2012; Noudoost & Moore, 2011; Pouget et al., 2009). However, FEF neurons projecting to V4 receive input from area 46, whereas the FEF neurons projecting to MT receive input from area 46 plus SEF (Ninomiya et al., 2012). Thus, intracortical projections from FEF convey different signals. How much such signals vary across cortical targets of FEF efferents is unknown.

Most of the categories with visual responses were also characterized by modulation associated with saccade production. These are typically referred to as visuomovement neurons. While these data support no conclusions about the unique functional contributions of the four visuomovement categories, several characteristics warrant discussion. First, categories 3_{con} and 4_{con} have noticeably stronger visual

responses than categories 6_{con} and 7_{con}. Perhaps categories 3_{con} and 4_{con} occupy an earlier position in the visuomotor transformation. The saccade-related activity of these two categories is similar, so they may contribute equally to the production of saccades. However, the timing of the peak visual responses differs in a manner similar to categories 1_{con} and 2_{con}. The earlier peak activity of category 3_{con} is consistent with receiving magnocellular pathway inputs, perhaps via category 1_{con} neurons. Meanwhile, the later peak activity of category 4_{con} is consistent with receiving parvocellular pathway inputs directly or via category 2_{con} neurons.

Categories 6_{con} and 7_{con} have similar visual responses but are distinguished by the magnitude of delay activity and the return to baseline following saccade. Category 6_{con} activity returns to baseline quickly after the saccade, indicating that this category may be more intimately involved in saccade dynamics than category 7_{con}. This is consistent with the higher delay activity in category 7_{con}, which may indicate that category 7_{con} is primarily involved in maintaining the stimulus location in working memory and therefore occupies an executive role as opposed to a direct role in saccade production. Of course, the lack of corroborating differences in other factors including tuning characteristics, spike timing, and spike widths may indicate that these categories are an excessive parsing of one continuum or that the measures are insensitive, but additional work is warranted to determine whether this is the case. For example, during visual search tasks, all visually responsive neurons respond equivalently to a target or a distractor in the receptive field (e.g., Schall et al. 1995). Visual neurons with transient responses do not contribute to selection of the target from distractors, but visually responsive neurons with prolonged activity do select the target

of a search array when saccades are accurate (14% transient and 86% sustained; Thompson et al. 1996). When arbitrary stimulus-response mapping is required after visual search, many visually responsive neurons select the attended stimuli, while other select only the endpoint of the saccade (Sato & Schall, 2003). Further research is needed with this task and these categorization methods to determine how this previously observed distinction maps onto these new functional categories. When monkeys perform visual search for a target among distractors of fixed features, approximately 50% of visually responsive neurons in FEF exhibit feature selective from the initial response (Bichot et al., 1996). The same distinction may also explain feature-based attention differences identified in FEF neurons in other studies (e.g., Bichot & Schall, 2002; Gregoriou et al., 2009; Zhou & Desimone, 2011). Other distinctions among FEF neuron categories have been described in perceptual choice (Ding & Gold, 2012). Finally, the relationship of the dynamics of visuomovement and movement neurons to saccade initiation can be distinguished using the saccade countermanding task (Ray et al., 2009).

Further insight may be gained by testing how the different categories contribute to eye-head coordination and visual-motor reference frame updating (Sajad et al., 2015, 2016). FEF neurons have also been implicated in remapping and transsaccadic stability (Crapse & Sommer, 2008, 2012; Shin & Sommer, 2012; Umeno & Goldberg, 1997). These operations require information about the just-executed saccade. A single consensus cluster of post-saccadic neurons was identified (5_{con}). These neurons also had visual responses. Previous research has suggested that this type of neuron can support remapping and trans-saccadic stability by signaling the vector of the saccade

that was just executed (Goldberg & Bruce, 1990). To produce sequences of saccades without visual guidance, the vector of the most recent saccade would be subtracted from the vector from the initial fixation point to the location of the second stimulus to account for the location of the second stimulus relative to the new fixation point rather than the point from which the location was initially encoded.

Antidromic stimulation studies agree that movement and fixation neurons project to the SC and brainstem but they disagree about the projection of visual and visuo-movement neurons (Segraves & Goldberg, 1987; Sommer & Wurtz, 2000). Perhaps the disagreement may be resolved by considering more refined categories of neurons. For example, perhaps only visuomovement neurons belonging to categories 6_{con} or 7_{con} with modest visual response, relative to categories 3_{con} and 4_{con}, project from FEF to SC.

2.4.3 Limitations and Extensions of Clustering Procedures

Each of the individual clustering procedures is limited by the distance measure used to calculate pairwise similarity, by the measurement of the responses, and by the quality of the discharge rate samples. Different distance measures emphasize different aspects of the variability across units. Whereas Euclidean distance emphasizes similarity in absolute discharge rates, correlation distance emphasizes similarity in the pattern of modulation of discharge rates. Different measurements of the variation of discharge rate emphasize different aspects of the variability across units. Measuring the mean firing rate in different epochs captures absolute discharge rates but ignores dynamics. Measuring the slopes of the SDF in different epochs ignores absolute discharge rates. However, measuring both the means and slopes across many epochs

or, indeed, using the SDF from the entire trial can expose the clustering algorithm to excessive incidental variation.

Different approaches to scaling the SDF across units emphasize different aspects of the variability across units. As shown in Figs. 2.3-2.5, different methods of scaling the SDF across units can result in category means that do not accurately represent the individuals comprising those categories. Naturally, different scaling procedures emphasize useful information about the units. For example, z-scoring the SDF based on the pre-stimulus baseline activity emphasizes the magnitude of modulation relative to the variation in the baseline. On the other hand, z-scoring the SDF based on the entire trial reduces the skewed variation of discharge rates. Analytical choices must be made, so confidence in the outcome of every particular clustering pipeline can be questioned.

Consensus clustering increases confidence in distinctions identified across measurements and clustering procedures by minimizing spurious classifications arising from incidental analysis choices or unreliable data. Moreover, the consensus clustering approach affords the opportunity to include as many other measures and clustering procedures as desired. In particular, biophysical spiking properties are certainly useful for categorizing neurons. The eventual inclusion of such features will surely add complexity but should certainly approach an accurate account of the true diversity of functional neuron categories in FEF. A correct account of such diversity is necessary to support the next generation of microcircuit models (Brown et al., 2004; Hamker, 2006; Heinzle et al., 2007; Mitchell & Zipser, 2003).

CHAPTER 3: CONTRIBUTIONS OF PREFRONTAL AND PREMOTOR CORTEX TO VISUALLY GUIDED SACCADES

3.1 INTRODUCTION

For more than a century, an area known as the frontal eye field (FEF) has been identified with the guidance and control of eye movements (reviewed by Schall 2015; Schall et al. 2017). Although much is known about the properties of FEF neurons and connectivity with cortical and subcortical structures, the boundaries of FEF and functional transitions with neighboring areas are uncertain. FEF has been defined as the subregion of granular area 8 in which low-current microstimulation elicits saccades (Bruce et al., 1985; Huerta et al., 1987; Robinson & Fuchs, 1969; Stanton et al., 1988). Confusion about the caudal boundary of FEF arises based on reports that microstimulation of a region caudal to the arcuate sulcus corresponding cytoarchitectonically to agranular area 6 and structurally to premotor cortex (F2 of Luppino et al. 2003) also elicits saccadic eye movements (Fujii et al., 2000; Neromyliotis & Moschovakis, 2017a) and is interconnected with SEF (Huerta & Kaas, 1990). Though premotor cortex is traditionally considered to be involved in guidance of limb movements (Cisek & Kalaska, 2005; Kalaska et al., 1998; Kalaska et al., 1997; Neromyliotis & Moschovakis, 2018; Neromyliotis & Moschovakis, 2017b; Thura & Cisek, 2014; Wise, 1985; Wise et al., 1992; Wise et al., 1996), the rostral premotor region also shows fMRI activation in saccade tasks (Baker et al., 2006; Koyama et al., 2004) and gaze modulation of reach signals (Boussaoud, 1995; Boussaoud et al., 1993a; Boussaoud et al., 1998; Cisek & Kalaska, 2002; Mushiake et al., 1997). Single-unit recordings in the rostroventral premotor region (F5) have identified neurons with motor

responses in both manual and oculomotor tasks (Neromyliotis & Moschovakis, 2018), including some neurons modulated regardless of the effector (Neromyliotis & Moschovakis, 2017b).

Based on these motor characteristics, this postarcuate region has been referred to as a premotor eye field (Amiez & Petrides, 2009; Neromyliotis & Moschovakis, 2017b, 2018). However, whether this cortical region contributes to more complex tasks and whether it should be considered as a caudal extension of FEF is undecided. Thus, we compared and contrasted single neuron discharges sampled in both banks of the arcuate sulcus during a memory-guided saccade task and a shape singleton search task. Specifically, because of suggested anatomical and physiological distinctions between dorsal and ventral premotor (F2 and F5; see Hoshi & Tanji, 2007 for review) and a distinction within dorsal premotor cortex where cognitive functions are represented more rostrally and motor functions more caudally (Abe & Hanakawa, 2009; Nakayama et al., 2016), we targeted the rostroventral portion of the dorsal premotor cortex (F2vr) in the caudal bank. We found the proportions of response modulation types differed between these two regions, but among similar neurons there were

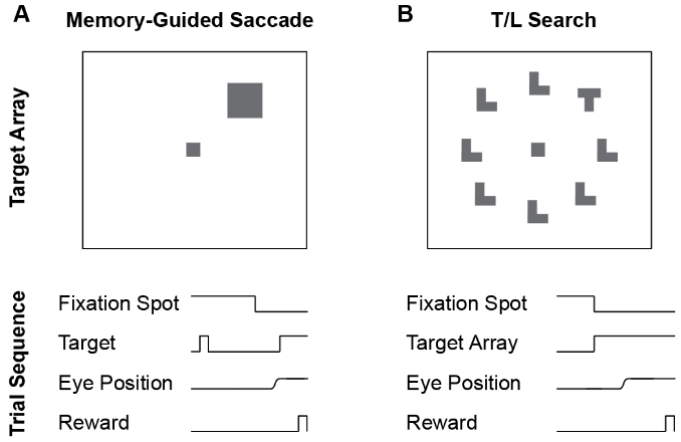

Figure 3.1. Task diagrams. (A) Memory-guided saccade task. The task begins with a fixation spot on. After a 500 ms fixation period, a single square target is briefly presented in the periphery. After the target disappeared, the monkey maintains fixation on the fixation spot for a variable delay period of 300 to 800 ms. After this delay, the fixation spot disappears and the monkey makes a saccade to the cued location. When the saccade is made to the correct location, the target is reappears to provide feeedback for thecorrect location for fixation. If the target is successfully fixated for 500 ms, reward is delivered. (B) Shape singleton search task. An example search array (top) is shown with a singleton T among seven distractor Ls. Trial sequence (below) indicates key trial events. The trial begins when a fixation spot is shown. After a delay, the fixation spot disappears and a search array is shown. A saccade is made to the shape singleton and fixation is maintained on it. If the target is successfully fixated for 200 ms, reward is delivered.

no consistent, identifiable differences between other properties. A preliminary analysis of some of these data have been presented previously in abstract form (Zinke et al., 2015).

3.2 METHODS

3.2.1 Subjects

Data were collected from three male macaque monkeys (*M. radiata*) weighing approximately 8.0 kg and ranging in age from 7-9 years. All procedures were in accordance with the National Institutes of Health Guide for the Care and Use of Laboratory Animals and approved by the Vanderbilt Institutional Animal Care and Use Committee.

3.2.2 Behavioral Task

Monkeys performed two tasks in this study. One task was a memory-guided saccade task (Fig. 3.1A). The details of this task have been described previously (Lowe & Schall, 2018). Briefly, after fixating a central point for a period of 500 ms a peripheral target stimulus was presented for 16.7 ms while the monkey maintained fixation. After a variable delay period (range 300 to 800 ms), the fixation point disappeared and the monkey was rewarded for making a saccade to and maintaining fixation on the cued location. To provide a fixation stimulus, the peripheral target was reilluminated when the monkey attained fixation on the remembered location. A juice reward was delivered if the monkey successfully fixated on the remembered location for 500 ms. The trial was aborted and a 2000 ms timeout was delivered if the monkey broke central fixation

prematurely, made a saccade to an incorrect location, or broke fixation on the peripheral target after an initially correct saccade.

The second task monkeys performed was a shape-singleton visual search task that has been described previously (Cosman et al., 2018). In short, monkeys were presented an array of eight stimuli comprising either gray Ts or Ls (Fig. 3.1B). Within one session these stimuli were presented with one of four possible orientations. One stimulus was a shape singleton; one T could be presented among seven Ls or one L among seven Ts. After a variable fixation period of 300 to 800 ms, the stimulus array was presented and the monkey was required to make a saccade to the singleton shape. A juice reward was delivered if the monkey successfully fixated the target for 200 ms. Trials were aborted if the monkey broke fixation prematurely, made a saccade to an incorrect stimulus, or broke fixation from the target prematurely after an initially correct saccade. On a subset of trials a color singleton distractor was presented within the array; one of the distractors was chromatic. Results with trials using a salient distractor were reported elsewhere (Cosman et al. 2018); these trials were excluded from the present analysis.

3.2.3 Recording Techniques

MRI compatible headposts were placed alongside recording chambers over the arcuate sulcus. Surgery was conducted under aseptic conditions with animals under isoflurane anesthesia. Antibiotics and analgesics were administered postoperatively. Details have been described previously (Schall et al., 1995a; Sato et al., 2001; Cohen et al., 2009b). Data were streamed to a data acquisition system: MNAP (40 kHz, Plexon, Dallas, TX - monkeys Da, Ga, and He) or a TDT System 3 (25 kHz, Tucker Davis

Technologies – monkey Da). Eye position was collected using EyeLink 1000 (SR Research). Eye position was calibrated daily and streamed to the data acquisition system and stored at 1 kHz. Electrophysiological data was obtained from linear electrode arrays, either a 24-channel Plexon Uprobe (monkeys Ga, He) or a 32-channel Neuronexus Vector Array (monkey Da). Both probes had a 150 µm recording contact spacing. Single units were identified online using a window discriminator (Plexon) or principal component analysis (TDT). Units recorded from the TDT system were sorted offline using Kilosort (Pachitariu et al., 2016).

FEF was localized using anatomical MRI reconstructions with a chamber grid (Crist instruments) projected onto the reconstructions. We identified grid locations whose trajectory pass through the rostral bank anterior to the genu of the arcuate sulcus, the anatomical location of the functionally defined FEF (Stanton et al., 1988). Neural responses were typical of FEF neurons and microstimulation with low currents (<50 µA) elicited saccades. F2vr was identified in a similar manner, but in grid locations whose trajectory pass through the caudal bank of the arcuate sulcus. For the two animals that expressed a clear spur (Da and Ga), grid locations were chosen with a trajectory passing through the dorsal bank of the spur (F2vr), for the animal without a spur (He), the locations were chosen in the caudal bank opposite to FEF. Microstimulation was not used to elicit saccades in these recording locations. Locations of the recording sites for neurons recorded in each task are projected onto each subject's sulcal pattern in Fig. 3.2.

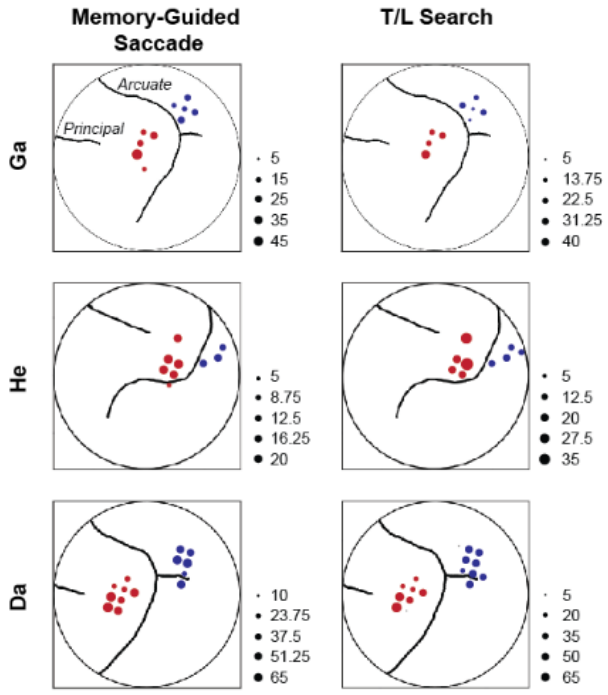

Figure 3.2. Recording sites. Sulcal patterns for each of the three monkeys are illustrated. Principal and arcuate sulci are labeled for Ga in the top left. Patterns are mirrored for monkeys Ga and He such that all three illustrations depict anterior to the left, posterior to the right, medial to the top and lateral to the bottom. Neuron counts for each location are depicted by the size of the circle, with larger circles indicating a larger neuron count. FEF recording locations are red, premotor cortex recording locations are blue. Neuron counts for the memory-guided saccade task are shown on the right and for shape singleton search on the right.

3.2.4 Data Analysis

Spike density functions (SDFs) were calculated by convolving spike trains with a kernel that resembles the postsynaptic potential elicited by an action potential (Thompson et al., 1996). For averaging across neurons, SDFs were normalized by z-scoring across the full trial and performing a baseline subtraction (Lowe & Schall, 2018). That is, the mean and standard deviation used for z-scoring were calculated across the whole trial and an additional subtraction of the pre-stimulus baseline activity was performed. This method of scaling responses reduces the skewness of the SDF across the population and generates a comparable range of activity across neurons without erroneously scaling neurons with little modulation (Lowe & Schall, 2018). Because these measures are not strictly z-scores, they will be referred to as arbitrary units (AU).

Receptive fields (RFs) were defined as the location in which the visual response was greatest for a correct saccade made to that location. For visually responsive neurons this is the visual receptive field whereas for movement-related neurons this is more comparable to a movement field. Target selection times (TST) were determined from the difference of SDFs of trials where the search target was presented within and

trials where the target was presented opposite to the RF. For each neuron, we calculated a z-scored difference function by subtracting the mean pre-stimulus baseline activity (300 ms before the onset of the search array) and dividing by the standard deviation of the pre-stimulus baseline activity. TST was defined as the earlier of two times (1) the time the z-scored difference function exceeds 2 and continues to exceed 6 for at least 20 ms continuously or (2) the time the difference function exceeds 2 standard deviations of the baseline difference for at least 50 ms continuously. Visual latency was calculated in a similar fashion but the SDFs themselves aligned on array onset were required to meet the above criteria. To assess the onset of presaccadic activity, the SDF was smoothed with a 20 ms uniform kernel. Then, starting at the time of the saccade, the correlation of the smoothed SDF across time was calculated in a 100 ms window. This window was moved backward in time until the correlation was no longer significant. The end of the window which produced the first non-significant correlation was taken as the time of presaccadic activity onset. Peak presaccadic activity was defined as the time at which the smoothed SDF reached its highest value. Neurons for which the algorithm identified time of peak presaccadic activity as preceding the presaccadic activity onset by more than 20 ms are excluded from analysis.

For neural classification, the presence or absence of visual activity was determined by the visual latency. If the visual latency was less than 200 ms, the neuron was considered to have visual activity. Similarly, if the neuron had elevated activity at the time of the saccade using an identical algorithm as well as a positive correlation of

response across time in the 20 ms before the saccade, the neuron was considered to have movement-related activity.

Subsequent classification was accomplished using a consensus clustering algorithm (Lowe & Schall, 2018). First, we applied the algorithm to all neurons in the sample regardless of region. For this clustering, we set a minimum cluster size of 20; Lowe & Schall set a minimum cluster size of 10 but applied the algorithm to one area, so we doubled the minimum cluster size to accommodate the second region. Then, we applied the algorithm to each region separately. For this clustering, we kept the minimum cluster size as 10. Importantly, we also included responses to stimuli outside the neurons' RFs. Otherwise, the clustering was identical to Lowe & Schall (2018).

3.3 RESULTS

3.3.1 Neuron Types

To compare neuronal modulation in the two eye fields, neurons were classified according to canonical FEF criteria observed during memory-guided saccades (Bruce & Goldberg, 1985; Schall 1991). Specifically, based on increased activity during the visual, presaccadic, both, or neither period of modulation neurons were classified as visual, movement, visuomovement, and unclassified. The average SDFs of the neurons of each type in each region are shown in Fig. 3.3.

In FEF, 32.2% of neurons were classified as visual, 16.9% as purely movement, 35.0% as visuomovement, and 16.0% were unclassified. In F2vr, 25.4% of neurons were classified as visual, 23.0% as purely movement, 24.2% as visuomovement, and 27.5% were unclassified. These proportions were significantly different (Contingency test $X^2(3) = 21.4$, $p < 0.001$). Relative to FEF, in F2vr fewer neurons had visually related activity and more neurons had exclusively presaccadic activity or were unclassified. This was true for monkey Da ($X^2(3) = 12.9$, $p = 0.005$) and Ga ($X^2(3) = 13.5$, $p = 0.004$), but not He ($X^2(3) = 0.9$, $p = 0.397$).

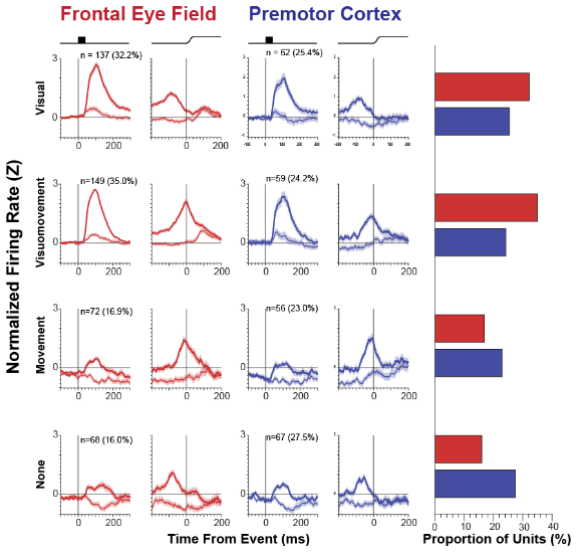

Figure 3.3. Traditional neuron classes. FEF neurons are frequently categorized as visual, visuomovement, or movement neurons. The present sample of neurons from each area was categorized according to these criteria. The mean ± SEM of the normalized SDF aligned on target onset (left) and saccade (right) for the neurons are plotted in red for FEF and blue for premotor cortex. Visual neurons are in the top row, visuomovement neurons in the second row, movement neurons in the third row, and uncategorized neurons in the bottom row. Number of neurons in each category and their proportions are shown. On the right, proportions of each neuron type in each area is shown.

3.3.2 Neuronal Modulation Timing

Given that neurons with visual and presaccadic activity are present in samples from both regions, we measured how visual latency, delay period activity, onset of presaccadic activity, and time of peak presaccadic activity of neurons in each region related to visually guided saccade production. Cumulative distributions of these values are shown in Fig. 3.4. Across regions, latencies of visual responses in the memory-guided saccade task were indistinguishable. In FEF, the median response latency of neurons with visual activity was 51 ms. In F2vr, the median response latency of neurons with visual activity was 55 ms. The distributions of response latencies were not significantly different (Wilcoxon rank-sum $Z = -1.29$, $p = 0.198$).

In contrast, the mean delay period activity in FEF when the singleton was in the RF was 0.01 AU, and that in F2vr was -0.02 AU. The distributions were not significantly different (Wilcoxon rank-sum Z=1.43, p = 0.153). Similarly, the mean delay period activity in FEF when the singleton was not in the RF was -0.18 AU, and that in F2vr was -0.37 AU. The distributions were significantly different (Wilcoxon rank-sum Z=2.12, p = 0.034). Combining these measures, the magnitude of selectivity during the delay period in FEF was 0.29 AU, and in F2vr was 0.37 AU. These distributions were not significantly different (Wilcoxon rank-sum Z= -0.40, p = 0.689).

The median onset of presaccadic activity before saccade onset was 88.5 ms in FEF and 68.0 ms before saccade onset in F2vr. The distributions were significantly different (Wilcoxon rank-sum Z = -5.52, p < 0.001). However, this was only true for one of the monkeys, monkey Ga (Z= -2.22, p = 0.027), but not Da (Z = -1.25, p = 0.213) or He (Z = -0.57, p = 0.571), so this finding should be taken with caution.

The median time when presaccadic activity peaked relative to saccade initiation in FEF was -1.0 ms and in F2vr was -5.0 ms. The distributions were not significantly different (Wilcoxon rank-sum Z = 1.39, p = 0.166).

3.3.3 Modulation During Visual Search

The response modulation of neurons in F2vr during a visual search task that frequently is used to characterize FEF neurons was also assessed and compared to FEF neurons. Monkeys were required saccade towards and fixate a singleton T among Ls or a singleton L among Ts (see Methods). FEF neurons exhibited frequently reported target selection; responses initially did not discriminate target from distractors but eventually became greater when the singleton shape was in the RF and reduced when

a distractor was in the RF (Fig. 3.5a). Surprisingly, a sample of F2vr neurons also exhibited target selection (Fig. 3.5B). However, fewer neurons in F2vr exhibited target selection (n = 135, 51.5%) than in FEF (n = 218, 70.8%). This difference was statistically significant (Contingency test $X^2(1) = 22.3$, $p < 0.001$).

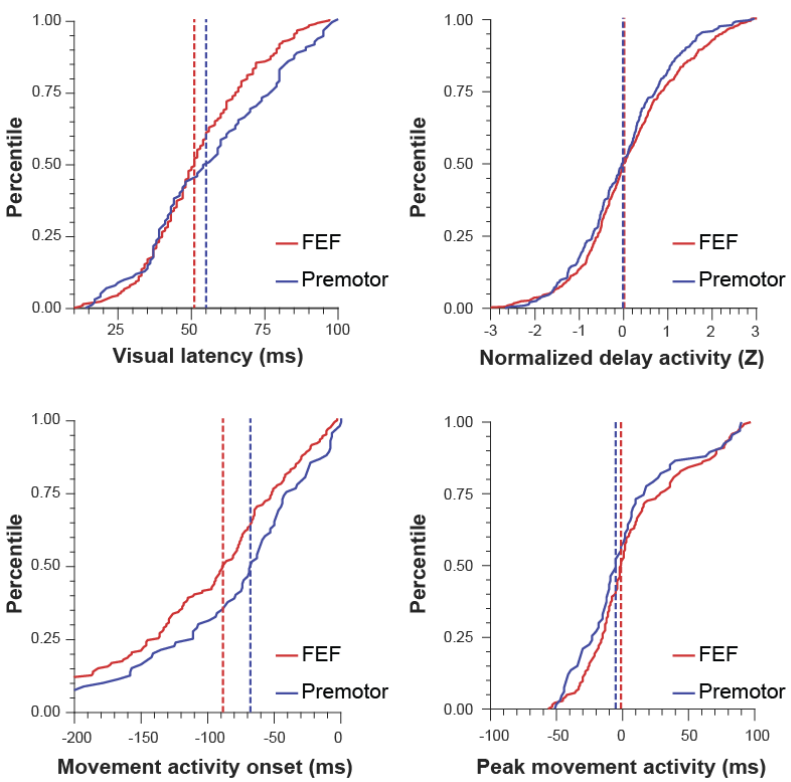

Figure 3.4. Neural characteristics of memory-guided saccades. Cumulative distributions for four metrics of neural activity are shown for FEF (red) and Premotor cortex (blue). (A) Visual latency distributions for both regions. Medians for each measure are shown as vertical lines in the corresponding color, (B) Normalized delay activity distributions when the singleton was in the RF. Conventions as in (A). (C) Movement activity onset. Conventions as in (A). (D) Time of peak movement activity in the bottom right. Conventions as in (A).

Of the neurons that did exhibit target selection, the timing of selection was indistinguishable between the two regions (Fig. 3.5B). The median target selection time in FEF was 155.0 ms (mode = 117.5 ms) and in F2vr was 144.0 ms (mode = 113.5 ms). The distributions were not significantly different Wilcoxon rank-sum Z = 0.35; p = 0.723).

The interpretation of this observation must be qualified by appreciating how the target selection time can vary across sessions in proportion to variation of response times or other factors. Hence, we compared the selection time of neurons recorded simultaneously in FEF and F2vr. The distribution of differences in target selection times in the two regions in these simultaneously recorded sessions are shown in Fig. 3.5C.

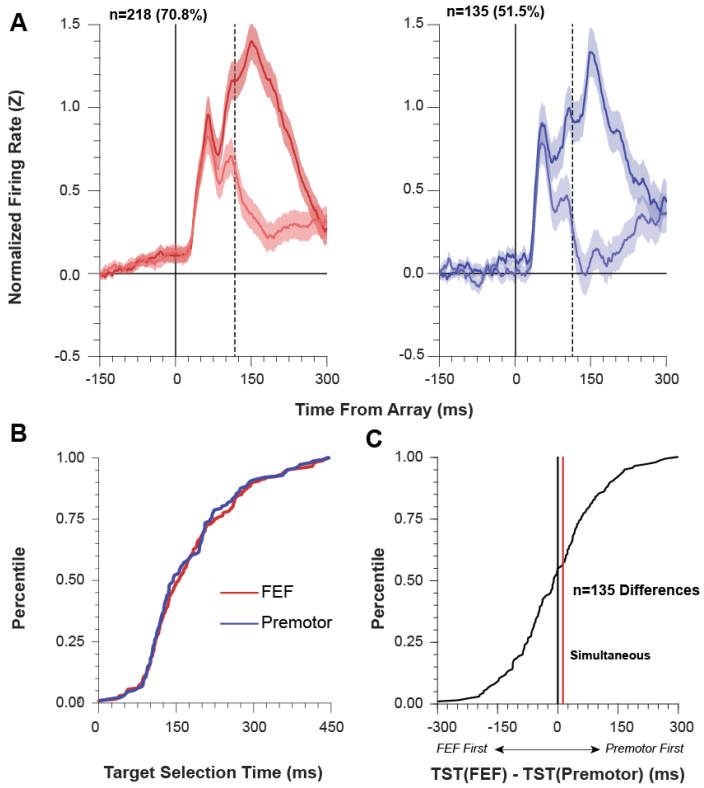

Figure 3.5. Neural responses during search. (A) Mean ± SEM of SDFs of target selective neurons during search in FEF (red, left) and premotor cortex (blue, right). Saturated colors indicate trials with the search target in the RF of the recorded neurons and desaturated colors indicate trials with the search target was outside and a distractor within the RF. Vertical dashed line indicates median TST. Neuron count and proportion of neurons within area are labeled. (B) Cumulative distributions of target selection times in FEF (red) and premotor cortex (blue). Target selection times were effectively identical across areas. (C) Distribution of target selection time differences in simultaneously recorded pairs of neurons in FEF and premotor cortex. By convention, when an FEF neuron precedes a premotor cortex neuron, the difference is negative. The median difference is shown as a vertical red line.

The mean difference in TST between such FEF-F2vr pairs was 10.0 ms (mode = 13.0). This distribution was not significantly different from zero ($t(134) = -0.55$, $p = 0.585$). Thus, target selection in FEF and in F2vr occur simultaneously.

We assessed whether the magnitude of the modulation signaling target selection was similar in the two regions. The average neural response 150 to 200 ms after array presentation was calculated for each neuron when either a target or distractor was in the RF. The modulation index was defined as the difference in the two trial conditions divided by the sum, $(r_{in} – r_{out})/(r_{in} + r_{out})$. The median selection index for FEF neurons was 0.133, whereas the median selection index for F2vr neurons was 0.100. The distributions of the selection indices were not significantly different (Wilcoxon rank-sum $Z = 1.26$; $p = 0.207$).

3.3.4 Consensus Clustering

To characterize and compare more detailed the diversity of neuron types within in FEF and F2vr, we applied a consensus clustering algorithm to the mean SDFs of each neuron (Lowe & Schall, 2018). We extended the algorithm for identifying clusters by including target out of RF conditions in addition to target in RF. In this first application of this method across cortical regions, we will adopt multiple analysis approaches. The first approach will determine clusters of units for both regions together. The second approach will determine clusters of units for each region separately. The first approach demonstrates the similarities of neuron categories across the two regions and assesses the relative proportion of neurons attributed to that category. The second approach will both refine the categories for each region and assess the presence or absence of these clusters in the other. This is done by identifying categories in one region and use a classifier to assign units from the other region to these categories.

Clustering the population.

To identify clusters present across both regions, we first performed the clustering of all units for both regions combined. This method allows the assessment of common neural response profiles across the two regions. To disambiguate results from different tasks, categories are labeled with subscripts for the task used: MG for memory-guided saccade task and VS for shape singleton visual search task. During the memory-guided saccade task, the algorithm identified six categories (Fig. 3.6). Categories 1_{MG} and 2_{MG} demonsrated suppressed responses and are distinguished by the presence (category 1_{MG}) or absence (category 2_{MG}) of a small initial visual transient. Categories 3_{MG}, category 5_{MG}, and category 6_{MG} are characterized by a spatially selective visual

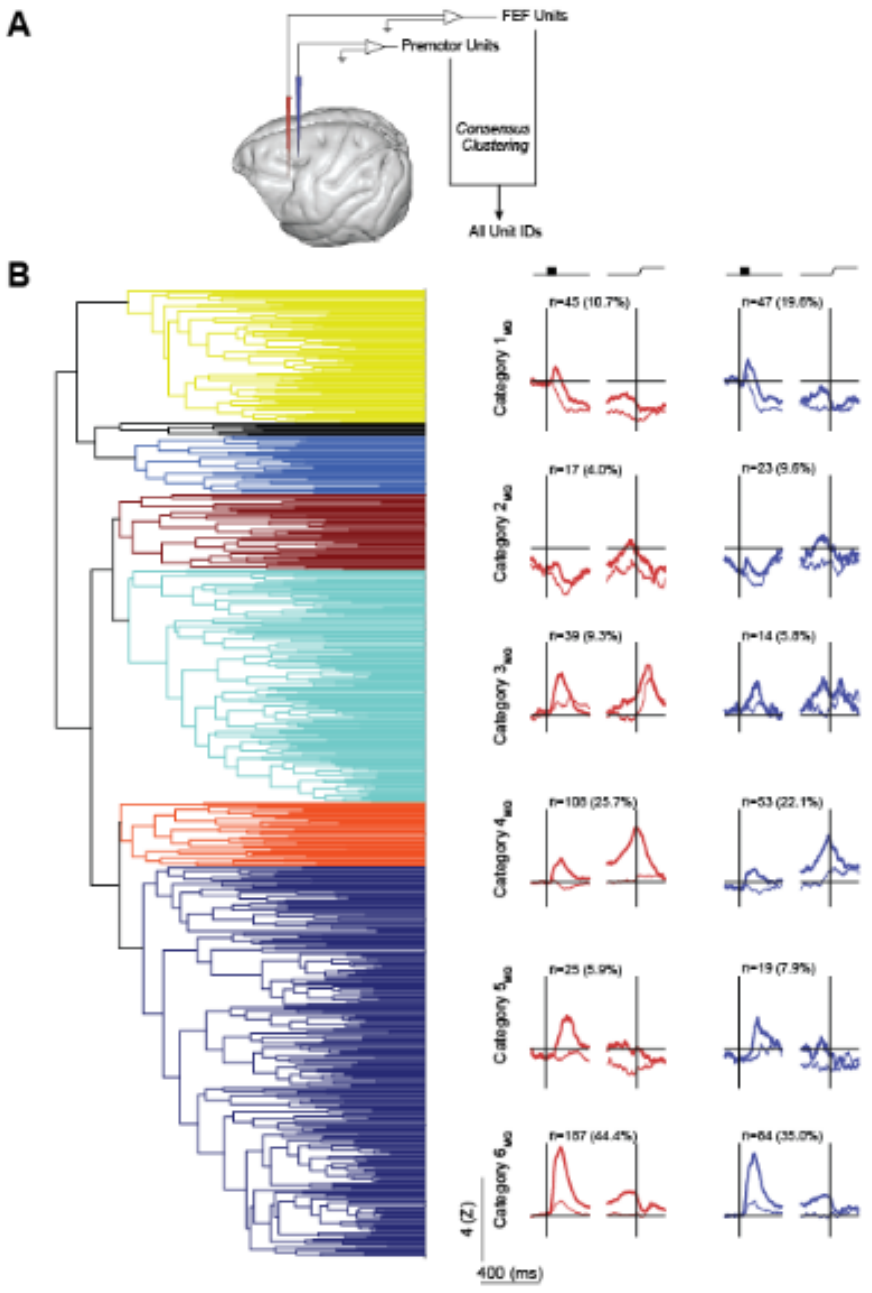

Figure 3.6. Memory-guided consensus clusters. A consensus clustering algorithm was applied to identify different categories of neurons in FEF and premotor cortex during the memory-guided saccade task. (A) Schematic of recording and clustering pipeline. Recordings were performed from both FEF (red electrode) and premotor cortex (blue electrode). Clustering was applied to the sample of neurons across regions. (B) Dendrogram of clustering results is shown on the left. Black lines indicate neurons that were not included in any of the six identified categories. Other colors are arbitrarily assigned by category. Category numbers are assigned from the top of the dendrogram to the bottom. Mean SDFs for target in (thick) and out of (thin lines) RF are shown on the right for FEF (red) and premotor cortex (blue). SDFs are aligned on target onset (left column of each pair) and saccade (right column of each pair). Number and proportion within area are labeled for each category and area combination.

response with no presaccadic activity and are differentiated by whether the response to the non-preferred location decreases below 0 (category 5_{MG}) or not (categories 3_{MG}, 6_{MG}), or whether the response to the preferred location remains above 0 during the delay (category 6_{MG}) or not (categories 3_{MG}, 5_{MG}).

The six categories were distributed unequally across regions (Contingency test $X^2(5) = 23.7$, $p < 0.001$). Post-hoc contingency tests indicate that categories 1_{MG}, 2_{MG},

and 6_{MG}. Categories 1_{MG} and 2_{MG} were more prevalent in F2vr than in FEF, and category 6_{MG} was more prevalent in FEF than in F2vr.

We also performed this analysis for neural responses during shape singleton search and found seven categories of neurons (Fig. 3.7). Two categories, category 1_{VS} and 2_{VS}, were characterized by suppressed responses. They were differentiated by the presence (category 1_{VS}) or absence (category 2_{VS}) of a visually aligned increase in firing rate. Category 3_{VS} was characterized by exclusively presaccadic responses with no visual

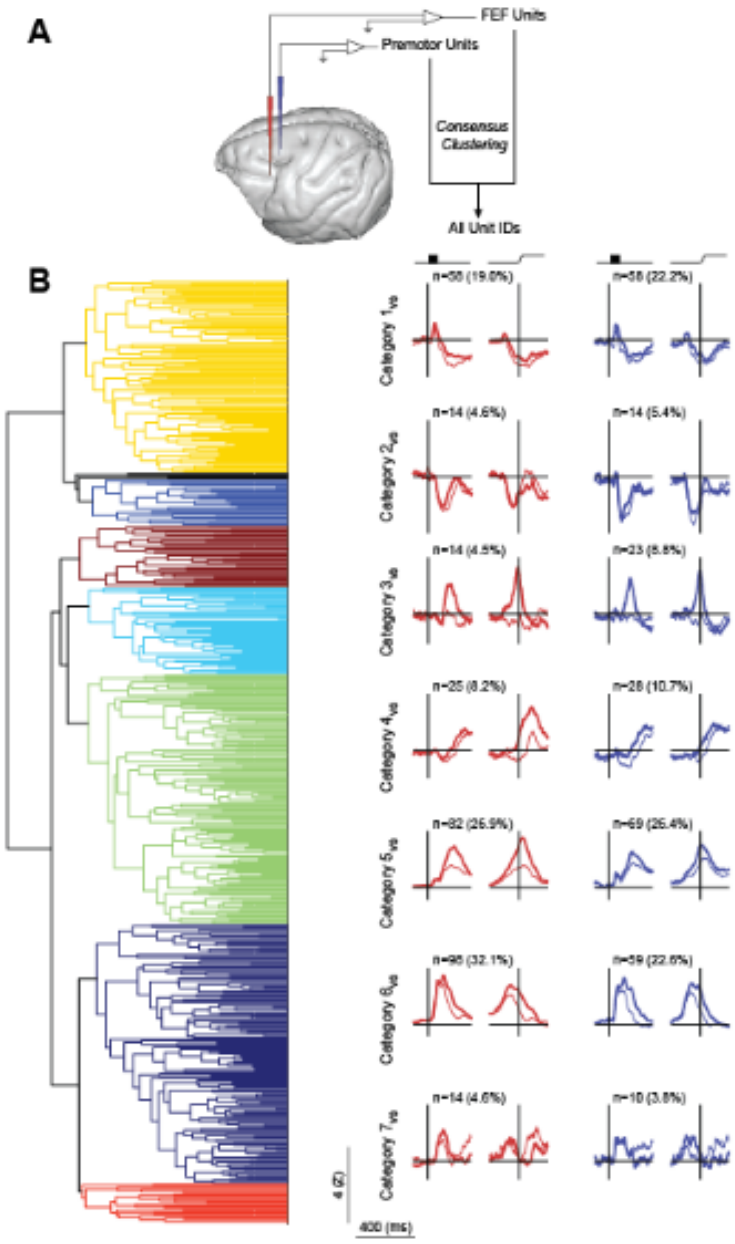

Figure 3.7. Search consensus clusters. A consensus clustering algorithm was applied to identify different categories of neurons in FEF and premotor cortex during the shape singleton search task. (A) Schematic of recording and clustering pipeline. Recordings were performed from both FEF (red electrode) and premotor cortex (blue electrode). Clustering was applied to the sample of neurons across regions. (B) Dendrogram of clustering and mean SDFs for each category. Conventions as in Fig. 3.6B.

response. Category 4_{VS} was characterized by post-saccadic responses. These responses were spatially selective in FEF, but not in F2vr. Categories 5_{VS}-7_{VS} are characterized by visual responses. Category 7_{VS} had only a small magnitude of response and was not spatially selective. Category 5_{VS} is the most canonical neuron type seen in visual search, whose visual response strongly discriminated the target location and whose presaccadic response peaked at the time of the saccade. Category 6_{VS} is strongly visual but has only a small magnitude of spatial selectivity. Insufficient data was collected in both memory-guided saccade and visual search tasks to support comparison of the categories of neurons across tasks.

Unexpectedly, the categories were distributed evenly across FEF and F2vr (Contingency test $X^2(6) = 10.5$, $p = 0.106$). When individual categories were compared, category 6_{VS} neurons were more prevalent in FEF than in F2vr, whereas category 3_{VS} neurons were more prevalent in F2vr than in FEF. These differences are consistent with the between area differences observed in the memory-guided clusters and the traditional categorization.

Clustering within region.

Next, to identify variation within regions, we separately applied the clustering algorithm to units recorded from FEF and to units recorded from F2vr. Then, in order to directly compare regions with the same set of clusters, we trained a classifier on the units from the clustered region and assigned the units from the unclustered region to these categories to identify categories in FEF and use a classifier to assign units from F2vr to these categories, and vice versa. This method allows the assessment of specific neural response profiles in one region and whether they exist in the other region as well. To

disambiguate results from different clustering approaches, categories are labeled with subscripts for the region to which clustering was applied and for the task used. Thus, a neuron from either region that was categorized as category 1 in a clustering of FEF neurons during memory-guided saccades will belong to category $1_{FEF,MG}$. A neuron from either region that was categorized as category 1 in a clustering of premotor neurons during visual search will belong to category $1_{PM,VS}$.

During memory-guided saccades, six categories were identified in FEF (Fig. 3.8). Then, a classifier was used to assign the premotor neurons to these categories. These composite categories, formed by the clustering algorithm and classification, were distributed unequally across FEF and F2vr (Contingency test $X^2(5) = 25.6$, $p < 0.001$). Post-hoc contingency tests indicated that this difference was driven by the distributions of categories $2_{FEF,MG}$, $3_{FEF,MG}$, $4_{FEF,MG}$, $5_{FEF,MG}$, and $6_{FEF,MG}$. Notably, one of the two purely visual categories, category $2_{FEF,MG}$ was more prevalent in FEF than in F2vr, whereas the other purely visual category, category $6_{FEF,MG}$, was more prevalent in F2vr than in FEF. These categories are distinguished by the presence (category $6_{FEF,MG}$) or absence (category $2_{FEF,MG}$) of post-saccadic activity. The purely presaccadic category, category $3_{FEF,MG}$, and a category with suppressed responses, category $4_{FEF,MG}$, were more prevalent in F2vr than in FEF. One of the visuomovement categories, category $5_{FEF,MG}$ was more prevalent in FEF than in F2vr and is defined by a longer return to baseline after the saccade. These results are consistent with the differences between neuron types using the traditional classification.

For the memory-guided saccade task, six categories were identified in F2vr (Fig. 3.9). Then, a classifier was used to assign the FEF neurons to these categories. These

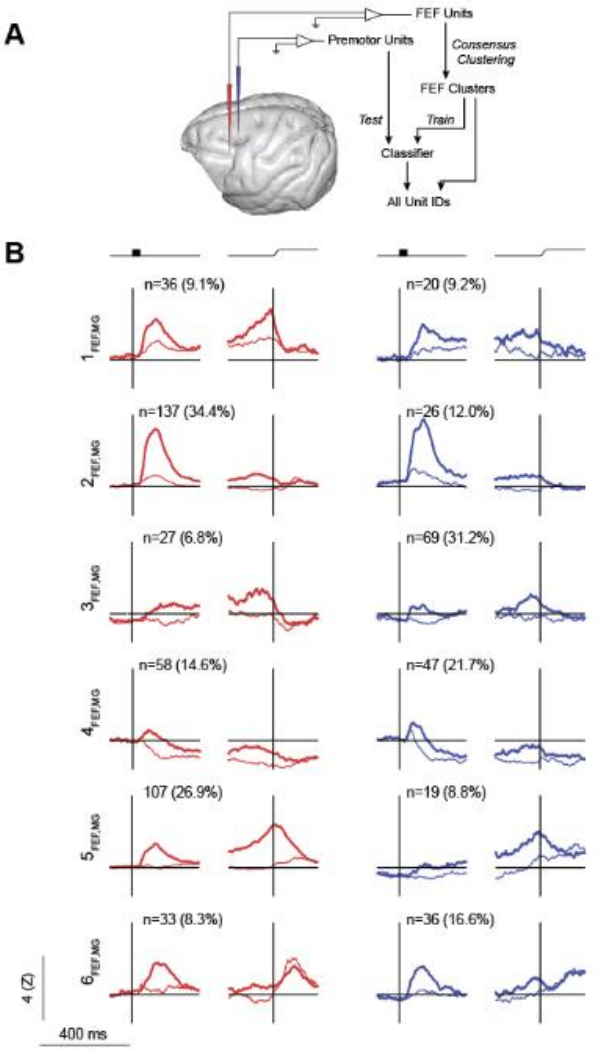

Figure 3.8. Memory-guided consensus clusters for FEF neurons. A consensus clustering algorithm was applied to identify different categories of neurons in FEF during memory-guided saccades, and a classifier was used to assign neurons in premotor cortex to these categories. (A) Schematic of recording and clustering pipeline. Recordings were performed from both FEF (red electrode) and premotor cortex (blue electrode). Clustering was applied to the sample of neurons from FEF. The FEF clusters were used to train a classifier and premotor neurons were tested by this classifier to assign the premotor neurons to the FEF clusters. These were used to create a composite set of cluster IDs across both regions. (B) Mean SDFs for the nine clusters. Conventions as in Fig. 3.6B.

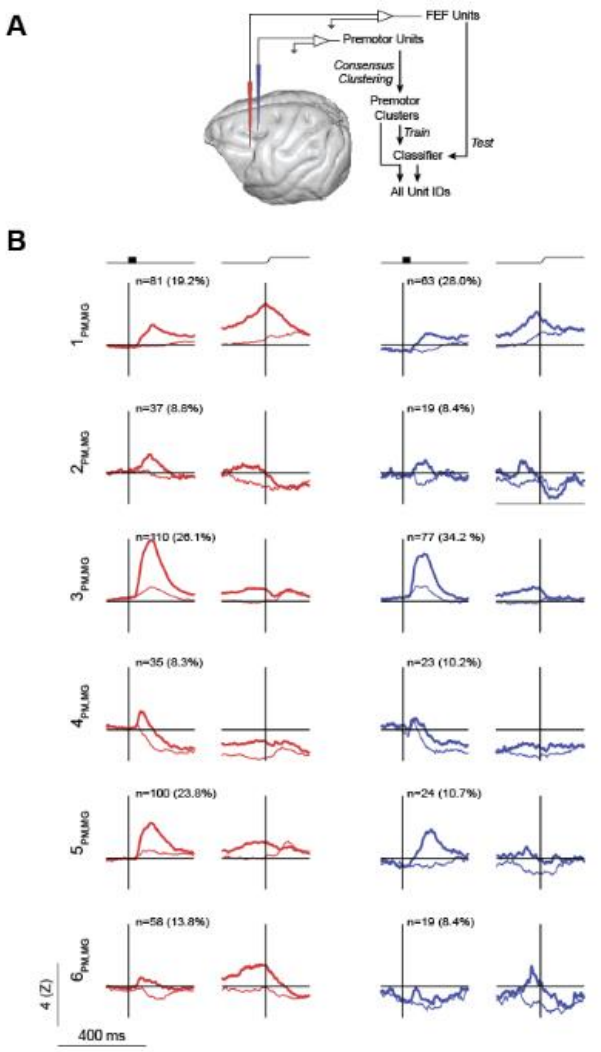

Figure 3.9. Memory-guided consensus clusters for premotor neurons. A consensus clustering algorithm was applied to identify different categories of neurons in premotor cortex during memory-guided saccades, and a classifier was used to assign neurons in FEF to these categories. (A) Schematic of recording and clustering pipeline. Recordings were performed from both FEF (red electrode) and premotor cortex (blue electrode). Clustering was applied to the sample of neurons from premotor cortex. The premotor clusters were used to train a classifier and FEF neurons were tested by this classifier to assign the FEF neurons to the premotor clusters. These were used to create a composite set of cluster IDs across both regions. (B) Mean SDFs for the eight clusters. Conventions as in Fig. 3.6B.

composite categories, formed by the clustering algorithm and classification, were distributed unequally across FEF and F2vr (Contingency test $X^2(5) = 25.6$, $p < 0.001$). Post-hoc contingency tests indicated that this difference was driven by the distributions

of categories $1_{PM,MG}$, $5_{PM,MG}$, and $6_{PM,MG}$. Interestingly, category $1_{PM,MG}$ is a visuomovement category, but more prevalent in F2vr than in FEF. One purely visual category, category $5_{PM,MG}$ was more prevalent in FEF than in F2vr, as was a category with pre-saccadic activity. Notably, the members of category $6_{PM,MG}$ appear different between the two areas; FEF members of this category exhibit delay period activity and a peak saccade-aligned response at the time of saccade initiation whereas F2vr members of this category exhibit suppressed responses aligned on the array and peak saccade-aligned response prior to saccade initiation.

During visual search, 5 categories were identified in FEF (Fig. 3.10). Then, a classifier was used to assign the premotor neurons to these categories. These composite categories, formed by the clustering algorithm and classification, were distributed unequally across FEF and F2vr (Contingency test $X^2(4) = 90.2$, $p < 0.001$). Post-hoc contingency tests indicated that this difference was driven by the distributions of categories $1_{FEF,VS}$, $2_{FEF,VS}$, $3_{FEF,VS}$, and $5_{FEF,VS}$. Category $1_{FEF,VS}$ is purely peri-saccadic, with activity ramping before the saccade but peaking after the saccade, and was more prevalent in F2vr than in FEF. Category $2_{FEF,VS}$ and category $3_{FEF,VS}$ both have visual responses and are more prevalent in FEF than in F2vr. Category $2_{FEF,VS}$ is spatially selective and visuomovement whereas category $3_{FEF,VS}$ is not spatially selective and does not have pre-saccadic activity. Category $5_{FEF,VS}$ has a suppressed response and is more prevalent in F2vr than in FEF.

During visual search, seven categories were identified in F2vr (Fig. 3.11). Then, a classifier was used to assign the FEF neurons to these categories. These composite categories, formed by the clustering algorithm and classification, were distributed

unequally across FEF and F2vr (Contingency test $X^2(6) = 18.5$, $p = 0.005$). Post-hoc contingency tests indicated that this difference was driven by the distributions of categories $2_{PM,VS}$, $4_{PM,VS}$, and $5_{PM,VS}$. Category $2_{PM,VS}$ had a suppressed response to the

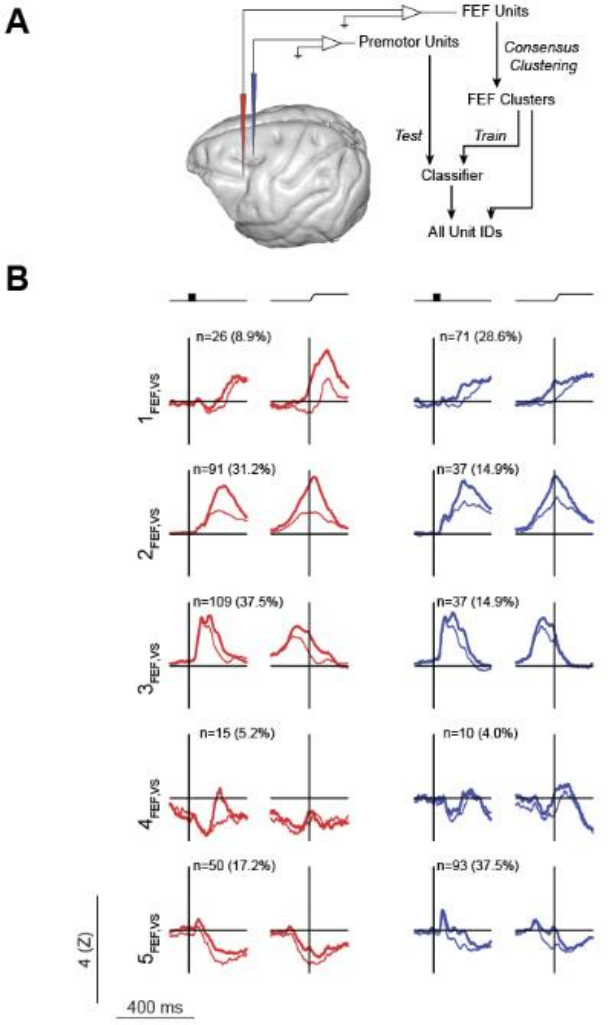

Figure 3.10. Search consensus clusters for FEF neurons. A consensus clustering algorithm was applied to identify different categories of neurons in FEF during the shape singleton search task, and a classifier was used to assign neurons in premotor cortex to these categories. (A) Schematic of recording and clustering pipeline. Recordings were performed from both FEF (red electrode) and premotor cortex (blue electrode). Clustering was applied to the sample of neurons from FEF. The FEF clusters were used to train a classifier and premotor neurons were tested by this classifier to assign the premotor neurons to the FEF clusters. These were used to create a composite set of cluster IDs across both regions. (B) Mean SDFs for the 11 clusters. Conventions as in Fig. 3.6B.

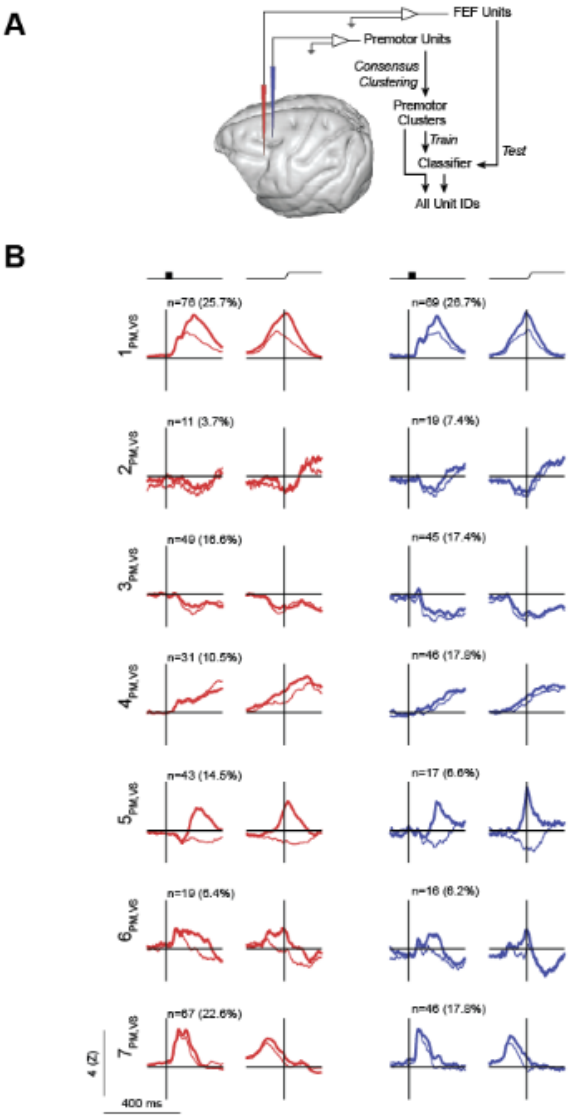

Figure 3.11. Search consensus clusters for premotor neurons. A consensus clustering algorithm was applied to identify different categories of neurons in premotor cortex during the shape singleton search task, and a classifier was used to assign neurons in FEF to these categories. (A) Schematic of recording and clustering pipeline. Recordings were performed from both FEF (red electrode) and premotor cortex (blue electrode). Clustering was applied to the sample of neurons from premotor cortex. The premotor clusters were used to train a classifier and FEF neurons were tested by this classifier to assign the FEF neurons to the premotor clusters. These were used to create a composite set of cluster IDs across both regions. (B) Mean SDFs for the nine clusters. Conventions as in Fig. 3.6B.

array followed by a post-saccadic response and was more prevalent in F2vr than in FEF. Category $4_{PM,VS}$ had a gradual non-specific increase in activity that peaked well after the saccade and was also more prevalent in F2vr than in FEF. Surprisingly, category $5_{PM,VS}$, which had sharp, transient increases in response that peaked at the time of the saccade, was more prevalent in FEF than in F2vr.

In all, the results of the clustering, whether regions were grouped for the clustering or separated, were internally consistent and are also consistent with the distribution of neuron types assessed by the traditional classification. FEF has higher proportions of visually related responses whereas F2vr has higher proportions of purely movement-related responses.

3.4 DISCUSSION

The caudal boundary of frontal eye field, located in area 8 in primates, is ambiguous. Neural responses just caudal to frontal eye field in the posterior bank of the arcuate sulcus, in area 6 or premotor cortex, specifically F5, are similar to responses in FEF in simple oculomotor tasks. Here, we show that these similarities extend to a more complex task a singleton shape visual search task in the ventral portion of the dorsal premotor cortex (F2vr). However, we did identify several distinguishing characteristics in both simple and complex tasks that may reveal the functional distinctions between these two regions. Below, we will first discuss the subdivisions of premotor cortex and the targeting of F2vr specifically to compare to FEF. Next, we discuss similarities between the two cortical regions. Then, we will discuss the differences and their potential for distinguishing functional specificity. Finally, we will discuss the relationship between these regions and the putative homologues in humans.

3.4.1 Subdivisions of Premotor Cortex

Premotor cortex is an anatomically and functionally diverse area, and its subdivisions have important implications for functional relationships to other areas. Primarily, premotor cortex can be divided into dorsal (PMd or F2) and ventral (PMv or F5) divisions based on cytoarchitecture (Geyer et al., 2000; Luppino et al., 2003) and connectivity (Ghosh & Gattera, 1995; Luppino et al., 2003; Tanné-Gariépy et al., 2002). These anatomical subdivisions correspond with functional differences in visuomotor behavior (see Hoshi & Tanji, 2007 for review). Specifically, PMd seems to be related more closely to dynamics and directions of motions as well as stimulus-response rule associations (Coallier et al., 2015; Cromer et al., 2011; Riehle & Requin, 1989; Romo et al., 2004; Wallis & Miller, 2003; Yamagata et al., 2012) whereas PMv seems to be more closely related to the visual information instructing a movement (Boussaoud & Wise, 1993a, 1993b; Hoshi & Tanji, 2000, 2004). Further, within PMd, visual responses are preferentially located in its rostrolateral extent, corresponding to F2vr (Fogassi et al., 1999), and rostral PMd is associated with more cognitive functions whereas caudal PMd is associated with motor funtions (Abe & Hanakawa, 2009; Nakayama et al., 2016). Thus, to identify whether the posterior bank of the arcuate sulcus is similar to FEF with respect to cognitive and visuomotor functions, we specifically targeted F2vr due to its putative cognitive specialization and action selection responses. This targeting was possible due to our use of MRI guided electrode penetrations to ensure recordings were in this small, specific target region (Fig. 2.2).

3.4.2 FEF and F2vr Have Similar General Characteristics

For the purpose of identifying the cognitive contributions of F2vr to visuomotor behavior, we recorded from neurons in this region during a shape singleton search task. In this task, we found that neurons in F2vr exhibit target selection, as has been seen repeatedly in FEF (e.g., Schall et al., 1995a; see Schall, 2015 for review). As a population, we found no differences between target selection time between the two regions. While the similarity of movement-related neurons in the FEF and ventral premotor cortex (F5) has been demonstrated (Neromyliotis & Moschovakis, 2018; Neromyliotis & Moschovakis, 2017b), importantly we now demonstrate that the ventral portion of the dorsal premotor cortex (F2vr) has similar visual and movement-related responses to FEF.

Though the target selection times may be similar in the two regions, the speed of calculating this discrimination may differ. We found no differences between visual latencies of the two regions. Thus, neither the time of target selection *per se* nor the timing of the target selection operation are different between F2vr and FEF. Further, we found that the time of onset of presaccadic activity is also not different between the two regions in two of the three monkeys. Thus, the visuomotor transformation occurs on similar timescales in both regions. This similarity in presaccadic activity onset is at odds with the results of Neromyliotis & Moschovakis (2018). However, their recordings were preferentially directed toward ventral premotor cortex (F5), whereas the present recordings were directed toward dorsal premotor cortex (F2vr). Because a mediolateral distinction has been observed in FEF (e.g., Markov et al., 2014; Suzuki & Azuma, 1983), and premotor cortex (for review, see Hoshi & Tanji, 2007), the regional

differences may account for the present results. Thus, we here demonstrate visual and motor responses in an oculomotor task exist in PMd as well as in PMv.

Other metrics, specifically delay period activity and the time of the peak movement-related response, also did not differ between the areas. Thus, the functional properties of the two regions are indistinguishable.

3.4.3 Differences Between FEF and F2vr

Though several gross metrics of visuomotor function are identical across FEF and F2vr, we did identify several key differences between the regions. Most notably, we found a difference in the proportion of neuron types across the regions. By classifying neurons according to a canonical visual, visuomovement, and movement classification scheme (Bruce & Goldberg, 1985), we found that the distribution of these neuron types was significantly different between the two regions. Specifically, FEF has more visual and visuomovement neurons than F2vr, whereas F2vr has more movement related and unclassified neurons. These differences were reinforced by the results of the consensus clustering identifying additional nuance in neuronal diversity. The categories identified in the memory-guided saccade task, after including responses to stimuli outside the RF, were consistent with those previously identified by Lowe & Schall (2018) which used only responses to stimuli inside the RF from these neurons, indicating robustness of the algorithm with additional conditions included in the clustering as well as the ability of this algorithm to differentiate between highly similar brain regions, and increasing confidence in this general finding.

This difference in neuron proportion may explain functional differentiation between the regions. Premotor cortex is generally considered to be an area involved in

skeletal movements, specifically manual responses (Cisek & Kalaska, 2005; Kalaska et al., 1998; Kalaska et al., 1997; Neromyliotis & Moschovakis, 2018; Neromyliotis & Moschovakis, 2017b; Thura & Cisek, 2014; Wise, 1985; Wise et al., 1992, 1996) and has neurons whose motor responses are modulated by eye position (Boussaoud, 1995; Boussaoud et al., 1993a; Boussaoud et al., 1998; Cisek & Kalaska, 2002; Mushiake et al., 1997). In contrast, FEF neurons are predominantly involved in eye movements (Lawrence & Snyder, 2009), either unresponsive during manual tasks (Thompson et al., 2005b) or lacking response modulation by arm movements (Mushiake et al., 1996). The difference in neuron type proportion may be due to the specialization of effectors.

Similarly, the proportion of neurons exhibiting target selection was greater in FEF than in F2vr. Thus, although both regions are involved in oculomotor search, FEF seems more specialized for this function. Interestingly, the proportion of neurons in each region with visual responses is almost exactly the proportion of neurons exhibiting target selection. While not all visual neurons exhibit target selection (Schall et al., 1995a; Thompson et al., 1996), the majority of those that do are more closely related to visual processing than saccade planning (Thompson et al., 1996). Thus, the difference in proportion of neurons exhibiting target selection between the two regions may be related to the proportion of visually responsive neurons and explained by putative specificity of effectors. This supposition is further supported by the magnitude of target selection; among those neurons in each region that did exhibit significant target selection, the magnitude of this selection did not differ between regions. However, FEF has been shown to exhibit target selection when no overt response is required (Thompson et al., 1997) and even when an arm movement is required in lieu of an eye

movement (Thompson et al., 2005b), suggesting that FEF may have a more general role in directing covert and overt attention. Further studies with multiple effectors are necessary to disambiguate the role of each region in effector-specific and effector-invariant target selection.

Because we did not have the monkeys perform any manual task, we could not identify neurons that select a response regardless of effector and thus we may be collapsing across dissimilar neural categories, and we cannot quantify the timing of inter-effector responses. Further, we may have found more similar proportions of response types. In FEF, responses to visual stimuli are attenuated if they are not potential saccade targets (Goldberg & Bushnell, 1981), and a similar attenuation has been observed for stimuli that are not potential reach targets (Wise et al., 1992). Our laboratory certainly appreciates the impact of neuronal diversity (Lowe & Schall, 2018), thus we realize that further direct comparisons would require tasks with manual responses.

3.4.4 Connectivity of Premotor Cortex and FEF

An important consideration for the differentiation between FEF and premotor cortex is the pathways by which the demonstrated visuomotor activity may arrive or be sent to different areas. In a seminal study examining the signals sent to the superior colliculus from FEF, Segraves & Goldberg (1987) demonstrated an example in which one site in the caudal bank of the arcuate was antidromically activated by stimulation in the superior colliculus. Thus, premotor cortex can supply visuomotor information to the superior colliculus (see also Distler & Hoffmann, 2015), which is one step closer to the brainstem saccade generator (e.g., Crapse et al., 2018).

FEF and the sulcal region of premotor cortex also share similar afferents. In one study, anterograde tracers were injected into parietal area LIP which resulted in labeling of the caudal bank of the arcuate sulcus, though these labels were more sparse than in the rostral bank (Schall et al., 1995b). Interestingly, anterograde tracers injected into temporal area TEO did not show this labeling, but retrograde tracers in both areas showed labeling in both FEF and the sulcal region of premotor cortex. This suggests that both premotor cortex and FEF are reciprocally connected with the dorsal stream, whereas premotor cortex sends but does not receive projections from the ventral stream. FEF is reciprocally connected with the ventral stream. These general findings were also demonstrated for connections with V4 in the ventral stream (Ungerleider et al., 2008) and again for LIP in the dorsal stream (Blatt et al., 1990; Petrides & Pandya, 1984). This suggests that premotor cortex may be primarily involved in spatial attention (e.g., Lebedev & Wise, 2001) but not feature attention, whereas FEF is involved in both (Lowe & Schall, 2019; for examples of feature attention, see Bichot et al., 2015, 1996; Peng et al., 2008; Xiao et al., 2006). Additional tasks requiring feature information may provide additional evidence differentiating these two eye fields.

3.4.5 Relation to Human Literature

One controversy in assessing the homology of human and macaque FEF has been the identification of the actual location of FEF in humans. In humans, FEF is frequently localized to area 6 (for review, see Amiez & Petrides, 2009; Paus, 1996; Schall et al., 2017; Tehovnik et al., 2000), whereas in macaques FEF is localized to area 8 (Huerta et al., 1987; Stanton et al., 1988). However, this may be explainable by the methodology; the studies in humans that localize FEF to area 6 use neuroimaging (PET and fMRI)

whereas the studies in macaques use intracranial microstimulation. In humans, FEF as identified by microstimulation is in area 8 (Blanke et al., 2000). If this is the case, and the “true human FEF” is in area 8 (Tehovnik et al., 2000), then why is FEF commonly found in area 6 of humans?

The present results may shed light on this question. Because of the remarkable similarity between the two regions as seen in the single neuron responses, both visual and motor, these two regions may be confusable in more gross measures such as fMRI. Further, the role of human FEF in anti-saccades is unclear (see Neggers et al., 2012; Paus, 1996), whereas in macaques area 8, or FEF, is differentially responsive to pro- and anti-saccades even in fMRI (Ford et al., 2009). The variability in studies of human FEF may be due to the localization of FEF. That is, such a difference between pro- and anti-saccades may be found when FEF is defined as in area 8 whereas it may be absent when FEF is defined as in area 6. In the present study, we found that some cognitive characteristics are more pronounced in FEF than in F2vr, specifically the delay period activity maintaining spatial information during memory-guided saccades. This lack of cognitive contributions to oculomotor tasks may extend to anti-saccades in F2vr. However, premotor cortex does modulate in anti-reach tasks (Crammond & Kalaska, 1994), but the generality of the effector is unknown. In any case, the appreciation of the distinction between FEF and F2vr presents an avenue by which these questions of homology can be addressed.

CHAPTER 4: SELECTIVE INFLUENCE AND SEQUENTIAL OPERATIONS: A RESEARCH STRATEGY FOR VISUAL SEARCH

4.0 SUMMARY

Chapter 3 defined functional categories of neurons that can be identified in search. But much as cataloguing these functional neuron types is necessary to understand the scope of the neurobiology, understanding the psychology underlying visual search is necessary to understand the scope of the behavior. As described in the Introduction, this is no trivial goal. Thus, two central questions frame this aim: (1) is visual search comprised of multiple distinct processing operations and (2) what is the architecture of those operations? Without establishing the existence of processing operations and their relationships, the subsequent analyses will lack the essential bridge between neurobiology and behavior.

There is evidence that visual search in a saccadic paradigm can be broken down to at least visual and motor operations (Thompson et al., 1996; Woodman et al., 2008), satisfying a positive conclusion to question (1). Next, the architecture of processing operations has been central to Sternberg's additive factor method (Sternberg, 1969, 2001) as well as Townsend's systems factorial technology (Houpt et al., 2014; Townsend & Nozawa, 1995), as well as to visual search research in general. The additive factor method can identify separate modifiability of any number of processing stages, though only in a serial architecture. SFT is restricted to 2x2 designs but is able to differentiate serial from parallel architectures and self-terminating from exhaustive stopping rules, while also differentiating between selective and non-selective influence

(i.e., coactivity). By designing a 2x2 factorial paradigm amenable to SFT (see Methods, Lowe et al., 2019), processing architectures of visual search will be assessed.

We developed a GO/NO-GO search task in which a search singleton is defined by its chromatic uniqueness, and the aspect ratio of this search singleton cues a GO/NO-GO rule. A notable foil for this study was performed by Sato and colleagues (2001). In this study, singleton identifiability was similarly manipulated by chromatic similarity between singleton and distractors, as in the present study. Response preparation was manipulated by changing the location of the singleton at some time between array onset and response. Conceptually, both this study and the present one intend to manipulate search efficiency and response preparation. The study by Sato and colleagues found response time differences from both manipulations, as does the present study. Two critical differences exist between these studies: (1) in the previous study, the response preparation manipulation still involved a saccade, and this saccade was directed in a different direction than the original singleton and (2) in the previous study the two manipulations were not performed during the same session. The new design provides theoretical advantages by (1) assessing the effects of the two manipulations when all necessary information is available within a given neuron's response field on every trial and (2) specifically addressing the question of whether the same individual neurons (not category of neurons, as per the visual neurons assessed by Sato and colleagues) carry information relevant to both manipulations.

In the remainder of this chapter I apply SFT to the response times in the task to characterize the cognitive architecture used to perform the task. This chapter has been published as Lowe et al. (2019).

4.1 INTRODUCTION

This introduction surveys the literature on visual search in the context of describing the underlying neuro-computational mechanisms and motivating a new experimental approach. To understand the neural mechanisms of visual search requires discovering the mapping between neural processes and visual, attention, and motor processes. Neural processes supporting visual search have been investigated in human studies using noninvasive measures of EEG and fMRI and in nonhuman primates using invasive sampling of neural discharges. Hence, to understand the neural mechanisms of visual search requires building a conceptual and empirical bridge between levels of explanation, neural measures, and species. This paper will situate the problem more definitely, briefly survey relevant performance and neural data, and introduce a program of research that can elucidate more specifically how neural circuits accomplish visual search.

Seeking to understand the relationship between neural and mental processes is hardly a new problem. For example, in 1865 Ernst Mach explained, “To every psychical there corresponds a physical, and conversely. Like psychical processes correspond to like physical, unlike to unlike. If a psychical process can be resolved, in a purely psychological manner, into a multiplicity of qualities, a, b, c, then to these there correspond an equal number of different physical processes, α, β, γ. Particulars of the physical correspond to all the particulars of the psychic.” (Boring, 1942). In 1970 Donald Davidson wrote, “… mental characteristics are in some sense dependent, or supervenient, on physical characteristics. Such supervenience might be taken to mean that there cannot be two events alike in all physical respects but differing in some mental respects, or that an object cannot alter in some mental respect without altering in

some physical respect." (Davidson, 1970). These axioms frame cognitive neurophysiology research.

The relationship between mental and physical descriptions can be articulated through linking propositions that specify the nature of the mapping between particular behaviors or cognitive states and associated neural states (Brindley, 1970; Teller, 1984; Teller & Pugh, 1983). Different kinds of linking propositions can be distinguished, e.g., identity, similarity, and analogy (Teller 1984). To illustrate, consider this linking proposition: the *nerve impulse* is an *action potential*. The nerve impulse is an event that caused muscle contraction after nerve irritation that was discovered by Galvani and characterized by Swammerdam (McComas, 2011). Its speed was first measured by Helmholtz in 1850. The action potential (or nerve current) was first measured by du Bois-Reymond in 1848 and its ionic nature was first described by Bernstein and Lillie and elucidated by Hodgkin and Huxley. How do we know that the behavioral nerve impulse is the ionic action potential? This may seem obvious today, but it was not always. Indeed, the identity was established beyond doubt only by Huxley & Stämpfli (1949). They reported, "It was found that the muscle twitched when the nerve was stimulated if, but only if, the thread connecting the fluids on the two sides of the gap was in place. … This demonstrates that the transmission of the nervous impulse depends on currents flowing outside the myelin sheath…"

What linking propositions are necessary to explain how the brain does visual search? How should such linking propositions be articulated and tested? Adopting Marr's hierarchy of computational theory, algorithm, and implementation, it seems clear that explaining how the brain does visual search requires translating between these

levels of explanation. Several complementary and competing computational theories of visual search and attention have been formulated. These include the Theory of Visual Attention (Bundesen, 1990), COntour Detector (Logan, 1996), Feature Gate (Cave, 1999), and Guided Search (Wolfe et al., 2015; Wolfe et al., 1989; Wolfe, 1994, 2007). Other computational approaches are designed to solve pragmatic, real-world search problems (Bruce et al., 2015; Itti & Koch, 2000). Some of these computational models have been articulated in terms of neural circuits at various levels of specificity from identification with specific brain structures and circuits (Adeli et al., 2017; Bundesen et al., 2011; Murray et al., 2017; Schwemmer et al., 2015) to microcircuitry of a cortical area (Heinzle et al., 2007) and with convolutional neural networks (e.g., Adeli & Zelinsky, 2018). Another approach has embedded neural signals measured during visual search performance into the stochastic accumulator framework (Purcell et al., 2010; Purcell et al., 2012b).

These diverse computational and algorithmic approaches offer tools appropriate to translate between the neural and cognitive processes producing an observed pattern of performance. They serve another scientific function too. The literature on visual search and selective attention is governed by ambiguous and vague terms such as attention (both as cause and as effect), capacity, capture, disengage, efficiency, engage, map, priority, salience, selection, and shift. Formal models are needed to explain what these terms mean by identifying them with specific components, processes, or outputs.

4.1.1 Human and Nonhuman Primate Visual Search Performance

Visual search has been investigated in many laboratories in many ways. Nevertheless, some general attributes have been established in human studies and replicated in macaque studies. The first key attribute is this: visual search takes time. A minimal amount of time is needed for visual encoding and response preparation. Not much more time is needed if the sought for object is easily discriminated from distracting objects, but progressively more time is needed if the distracting objects are more visually similar to the sought for target object and there are more such distracting objects (e.g., Duncan & Humphreys, 1989; Treisman & Gelade, 1980). Additional time may be taken if one of the non-target items is especially conspicuous (e.g., Bacon & Egeth, 1994; Theeuwes, 1994) or if the target item is in the same location as a previously attended target (Klein, 2000; Posner & Cohen, 1984). More time is needed if the response to the target object requires any kind of arbitrary mapping from stimulus location or property to response.

To investigate mechanisms of visual search at the neural circuit level requires systematic testing in nonhuman primates. For such studies to be relevant for understanding human performance, we must verify that nonhuman primates exhibit chronometric characteristics of search performance corresponding to humans. Fortunately, when sought, this confirmation has been found. Macaque monkeys exhibit dependence of visual search on target-distractor similarity and set size during singleton search (Arai et al., 2004; Azzato & Butter, 1984; Balan et al., 2008; Buracas & Albright, 1999; Camalier et al., 2007; Cohen et al., 2009b; Lee & McPeek, 2013; McPeek & Keller, 2001; Motter & Holsapple, 2007, 2000; Nothdurft et al., 2009; Sato et al., 2001; Song et al., 2008) and conjunction search (Bichot & Schall, 1999; Motter & Belky, 1998; Shen & Paré, 2006). They can exhibit feature search asymmetries (Nakata et al., 2014).

They can exhibit inhibition of return (Bichot & Schall, 2002; Fecteau & Munoz, 2003; Torbaghan et al., 2012). Visual search is guided by memory as well as sensation. On the shortest time scale, performance of popout search varies if the search feature dimensions change (Maljkovic & Nakayama, 1994). Called priming of popout, this demonstrated the limits of automaticity in visual search. Monkeys also exhibit priming of pop out (Bichot & Schall, 2002; Purcell, et al., 2012b). Macaque monkeys can also perform visual search filtering tasks that require search on one feature dimension and response according to another (Katnani & Gandhi, 2013; Sato & Schall, 2003). Most recently, we have shown that monkeys also show contingent capture of attention by conspicuous non-target items (Cosman et al., 2018). Hence, macaque monkeys are a valid model of human visual search.

4.1.2 Nonhuman Primate Visual Search Neurophysiology

Establishing that macaque monkeys perform visual search like humans provides the opportunity to investigate at the neurophysiological level the various operations, processes, and stages supporting visual search. To orient the reader to this literature, we offer a selective survey of the neurophysiological correlates of visual search.

The first such studies were published by Chelazzi et al. (1993) in inferotemporal cortex and Schall and Hanes (1993) in frontal eye field. Both studies found that neurons that initially did not distinguish the target from distractors eventually came to discharge more spikes when the target relative to a distractor was in the response field. Subsequent studies across numerous laboratories have replicated and extended the original observations during visual search tasks in frontal eye field (Bichot et al., 2001a; Bichot et al., 2001b; Cohen et al., 2007, 2009; Costello et al., 2013; Heitz & Schall,

2012; Miller & Buschman, 2013; Mirpour et al., 2018; Monosov et al., 2008; Monosov & Thompson, 2009; Murthy et al., 2009; Nelson et al., 2016; Phillips & Segraves, 2010; Purcell et al., 2013; Ramkumar et al., 2016; Sapountzis et al., 2018; Sato et al., 2001; Sato et al., 2003; Sato & Schall, 2003; Schall et al., 1995a; Schall, 2004b; Thompson et al., 1996; Thompson et al., 2005a, 2005b; Thompson et al., 1997; Trageser et al., 2008; Woodman et al., 2008; Zhou & Desimone, 2011), in other prefrontal regions (Bichot et al., 2015; Hasegawa et al., 2000; Iba & Sawaguchi, 2003), in extrastriate visual areas like MT (Buracas & Albright, 2009) and V4 (Arcizet et al., 2018; Bichot et al., 2005; Chelazzi et al., 2001; Gee et al., 2010; Ipata et al., 2012; Mazer & Gallant, 2003; Motter, 1994; Ogawa & Komatsu, 2006; Zhou & Desimone, 2011), as well as areas in the temporal lobe (Chelazzi et al., 1998; Monosov et al., 2010; Mruczek & Sheinberg, 2007a, 2007b, 2012) and the parietal lobe (Arcizet et al., 2018; Balan et al., 2008; Constantinidis & Steinmetz, 2001; Ipata et al., 2006a, 2006b; Meyers et al., 2018; Mirpour et al., 2009, 2010; Mirpour & Bisley, 2013; Nishida et al., 2013, 2014; Ogawa & Komatsu, 2009; Sapountzis et al., 2018; Steenrod et al., 2013; Tanaka et al., 2015; Thomas & Paré, 2007) as well as subcortically in the superior colliculus (Lovejoy & Krauzlis, 2017; McPeek & Keller, 2002; Reppert et al., 2018; Shen & Paré, 2007, 2014; Song & McPeek, 2015; White et al., 2009, 2017), substantia nigra of the basal ganglia (Basso & Wurtz, 2002), and central thalamus (Costello et al., 2016).

Viewing these diverse results with a goal of formulating a mechanistic model of visual search, we must appreciate that each of these cortical areas and subcortical structures is comprised of a diversity of neurons distinguished by morphology and connectivity. Only some of the neurons in these various neural loci contribute to visual

search. The detailed connectivity of this network has yet to be worked out, but some results point toward nuances that will constrain such a mechanistic model. For example, different neurons in FEF project to V4 and to MT, and the two pools of neurons have different frontal lobe inputs (Ninomiya et al., 2012). Also, FEF is connected with at least 80 cortical areas (Markov et al., 2014; Schall et al., 1993; Schall et al., 1995b). Similarly, the superior colliculus receives inputs from effectively as many cortical areas (Cerkevich et al., 2014; Fries, 1984). Crucially, pyramidal neurons in the cerebral cortex do not project to more than one cortical area (Markov et al., 2014). Likewise, pyramidal neurons in layer 5 that project to the superior colliculus do not also project to cortical areas (Pouget et al., 2009). Hence, if each pyramidal neuron projecting to a different target conveys a different signal, then a cortical area like FEF must have dozens of distinct types of pyramidal neurons. The extent of this functional variability has only recently been investigated quantitatively (Lowe & Schall, 2018).

Research has demonstrated that different neurons support different operations. For example, the target selection process manifest by visually responsive neurons is distinct from saccade production. For example, in FEF the target selection process happens if no saccade to the target is made (Thompson et al., 2005b; Thompson et al., 1997) or if the endpoint of the saccade is not at the search target (Murthy et al., 2009; Sato et al., 2003). Moreover, the target selection process does not automatically produce saccade preparation (Juan et al., 2004; cf. Katnani & Gandhi, 2013). Corrective saccades are produced by FEF (and related) movement neurons independent of state of the visual neurons (Murthy et al., 2007).

The claim that anatomically and functionally different populations of neurons accomplish visual search requires an explanation of the relationship between those populations. One approach was formalized in the Gated Accumulator Model (Purcell et al., 2010; Purcell et al., 2012b). This model explains the relationship between visual target selection and saccade preparation by using the observed responses of FEF visual neurons as inputs to a network of accumulators. The salience evidence that is accumulated is just the spike trains recorded from visually responsive neurons in FEF. Accumulated variability in the firing rates of these neurons explains choice probabilities and the distributions of correct and error response times with search arrays of different set sizes if the accumulators are mutually inhibitory. The dynamics of the stochastic accumulators quantitatively predict the activity of presaccadic movement neurons that initiate eye movements if gating inhibition prevents accumulation before the representation of stimulus salience emerges. This formal modeling approach demonstrates the viability of combining neurophysiological data and computational models to identify neural substrates of visual attention and to formalize the otherwise vague concepts and terms listed above.

4.1.3 Human and Nonhuman Primate Visual Search Electrophysiology

Establishing similarities between macaque and human measures of visual search is necessary to enable mapping between monkey neurophysiology and human cognition. We reviewed similarities of macaque and human performance above. Here, we briefly summarize another empirical bridge, recording event-related potentials in nonhuman primates to obtain measures parallel to those of human studies. First, the ERP signature known as contralateral delay activity has been measured in macaque

monkeys (Reinhart et al., 2012), so the contribution of working memory in guiding search can be investigated with macaque monkeys in parallel to human studies (e.g., Woodman et al., 2007). Next, the allocation of visual attention during visual search is indexed by an event-related potential known as the N2pc (e.g., Liesefeld et al., 2017; Luck & Hillyard, 1994; McCants et al., 2018). Also, the suppression of salient distractors is indexed by an event-related potential known as the Pd (Hickey et al., 2008; Liesefeld et al., 2017; Sawaki & Luck, 2010). Previous research has confirmed that macaque monkeys manifest the N2pc (Cohen et al., 2009a; Heitz et al., 2010; Purcell et al., 2013; Woodman et al., 2007). Recent work has also demonstrated monkeys manifest the Pd component associated with suppression of salient distractors (Cosman et al., 2018). The relationship of intracranial single-unit signals and extracranial EEG signals requires much further investigation, because for unknown reasons the neural events signaling search target location arise in FEF before the N2pc (Cohen et al., 2009a). To understand these timing relationships, data from a likely generator of the N2pc, such as area V4, is needed (e.g., Hopf et al., 2000).

4.1.4 Linking Propositions Through Combined Neural and Mental Chronometry

To claim that we understand the neural mechanisms of visual search, we will need to explain the neural processes that occupy the different amounts of time taken during visual search under various conditions. As visual search time increases, do a fixed number of neuro-computational processes just take longer? Or does an increase of visual search time happen because additional neuro-computational processes are inserted between encoding and responding? If additional processes are invoked, how do the multiple processes interact?

We believe that the answers to these questions will end with neurophysiological data, but they must begin with a clear appreciation of the psychological perspective on visual search and the history of response time models. A conceptually and historically foundational hypothesis posited that response time (RT) in complex tasks is the summation of functionally distinct stages (Donders, 1868). This stage assumption is foundational to the predominant model of “decision-making”, which consists of a single stochastic sequential-sampling process following an uninteresting visual encoding stage and preceding a delayed response production stage (Ratcliff et al., 2016; Michael N. Shadlen & Kiani, 2013). Such models explain performance and account for neural activity in visual discrimination tasks as well as visual search with direct stimulus-response mapping (Purcell et al., 2010; Purcell et al., 2012b). But, if RT is not comprised of dissociable stages, or if RT is comprised of multiple stochastic sequential-sampling processes, then models like drift diffusion seem disqualified. If that is so, then alternative models must be considered. One possibility is a cascade architecture in which multiple levels of processing are arranged serially with information continuously propagating from one level to the next (e.g., McClelland, 1979). Another, intermediate possibility is known as asynchronous discrete flow in which the processing of multiple features is accomplished discretely, independently but in parallel and finishing at different times (Miller, 1988). These qualitatively different mechanisms with aspects of simultaneity of processing have been overlooked in the canonical literature on the neural mechanisms of decision making.

Crucially, models with a single stochastic decision process cannot explain tasks that require multiple, sequential operations. Consider a visual search filtering task like

the one used in this study. In the vernacular of this literature, accomplishing such a task requires a “decision” about the location of a color singleton, a “decision” about the shape of the singleton, a “decision” about the shapes of distractors, a “decision” about the congruency of the singleton and distractor shapes, a “decision” about the instructed stimulus-response mapping, a “decision” about the correct endpoint of the saccade, and a “decision” about when to initiate the saccade. This confusion can be eliminated by using the term “decision” to describe the deliberations and actions of agents but not to characterize particular neuro-computational processes (Schall, 2001).

If neuro-computational modules are distinct and independent, then it should be possible to change one process without changing another. This idea underlies the logic of separate modifiability formulated by Saul Sternberg (1969, 2001). If mental modules are distinct and independent, then it should be possible to change one process without changing the other. The logical, mathematical, and statistical formulation developed by Sternberg specifies how to interpret the effects of specific causal manipulations on performance and neural measures. For example, if factors *F* (e.g, singleton-distractor identifiability) and *G* (stimulus-response cue discriminability) influence two sequential processes, **A** and **B**, selectively, then RT = $\text{Duration}_{\mathbf{A}}(F) + \text{Duration}_{\mathbf{B}}(G)$. If **A** and **B** are distinct, sequential processes, then in an *F* x *G* factorial experiment, changes of RT over variation of *F* will be independent of changes of RT over variation of *G* (Figure 4.1). This approach has already revealed additivity and mutual invariance of singleton-distractor similarity and response interference in monkey cognitive neurophysiology studies (Mouret & Hasbroucq, 2000; Sato et al., 2001) and human ERP studies (e.g.

Osman et al., 1992; Servant et al., 2015; Smulders et al., 1995; see also Liesefeld, 2018).

Although this approach has proven effective, distinct and independent modules need not result in total additivity. If factors *F* and *G* selectively influence distinct but simultaneous processes, A and B, then RT < Duration$_A$(*F*) + Duration$_B$(*G*) (Figure 1). The literature is divided on how filtering tasks, like the one we used, are performed. The most common view is that selection and categorization of an object are separate sequential stages (Figure 1A) (e.g., Broadbent, 1971; Hoffman, 1978; Treisman, 1988; Wolfe et al., 2015). An alternative view is that objects are selected and categorized through parallel processes (Figure 4.1B) (e.g., Bundesen, 1990; Logan, 2002).

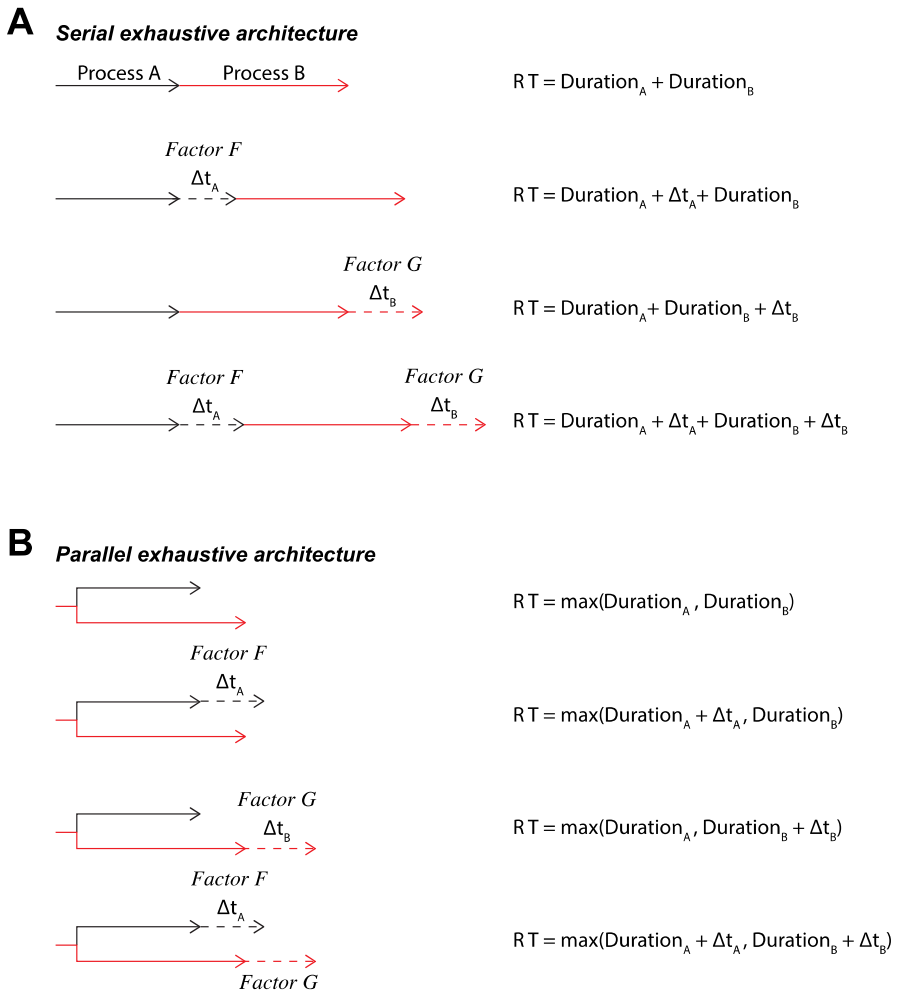

Figure 4.1. Two alternative architectures for the interaction of two distinct processes. (**A**) Serial exhaustive architecture. Both processes must complete before a response can be initiated. The durations of the two stages of processing, A and B, are under the selective influence of factors, *F* and *G*. Mutual invariance is satisfied when manipulation of factor *F* (or *G*) alters the duration of stage A (or B) but not B (or A). Additivity is satisfied when the total RT equals the sum of the durations of the separate processes. (**B**) Parallel exhaustive architecture. The two processes operate concurrently but both must complete before a response can be initiated. Manipulation of factor *F* (or *G*) alters the duration of stage A (or B) but not B (or A). The variation of RT across the two manipulations is additive or under-additive.

The fundamental problem of distinguishing serial

from parallel processing has proven challenging because particular serial and parallel architectures can be mathematically indistinguishable (e.g., Townsend, 1972; Townsend, 1990). However, a mathematically rigorous approach to investigating alternative process architectures was developed by James Townsend and colleagues, known as systems factorial technology (Harding et al., 2016; Houpt et al., 2014; Townsend & Nozawa, 1995). Based on mathematical axioms, postulates, and theorems, systems factorial technology offers strong tests of alternative architectures. Under conditions of selective influence, distinct predictions about response time dynamics are made for serial and parallel models with different decision stopping rules. Through a series of specific analyses of response time distributions, systems factorial technology can discriminate between five types of information processing architectures that could accomplish a task. These are (1) serial self-terminating, (2) serial exhaustive, (3) parallel self-terminating, (4) parallel exhaustive, and (5) coactive. Of course, distinguishing serial from parallel processing in visual search has a long and some may say discouraging history (Townsend, 1990; Treisman & Gelade, 1980; see also Liesefeld & Müller, 2020; Moran et al., 2016; Thornton & Gilden, 2007); yet, progress on this issue remains possible. Through systems factorial technology, when selective influence is applied effectively in visual search, predictions of serial and parallel models and their stopping rules are mathematically distinct and experimentally discriminable (Fifić et al., 2008b).

4.1.5 Prerequisites for Linking Neurophysiology and Systems Factorial Technology

The integration of neurophysiology and systems factorial technology has three prerequisites: (1) the existence of distinct operations or stages that can be selectively

influenced by experimental manipulations; (2) a factorial task design that selectively influences these distinct operations or stages; and (3) evidence that macaque monkeys can perform such a factorial experiment in a manner that can be analyzed by SFT. For perspective, prerequisites like this had to be satisfied when this laboratory began using the stop signal saccade countermanding task (Hanes & Schall, 1995).

The first prerequisite has already been satisfied empirically. During cognitive neurophysiological experiments, RT can be divided into distinct processing stages during visual search (Thompson et al., 1996; c.f. Costello et al., 2013). The singleton selection stage takes longer during less efficient search when the target is more similar to distractors (Sato et al., 2001). Saccade preparation is delayed in less efficient relative to more efficient visual search (Woodman et al., 2008). Requiring arbitrary stimulus-response mapping reveals more neuro-computational processes because it requires more operations that occupy different intervals including singleton selection, encoding the stimulus-response rule, and saccade endpoint selection (Sato et al., 2003; Schall, 2004).

Here, we present the second and third prerequisites. We have developed a filtering task that requires search on color and response on shape with factorial manipulations of singleton selection through singleton-distractor chromatic similarity and of stimulus-response mapping through stimulus elongation. We then provide the first demonstration that such tasks can be performed by macaque monkeys. We also show that performance can be analyzed using the methods of systems factorial technology producing results that support substantive inferences about the processing architectures underlying the performance. Importantly, the processing architectures discovered for

two monkeys differed. We regard this as a positive indication about the utility of systems factorial technology to discriminate different strategies. Using the large datasets provided through cognitive testing of macaque monkeys, we addressed other questions that have not been possible using systems factorial technology with the smaller datasets typical of human studies. These include relating processing architecture to the quality of performance and to the production of error responses. These novel results establish a foundation for neurophysiological investigation using the logic of separate modifiability and the tools of systems factorial technology, which will provide unprecedented insights into the neuro-computational mechanisms of visual search.

4.2 METHODS

4.2.1 Subjects, Surgical Procedures, and Gaze Acquisition

All procedures were approved by the Vanderbilt Institutional Animal Care and Use Committee in accordance with the United States Department of Agriculture and Public Health Service Policy on Humane Care and Use of Laboratory Animals.

Behavioral data were collected from two macaque monkeys, *Macaca mulatta* and *M. radiata*, identified as Le and Da. The monkeys weighed approximately 12 kg (Le) and 8 kg (Da) and were aged 6 years (Le) and 12 years (Da) at the time of the study. Monkeys were surgically implanted with a headpost affixed to the skull via ceramic screws under aseptic conditions with isoflurane anesthesia. Antibiotics and analgesics were administered postoperatively. Monkeys were allowed at least 6 weeks to recover following surgery before being placed back on task. Gaze was tracked using an Eyelink 1000 system (SR Research; sampling rate = 1,000 Hz).

4.2.2 Task Design and Protocol

Monkeys performed 30 sessions of a go-nogo visual search task in which response was cued by the shape of a color singleton. Trials began with the monkey fixating a central stimulus for 800-1200 ms, after which eight iso-eccentric, isoluminant stimuli were presented with eccentricity = 6.0 deg. Stimuli were either square or rectangular. All eight stimuli had the same shape on each trial. If the singleton and distractors were square, cueing a no-go trial, monkeys were rewarded for maintaining fixation at the central spot for 1000 ms. No-go trials comprised ~20% of all trials in each session. If stimuli were rectangular, monkeys were rewarded for shifting gaze to the singleton and maintaining fixation for 800 ms (monkey Le) or 1000 ms (monkey Da). The inter-trial interval was fixed at 2 sec.

Task difficulty varied along two dimensions (Figure 4.2): singleton-distractor color similarity and stimulus elongation. Singleton-distractor color similarity manipulated singleton identifiability. Stimulus elongation manipulated cue discriminability. All stimuli had four possible colors: red (CIE x 628, y 338, Y 4.4 or x 604, y 339, Y 5.2), off-red (CIE x 552, y 399, Y 4.5 or x 520, y 405, Y 6.6), green (CIE x 280, y 610, Y 4.6 or x 292, y 575, Y 6.1), and off-green (CIE x 322, y 558, Y 4.6 or x 364, y 426, Y 6.8) presented on a gray background (CIE x 275, y 228, Y 0.54 or x 334, y 375, Y 0.6). Stimuli had three possible aspect ratios: square for nogo trials, and either 1.4 or 2.0 for go trials. The orientation of elongation was counterbalanced between the two monkeys; for monkey Da a vertical rectangle signaled go, whereas for monkey Le a horizontal rectangle signaled go.

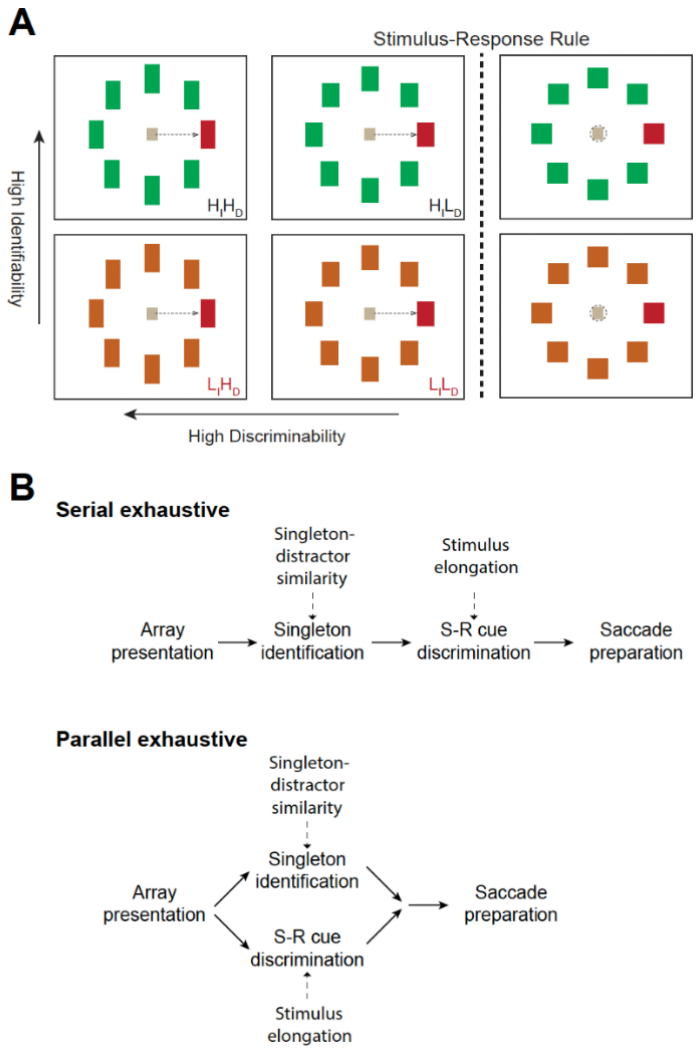

Figure 4.2. Visual search task designed to elucidate distinct operations. (**A**) Visual search task with go-nogo stimulus-response mapping. Six representative trial types are depicted. Correct gaze behavior is illustrated with dotted arrows for go trial saccades or dotted circle for nogo maintained fixation. The singleton is illustrated as always red and located on the right for purposes of illustration. Singleton shape cued the response rule. If the singleton was square (*right*), it cued withholding of the saccade. If the singleton was elongated (*left* and *middle*), it cued a pro-saccade. Two factors were manipulated independently. Stimulus-response cue discriminability was either High (aspect ratio = 2.0, $H_{Discrim}$ or H_D) or Low (aspect ratio = 1.4, $L_{Discrim}$ or L_D). On each trial, all distractors shared the degree of elongation with the color singleton. Singleton identifiability was either High (larger chromatic difference between singleton and distractors, H_{Ident} or H_I) or Low (smaller chromatic difference between singleton and distractors, L_{Ident} or L_I). The task offered 4 basic types of trials: High Identifiability and High Discriminability ($H_{Ident}H_{Discrim}$), Low Identifiability and High Discriminability ($L_{Ident}H_{Discrim}$), High Identifiability and Low Discriminability ($H_{Ident}L_{Discrim}$), and Low Identifiability and Low Discriminability ($L_{Ident}L_{Discrim}$). To assess the additivity and mutual invariance of these factors, trial types were interleaved in a 2x2 design. (**B**) Alternative processing architectures for the double factorial visual search task. Singleton identification is influenced by target-distractor similarity but not singleton elongation. Stimulus-response cue discrimination is affected by singleton elongation, but not target-distractor similarity. Under the serial exhaustive architecture (top), singleton identification is completed before cue discrimination, which must then be completed before production of the response. Under the parallel exhaustive architecture (bottom) singleton identification and cue discrimination operate concurrently and must both finish before production of the response.

4.2.3 Assessment of Operations, Stages and Strategies

To assess alternative process architectures supporting performance of this task, we applied systems factorial technology (Harding et al., 2016; Houpt et al., 2014; Townsend & Nozawa, 1995). Statistical details of systems factorial technology and reporting conventions can be found in these references. Systems factorial technology typically requires a 2x2 manipulation of factors that selectively influence distinct processing operations (cf. Yang et al., 2014). As illustrated in Figure 4.2, the first manipulation was *singleton identifiability* through interleaved presentation of search arrays with low singleton-distractor similarity (e.g., red among green) (High Identifiability, H_{Ident}) and search arrays with high singleton-distractor similarity (e.g., red among off-red) (Low Identifiability, L_{Ident}). The second manipulation was *cue discriminability* through interleaved presentation of array items with higher aspect ratio (High Discriminability, $H_{Discrim.}$) and array items with lower aspect ratio (Low Discriminability, $L_{Discrim.}$). The cue discrimination was enforced by interleaving 20% nogo trials. This 2x2 design results in four types of trial. The easiest were High Identifiability with High Discriminability ($H_{Ident}H_{Discrim.}$). The most difficult were Low Identifiability with Low Discriminability ($L_{Ident}L_{Discrim}$). The two intermediate difficulty were Low Identifiability with High Discriminability ($L_{Ident}H_{Discrim}$) and High Identifiability with Low Discriminability ($H_{Ident}L_{Discrim}$).

4.2.4 Statistical Analyses

All t-tests presented are two-sided, unless otherwise stated. ANOVA were calculated on across-session mean response times and accuracy rates. Also, to account for incidental variation across sessions while preserving relative relationships between conditions,

ANOVA were repeated with per-session response times after subtracting the session mean from each response time (*adjusted session means*). To avoid edge effects, accuracy rates were transformed using the logit transformation (Warton & Hui, 2011).

4.3 RESULTS

Each monkey performed 30 sessions of the search task. On average, Da performed 649 correct trials per session providing a total of 19470 correct trials, and Le performed 642 correct trials per session, providing a total of 19260 correct trials.

4.3.1 Monkeys are Sensitive to Cue Discriminability and Singleton Identifiability

Response times (RT) of both monkeys were affected by both task manipulations. The RTs for each condition are plotted in Figure 4.3A and listed in Table 4.1. As expected, response times were longer for trials in which the singleton was more chromatically similar to distractors and thus harder to identify. Likewise, response times were longer when the cue was less discriminable. These differences were statistically significant when evaluated as simple session means or when accounting for variation in means

Table 4.1. Response time mean ± SD (ms) and associated ANOVA table.

				Predictor	Sum of squares	df	Mean square	*F*	*p*
Monkey Da				**Session mean**					
		Cue discrimiminability		Discriminability	83,468.7	1	83,468.7	234.6	0.000
		High	Low	Identifiability	38,471.7	1	38,471.7	108.1	0.000
Singleton identifiability	High	206 ± 15	266 ± 29	Discriminability × Identifiability	1754.7	1	1754.7	4.9	0.028
	Low	249 ± 13	295 ± 14	Error	41,274.0	116	355.8		
				Adjusted session mean					
				Discriminability	83,468.7	1	83,468.7	535.1	0.000
				Identifiability	38,471.7	1	38,471.7	246.6	0.000
				Discriminability × Identifiability	1754.7	1	1754.7	11.2	0.001
				Error	18,094.8	116	156.0		
Monkey Le				**Session mean**					
		Cue discriminability		Discriminability	41,155.0	1	41,155.0	65.3	0.000
		High	Low	Identifiability	38,966.6	1	38,966.6	61.8	0.000
Singleton identifiability	High	213 ± 11	242 ± 23	Discriminability × Identifiability	1577.8	1	1577.8	2.5	0.116
	Low	241 ± 11	286 ± 42	Error	73,131.6	116	630.4		
				Adjusted session mean					
				Discriminability	41,155.0	1	41,155.0	170.2	0.000
				Identifiability	38,966.6	1	38,966.6	161.1	0.000
				Discriminability × Identifiability	1577.8	1	1577.8	6.52	0.012
				Error	28,054.8	116	241.8		

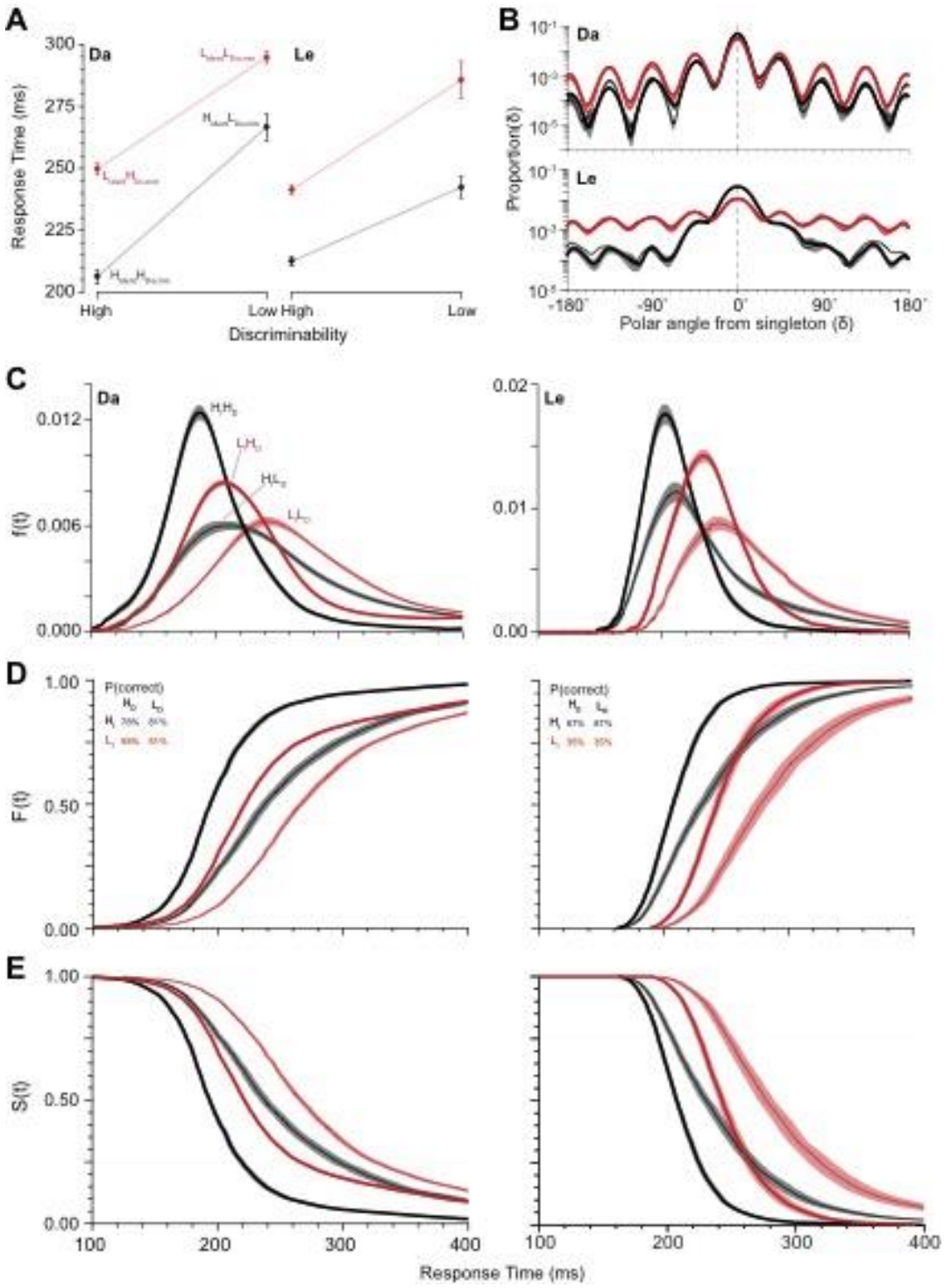

Figure 4.3. **Basic performance measures.** (**A**) Mean RT ± SEM for each trial type of the double factorial paradigm. There were four trial types: $H_{Ident}H_{Discrim}$, $H_{Ident}L_{Discrim}$, $L_{Ident}H_{Discrim}$, and $L_{Ident}L_{Discrim}$ Trials with High and Low singleton identifiability are shown in black and red, respectively. Monkey Da exhibited under-additivity of RT, whereas monkey Le exhibited over-additivity of RT across the two manipulations. (**B**) Log plot of the probability density of saccade endpoints relative to singleton location for High (black) and Low (red) singleton identifiability and High (bold) and Low (thin) cue discriminability. Spacing between search stimuli was 45˚ in polar angle. Both monkeys exhibited higher incidence of error saccades to the location adjacent to the singleton. Error bands are SE across sessions. (**C**) Probability density of RT, f(t). (**D**) Cumulative distribution of RT, F(t). Percent correct for each trial type is inset. (**E**) Survivor function of RT, S(t) = 1 – F(t).

across sessions (Table 4.1). In session means we found a significant interaction of the

factors for monkey Da but not Le. In adjusted session mean values, the interaction was evident for both monkeys.

The endpoints of errant saccades were not distributed randomly and were thus informative. Both monkeys made false alarm saccades toward the color singleton when it was a square (Da: 11.5 ± 5.2% H_{Ident}, 11.3 ± 3.3% L_{Ident}; Le: 26.7 ± 15.0% H_{Ident}, 7.2 ± 7.1% L_{Ident}). This demonstrates that squares and the less elongated rectangles were sufficiently similar to invoke cue discriminability confusion.

Saccade endpoint was affected more by singleton identifiability than by shape discriminability (Figure 4.3B, Table 4.2). As expected, accuracy was significantly higher under high identifiability relative to low identifiability for both monkeys. However, the effect of cue discriminability on saccade endpoint accuracy was different for the two monkeys. Monkey Le was equally accurate when stimulus shape was more or less discriminable. Curiously, monkey Da was more accurate when stimulus shape was less discriminable. Finally, as observed previously (e.g., Findlay, 1997), on error trials both monkeys more commonly shifted gaze to a distractor adjacent to the color singleton (Figure 4.3B).

The average trends are commonly all that is reported. However, the approach we will use begins with recognizing that singleton identifiability and cue discriminability influenced the shape of the RT distributions. To prepare for the systems factorial

Table 4.2 Percent correct mean ± SD (%) and associated ANOVA table

				Predictor	Sum of squares	df	Mean square	*F*	*p*
Monkey Da				**Logit transformation**					
		Cue discrimiminability		Discriminability	1.26	1	1.26	9.25	0.000
		High	Low	Identifiability	42.92	1	42.92	315.26	0.003
Singleton identifiability	High	78.3 ± 4.4	80.6 ± 4.2	Discriminability × identifiability	0.12	1	0.12	0.91	0.343
	Low	51.2 ± 10.0	57.6 ± 11.4	Error	15.79	116	0.1361		
Monkey Le				**Logit transformation**					
		Cue discriminability		Discriminability	0.01	1	556.10	0.04	0.850
		High	Low	Identifiability	209.50	1	0.04	843.65	0.000
Singleton identifiability	High	87.2 ± 5.4	86.9 ± 5.6	Discriminability × identifiability	0.00	1	< 0.001	< 0.001	0.968
	Low	35.1 ± 7.2	35.5 ± 10.0	Error	28.81	116	66.60		

analysis, we illustrate the variation of the RT distributions in three formats. The first is the simple probability density ($f(t) = Prob(t < RT < t+\Delta t)$), which is the probability of a response at a given time (Figure 4.3C). The second is the cumulative distribution ($F(t) = \int f(t)dt = Prob(RT \leq t)$), which is the probability of a response being produced at a time less than or equal to t (Figure 4.3D). The third is the survivor function ($S(t) = Prob(RT > t) = 1 – F(t)$), which is the probability that a response has not yet been produced by time t (Figure 4.3E). The influence of both factors on the shape of these distributions is clear for both monkeys. However, much deeper computational insights are available through the next analytical steps.

4.3.2 Systems Factorial Technology-Based Assessment of Visual Search Performance

Systems factorial technology is used to assess processing stage architecture and performance strategy by analyzing the RT distributions of each condition within a 2x2 factorial design (Harding et al., 2016; Houpt et al., 2014; Houpt & Townsend, 2010; Townsend & Nozawa, 1995). Given that each factor (singleton identifiability and cue discriminability) affected RT, we assessed the manner in which one factor affected RT while the other factor was fixed. In other words, how stimulus shape affects RT on trials with dissimilar singleton and distractors may or may not be the same as how shape affects RT on trials with similar singleton and distractors.

To illustrate the rationale and implementation of systems factorial technology, we performed a system of simple simulations (Figure 4.4). The 5 alternative architectures were simulated with pairs of linear accumulators embodying two processes, designated **A** and **B** (S. D. Brown & Heathcote, 2008; Carpenter & Williams, 1995)**.** The finishing times of the accumulators were determined by four parameters: threshold, drift rate, drift

rate variability, and non-decision time. To simplify, both accumulators shared an

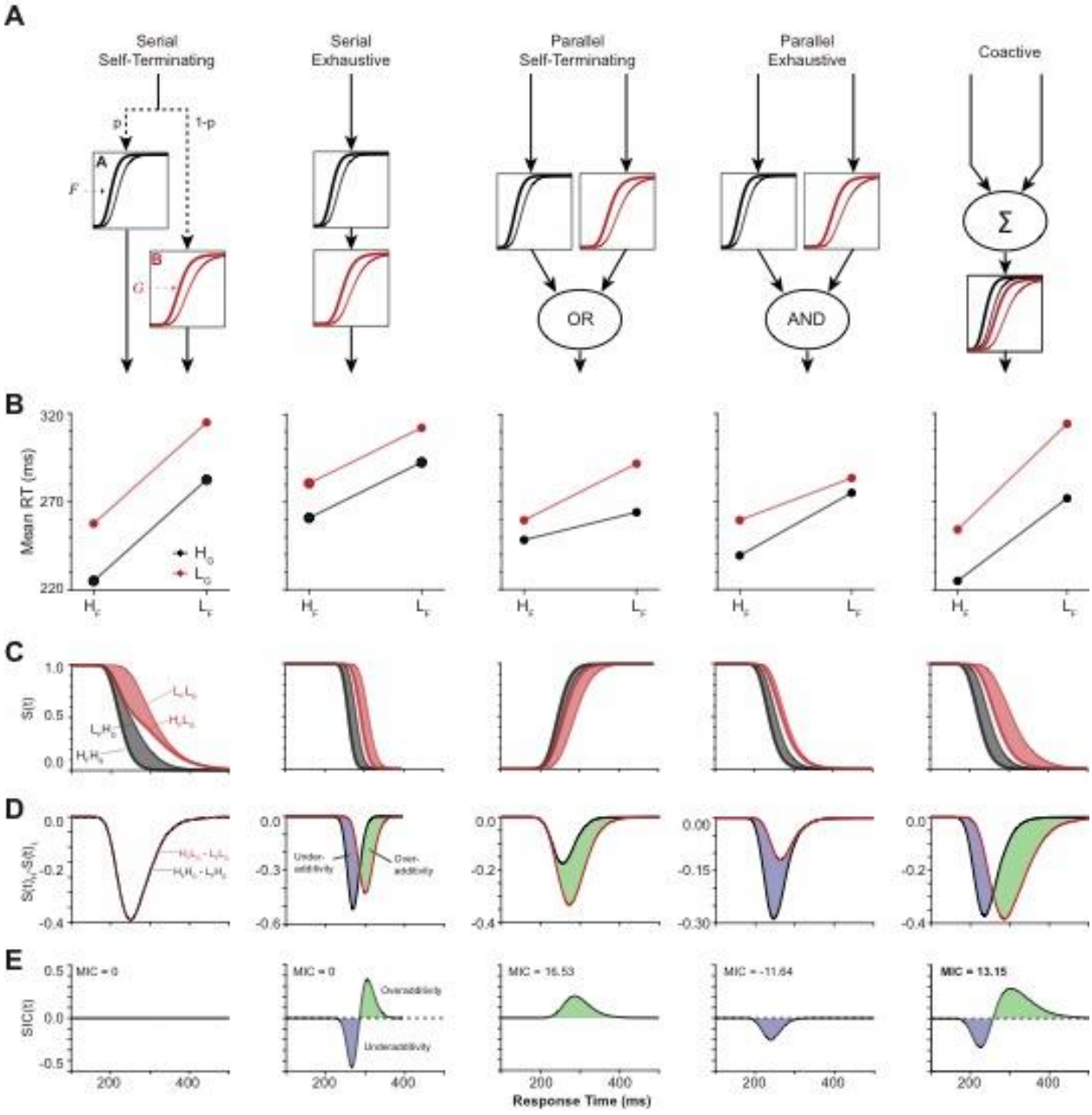

Figure 4.4. Systems factorial technology simulations. (**A**) Each of five processing architectures were modeled using two simple linear accumulator models, each representing an independent operation or stage. The two operations, A and B, were assumed to be under the selective influence of Factors *F* and *G*. Stage A varied with Factor *F* (but not *G*), and Stage B varied with Factor *G* (but not *F*). Essential features of each architecture are shown with depictions of relative stage durations. (**B**) Mean interaction contrast. Plots of mean RT for each trial type of the double factorial setup. Lines in red and black refer to Low and High levels of Factor *G*. (**C**) Survivor function *S(t)* for each trial type. The gray and red shadings highlight the effects of Factor *F* on *S(t)* at fixed levels of Factor *G*. (**D**) Difference in survivor function *S(t)* for fixed levels of Factor *G*. Regions of blue and green denote intervals of underadditivity and overadditivity, respectively. (**E**) Survivor interaction contrast *S(t)*. The serial self-terminating architecture produced a SIC that did not differ from 0.0 for all time. The serial exhaustive architecture produced a SIC that deviated to under-additivity followed by over-additivity, with equal area under each region. The parallel self-terminating architecture produced a SIC with overadditivity. The parallel exhaustive architecture produced a SIC with underadditivity. The coactive architecture produced a SIC that deviated to underadditivity followed by overadditivity, with greater area under the overadditive region for net overadditivity.

equivalent arbitrary threshold and a non-decision time of zero. An arbitrary mean drift rate was assigned for the more efficient condition of each factor, and a slower drift rate was assigned for the less efficient condition of each factor. Each manipulation was also assigned identical drift rate variability. For the combined manipulation, the drift rate effects were added. Each replicate for each condition had a drift rate sampled from a normal distribution centered on the assigned mean drift rate and with a standard deviation of the assigned drift rate variability. The parameters of each simulation were adjusted to produce similar ranges of RT. The resultant process durations were assessed by 10000 random samples defined by each manipulation's drift rate parameterization.

We explore the influence of two factors, designated F and G, either of which can cause higher (H) or lower (L) efficiency. For example, factor *F* could be identified with singleton-distractor similarity that influences the duration of singleton identification (process **A**), and factor *G* could be identified with singleton elongation that influences the duration of response cue discrimination (process **B**). Importantly, depending on task demands not all processing architectures are candidates for task performance. For example, if a response is specified by a conjunction of two features, self-terminating architectures will result in high error rates. Conversely, if a response can be determined from a single source of information and not necessarily both, exhaustive architectures will result in inefficient performance. Nevertheless, because no particular task is being modeled in these simulations, SFT can be applied to simulated outcomes produced by all 5 architectures. We present these simulations to aid in conceptualizing the differences in the architecture details and in recognizing how the signatures of each

architecture are produced. We now present the 5 possible processing architectures resolved by SFT.

Consider first processes **A** and **B** as serial self-terminating processes (Figure 4A). The two processes are queued sequentially, but only one needs to be completed for the overt response to be produced. Formally, the order of sub-processes is unknown and random. The two levels of factor *F* result in two distributions of process finishing times that overlap but have different modal values. Similarly, the two levels of factor *G* result in two distributions of finishing times that overlap but have different modal values. In this architecture, RT on each trial corresponds to the finishing time of the fastest process. Of course, process **A** or **B** might finish first on a given trial, but on average the systematic variation of RT will depend on the influence of the respective factors on each process. Crucially, under this architecture the influence of each factor on each process is independent. This results in mutually invariant, additive differences in average RT (<RT>) of both processes across both factors. In other words, a plot of average RT produced for each combination of the 2x2 design will produce parallel relations with no interaction across factors. The nature of the interaction across factors can be summarized by a value known as the *Mean Interaction Contrast* (MIC), which is calculated as

$$MIC = (\langle RT \rangle_{HH} - \langle RT \rangle_{HL}) - (\langle RT \rangle_{LH} - \langle RT \rangle_{LL}).$$

In this formula $\langle RT \rangle_{HH}$ is the mean RT on trials with both factors allowing high efficiency for their respective processes, which tends to make it the smallest value. In comparison, $\langle RT \rangle_{LL}$ is the mean RT on trials with both factors allowing low efficiency for their respective processes, which tends to make it the largest value. Likewise, $\langle RT \rangle_{HL}$ and

$\langle RT \rangle_{LH}$ are the mean RT on trials with one factor allowing high efficiency for its process with the other factor allowing only low efficiency for its process, which tends to make these intermediate values.

For the serial self-terminating processes, MIC = 0, which indicates perfect additivity of the underlying processes. Non-zero values of MIC signify an interaction among the processes. Such an interaction can be underadditive (MIC < 0) or overadditive (MIC > 0). MIC > 0 identifies either parallel self-terminating or coactive process architectures, and MIC < 0 identifies parallel exhaustive processes. Thus, the MIC offers some insight into the nature of the interaction between sub-processes. However, MIC cannot discriminate between the self-terminating or exhaustive stopping rules for serial architectures or discriminate between coactive and parallel self-terminating architectures (Townsend & Nozawa, 1995).

Further insight is available through examination of the production of responses through time across conditions. The effects of the combination of conditions can be assessed as a function of time over the production of the responses by measuring the difference of the survivor functions. The justification and rationale for this approach is detailed by Townsend and colleagues (Houpt et al., 2014; Houpt & Townsend, 2010; Townsend & Nozawa, 1995). The purpose of the analysis is to determine the extent to which the two levels of each factor influence the rate of response production through time. This is quantified by measuring the difference between response production when one factor is highly efficient (H_F) and when it is less efficient (L_F), while the other factor is more (H_G) or less (L_G) efficient.

The interaction between the two manipulations is known as the *survivor interaction contrast (SIC).* The SIC is a distribution-free measure for assessing the architecture (i.e., serial or parallel) and stopping rule (i.e., race minimum time or exhaustive maximum time) of information processing, which indexes the difference in levels of *G* between the levels of *F*, is calculated similar to the MIC by subtracting the two resulting difference functions over time:

$$SIC(t) = [S_{HH}(t) - S_{HL}(t)] - [S_{LH}(t) - S_{LL}(t)]$$

where $S_{HH}(t)$ is the value of the survivor function at time t when both factors are more efficient (H_FH_G), $S_{LL}(t)$ is the value of the survivor function at time t when both factors are less efficient (L_FL_G), $S_{HL}(t)$ is the value of the survivor function at time t when factor *F* is more efficient and factor *G* is less efficient (H_FL_G), and $S_{LH}(t)$ is the value of the survivor function at time t when factor *F* is less efficient and factor *G* is more efficient (L_FH_G). These operations are commutative thus the effect of varying *G* with respect to varying *F* is expected to be equivalent. The SIC measures the interaction contrast throughout the duration of all processes. The basic concepts of additivity, underadditivity, and overadditivity apply to the SIC; they just apply through time. Under the assumptions of systems factorial technology (e.g., stochastic independence of the processes), the form of SIC(t) is diagnostic of the 5 processing architectures. The statistical issues involved in evaluating SIC curves have been detailed (Houpt & Townsend, 2010).

The purely additive influence of factors in the serial self-terminating architecture result in SIC values that do not vary over time. However, the SIC produced by the other 4 architectures varies through time, each producing a different pattern of variation.

Accordingly, the pattern of variation of the SIC curves can diagnose which underlying architecture produced a given pattern of RTs in the 2x2 factorial experimental design.

Consider next the serial exhaustive architecture. The processes are queued sequentially and the overt response is produced only when both processes have finished. Formally, the order of processes is unknown and SFT is unable to identify which one acted first. The mean RTs across factors exhibit no sign of interaction, so the MIC = 0 for this architecture as well. However, through time this architecture produces first underadditivity then overadditivity. That is, the SIC exhibits a negative-going followed by a positive-going deflection. Importantly, to satisfy the requirement that MIC = 0, the areas under the negative-going and positive-going deflections are equivalent. This time varying SIC is then used to resolve ambiguities when MIC = 0.

Consider next the parallel self-terminating architecture. Both processes operate simultaneously, so a stopping rule must be specified. Specifically, if a response can be made when one stage is complete, then the combined process is parallel self-terminating. In this architecture, the overt response is produced as soon as either process finishes. This architecture is also known as a race and predicts overadditivity. Thus, MIC > 0, and the SIC curve deviates only positively.

Consider next the parallel exhaustive architecture in which a response can only be made when both stages are complete. Both processes operate simultaneously, but the overt response is produced only after both processes have finished. This architecture predicts underadditivity. Thus, MIC < 0, and the SIC curve deviates only negatively. The performance of one of the monkeys will have this appearance.

Consider finally the coactive architecture. While more complex and less explicit in form, it can be distinguished in function through these methods. In this architecture processes interact in a manner that can be characterized as finer grain coordination such as summation of the respective states through time. This can be realized if neither of the two processes **A** nor **B** produce the overt response but instead provide activations to a third process that sums the activations from **A** and **B** and thereby produces the overt response. This architecture, like a serial exhaustive architecture, predicts first underadditivity and then overadditivity. However, unlike a serial exhaustive architecture, for the co-active architecture, MIC > 0. Therefore, the area under the positive-going, over-additive deflection is greater than the area under the negative-going under-additive deflection and the architecture predicts a net overadditivity. Accordingly, although this architecture has an initial negative dip and a positive deflection (like serial processing) and has an MIC greater than 0 (like parallel self-terminating), the combination of SIC and MIC differentiates it from either of these other architectures. The performance of another monkey will have this appearance.

4.3.3 Processing Architectures Supporting Visual Search

We applied systems factorial technology to the visual search data obtained from two macaque monkeys. Figure 4.5A presents mean survivor functions for each level of the 2x2 factorial design for each monkey. At a fixed level of singleton identifiability, the difference between survivor functions represents the effect of shape discriminability. Figure 4.5B plots the difference in survivor functions for each level of singleton identifiability. The shape of these differences reveals the effect of the separate factors on response production through time. Figure 4.5C plots the difference of these

differences, which is the survivor interaction contrast (SIC). The SIC summarizes the influence of the two factors through time. We will report SIC results by first describing the shape of the curve, then reporting the MIC, then reporting the inferred architecture.

For monkey Le, the SIC exhibited a pronounced period of underadditivity followed by a prolonged period of overadditivity. The integral of the period of

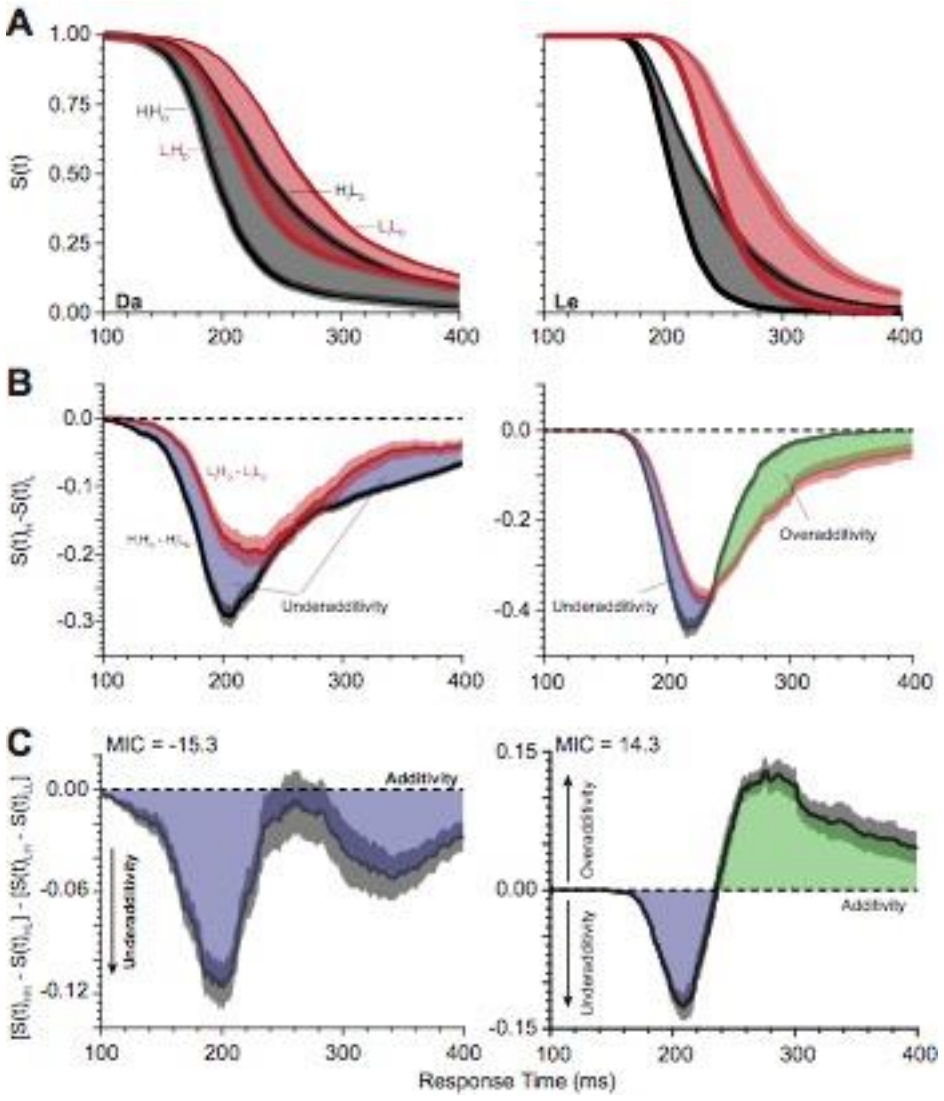

Figure 4.5. Systems factorial analysis of RT distributions from the double factorial visual search task. (**A**) Survivor functions *S(t)* for each combination of singleton identifiability and cue discriminability. Black and red lines depict High and Low singleton identifiability. Thick and thin lines depict High and Low cue discriminability. The difference between survivor functions for High and Low cue discriminability is shaded in black (High singleton identifiability) and red (Low singleton identifiability). (**B**) Difference between survivor functions for High and Low cue discriminability, computed at fixed levels of singleton identifiability. Shaded regions represent period of underadditivity (blue) and overadditivity (green) for Low (red) and High (black) singleton identifiability. Error regions are SE across sessions. (**C**) Survivor interaction contrast curves. The SIC curve for monkey Da was exclusively sub-additive, consistent with the parallel exhaustive architecture. The SIC curve for monkey Le exhibited a change from under- to over-additivity, consistent with the parallel coactive architecture.

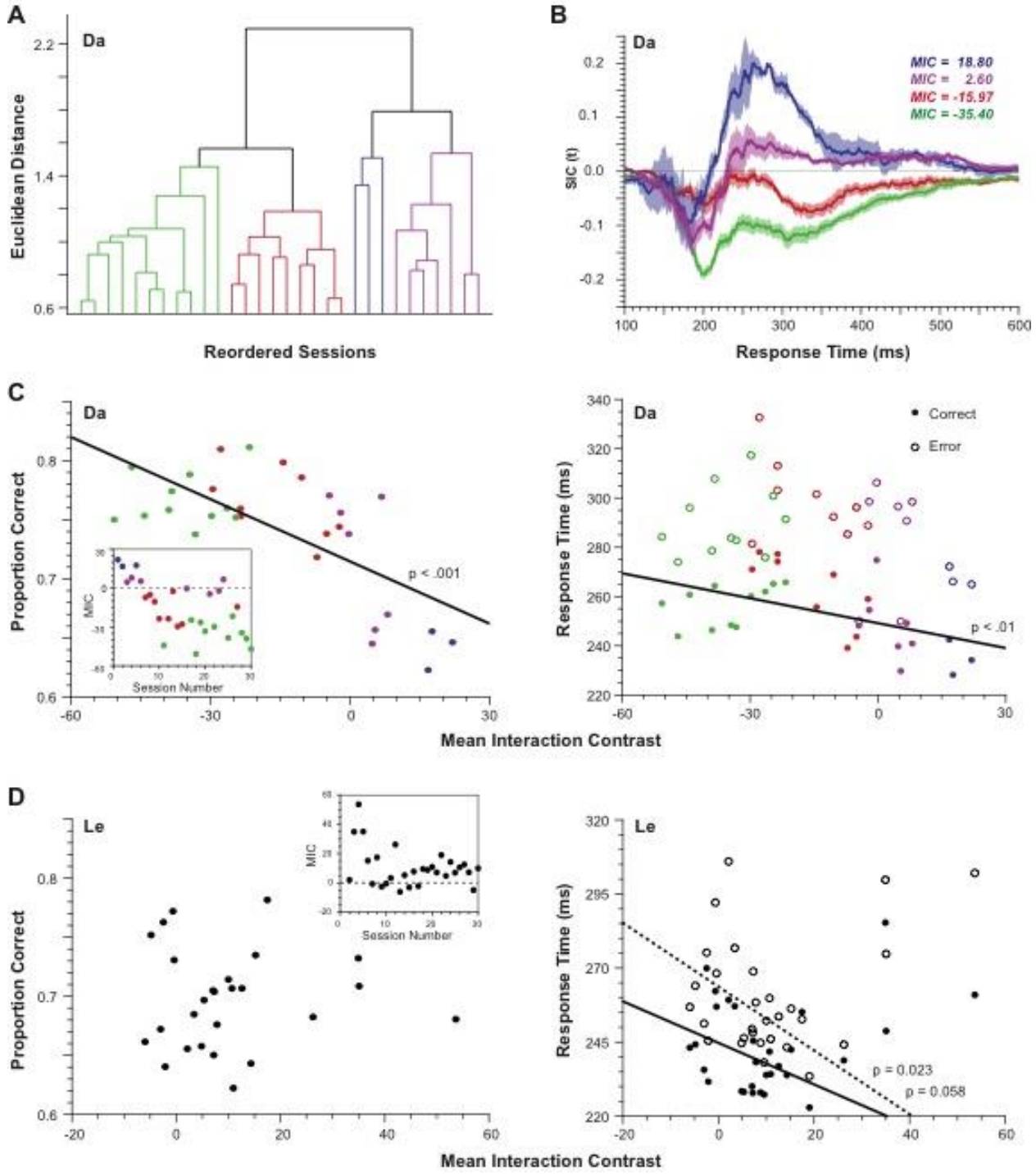

Figure 4.6. **Variation of performance across sessions.** (**A**) Dendrogram resulting from clustering of SIC curves across sessions for monkey Da based on Euclidean distance. Four clusters were evident, suggesting the use of different strategies. (**B**) Form of the four clusters of SIC curves. Two (blue, magenta) corresponded to the co-active architecture, and two (red, green) were unlike the SIC of any architecture. (**C**) (*left*) Proportion correct as a function of MIC across sessions for monkey Da. A strong correlation was observed. MIC across session number inset. Points are colored in accordance with their cluster identity. (*right*) Mean RT for correct (filled) and error (open) trials as a function of MIC across sessions. Error RT were longer than correct RT, and a strong correlation with MIC was observed for correct but not error RT. (**D**) (*left*) Proportion correct as a function of MIC across sessions for monkey Le. MIC across session number inset. A significant correlation was not observed. (*right*) Mean RT for correct (filled) and error (open) trials as a function of MIC across sessions. Error RT were longer than correct RT, and a correlation with MIC was observed for error RT and a trend toward correlation with MIC was observed for correct RT.

overadditivity exceeded that of the underadditivity, indicative of a positive mean

interaction contrast (MIC = 14.3). This outcome is characteristic of the coactive processing architecture (Figure 4.4, fifth architecture).

For monkey Da, the SIC exhibited only a prolonged underadditive deflection with MIC = -15.3. This outcome is characteristic of the parallel exhaustive architecture (Figure 4.4, fourth architecture). Note that neither monkey exhibited a self-terminating architecture. This is reassuring because a correct response requires both singleton identification and cue discrimination. Either serial or parallel self-terminating architectures would produce a response with only half of the necessary information and thus nearly chance performance.

SFT analyses are typically performed on a per-subject basis rather than the present repeated testing across many sessions that can be done with monkeys. Thus, it is possible that the performance strategy associated with different processing architectures or dynamics varies across sessions. If so, then the multiphasic SIC curves could be artifacts of averaging sessions performed with different strategies. To assess whether the average SIC curve is a mixture of multiple architectures across different sessions, we performed a hierarchical agglomerative cluster analysis of SIC curves. We contrasted the use of Euclidean distance, which emphasizes the magnitudes of the SIC curves, and correlation distance, which emphasizes the shapes of the SIC curves, as similarity metrics.

For monkey Da, using Euclidean distance as the similarity metric, we identified four clusters (Figure 4.6A). Using correlation distance as a similarity metric was less discriminating. We believe this indicates that the major differences in SIC are in magnitude rather than shape. To examine the systematic variability across sessions, we

plotted the SIC for each cluster (Figure 4.6B). With MIC > 0 and a later overadditive deflection exceeding the early underadditive deflection of the SIC, two of the clusters identified the coactive architecture. With MIC < 0 and only underadditive SIC deflections, the other two clusters identified the parallel exhaustive architecture. Notably, the biphasic SIC was evident in individual clusters. Even the most clearly underadditive SIC cluster had bimodal characteristics.

For monkey Le, neither Euclidean nor correlation distance yielded distinct clusters. The coactive architecture was identified by the MIC values and SIC forms from each session, although MIC magnitude varied across sessions.

The variation in MIC values across sessions offers a unique opportunity to assess whether qualitative or quantitiative differences in processing strategies result in predictable differences in performance. Hence, we examined the relationship between the per-session MIC, accuracy and response times (Figure 4.6C). For monkey Da, we found a significant negative correlation between percent correct and MIC ($r = -0.69$, $p < 0.001$). We also found a significant negative correlation between RT of correct responses and MIC ($r = -0.49$, $p < 0.01$). However, we found no relationship between MIC and RT on error trials ($r = -0.30$, $p = 0.11$).

For monkey Le, some early sessions had MICs much greater than the majority of sessions. Treating these as outliers, we found no relationship between percent correct and MIC ($r = -0.21$, $p = 0.32$), but RT and MIC trended toward a significant negative correlation for correct RTs ($r = -0.38$, $p = 0.058$) and were significantly negatively correlated for error trials ($r = -0.45$, $p = -0.022$). Relationships like these have not been reported before.

4.3.4 Processing Architectures for Correct and Error Performance

SFT analyses commonly assume a low error rate. The performance of our monkeys had relatively high error rates. However, other investigators have demonstrated that conclusions from SFT are reliable in spite of error rates approximating what we obtained (Fifić et al., 2008a). We utilized the large amount of data obtained across sessions to investigate for the first time whether performance strategies differed between correct trials and errors. Given the prevalence of erroneous saccades to the distractor adjacent to the singleton, we distinguished two categories of errors. First, we will examine informed errors made to the stimulus adjacent to the singleton. Second, we will examine guess errors made to any other location.

Figure 4.7 illustrates the progression of distributions used for the SFT analysis for correct responses, informed errors, and guesses for both monkeys. The factorial manipulation trial types were assigned according to the configuration of the search array and not saccade endpoint. That is, H_I, L_I, H_D, and L_D were assigned with respect to the identifiability and discriminability of the singleton.

For monkey Da, both informed errors and guesses were generated with SIC deflecting only in the underadditive direction (MIC < 0), like the correct responses. Hence, like correct responses, errors were identified with the parallel exhaustive architecture. In other words, qualitatively a single architecture produced both correct and error responses. However, quantitatively, MIC for guesses was more underadditive than MIC for informed errors, which was more underadditive than MIC for correct responses. Also, the SIC for error responses was prolonged but lacked the pronounced

multiphasic pattern obtained from correct trials. Thus, the evidence suggested that

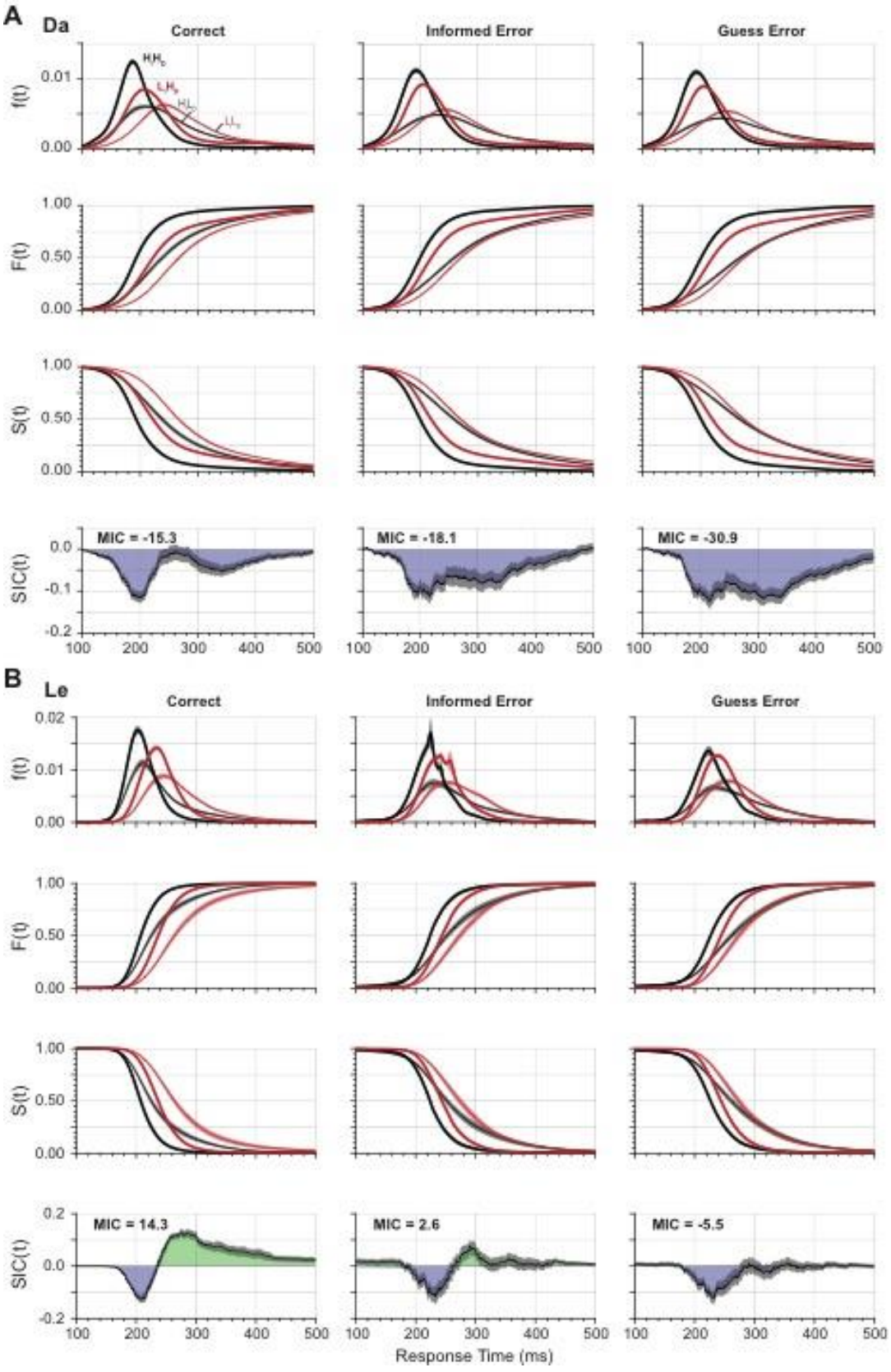

Figure 4.7. **SFT analysis for different trial outcomes.** (**A**) SIC curves derived from monkey Da performance on correct (left), informed errors adjacent to the singleton (middle) and guess errors (right). SIC curves for informed and guess errors exhibit more underadditivity relative to correct trials. All three SIC curves resemble that of the parallel exhaustive architecture. (**B**) SIC curves derived from monkey Le performance on correct (left), informed errors adjacent to the singleton (middle) and guess errors (right). SIC curves for errors exhibit more underadditivity (less overadditivity) relative to correct trials. The SIC curve for guess errors resembles the parallel exhaustive architecture, for informed errors, the serial exhaustive architecture, and for correct trials, the coactive architecture.

monkey Da employed similar architectures on both error and correct trials.

For monkey Le, we observed qualitative variation in MIC and SIC for error relative to correct trials. As noted, correct trial performance produced MIC and SIC values that identified the coactive architecture. However, for guess errors, the SIC deviated only in the underadditive direction (MIC < 0), which identify the parallel exhaustive architecture. Meanwhile, for the informed errors, the SIC deflected more in the under- than overadditive direction (MIC slightly greater than zero). This pattern seems to approximate at least the parallel exhaustive architecture. Thus, for monkey Le, errors may originate from a processing architecture different from that resulting in correct trials.

For both monkeys, although their overall SIC curves have different shapes, the MIC for correct responses (Da: MIC = -15.3; Le: MIC = 14.3) was more positive than the MIC for informed errors (Da: MIC = -18.1; Le: MIC = 2.6), which was more positive than the MIC for guess errors (Da: MIC = -30.8; Le: MIC = -5.5). It should be noted that for both monkeys this difference appears most pronounced around the time of the second negative peak in Da's biphasic SIC curve.

4.4 DISCUSSION

Through the present results, we have demonstrated the ability of monkeys to perform a speeded response task with 2x2 factorial manipulations of difficulty. To our knowledge, this is a first application of this experimental design in nonhuman primate research. We

have also demonstrated the utility of systems factorial technology in assessing behavioral responses to infer underlying processing architectures. These findings pave the way for developing studies in monkeys that are directly comparable to studies in humans and to extend investigation to the neurophysiology producing the performance. We discuss two potential limitations of these current results: inter-monkey differences and error-prone performance. We conclude that neither of these considerations undermines the utility of this new experimental approach for nonhuman primate cognitive neurophysiology. In fact, the inter-monkey differences highlight the utility of systems factorial technology in diagnosing visual search strategy. We then situate this work in the context of related research using other approaches.

4.4.1 Individual Differences Between Monkeys

We identified a plausible processing architecture for both monkeys. Technically, it should be noted that the approach could have resulted in implausible architectures. Interestingly, the results differed, indicating that the two monkeys used different strategies. While such lack of replication invites further research with more subjects, we believe useful insights are still available for two reasons. First, although both monkeys showed the same main effects of the factorial manipulations, subtle differences in RT distributions were evident across monkeys. However, in and of themselves, these differences offer no insights into the source of those differences. The use of systems factorial technology provided distinctively different results for both monkeys. This outcome offers additional inferences about the mechanisms producing the RT distributions.

Second, these different inferences provide starkly contrasting predictions for the neurophysiological underpinnings of this behavior. For example, for monkey Da, whose RT distributions suggest a parallel exhaustive processing architecture, separate populations of neurons may carry signals related to singleton identifiability or cue discriminability. In contrast, for monkey Le, whose RT distributions suggest a coactive processing architecture, one population of neurons may carry signals related to singleton identifiability and cue discriminability. These are just two of multiple alternatives that can be formulated but are beyond the scope of this paper. Further insights are available through quantifying the degree and timing of saccade preparation assessed through the activity of movement neurons (e.g., Bichot et al., 2001a; Hanes & Schall, 1996; Woodman et al., 2008).

The differences across monkeys could be due to one of two differences in the task. First, the two monkeys were required to fixate the search stimuli for different amounts of time. We doubt that this modest difference in fixation duration can explain the major difference in strategy. Because the fixation interval follows both array presentation and response time and are identical for all go-trial conditions, we do not see a mechanism by which this post-response fixation interval would affect the processing of the array during the trial. Still, further research can verify this supposition. Second, the elongated stimuli seen by Da were vertical whereas those seen by Le were horizontal. The orientations of the stimuli result in different edge-to-edge distances of stimulus pairs which may influence stimulus salience. We doubt that stimulus shape explains the difference in strategy. This rotation of the stimuli would be balanced across the two monkeys, where the edge-to-edge distance of the stimuli on the left and right for

monkey Da would be the same as the edge-to-edge distance of the stimuli on the top and bottom for monkey Le. Similarly, the stimuli on the top and bottom for Da have the same edge-to-edge distance as the stimuli on the left and right for Da. If this did explain the difference in processing architectures, then these stimulus location sets (Da: left/right, Le: top/bottom and Da: top/bottom, Le: left/right) should also be systematically different. We have compared results across these stimulus configurations and found no differences. Therefore, differences in array configuration cannot explain the differences in inferred processing architectures.

Further, the dissociation between parallel exhaustive and coactive architectures has been described previously. Fifić and colleagues (2008a) had human participants perform a multidimensional classification task for stimuli with dimensions that were either separable or integral. Performance during classification of separable-dimension stimuli was marked by the use of a parallel exhaustive architecture whereas performance during classification of integral-dimension stimuli was marked by the use of a coactive architecture. This performance strategy difference, revealed only through systems factorial technology, resembles the performance strategy difference identified here. Because the shape and chromatic dimensions of the current stimuli are different, they could be treated as separable dimensions. However, because both dimensions are carried by the same object they could be seen as integral. Monkey Da had performed several visual search tasks prior to this study in which shape and color cue different aspects of the response rules (Heitz & Schall, 2012; Reppert et al., 2018). This experience may enable the parallel exhaustive strategy by treating these feature dimensions separately. Monkey Le, on the other hand, had not performed other tasks

prior to this study and thus may integrate the two feature dimensions through a coactive strategy. Alternatively, monkey Le may have analyzed the distractors, or the whole array holistically, to determine the stimulus-response rule. If he did not individuate stimuli, this may also explain the coactive processing strategy, pooling all sources of information.

Many other investigators have addressed the problem of the architecture underlying visual search. All now agree that the slope of RT with set size is not an effective criterion. More complex tasks are needed. For example, previous work studying a wide variety of visual search displays with multiple targets concluded that whereas most search conditions are accomplished through parallel limited-capacity process, a few conditions require serial search (Thornton & Gilden, 2007; see also Moran et al. 2016). A previous investigation of visual search with manipulation of target-distractor similarity employed systems factorial technology (Fifić et al., 2008b). These authors reported systematic departure from parallel or serial processing and concluded that the results were consistent with co-active processing.

4.4.2 Potential Problems of Error-Prone Performance

Systems factorial technology generally assumes perfect or near-perfect performance, because errors can contaminate RT distributions through speed accuracy tradeoffs. However, performance was not perfect in the data presented here. Thus, it is valid to wonder whether the SIC calculations and processing architecture inferences are invalidated by contamination of errors. This seems unlikely for two reasons. First, the SIC curves for both monkeys are qualitatively similar to those obtained in several other studies in humans with low error rates. Thus, the inferences supported by the findings

are sensible in the context of separable and integral feature dimensions as discussed above.

Second, simulation approaches that are allowed to produce errors have shown that the MIC and SIC signatures are robust with moderately high error rates (Fifić et al., 2008a; Townsend & Wenger, 2004). Specifically, only the coactive architecture signatures degrade with errors by losing their overadditivity. However, such an outcome means that a coactive architecture would be mistakenly identified as serial exhaustive. Hence, if performance supports the inference of the coactive architecture in spite of high error rates, then this should only increase confidence in the validity of the inference. If anything, we suspect that the high error rate may have resulted in the uncharacteristic bimodality of the SIC curve for monkey Da, but the nature of this bimodality is not at odds with the overall inference of a parallel exhaustive architecture.

Further evidence that errors do not prevent interpretation of system factorial results is found in the interesting relationships we discovered between MIC and SIC values and error production. For monkey Da, although both error and correct responses arose from the same parallel exhaustive architecture, the magnitude of additivity assessed through MIC values was lower for errors relative to correct trials. This indicates that errors arose from quantitative, not qualitatively different processing. In contrast, for monkey Le, errors arose from qualitatively different processing. Correct trials arose from the coactive architecture, but errors arose from the parallel exhaustive architecture. We surmise, therefore, that rather than system factorial technology being challenged by errors, with large enough samples, errors can be interpreted by systems factorial technology. This is an innovative extension.

4.4.3 The Logic of Selective Influence, Additivity, Race Inequalities, and Systems Factorial Technology

As noted above, the overall goal of applying the logic of selective influence is to distinguish cognitive, motor, and sensory, or, more generally, computational processes. The experimental approach of creating dissociations to discover separable processes is well-known in ocular motor and visual neuroscience. For example, memory-guided saccades were devised to dissociate visual processing from saccade production (Bruce & Goldberg, 1985; Hikosaka & Wurtz, 1983). Double-step saccades were devised to dissociate retinal location and eye position in saccade production (Hallett & Lightstone, 1976). Anti-saccades are contrasted with pro-saccades to distinguish contributions of voluntary stimulus-response mapping (Hallett & Adams, 1980). Bistable visual stimuli afford a distinction between explicitly perceiving an object from simply responding to stimuli (Blake & Logothetis, 2002; Logothetis & Schall, 1989). Visual search was used to dissociate presentation of a stimulus in a neurons response field from that stimulus being the target of a saccade (Schall & Hanes, 1993). And so on.

The straightforward framing hypothesis that RT is the summation of functionally distinct stages (Donders, 1868) was challenged on multiple grounds during the early years of experimental psychology. Indeed, in the 1938 edition of his textbook *Experimental Psychology*, Robert S. Woodworth wrote, “If we cannot break up the reaction into successive acts and obtain the time of each act, of what use is the reaction time?” (page 310). However, this pessimistic conclusion was removed from a revised edition (Woodworth & Schlosberg, 1954). Further progress on inferring processing architecture from systematic variation of RT was sparked by the formulation of the additive factors method (Sternberg, 1969). To determine whether two factors affect the

same or separate stages, the method assesses additivity of mean response times and of their variances. When response times from two or more factors are additive, the factors are taken to affect separate independent stages.

The formulation of critiques (Townsend, 1972) and extensions (e.g., Ashby & Townsend, 1980; Schweickert, 1978; Taylor, 1976; Townsend, 1984) energized more sophisticated approaches to decomposing RT. For example, additive factors assumes a strictly serial architecture. As demonstrated in Figure 1, though, in a parallel architecture two factors can independently affect processing stages without affecting response times in an additive fashion. Today, the theoretical foundation and empirical effectiveness of the approach has been established in multiple research domains of experimental psychology and cognitive neuroscience (e.g., Sternberg, 2001; Townsend & Ashby, 1983).

Today, systems factorial technology offers the most complete method to infer processing architectures from performance of a double-factorial task (Townsend and Nozawa 1995). Here, we manipulated singleton identifiability by varying singleton-distractor similarity and cue discriminability by varying singleton elongation. Other factors can be manipulated, of course. Indeed, the selective influence approach enables discovery of which factors influence common or different sub-ordinate processes. In the context of visual search, additional factors that merit investigation include set size, feature conjunctions, inhibition of return, priming of popout, attentional capture, and stimulus-response mapping difficulty. For example, the relationship between singleton-distractor similarity and stimulus-response mapping could be assessed by adding an additional stimulus-response mapping rule, e.g. instructing pro-saccades or anti-

saccades (Sato & Schall, 2003). By iteratively and systematically testing the independence and interactions of pairs of factors, we will gain a deeper understanding of the existence of and relationships among the computational processes accomplishing visual search. Further validation would entail simulation as illustrated in Figure 4 and identification of neural signaling corresponding to the timing of the hypothetical constituent processes.

We should note that other, more specific approaches to inferring processing architecture and duration have been developed. For example, Miller (1982) described the race model inequality to distinguish between parallel channels and coactive processing. In this conception, if two sources of information are in separate parallel channels, then the probability of responding to two sources of information at a given time *t* must be less than the probability of responding to either individual source alone at time *t*. Otherwise, processing must be coactive. This model holds for self-terminating architectures, such as a race model, because it assumes that either piece of information can elicit a response. However, if both pieces of information are needed to produce a response, then this assumption does not hold and violations of the inequality do not necessarily indicate coactivity.

Similarly, Logan & Cowan (1984) used the race model formulation to explain performance of the stop signal (countermanding) task. This model affords estimation of the duration of a covert stopping process that happens to correspond precisely to the moment of modulation of particular sensory-motor neurons (Costello et al., 2013; Hanes et al., 1998; Mallet et al., 2016; Murthy et al., 2009; Paré & Hanes, 2003). The relationship between the abstract race model and the neurophysiological findings was

elucidated through development and validation of the interactive race model (Boucher et al., 2007; Logan et al., 2015).

Systems factorial technology improves upon both of these methods by distinguishing self-terminating and exhaustive stopping rules and is not limited to additivity which allows the assessment of both serial and parallel processing architectures. Thus, if an experiment can be designed such that the response times are amenable to systems factorial technology, it is the more powerful method because it can differentiate all possibilities. Ultimately, we believe that similar mappings between abstract model architectures and neural processes can be achieved using the logic of selective influence and the tools of systems factorial technology.

4.4.4 Conclusions

RT in complex tasks is the summation of functionally distinct operations or stages. While not emphasized, the stage assumption is fundamental to the predominant model of “decision- making” – a single sequential-sampling process intervening between uninteresting visual encoding and response production stages. Such models explain performance and account for neural activity in visual discrimination tasks as well as visual search with direct stimulus-response mapping. But, if RT is not comprised of dissociable stages, then models like drift diffusion may be disqualified and alternative models are endorsed, such as cascade (e.g., McClelland, 1979) or asynchronous discrete flow (Miller, 1988), which are qualitatively different mechanisms.

The most effective and perhaps only method for assessing the existence and characterizing the properties of modules or stages is the logic of separate modifiability. Crucially, single-stage decision-making models cannot explain tasks that require

multiple, sequential operations. The term “decision” is hopelessly ambiguous when applied to a task that requires a “decision” about the location of a color singleton, a “decision” about the shape of the singleton, a “decision” about the shapes of distractors, a “decision” about the congruency of the singleton and distractor shapes, a “decision” about the instructed stimulus-response mapping, a “decision” about the correct endpoint of the saccade, and a “decision” about when to initiate the saccade. We have established that macaque monkeys can perform a task with simultaneous, independent factorial manipulations, producing performance measures that produce interpretable outcomes using the most advanced computational analytical approaches. This paves the way for a next step in cognitive neurophysiology of visual search by providing the ability to assess whether individual neural processes are prolonged, more numerous, or interacting.

CHAPTER 5: SEQUENTIAL OPERATIONS REVEALED BY SERENDIPITOUS FEATURE SELECTIVITY IN FRONTAL EYE FIELD

5.0 SUMMARY

In Chapters 2 and 3, I characterized functional neural diversity by way of a consensus clustering algorithm. In Chapter 4, I characterized the cognitive architectures underlying the GO/NO-GO search task by way of SFT and workload capacity analyses. To complete the link between observations at the neural and behavioral levels, we must first establish that some categories of neurons instantiate cognitive operations. In this chapter, I analyze FEF neural responses during a related pro-/anti-saccade search task (Sato & Schall, 2003). Specifically, by leveraging an imbalanced stimulus-reward contingency across stimulus features, I identify separate, sequential stimulus selection and saccade selection processes in visually responsive FEF neurons. This identification demonstrates the ability to define neural indices of the finishing times of separate cognitive operations. This chapter has been uploaded to bioRxiv as Lowe & Schall (2019).

5.1 INTRODUCTION

To navigate in and interact with the visual world, primates must locate and identify objects to scrutinize through gaze. To understand how this localization, identification and gaze shifting is performed, we use visual search tasks in which targets for gaze shifts are presented with distracting stimuli. Target stimuli can be distinguished from distractors by some feature or set of features (Wolfe & Utochkin, 2019). Targets are

sought through an interplay of localization, identification, and saccade preparation manifest as covert and overt orienting.

The frontal eye field (FEF), in prefrontal cortex, is known to support attention and eye movements and the performance of visual search (see Bisley & Mirpour, 2019; Schall, 2015 for review). Neurons in FEF respond to visual stimulation, before eye movements, or both (Bruce & Goldberg, 1985; Lowe & Schall, 2018; Schall, 1991). FEF has been conceptualized as a salience or priority map (Bisley, 2011; Fernandes et al., 2014; Thompson & Bichot, 2005), meaning that its responses are related to whether a stimulus is important for attention or gaze shifts regardless of what features make it important (Mohler et al., 1973; Monosov et al., 2010; Ogawa & Komatsu, 2006; Ramkumar et al., 2016; Schall et al., 1995a; Zhou & Desimone, 2011). However, FEF is also an ocular motor center (Schall, 2015). Therefore, experimental manipulations are needed to dissociate selection of a stimulus as a conspicuous object, selection of a stimulus as a potential endpoint of a gaze shift, or preparation of a saccade (Matsushima & Tanaka, 2014; Murthy et al., 2001; Sato et al., 2001; Sato & Schall, 2003; Scerra et al., 2019; Thompson et al., 1996; Trageser et al., 2008; c.f. Costello et al., 2013).

Our laboratory designed a visual task to dissociate localization of a color singleton from the endpoint of a saccade reporting its location (Sato & Schall, 2003; Schall, 2004). The orientation of a color singleton cued monkeys to produce either a pro-saccade to the singleton or an anti-saccade to the distractor at the opposite location. We have improved the task by making the distractors elongated. This requires monkeys to select on color but respond on shape, resembling classic filtering tasks

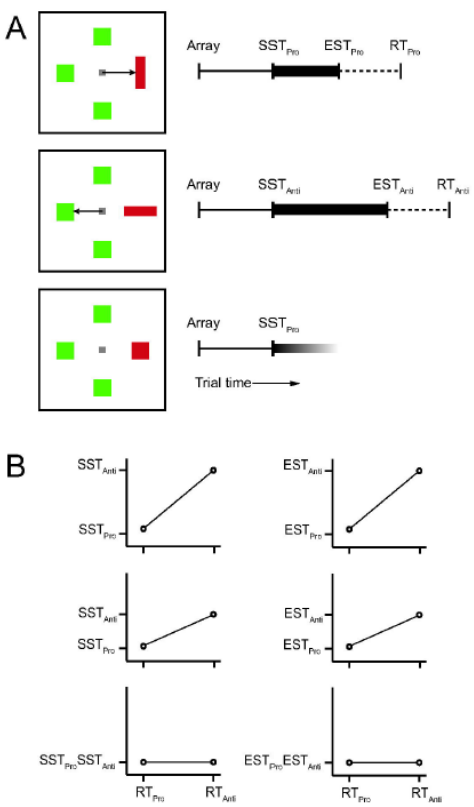

Figure 5.1. Visual search with explicit stimulus-response mapping. (A) Visual search task in which the orientation of a color singleton cues a pro-saccade (vertical), an anti-saccade (horizontal), or no saccade (square). Response times can be subdivided into three states or operations. Array presentation is followed by stimulus encoding and localization (thin line); the conclusion of this operation is indexed by singleton selection time (SST). Next, stimulus-response mapping and selection of the saccade endpoint happens if a pro- or anti-saccade will be produced (thick line); the conclusion of this operation is indexed by endpoint selection time (EST). This operation may not occur when no saccade is made (grayed thick line). Finally, saccade preparation leads to initiation of the saccade which is manifest as the measurement of RT (dotted line). (B) Response time on anti-saccade trials (RT_{Anti}) is systematically longer than that on pro-saccade trials (RT_{Pro}). Measurements of SST and EST provide insight into the operations contributing to the variation of RT. Theoretically, a difference between SST_{Anti} and SST_{Pro} (left) or between EST_{Anti} and EST_{Pro} (right) could explain all (top), some (middle), or none (bottom) of the variation of RT.

(Eriksen & Eriksen, 1974; Sperling, 1960; Theeuwes, 1992; Treisman & Gelade, 1980). The literature is divided on whether selecting an object and categorizing it are separate, sequential stages (Broadbent, 1971; Hoffman, 1978; Treisman, 1988; Wolfe et al., 2015) or objects are selected and categorized in a single step (Bundesen, 1990; Logan, 2002). Thus, whether covert and overt orienting processes are comprised of distinct operations or stages remains uncertain.

These differing views can be resolved through measurements of neural chronometry (Fig. 5.1). In the pursuit of this research aim, reward contingencies allowed one monkey to discover a strategy that prioritized the shape of the stimuli. Unexpectedly, some neurons recorded during this task exhibited rapid selectivity for stimulus shape. Here, we compare these findings to a previous report of color selectivity in FEF (Bichot et al., 1996) and characterize the neural chronometry of these FEF

neurons. The results provide new evidence that selection of objects and saccade endpoints are distinct operations, both accomplished by visually responsive FEF neurons. The time course of this feature selectivity provides new evidence that visual search is accomplished through sequential operations.

5.2 METHODS

5.2.1 Subjects

Data from one male macaque monkey (*M. radiata*) was compared to data previously collected from four male macaque monkeys (*M. mulatta*). All procedures were in accordance with the National Institutes of Health Guide for the Care and Use of Laboratory Animals and approved by the Vanderbilt Institutional Animal Care and Use Committee.

5.2.2 Visual Search Task

All macaque monkeys performed color singleton visual search tasks. For two monkeys (A, C) the colors of singleton and distractor were constant, giving rise to strong search performance asymmetries (Bichot et al., 1996). For two monkeys (B, Q) the singleton and distractors alternated between red/green or green/red across sessions. New performance and neurophysiology data were collected from another monkey (Da) performing the visual search task with pro- and anti-saccades (Sato & Schall, 2003). The orientation of the singleton cued the pro- or anti-saccade and was presented with elongated distractors. The monkey was trained to fixate a central point whose appearance marked the beginning of the trial. After fixating this point for between 300 and 800 ms, an array of four rectangular stimuli appeared between 3° and 10°

eccentricity. One of these stimuli was a color singleton (either red with green distractors or green with red distractors). The color of the singleton and distractors were randomly assigned on a trial by trial basis. All stimuli had an area of 1 square degree. Singletons could be either vertical (aspect ratio = 4.00) or horizontal (aspect ratio=0.25). Distractors could be either vertical, horizontal, or square (aspect ratio = 1.00). The aspect ratio of the color singleton indicated a response rule. If the singleton was vertical then reward was delivered for a saccade to the singleton (pro-saccade; Fig. 5.2A). If the singleton was horizontal then reward was delivered for a saccade to the stimulus located opposite to the singleton (anti-saccade). After making the saccade, the monkey was required to fixate the correct stimulus for 400 ms, until the fluid reward was delivered. If the monkey broke fixation or made a saccade to an incorrect location, a 2,000 ms time-out delay occurred.

Correct responses were defined by the orientation of the color singleton. Hence, the orientation of the distractors can influence response selection. Consequently, particular combinations of singleton and distractor orientations can cue congruent or incongruent saccades. The distractor opposite the singleton was a correct endpoint on anti-saccade trials, so congruency was operationalized by the relationship of the shape of the singleton and the distractor at the opposite location. If the distractor was vertical, a saccade may be planned toward it. If it was horizontal a saccade may be planned toward the color singleton. If the saccade consistent with the orientation of the opposite distractor corresponded to the saccade cued by the singleton, then the stimulus array was *congruent*. If the singleton and opposite distractor cued saccades in opposite

directions, then the stimulus array was *incongruent*. If the opposite stimulus was square, the stimulus array was *neutral*.

5.2.3 Data acquisition and analysis

Because all details have been described previously (Cohen et al., 2009b; Sato et al., 2001; Schall et al., 1995a), they will not be repeated. The following approaches and definitions are particular to this analysis.

For averaging across neurons, SDFs were normalized by z-scoring across the full trial and performing a baseline subtraction. That is, the SDFs aligned on array presentation and saccade for each condition were concatenated and the standard deviation of this concatenated vector was calculated. The SDFs for that unit were then divided by that standard deviation. Then, the mean baseline activity, the average value of the SDF in the 300 ms preceding array onset, was subtracted. This method of scaling responses reduces the skewness of the SDF across the population and generates a comparable range of activity across neurons without erroneously scaling neurons with little to no modulation (Lowe & Schall, 2018).

Selection times were calculated from the SDFs by subtracting the mean difference during the 300 ms before array onset from the difference between two conditions. Selection times were defined as the earlier of two times (1) the time the difference function exceeds 2 standard deviations of the baseline difference and continues on to exceed 6 standard deviations for at least 20 ms continuously or (2) the time the difference function exceeds 2 standard deviations of the baseline difference for at least 50 ms continuously. Visual latency was calculated in a similar fashion where the SDF itself meeting the above criteria as opposed to a difference function. Differences

among selection time distributions were assessed with a nonparametric Kruskal-Wallis test for equal medians.

Each selection time measure was calculated over all RTs and in groups of trials with shortest and longest RTs based on median split. The magnitude of any difference in selection times across RT groups was compared to the difference in RT across the groups through a two-tailed t-test and associated Bayes factor.

5.3 RESULTS

5.3.1 Performance Results

We begin by introducing a nomenclature used below. Correct saccades to vertical stimuli included pro-saccade trials with congruent, neutral, or incongruent arrays ($Pro^{C,N,I}$) and congruent anti-saccade trials ($Anti^{C}$). We also designate saccades to square stimuli as neutral anti-saccade trials ($Anti^{N}$) and saccades to horizontal stimuli as incongruent anti-saccade trials ($Anti^{I}$).

RT and accuracy both exhibited an influence of response mapping and singleton-distractor congruency (Fig. 5.2B). As expected, mean RT ± SEM on all anti-saccade trials (311 ± 48 ms) was significantly greater than RT on all pro-saccade trials (240 ± 28 ms) (ANOVA: $F(1,198) = 182.5$, $p < 0.001$. A Bayesian analysis suggested that the data were 2.8×10^{22} times as likely to have been observed in a model including stimulus-response mapping as a factor as compared to a null model. Also, RT on all incongruent trials (304 ± 57 ms) was significantly greater than RT on all neutral trials (282 ± 50 ms), which was significantly greater than RT on all congruent trials (260 ± 45 ms) (ANOVA: $F(2,198) = 20.9$, $p < 0.001$). A Bayesian analysis suggested that the data were 1.7×10^{7} times as likely to have been observed in a model including congruency in addition to

stimulus-response mapping as compared to a model with stimulus-response mapping alone. Thus, the shape of the distractors influenced the efficiency of visual search and saccade production. A Bayesian analysis did not provide evidence for or against an interaction; the data were nearly equiprobable (only 1.24 times as likely) in a model with no interaction as compared to a model with an interaction between stimulus-response mapping and congruency.

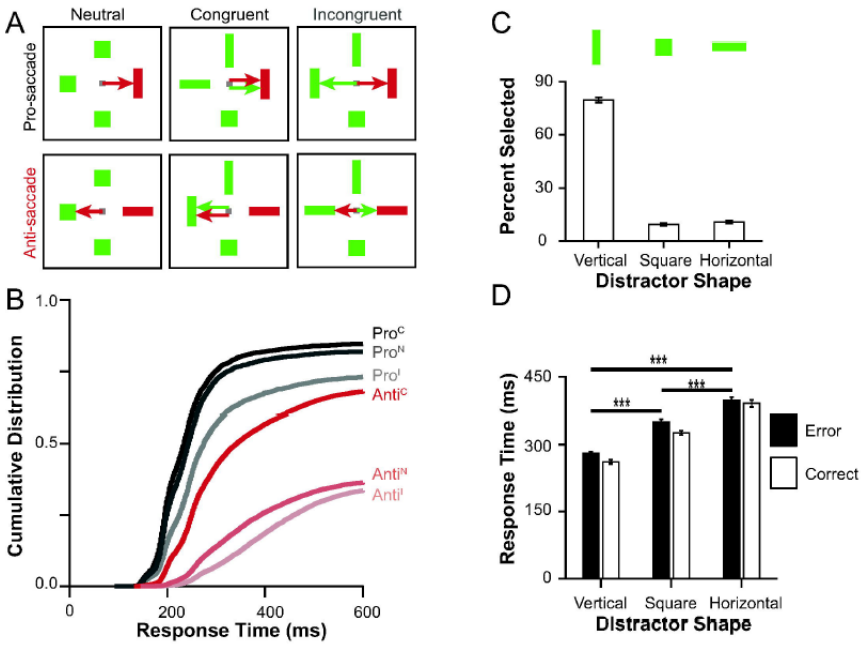

Figure 5.2. Search array configurations and task performance. (A) Visual search with pro-saccade (top) and anti-saccade (bottom) responses based on orientation of color singleton. Distractors could be square or elongated. Because shape of the singleton cues stimulus-response rule, the shape of the distractors may influence the efficiency of stimulus-response mapping via a congruency effect. We operationalized neutral trials as those in which the distractor opposite the singleton was square (left column), congruent trials as those in which the distractor opposite the singleton would cue the same saccade as the singleton (middle column), and incongruent trials as those in which the distractor opposite the singleton cued the opposite saccade (right column). The saccades cued by the singleton (distractor) are indicated as red (green) arrows. (B) Defective RT distributions for pro-saccade (black) and anti-saccade (red) trials with congruent arrays (full saturation), neutral arrays (intermediate saturation), and incongruent arrays (lowest saturation). Saccade latency was longer for anti- relative to pro-saccades, and longer of incongruent relative to neutral and congruent trials. (C) Proportions of error saccades made to each stimulus shape for trials in which at least one distractor was vertical (open). (D) RTs to each stimulus shape for error (filled) and correct (open) trials. Saccades to vertical items were shortest latency.

Analyzing the pattern of errors, we discovered that the monkey more commonly shifted gaze to a vertical item than to any other (Fig. 5.2C). Endpoint errors were significantly more common to vertical stimuli (80 ± 12% vertical, 10 ± 7 % square, 11 ± 7% horizontal; ANOVA: $F(2,117) = 833.92$, $p < 0.001$). A Bayesian analysis suggested that the data were 3.6×10^{65} times as likely to have been observed in a model including

shape as a factor as compared to a null model. The preference for vertical stimuli was evident also in the RT (Fig. 5.2D). RTs were significantly shorter for saccades to vertical (271 ± 38 ms), relative to square (339 ± 49 ms) and horizontal stimuli (394 ± 67 ms) (ANOVA: $F(2,234) = 110.15$, $p < 0.001$) regardless of correct or error trial outcome (ANOVA: interaction $F(2,234) = 0.58$, $p = 0.561$). A Bayesian analysis suggested that the data were 3.8×10^{30} times as likely to have been observed in a model including shape as a factor as compared to a null model. There was also no evidence of an interaction, as the data were 8.3 times as likely to have been observed in a model with only shape and trial outcome as factors as compared to a model with an interaction. The more frequent and faster responses to vertical stimuli indicate that the monkey adopted a strategy of searching for vertical items as opposed to guiding gaze by the stimulus-response rule provided by the singleton. In other words, the monkey divided attention to vertical items in the array rather than focusing attention on the singleton that cued the stimulus-response rule. Serendipitously, the short-cut used by the monkey revealed new properties of feature and spatial processing supporting visual search with arbitrary stimulus-response mapping.

5.3.2 Shape Selectivity in FEF

Based on previous observations during color singleton search with fixed target and distractor color assignments (Bichot et al. 1996), we tested whether the predisposition for vertical stimuli was associated with altered stimulus feature processing by FEF neurons. FEF is comprised of a diversity of neurons with visual, visuomovement, movement, and other patterns of modulation (Lowe & Schall 2018). The sample of neurons analyzed for this report consisted entirely of visually responsive neurons. This

is important to understand because we will describe a pattern of modulation that is related to saccade production but is distinct from the saccade preparation accomplished by movement neurons.

Responses to the different stimulus shapes was assessed when they were irrelevant distractors, i.e., not the color singleton nor the endpoint of an anti-saccade or error saccade. Responses to vertical, square, and horizontal irrelevant distractors from two example neurons are shown in Fig. 5.3A. Both neurons responded more to a vertical than to any other item in the RF. The time at which this difference between responses to vertical and non-vertical stimuli was defined as *feature selection time (*FST*)*. For neuron 1, FST occurred 136 ms after array presentation, 41 ms after the initial transient. FST for neuron 2 occurred 95 ms after array presentation, only 8 ms after the visual transient. These representative neurons exemplify two other distinctive properties. Whereas neuron 1 showed graded selectivity (vertical > square > horizontal), neuron 2 showed categorical selectivity (vertical > square = horizontal) (e.g., Ferrera et al., 2009). The average responses to vertical, square, and horizontal

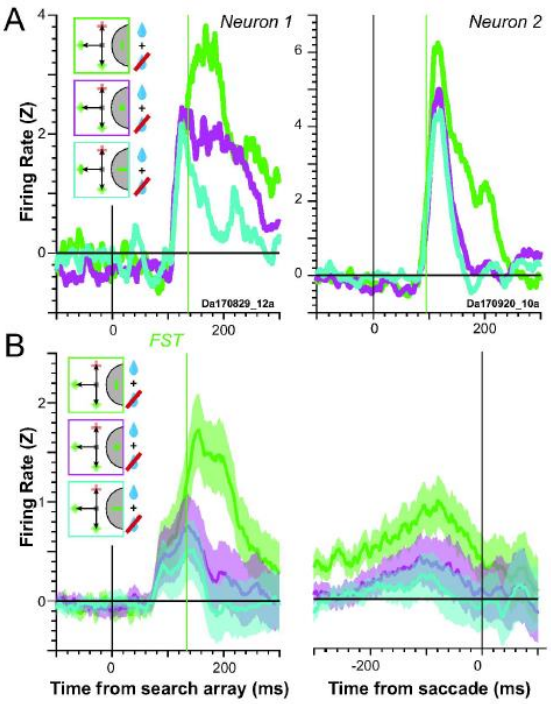

Figure 5.3 Feature selectivity in FEF. (A) Normalized firing rate for two example neurons that exhibited shape selectivity aligned on stimulus onset. Responses to vertical (green), square (magenta), and horizontal (cyan) stimuli that were irrelevant distractors across correct (blue drop) and error (crossed blue drop) pro- and anti-saccade trials. Trial types are indicated in the color-coded insets. The set of possible stimuli that can appear at a given location are superimposed. The singleton shown at 90° could have appeared at 270°; likewise, the distractors shown at 270° could have appeared at 90°. Feature selection time (FST) is indicated by the vertical green line. (B) Average normalized firing rate ± SEM for all feature selective neurons aligned on array presentation (left) and saccade initiation (right). Vertical green line plots the median FST for this population.

objects for the feature selective neurons is shown in Fig. 5.3B. The mean ± SEM FST was 130 ± 30 ms (mode = 134 ms; Table 1).

In monkeys performing color singleton search with constant target and distractor colors, the color-selective neurons in FEF responded with latencies not less than ~60 ms, while non-selective neurons responded with latencies as short as ~40 ms (Bichot et al., 1996). We compared the current results to those data (Fig. 5.4). For each neuron, an ANOVA was performed on the SDF values during the first 25 ms (corresponding to the interval used by Bichot et al. (1996)) or 100 ms after the visual transient. Of 124 neurons sampled, 13% showed shape selectivity in the first 25 ms and 24% in the first 100 ms. As observed previously, neurons with shape selectivity were not the earliest to respond. The earliest visual response of shape selective neurons was 66 ms (median 95 ms; mode 89 ms), later than the two earliest visual responses from non-shape selective neurons 52 and 58 ms). Combined across the two studies, the results show that neither shape nor color information arrives in FEF via the fastest visual pathway and indicate that the training conditions of the present study created the same feature selective state.

Measure	Mean ± SEM (ms)	Mode (ms)	$p(\frac{\Delta\ Selection\ Time}{\Delta\ Response\ Time} > 0)$	BF
FST	130 ± 30	134	0.683	0.22
$_{Corr}SST_{Pro}$	136 ± 37	137	0.377	0.28
$_{Corr}EST_{Anti}$	160 ± 34	134	0.002	24.62
$_{Corr}EST_{Pro}$	154 ± 51	133	0.027	2.55
$_{Err}EST$	155 ± 41	133	0.011	5.64
$_{Corr}EST^{C}_{Anti}$	149 ± 57	168	0.021	3.29

Table 5.1. Selection time summary statistics. For each selection time, the table reports the mean value ± SEM, modal value, probability that variation in selection time over interquartile range of the response times is equal to zero (i.e., the probability that selection time is synchronized to array presentation), and the Bayes factor for whether the change in selection time is synchronized to the change in RT (BF < 0) or not synchronized to the change in RT (BF > 0).

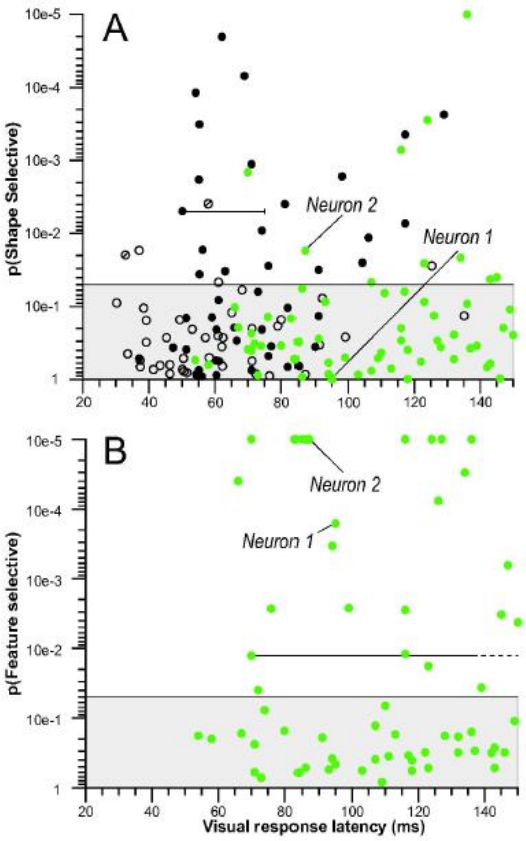

Figure 5.4. Relationship between feature selectivity and visual latency. Neurons sampled in this study (green) were compared to those reported previously in control monkeys that performed search with variable color assignments (open black circles) and experimental monkeys that performed search with constant color assignments (filled black circles) (Bichot et al. 1996). The probability of the response to the singleton in the receptive field being the same as the response to a distractor in the receptive field during the first 25 ms (A) and 100 ms (B) is plotted as a function of visual response latency. Horizontal lines indicate analysis window. In (B) the dashed portions of the line indicate that the 100 ms analysis window extends beyond the range of the plot. The shaded region indicates nonsignificant probability values greater than 0.05. In the previous study, of the 43 neurons from control monkeys, 39 fell in the nonsignificant area, two responded preferentially to the target, and two responded preferentially to the distractors of the search array field (marked by diagonal lines). In contrast, 21 of 47 neurons recorded from the experimental monkeys exhibited significantly greater initial responses when the singleton fell in the receptive field, and none showed the opposite effect. In the current study, of 124 neurons sampled, 16 showed shape selectivity in the first 25 ms and 30 in the first 100 ms. Example neurons 1 and 2 are identified as N1 and N2.

5.3.3 Relation of Feature Selection to Spatial Selection

The serendipitous discovery of orientation sensitivity in FEF offered an opportunity to relate these observations to previous findings (Thompson et al., 1996; Murthy et al., 2001; Sato & Schall, 2003; Schall, 2004b). We performed the following sequence of analyses. To report the findings most clearly and concisely, we introduce a nomenclature to distinguish the categories of neurons, the types of trials and the timing measures. First, as previou sly, we distinguish singleton selection time (SST) from saccade endpoint selection time (EST). Second, we distinguish whether measures were obtained in correct or error trials with left subscript, e.g., $_{Corr}$EST and $_{Err}$EST. Third, we distinguish whether measures were obtained in pro- or anti-saccade trials with right subscript, e.g., $_{Corr}$EST$_{Pro}$ and $_{Corr}$EST$_{Anti}$. Finally, we distinguish whether the measure was obtained in trials with congruent,

incongruent, or neutral search arrays with right superscript, e.g., $_{Corr}EST^{C,I}_{Pro}$ and $_{Corr}EST^{C,I}_{Anti}$. The absence of a particular superscript or subscript implies that the measure was obtained over all possible groups. The authors appreciate the complexity of this nomenclature, which is in keeping with that of more mature scientific fields such as chemistry, molecular biology, and physics that require non-intuitive but detailed nomenclatures and symbols.

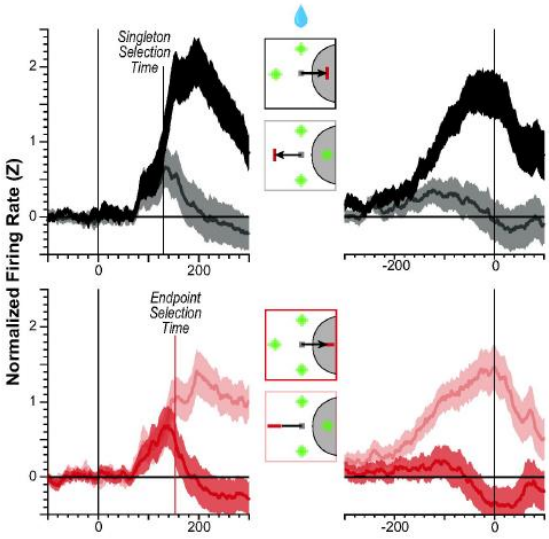

Figure 5.5. Singleton and saccade endpoint selection. (A) For the 30 feature selective neurons, average normalized SDF when the singleton appeared in (dark) or opposite (light) the RF during interleaved pro- (top) and anti-saccade (bottom) trials aligned on array presentation (left) and on saccade initiation (right). Insets illustrate the locations and orientations of the singleton and possible horizontal, square, or vertical distractors relative to RF (gray arc) plus the reward earned (drop icon) for each SDF. SST measures when the SDF for the singleton in the RF exceeds the SDF for a distractor in the RF. EST measures when the SDF for the anti-saccade endpoint opposite the RF exceeds the SDF for the singleton in the RF.

In the first analysis, responses during pro- and anti-saccade trials were assessed for the feature selective and the non-feature selective neurons to identify SST and EST as measured previously (Sato & Schall, 2003) (Fig. 5.5A). In pro-saccade trials, the average response became greater when the singleton was in the RF relative to when it was opposite the RF, replicating Sato & Schall (2003) and numerous other studies describing target selection in FEF during search (e.g., Bichot et al., 2015; Buschman & Miller, 2007; Glaser et al., 2016; Keller et al., 2008; McPeek, 2006; Mirpour et al., 2019; Monosov et al., 2010; Monosov & Thompson, 2009; Phillips & Segraves, 2009; Pouget et al., 2009; Scerra et al., 2019; Schall et al., 1995a; Schall & Hanes, 1993; Thompson et al., 1996; Wardak et al., 2006; Zhou & Desimone, 2011). Conversely, in anti-saccade trials, the average response

across the sample of feature selective neurons became greater when the endpoint of the saccade was in the RF relative to when the singleton was in the RF. Similar results were found for the non-feature-selective neurons (Fig. 5.5B).

These results generally replicate previous observations (Sato & Schall, 2003); however, the absence of SST during anti-saccade trials was unexpected. The monkey's performance strategy resulted in low accuracy for $Anti^{N}$ and $Anti^{I}$ trials. Hence, the absence of SST_{Anti} is consistent with a failure to focus attention on the singleton appropriately. Further, the aspect ratio of the stimuli used in this study was greater than that used by Sato & Schall and so was more easily discriminable from central fixation. However, when RTs were longer, due either to more deliberate focusing of attention on the singleton or overall slowing of processing, SST preceded EST during anti-saccade trials (Fig. 5.6). Therefore, the overall pattern of neural modulation observed in FEF is consistent with the performance data indicating that the monkey divides attention among vertical items, sacrificing accuracy for speed.

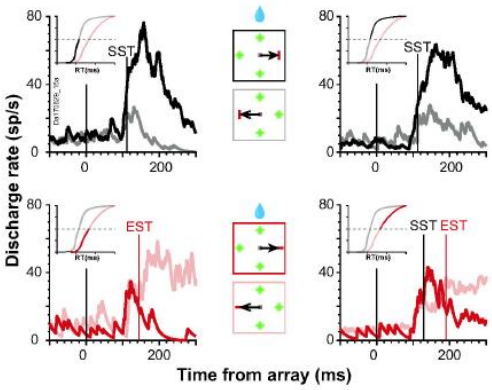

Figure 5.6. Singleton and saccade endpoint selection across response time. Representative neuron illustrating variation of SST and EST for shortest (left) and longest (right) RT (highlighted in inset cumulative RT distributions). In pro-saccade trials, SST does not vary with RT. In anti-saccade trials, SST was manifest in long but not short RT trials, followed by EST. Conventions as in Figure 5.4.

Across the sample of feature selective neurons, SST measured in pro-saccade trials ($_{Corr}SST_{Pro}$) preceded EST measured in anti-saccade trials ($_{Corr}EST_{Anti}$) Average values for these and all subsequent temporal indices ± SEM are found in Table 5.1. Statistical tests on all pairs of distributions are found in Table 5.2.

Having established that these relationships replicate previous observations (Sato & Schall, 2003), we can now explore the relationship of the new measure FST to SST and EST measured in the different types of trials. FST was not significantly different than $_{Corr}SST_{Pro}$. In contrast, FST was significantly earlier than $_{Corr}EST_{Anti}$.

The simultaneity of FST with $_{Corr}SST_{Pro}$ entails that they index a common process. If so, then FST can inherit the interpretation of SST. Accordingly, we conjecture that FST indexes the process of stimulus selection through attention allocation and not saccade endpoint selection.

The second analysis assessed how feature selection was related to spatial selection of locations other than the singleton or saccade endpoint. This was accomplished by contrasting responses of feature-selective neurons to fixated and non-fixated stimuli. Fig. 5.7A compares the activity of the two example neurons and of the sample of feature-selective neurons to vertical distractors in the RF that were not fixated, activity preceding correct pro-saccades to the vertical singleton in the RF, and activity when unchosen square or horizontal distractors were in the RF. Responses were greater when the vertical color singleton in the RF attracted a gaze shift relative to when a vertical distractor in the RF was not fixated, replicating the well-known enhancement effect (Goldberg & Bushnell, 1981). By comparing discharge rates when an unfixated, irrelevant vertical distractor was in the RF and when the fixated vertical color singleton was in the RF, we m easured *endpoint selection time* for pro-saccades ($_{Corr}EST_{Pro}$).

The time $_{Corr}EST_{Pro}$ identifies when the endpoint of the upcoming pro-saccade is specified by feature-selective neurons. This is a new measure. It is distinct from EST defined by Sato and Schall (2003), or $_{Corr}EST_{Anti}$ described above because it was not calculated from anti-saccade trials. Across the sample of feature selective neurons, $_{Corr}EST_{Pro}$ was significantly later than FST and $_{Corr}SST_{Pro}$, but was not different from $_{Corr}EST_{Anti}$.

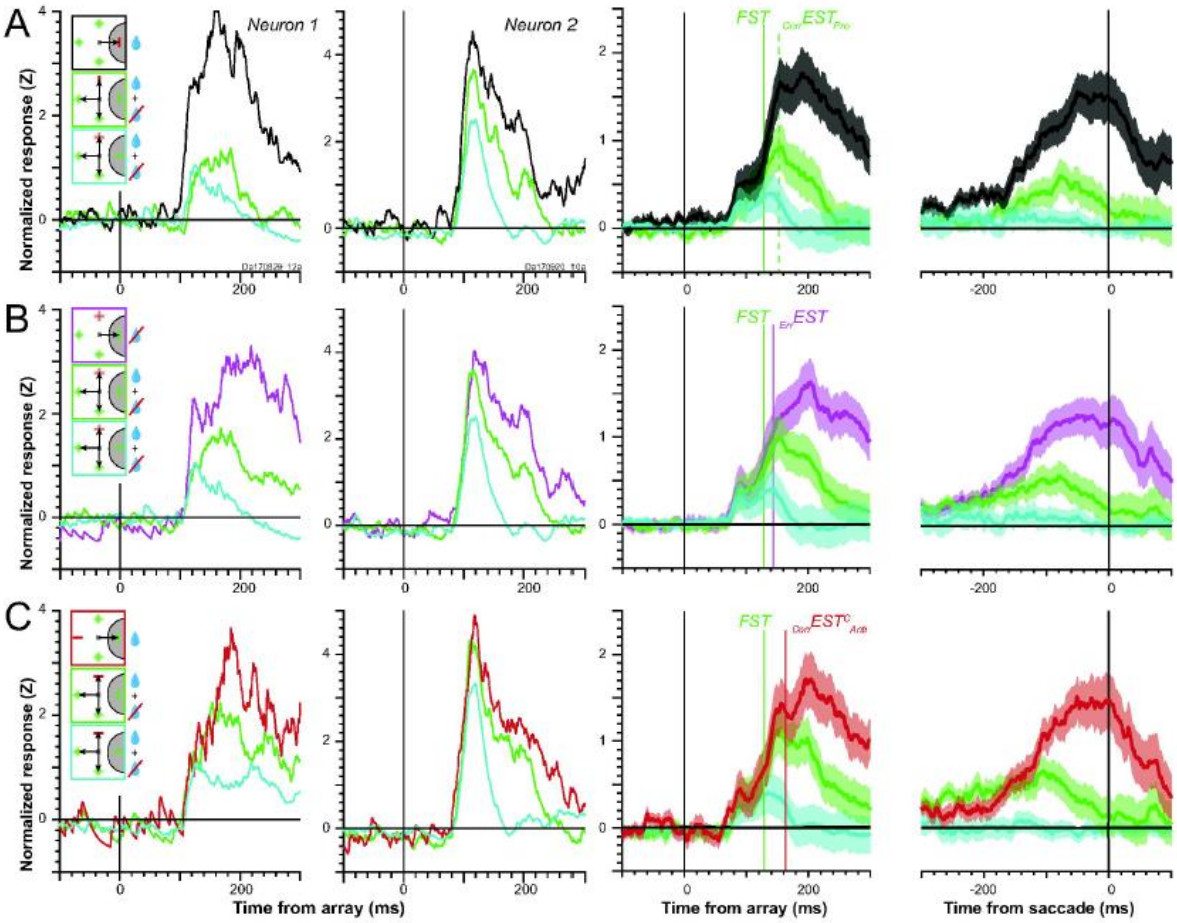

Figure 5.7. Distinction of feature selectivity from saccade selection. Normalized firing rates for neuron 1 (1st column) and neuron 2 (2nd column) aligned on array presentation, plus mean normalized SDF ± SEM of feature selective neurons aligned on array presentation (3rd column) and on saccade initiation (4th column). (A) Activity associated with irrelevant vertical (green), non-vertical (cyan), and the singleton in the RF (black) demonstrate enhancement associated with correct saccade selection, which distinguishes FST from $_{Corr}EST_{Pro}$. (B) Activity on pro- and anti-saccade trials associated with irrelevant vertical (green), non-vertical (cyan), and incorrectly selected vertical distractors in the RF (magenta) demonstrate enhancement associated with errant saccade selection, which distinguishes FST from $_{Err}EST$. (C) Activity on anti-saccade trials associated with irrelevant vertical (green), non-vertical (cyan), and correctly selected vertical distractor in the RF (red) demonstrate enhancement associated with anti-saccade selection, which distinguishes FST from $_{Corr}EST^{C}_{Anti}$.

The third analysis tested whether $_{Corr}EST_{Pro}$ was due only to the difference in color between the fixated and unfixated vertical items. This was accomplished by contrasting responses when an incorrect saccade was made to a vertical distractor in the RF relative to the un-fixated vertical distractor (Fig. 5.7B). The response to the fixated vertical distractor was greater than the response to the un-fixated vertical distractor. This replicates multiple previous findings that saccade endpoint errors during visual search arise when FEF neurons treated a distractor as if it were the target (Heitz et al., 2010; Reppert et al., 2018; Thompson et al., 2005a). We identify the time when this occurs as *endpoint selection time* for errors *(*$_{Err}EST$*)*. Across the sample of feature selective neurons, $_{Err}EST$ was significantly later than FST and trended toward being later than $_{Corr}SST_{Pro}$, but was not different than $_{Corr}EST_{Anti}$ or $_{Corr}EST_{Pro}$.

The fourth analysis tested whether the responses of feature-selective neurons varied across trial context. This was accomplished by comparing the responses observed with correct anti-saccades to the vertical item and responses to irrelevant vertical and non-vertical distractors (Fig. 5.7C). This analysis compared only items of the same color. Both example neurons produced most activity associated with fixated vertical stimuli in the RF relative to un-fixated vertical distractors, and least activity with square or horizontal distractors in the RF. Across the sample of feature selective neurons, the *endpoint selection time for congruent anti-trials (*$_{Corr}EST^{C}_{Anti}$*)* was significantly later than FST but was not different than $_{Corr}SST_{Pro}$, $_{Corr}EST_{Anti}$, $_{Corr}EST_{Pro}$, or $_{Err}EST$.

These analyses assess the temporal aspects of attention allocation and endpoint selection. Fig. 5.7 shows three conditions in which vertical items were fixated: correct

Pro trials, incorrect saccades to vertical items, and correct Anti^{C} trials. These were used to identify $_{Corr}$EST$_{Pro}$, $_{Err}$EST, and $_{Corr}$EST$^{C}_{Anti}$, respectively. In a fifth analyses, the magnitude of response in three conditions were compared at three time windows: 100 to 150 ms after array onset (around the time of FST and $_{Corr}$SST$_{Pro}$), 150 to 200 ms after array onset (around the time of EST), and -25 to 25 ms from saccade initiation (Fig. 5.8). The magnitude of the responses did not differ in the early visual time window ($F(2,87) = 0.022$, $p = 0.9774$), the late visual time window ($F(2,87) = 0.077$, $p = 0.9263$), or around the saccade ($F(2,87) = 0.106$, $p = 0.8994$). In short, responses were identical if a saccade was made toward a vertical item in the RF, regardless of context or whether such a saccade was correct or incorrect.

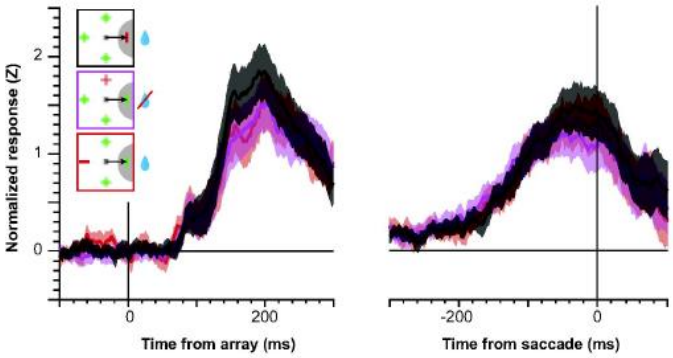

Figure 5.8. Magnitude of response during saccade selection. Mean normalized SDF ± SEM of feature selective neurons aligned on array presentation (left) and on saccade initiation (right). Activity associated with correct Pro saccades into the RF (black), incorrectly selected vertical distractors in the RF (magenta), and correct Anti^{C} saccades into the RF (red) do not differ, showing that this population does not differentiate type of saccade if a saccade is to be made.

5.3.4 Variation of Modulation Times in Relation to RT

Previous research using this task distinguished neurons by measuring whether SST and EST were synchronized on array presentation or varied with RT (Sato & Schall, 2003; Schall, 2004b). We performed the same analysis for these data, calculating FST, $_{Corr}$SST$_{Pro}$, $_{Corr}$EST$_{Anti}$, $_{Corr}$EST$_{Pro}$, $_{Err}$EST, and $_{Corr}$EST$^{C}_{Anti}$ in the fastest and slowest 50% of trials. The difference in selection times divided by the interquartile range of the RTs could range between 0.0 (synchronized on array presentation) to 1.0 (synchronized on saccade initiation).

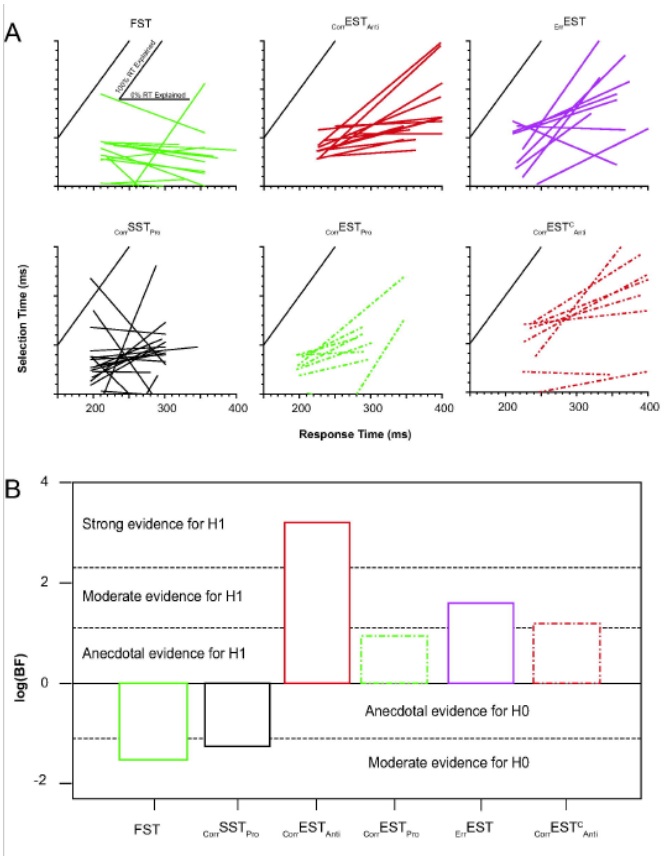

Figure 5.9. Chronometry of feature selection, singleton selection, and endpoint selection in relation to response time. (A) Selection times for faster and slower RT groups plotted as a function of the mean RT of each group. Each line corresponds to one neuron with a measurable selection time in both RT groups. The slope indicates the contribution of each selection time to RT. Inset in top left subplot (FST) illustrates range of possible influences of selection times on RTs. Selection times could be synchronized on array presentation and invariant with respect to RT (0% RT explained) or synchronized on saccade presentation (100% RT explained). Colors as in Fig. 6. Dashed lines indicate measures from non-feature-selective cells. (B) Bayes factors from statistical test of the slopes of each selection time relative to RT. Bayes factors less than 1 (log values less than 0) indicate evidence for the null hypothesis (H0) that the distribution mean is equal to 0. Bayes factors greater than 1 (logs greater than 0) indicate evidence for the alternate hypothesis (H1) that the distribution is greater than 0. Levels of evidence defined by the Bayes factor are indicated. Line and color assignments as in Fig 6. We found moderate evidence supporting the hypothesis that FST and $_{Corr}SST_{Pro}$ are synchronized on array presentation and not on saccade initiation. On the other hand, we found strong evidence that $_{Corr}EST_{Anti}$, anecdotal evidence that $_{Corr}EST_{Pro}$, and moderate evidence that $_{Err}EST$ and $_{Corr}EST^{C}_{Anti}$ were not synchronized on array presentation nor saccade initiation.

The proportion of RT accounted for by variation in selection times are shown in Fig. 5.9. We found that this proportion was not different than 0.0 for FST ($t(13) = -0.49$, $p = 0.683$) or $_{Corr}SST_{Pro}$ ($t(18) = 0.91$, $p = 0.377$). In terms of Bayes Factors (Rouder et al., 2009) we found moderate evidence that *FST* (BF = 0.22) and $_{Corr}SST_{Pro}$ (BF = 0.28) account for no variability of RT. In other words, the state indexed by FST and $_{Corr}SST_{Pro}$ arises at a time synchronized on array presentation.

In contrast, variation in all measures of endpoint selection in feature-selective cells accounted for a significant fraction of variation of RT. With strong evidence rejecting the null hypothesis (BF = 24.62), a significant proportion of the variation of RT was accounted for by variation in $_{Corr}EST_{Anti}$ ($t(13) = 3.92$, $p = 0.002$). At a moderate level of evidence, a significant proportion of the variation of RT was accounted for by variation in $_{Err}EST$ ($t(9) = 3.22$, $p = 0.011$, BF = 5.64) and $_{Corr}EST^{C}_{Anti}$ ($t(7) = 2.95$, $p =$

0.021, BF = 3.29). At an anecdotal level of evidence, a significant proportion of the variation of RT also was accounted for by variation of $_{Corr}EST_{Pro}$ (t(8) = 2.71, p = 0.027, BF = 2.55).

Although the measures of EST account for some RT variability, the average proportion of RT explained across all significant relationships is 24.8%. The additional RT variability will be accounted for by response preparation processes subsequent to EST and not included in these data.

5.3.5 Neural Chronometry of Feature and Spatial Selection

The various distinct response modulations reveal a temporal sequence of operations in FEF accomplishing this visual search task (Fig. 5.10; Table 5.2). Following array presentation, the first state transition is indexed by the response of visually responsive neurons after a characteristic latency. The next state transition was indexed by FST, which coincided with $_{Corr}SST_{Pro}$. The state indexed by $_{Corr}SST_{Pro}$ has been identified with the allocation of visual attention on th e singleton based on its salient visual attribute to encode the stimulus-response rule (Sato & Schall, 2003; Schall, 2004b). The discovery of feature-selection arising concomitantly with $_{Corr}SST_{Pro}$ reported here suggests that the monkey divided visual attention among the vertical items in the array. The allocation of

	FST	$_{Corr}SST_{Pro}$	$_{Corr}EST_{Anti}$	$_{Corr}EST_{Pro}$	$_{Err}EST$
$_{Corr}SST_{Pro}$	$X^2(1,42) = 0.02$, p = 0.888				
$_{Corr}EST_{Anti}$	$X^2(1,44) = 9.33$, p = 0.002 *	$X^2(1,46) = 8.35$, p = 0.004 *			
$_{Corr}EST_{Pro}$	$X^2(1,42) = 5.58$, p = 0.018 *	$X^2(1,44) = 4.31$, p = 0.038 *	$X^2(1,46) = 0.01$, p = 0.967		
$_{Err}EST$	$X^2(1,39) = 4.36$, p = 0.037 *	$X^2(1,41) = 3.56$, p = 0.059 †	$X^2(1,443) = 0.34$, p = 0.560	$X^2(1,41) = 0.20$, p = 0.652	
$_{Corr}EST^{c}_{Anti}$	$X^2(1,34) = 3.90$, p = 0.048 *	$X^2(1,36) = 2.75$, p = 0.097 †	$X^2(1,38) = 0.24$, p = 0.625	$X^2(1,36) = 0.01$, p = 0.905	$X^2(1,33) = 0.03$, p = 0.855

Table 5.2. Selection time comparisons. The distribution of each selection time was compared to the distribution of each other selection time using a Kruskal-Wallis test. The X^2 value, degrees of freedom, and *p* value of each pairwise test is shown. Because the tests are symmetric, only the lower diagonal is shown. Values that trend toward significance ($p < 0.10$) are marked with a dagger (†). Values that reach significance ($p < .05$) are marked with an asterisk (*).

spatial visual attention to spatially separated, noncontiguous items in a search array has been demonstrated (e.g., Bichot et al., 1999; Dubois et al., 2009). The next state transition was indexed by EST. The state indexed by EST has been identified with the specification of the endpoint of the saccade. Being different in time and relationship with RT, it is a state different from that identified by $_{Corr}SST_{Pro}$ (Sato & Schall, 2003; Schall 2004b) and likewise distinct from the presaccadic build-up of movement related neurons (Woodman et al., 2008), which accounts for the remainder of the variation of RT.

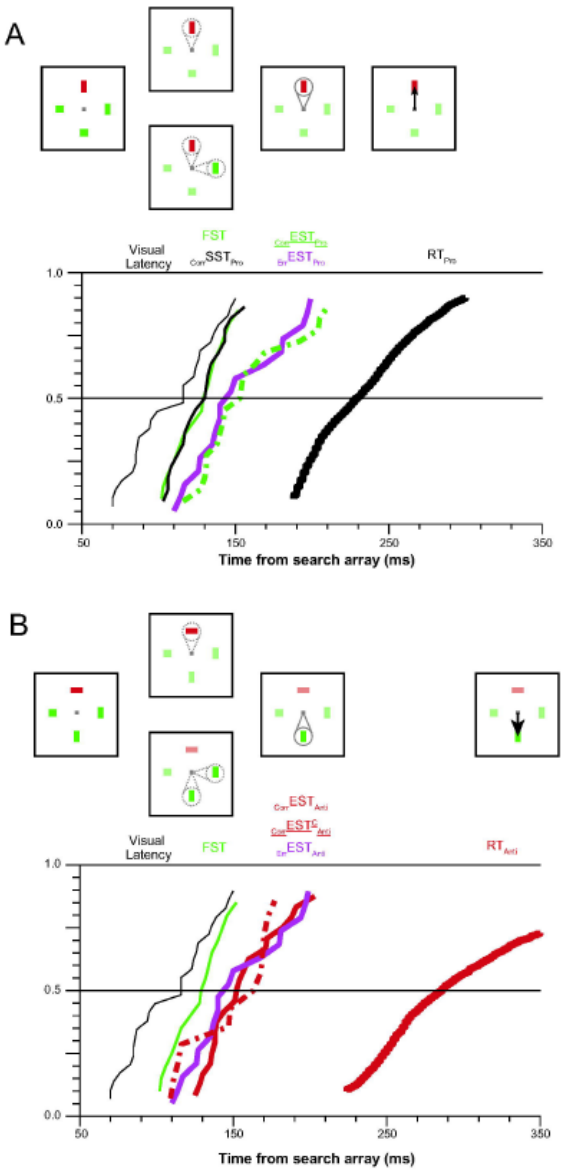

Figure 5.10. Distributions of feature selective processes. (A) Diagrams showing sequence of states during pro-saccades (top). The hypothesized spotlight of attention is shown in gray lines and a saccade is indicated by a solid arrow. Cumulative distributions of selection time metrics alongside visual response latency and Pro RT distribution (bottom). The colors are the same as the diagrams and previous figures and labeled above the plot boundary. Line thickness increases as stages become further from array onset and closer to RT. (B) Diagrams showing sequence of states during anti-saccades (top) and cumulative distributions of selection time metrics (bottom).

5.4 DISCUSSION

The present study demonstrates two primary findings: (1) besides color (Bichot et al., 1996), shape selectivity can arise in FEF when strategies commit feature attention and (2) this feature selectivity, which seems associated with divided attention, is functionally distinct from the

selection of the saccade endpoint. The first finding may seem at odds with the perspective that FEF selects targets regardless of the feature that identifies a stimulus as that target. However, adaptive performance strategies can explain this anomaly. Strategies are revealed by analyzing the responses made on error trials and RT in all trials. The increased prevalence of error saccades to vertical stimuli and the fastest RT to vertical stimuli reveals a priority for locating vertical stimuli.

The results are based on data obtained from a single monkey. Nevertheless, we believe they are reliable and interpretable for the following reasons. First, the observation of feature selectivity in FEF replicates previous findings (Bichot et al. 1996; Peng et al. 2008). A similar predisposition for motion direction has been described in the superior colliculus of monkeys performing a motion discrimination task with fixed stimulus-response mapping (Horwitz et al., 2004). The unexpected but clear robustness of this phenomenon should engender confidence in the replicability of the current observations. Second, the distinction of singleton selection and endpoint selection replicates previous findings (Sato & Schall, 2003; Schall 2004b). Such replication should increase confidence in the interpretability of the new findings. Finally, the novel observation of a distinct endpoint selection in pro-saccade trials is statistically robust, conceptually novel, and theoretically important. While we are confident that another monkey could be trained into this state, we judge that effort is better invested in more novel research goals. Indeed, we have discovered that the second monkey, trained without the opportunity to experience the confounds, employs a qualitatively different strategy to perform this task (Lowe et al., 2019).

5.4.1 Possible Sources of Feature Selection in FEF

We do not know whether the shape selectivity we observed is intrinsic to FEF, imparted by other prefrontal areas, inherited from earlier visual areas, or manifest from broad associations of stimulus, action, and reward. We consider each hypothesis below.

The hypothesis that feature selectivity is intrinsic to FEF runs counter to the framework of FEF as an area that contains a salience or priority map regardless of features defining salience or priority (Thompson & Bichot, 2005). However, some studies have reported differential activity to stimuli defined by features whose identities do not dictate different stimulus-response rules (Ferraina et al., 2000; Peng et al., 2008; Xiao et al., 2006). Mohler et al. 1973 reported 6% of FEF neurons (12.5% of those with visual responses) responding differently according to direction of motion or color. Peng and colleagues (2008) found that even during a passive fixation task a quarter of FEF neurons had responses that differed according to the form of the presented stimuli. These differences occurred at most 12 ms after the initial visual transient. This short delay between visual response onset and feature selectivity is consistent with the selectivity for color found previously (Bichot et al. 1996). However, the shape selectivity presented here was not as immediate. This may be due to the nature of the tasks across studies in that there are unbalanced reward contingencies of nonpreferred stimuli in the present study whereas all stimuli were evenly rewarded in the passive fixation and delayed match to sample tasks used by Peng et al. It is notable that the proportions of feature selective neurons found by Peng et al. are similar to those found in the present data, but are fewer than those found by Bichot et al. (1996). This could be due to differences in complexity of the stimuli, nature of the task, or sampling of units.

The hypothesis that feature selectivity in FEF can be imparted by another prefrontal area is motivated by the recent description of a ventral prearcuate area (Bichot et al. 2015), which has dense connections with FEF (Huerta et al., 1987). Neurons in this area have differential responses to complex visual stimuli during detection and delayed search tasks, and this feature selectivity preceded the selection of a saccade endpoint (Bichot et al., 2015). However, direct comparison between this and the current study is challenged by differences in experimental design and particular observations. For example, their target item was cued before array presentation and so was held in working memory, but our target item in this study was a long-term memory trace. Also, neurons in the ventral prearcuate area exhibited feature selectivity at approximately the same time as FEF, and the spatial selectivity identified in FEF was earlier than that observed in the present data ($_{Corr}SST_{Pro}$). Further research is needed, therefore, to clarify whether FEF receives feature information primarily from this area, or both areas have common inputs and process feature information in parallel.

The hypothesis that feature selectivity in FEF is inherited from feature selective responses earlier in the visual stream is motivated by the connections between FEF and effectively all extrastriate visual areas (Schall et al. 1995; Markov et al. 2014). V4 is one likely source because the neurons are selective for color (Schein & Desimone, 1990; Zeki, 1980; Zeki, 1973) and shape (Desimone & Schein, 1987; Pasupathy & Connor, 1999). In the previous (Bichot et al. 1996) and current study, neither color nor shape selectivity were carried by the FEF neurons with the shortest visual latencies. This is consistent with color and shape information arriving in relatively longer latency afferents (e.g., Schmolesky et al., 1998). Evidence from simultaneous recordings in FEF and V4

demonstrate an association of visual neurons in FEF with V4 (Gregoriou et al., 2012) and feature selectivity in V4 preceding FEF selective modulation (Zhou & Desimone, 2011). Further research is needed, though, to understand the interplay of feature selectivity and attentional modulation between FEF and extrastriate visual areas (Zhou et al., 2011; see also Monosov et al., 2010).

The hypothesis that feature selectivity in FEF is manifestation of the association of strategy and reward is motivated by well-known reports that visual responses in FEF are modulated by reward expectation (Glaser et al., 2016) or magnitude (Ding & Hikosaka, 2006). Parallel modulation is observed broadly in the visuo-motor network (e.g., Griggs et al., 2018; Platt & Glimcher, 1999; Sugrue et al., Newsome, 2004; Yamamoto et al., 2013). In human studies, both reward probability and magnitude have been shown to influence behavior. Della Libera & Chelazzi, (2009) found that by associating meaningless shape stimuli with high, low, or neutral reward in a practice phase resulted in facilitation or interference of response times, depending on task conditions. Similarly, attentional biases emerge when color stimuli are associated with high or low reward, whether or not participants are aware of the stimulus-reward associations (Kiss et al., 2009; Kristjánsson et al., 2010). These associations do not require physical salience as they are present with stimulus configurations that have only reward histories to differentiate stimuli and for which rewarded features are not the basis for selection (Anderson et al., 2011). These findings suggest that stimulus-reward associations can be learned and combined with physical salience to form an integrated priority map (Awh et al., 2012). These reward associations manifest themselves in neural activity (Anderson, 2016). The tail of the caudate is sensitive to learned reward

associations (Anderson et al., 2014). Learned value associations are reflected in BOLD signaling in attentional visual areas such as parietal cortex (Anderson et al., 2014) and are reflected in shifts of ERPs indexing attentional selection such as the N2pc (Kiss et al., 2009).

In conjunction search FEF neurons respond maximally when the correct saccade target is in the RF (Bichot et al., 2001b; Ogawa & Komatsu, 2006) but also show larger responses to a distractor that shares a feature with the correct saccade target than a distractor that shares no features (Bichot et al., 2001b). Similarly, FEF neurons respond more when a distractor that was the target on the previous session is in the RF than a distractor that shares no features with the current saccade target. This demonstrates that FEF neurons can differentially respond to features that are remembered to be rewarded even when not presently rewarded. Reward associations, specifically the lack thereof, can also participate in distractor suppression (Cosman et al., 2018). In a search task with salient distractors that "capture" attention (Theeuwes, 1991) two monkeys overcame capture with training and produced equal performance when the color singleton distractor was present or absent. Neurons recorded from those two monkeys showed a reduction in firing rate when the salient distractor was in the RF compared to a non-salient distractor was in the RF. Because the salient distractors were never a saccade target, but were nevertheless distinguishable from the other distractors, responses to them can be more actively and immediately suppressed than the other distractors. Bichot and colleagues (2001) also tested neural responses during a search task with a salient distractor and did not find distractor suppression. However, the monkeys in that study were behaviorally affected by the singleton distractor and thus

distractor suppression may not be expected. Further, the neurons analyzed by Bichot and colleagues were movement neurons whereas those analyzed here and by Cosman et al. had visual responses. This difference in neuron type may also explain the differences in results.

Interestingly, the third monkey in the study by Cosman and colleagues that was unable to overcome attentional capture was the same monkey Da whose data are reported here. Neurons from this monkey did not show such distractor suppression. Notably, this monkey also had neurons that retained an initial nonspecific visual response whereas monkeys A and C did not have such a response during the color singleton search task. Such an initial visual response is reduced in FEF neurons when stimuli are not saccade targets (or, alternatively, enhanced when they are saccade targets) in both search tasks (Thompson et al., 1997) and in single stimulus presentations (Goldberg & Bushnell, 1981; Mohler & Wurtz, 1976; Schall et al., 1995a). In the case of monkeys A and C, the stimuli whose colors were not the target color were never correct saccade targets and can thus be discounted and would have attenuated nonspecific responses to these stimuli, and this attenuation could be complete such that there is no such response. In the case of Da, square and horizontal stimuli were correct saccade endpoints on a subset of anti-saccade trials, thus they are still associated with reward to some degree and thus may require the retaining of the nonspecific visual transient.

5.4.2 Processing Operations and Neural Chronometry

We replicated the previous finding of distinct operations mediated by visually responsive neurons selecting a conspicuous stimulus and selecting the endpoint of the saccade

(Sato & Schall, 2003). The prior experiment did this by contrasting modulation in pro- and anti-saccade trials. The current experiment did this, innovatively, by contrasting modulation to preferred and non-preferred features and to fixated and non-fixated items among identified neurons exhibiting feature selectivity even for stimuli that should not be and were not selected. Specifically, we demonstrated quantitative differences between two measures of neural modulation: stimulus selection, indexed by FST and $_{Corr}SST_{Pro}$, and saccade endpoint selection, indexed by EST. The chronometric distinction between singleton selection and endpoint selection in both pro- and anti-saccade trials and the simultaneity of EST on pro- and anti-saccade trials having very different RT validates the conceptual distinction between these operations. These neural measures index some of the computational operations occupying response time in this task (Donders, 1868).

The delay between EST and saccade initiation identifies another operation preceding saccade initiation. This operation has been identified psychologically as response preparation and neurally as the presaccadic build-up of movement related neural activity, which does not occur until information about target items becomes available (Woodman et al., 2008) and is identified with the accumulation of sensory evidence (Purcell et al., 2010, 2012b; Servant et al., 2019). The final saccade initiation operation is accomplished by competitive interactions between movement cells (Purcell et al., 2010, 2012b). The time required for this competition resolution explains the additional time necessary for anti-saccades compared to pro-saccades. The relationship between stimulus selection, endpoint selection, and saccade preparation has been

investigated in monkeys (Juan et al., 2004; Katnani & Gandhi, 2013) and humans (Juan et al., 2008).

To verify the existence and elucidate the properties of these distinct operations and stages, and to resolve different explanations for causal manipulations, further research should employ the powerful logic of selective influence in factorial experimental designs (Sternberg, 2001; Townsend & Nozawa, 1995) with joint measures of mental and neural chronometry.

CHAPTER 6: NEURAL CORRELATES OF MULTIDIMENSIONAL DECISION-MAKING IN MACAQUE FRONTAL EYE FIELD

6.0 SUMMARY

In Chapters 2 and 3 I identified functional neuron categories in FEF. In Chapter 4 I identified cognitive architectures underlying our GO/NO-GO search task. In Chapter 5, I identified neural indices of cognitive operations. In this chapter, my goal is to identify neural indices of the cognitive operations in GO/NO-GO search, relate these neural indices to the architecture of those operations, and outline a mechanistic description of information processing between the array presentation and response.

In these recordings, I expect to identify neurons that exhibit *singleton selection*, or increased responses when a search singleton is located within the response field of FEF neurons as compared to when a search singleton is located outside its response field (Schall et al., 1995a; Schall & Hanes, 1993). Further, I expect to see that with increased singleton identifiability, the time at which this selection occurs, the *singleton selection time (SST)*, will be decreased (Sato et al., 2001). If the cognitive architecture is coactive, i.e., both factorial manipulations affect operations that are summed before a common decision operation, then SST should scale with response time across all four GO conditions. If cognitive architecture is not coactive, i.e., the two factorial manipulations affect different decision operations, then SST should not be impacted by cue discriminability, given that it is affected by singleton identifiability as expected. Conversely, this architecture implies the existence of a sub-population of neurons selective for aspect ratio. The time when GO and NO-GO conditions are differentiated will be termed *cue discrimination time (CDT)*, which should be faster when cue

discriminability is increased. I assess which of these subpopulations of neurons exist in FEF, and whether their responses are consistent with the behaviorally defined cognitive architectures. These analyses are in preparation for submission in a minimal and/or detailed form; the remainder of this chapter is the detailed version of the analyses.

6.1 INTRODUCTION

For more than a century, an area in the frontal lobe called frontal eye field (FEF) has been known to be involved in the production of eye movements (Ferrier, 1875). Recordings of single neurons in FEF have confirmed the presence of neurons whose discharge rate increases before eye movements (e.g., Bizzi & Schiller, 1970) as well as neurons that respond to visual stimuli (Bruce & Goldberg, 1985; Lowe & Schall, 2018; Schall, 1991). Movement-related neurons in FEF trigger saccade production when a critical discharge rate is achieved (Hanes & Schall, 1995). Visually driven neurons in FEF exhibit *target selection*, or a differential response when a search target is within as compared to outside its receptive field (Schall, 2015; Schall & Hanes, 1993; Thompson et al., 1996).

Now, FEF visual neurons are generally seen as containing a salience or priority map that defines the behavioral significance of locations or items in the visual field (for review, see Bisley, 2011; Thompson & Bichot, 2005). But the mechanism by which the visuomotor transformation, the conversion of visual salience to an oculomotor command, is not fully understood. Some investigators have focused on the coordinate system transformations in neurons during the delay period of a delayed saccade task (Sajad et al., 2016). Others tried to remove the motor planning component of neural responses by varying the visual processing time (Costello et al., 2013; Stanford et al.,

2010), or interfere with the motor plan by changing the target location (Goldberg & Bruce, 1990; Ray et al., 2009; Sato et al., 2001; Umeno & Goldberg, 1997) or introducing a stimulus-response mapping rule (Everling & Munoz, 2000; Lowe & Schall, 2019; Sato & Schall, 2003). Still others have focused on whether transmission between visual and movement neurons is continuous (Bichot et al., 2001a) or discrete (Woodman et al., 2008).

The latter question has been more or less resolved during search by the Gated Accumulator Model (Purcell et al., 2010, 2012b). A family of models with or without certain components, such as lateral inhibition, gating, leak, etc., were all generally able to fit behavioral data. This highlights the problem of *model mimicry* whereby multiple alternatives for underlying processes can explain behavior similarly well. However, only the model with gating between the visual and movement units was able to capture the neural dynamics.

This model provided convincing evidence that at least some gate is necessary during visuomotor transformations, specifically during search. However, while this finding can explain why movement neuron activity begins to rise after visual neurons select search targets, it cannot on its own explain the canceling of movement neuron buildup activity during saccade countermanding tasks (Boucher et al., 2007; Hanes & Schall, 1995). Nor can it explain why visual neurons can be influenced by target-distractor similarity in search but not changes of target position while response times (RT) are affected by both (Sato et al., 2001). Further, at least two subpopulations of visual neurons have been demonstrated in a pro-/anti-saccade search task with different relationships to RT across the two stimulus-response mapping rules (Sato &

Schall, 2003). In this task, type I visual cells seem to create the salience map whereas type II visual cells select the saccade endpoint. We have also demonstrated this dissociation between stimulus selection and saccade endpoint selection on pro-saccade trials with specific task manipulations (Lowe & Schall, 2019).

It seems as though there are additional gating mechanisms for stimulus-response mapping rules that interact with the visuomotor transformation demonstrated by the Gated Accumulator Model. Direct investigations of such interactions have not yet been performed, as there have not been studies that specifically and selectively manipulated the stimulus selection and saccade selection processes. Or, such tasks have not manipulated both processes within the same sessions and for the same neurons (e.g., Sato et al., 2001). Here we present results from such an approach.

By adding a response preparation manipulation to a search task, we can selectively manipulate the search efficiency and the response rule to probe additional interactions between visual and movement-related neurons. Behaviorally, these tasks are *filtering tasks* that require the selection of a stimulus based one feature and selection of a response based on a different feature. In psychology, these tasks have been studied extensively but the mechanisms by which stimulus selection and response selection are still unknown. The most common view is that stimulus selection and response selection are separate sequential stages (e.g., Broadbent, 1971; Hoffman, 1978; Treisman, 1988; Wolfe et al., 2015). An alternative view is that objects are selected and categorized through parallel processes (Bundesen, 1990; Logan, 2002).

Serial and parallel processing have a long and complex history which we have summarized previously (Lowe et al., 2019). In brief, these two processing architectures

were once seen as easily dissociable in tasks like search where the reliance of RT on set size was taken to be indicative of serial processing and a lack of such reliance was taken to be indicative of parallel processing (Treisman & Gelade, 1980). However more recent models have shown that mimicry is rampant between these architectures (e.g., Moran et al., 2016; Townsend, 1990; Wolfe, 2007). However, Townsend and colleagues (Houpt et al., 2014; Townsend & Nozawa, 1995) developed a method of identifying these architectures, *systems factorial technology (SFT)*, in a way that gives nearly unambiguous inferences of underlying processing architectures from RT distributions.

Each of the family of architectures discriminable through SFT make specific predictions of the underlying neurons involved in the task (Fig. 6.1). To test these predictions, and to understand the roles of response preparation and stimulus selection in the visuomotor transformation in FEF, we developed a filtering task in which the aspect ratio of a color singleton in a search array cued either a GO or NO-GO rule. To selectively manipulate the stimulus selection process, we changed the chromatic similarity of the singleton and distractor stimuli. To selectively manipulate the response preparation process, we changed the aspect ratio of the stimuli to be more or less similar to the NO-GO cue. These manipulations were performed independently of one another so that all trial types were available for comparison within a single session. The behavioral effects and application of SFT to this task has been reported previously (Lowe et al., 2019). Now, we recorded from neurons in the FEF of two monkeys performing this GO/NO-GO search task and compare the responses of the visual and movement-related neurons to the predictions of SFT.

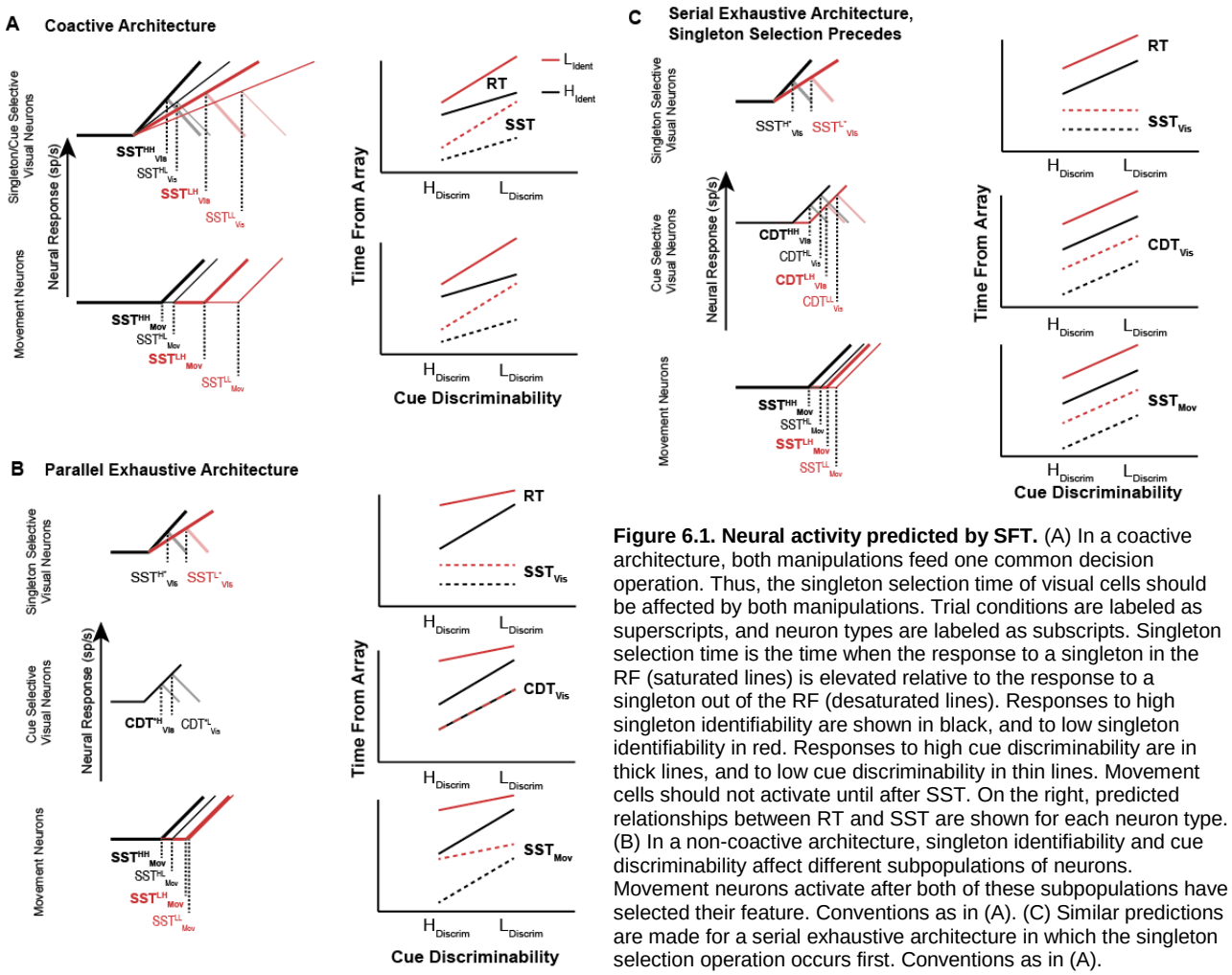

Figure 6.1. Neural activity predicted by SFT. (A) In a coactive architecture, both manipulations feed one common decision operation. Thus, the singleton selection time of visual cells should be affected by both manipulations. Trial conditions are labeled as superscripts, and neuron types are labeled as subscripts. Singleton selection time is the time when the response to a singleton in the RF (saturated lines) is elevated relative to the response to a singleton out of the RF (desaturated lines). Responses to high singleton identifiability are shown in black, and to low singleton identifiability in red. Responses to high cue discriminability are in thick lines, and to low cue discriminability in thin lines. Movement cells should not activate until after SST. On the right, predicted relationships between RT and SST are shown for each neuron type. (B) In a non-coactive architecture, singleton identifiability and cue discriminability affect different subpopulations of neurons. Movement neurons activate after both of these subpopulations have selected their feature. Conventions as in (A). (C) Similar predictions are made for a serial exhaustive architecture in which the singleton selection operation occurs first. Conventions as in (A).

6.2 METHODS

6.2.1 Monkeys, Surgical Procedures, and Gaze Acquisition

All procedures were approved by the Vanderbilt Institutional Animal Care and Use Committee in accordance with the United States Department of Agriculture and Public Health Service Policy on Humane Care and Use of Laboratory Animals.

Behavioral data were collected from two macaque monkeys, *Macaca mulatta* and *M. radiata*, identified as Le and Da. The monkeys weighed approximately 12 kg (Le) and 8 kg (Da) and were aged 7 years (Le) and 13 years (Da) at the time of the study. Monkeys were surgically implanted with a headpost affixed to the skull via ceramic

screws under aseptic conditions with isoflurane anesthesia. Antibiotics and analgesics were administered postoperatively. Monkeys were allowed at least 6 weeks to recover following surgery before being placed back on task. Gaze was tracked using an Eyelink 1000 system (SR Research; sampling rate = 1,000 Hz).

6.2.2 Assessment of Operations, Stages and Architectures

To assess alternative process architectures supporting performance of this task, we applied systems factorial technology (Harding et al., 2016; Houpt et al., 2014; Lowe et al., 2019; Townsend & Nozawa, 1995). Statistical details of systems factorial technology and reporting conventions can be found in these references. Systems factorial technology typically requires a 2x2 manipulation of factors that selectively influence distinct processing operations (cf. Yang et al. 2014). As illustrated in Figure 6.2, the first manipulation was *singleton identifiability* through interleaved presentation of search arrays with low singleton-distractor similarity (e.g., red among green; High Identifiability, H_{Ident}) and search arrays with high singleton-distractor similarity (e.g., red among off-red; Low Identifiability, L_{Ident}). The second manipulation was *cue discriminability* through interleaved presentation of array items with higher aspect ratio (High Discriminability, $H_{Discrim.}$) and array items with lower aspect ratio (Low Discriminability, $L_{Discrim.}$). The cue discrimination was enforced by interleaving 20% nogo trials. This 2x2 design results in four types of trial. The easiest were High Identifiability with High Discriminability ($H_{Ident}H_{Discrim.}$). The most difficult were Low Identifiability with Low Discriminability ($L_{Ident}L_{Discrim}$). The two intermediate difficulty were Low Identifiability with High Discriminability ($L_{Ident}H_{Discrim}$) and High Identifiability with Low Discriminability ($H_{Ident}L_{Discrim}$).

6.2.3 Task Design and Protocol

Monkeys performed 30 sessions of a GO/NO-GO visual search task in which response was cued by the shape of a color singleton. Trials began with the monkey fixating a central stimulus for 800-1200 ms, after which eight iso-eccentric, isoluminant stimuli were presented. Eccentricities varied between 4.0 and 8.0 degrees of visual angle and were adjusted per-session to drive isolated neurons. Stimuli were either square or rectangular. All eight stimuli had the same shape on each trial. If the singleton and distractors were square, cueing a no-go trial, monkeys were rewarded for maintaining fixation at the central spot for a random interval between 800 and 1200 ms. No-go trials comprised ~20% of all trials in each session. If stimuli were rectangular, monkeys were rewarded for shifting gaze to the singleton and maintaining fixation for 700 ms. The inter-trial interval was fixed at 1500 ms.

Task difficulty varied along two dimensions (Figure 6.2): singleton-distractor color similarity and stimulus elongation. Singleton-distractor color similarity manipulated singleton identifiability. Stimulus elongation manipulated cue discriminability. All stimuli had four possible colors: red (CIE x 628, y 338, Y 4.4 (monkey Da) or x 604, y 339, Y 5.2 (monkey Le)), green (CIE x 280, y 610, Y 4.6 (monkey Da) or x 292, y 575, Y 6.1 (Monkey Le)), off-red, or off-green presented on a gray background (CIE x 275, y 228, Y 0.54 or x 334, y 375, Y 0.6). CIE values for off-red and off-green stimuli were adjusted for each monkey to elicit a performance deficit when

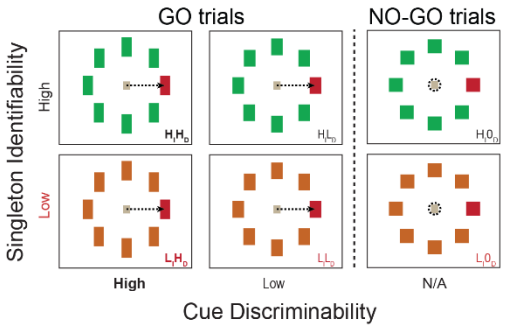

Figure 6.2. Task design. In this task an eight element search array was presented on each trial, with one color singleton and seven distractors. The aspect ratio of the singleton cued a GO response when elongated (indicated by dotted arrows) or a NO-GO response when square (indicated by a dashed circle around fixation). Task difficulty was manipulated by chromatic similarity, or singleton identifiability which could be either high (H_I) or low (L_I), and by the aspect ratio, or cue discriminability which could be either high (H_D) or low (L_D).

presented in a Low Identifiability condition. Stimuli had three possible aspect ratios: square for NO-GO trials, and either 1.4 or 2.0 for GO trials. The orientation of elongation was counterbalanced between the two monkeys; for monkey Da a vertical rectangle signaled GO, whereas for monkey Le a horizontal rectangle signaled GO.

6.2.4 Recording Techniques

MRI compatible headposts and recording chambers were placed over the arcuate sulcus. Surgery was conducted under aseptic conditions with animals under isoflurane anesthesia. Antibiotics and analgesics were administered postoperatively. Details have been described previously (Schall et al., 1995a; Sato et al., 2001; Cohen et al., 2009b). Electrophysiological data was obtained from 32-channel linear electrode arrays (Neuronexus Vector Array). Probes had either 100 or 150 μm recording contact spacing. Data were streamed to TDT System 3 (25 kHz, Tucker Davis Technologies). Single units were identified online using principal component analysis (TDT) and sorted offline automatically using JRClust (Jun et al., 2017) or manually using Plexon Offline Sorter (Plexon). Well isolated neurons were identified as units that met several criteria: a minimum firing rate during the pre-stimulus baseline period, a maximum Fano factor (variance divided by mean) during the pre-stimulus baseline period, a minimum signal-to-noise ratio of the spike waveforms (Joshua et al., 2007), and a minimum 10^{th} percentile of inter-spike intervals. Criteria for these values were assigned by visually inspecting distributions across the population and SDFs of the included neurons, but specific values did not substantially change the results reported here.

6.2.5 Cell Type Classification

First, we classified neurons according to traditional criteria and defined neurons as visually-responsive, visuomovement, movement-related, fixation, or post-saccadic (Bruce & Goldberg, 1985; Schall, 1991). Visually responsiveness was defined as a significant increase in response from pre-array baseline of more than 2 standard deviations for at least 50 ms beginning less than 150 ms after array onset. Movement-related activity was defined similarly, with the time period assessed being the 100 ms before saccade. Movement-related activity was also required to have a positive correlation over time in the 20 ms before saccade to eliminate the effect of delay period activity, and a peak of less than 100 ms post-saccade. Visuomovement neurons were those that exhibited both types of activity. Fixation neurons were those that decreased in response by more than 2 standard deviations from pre-array baseline around the time of the saccade. Post-saccadic neurons were those that met the movement-related criteria in the 100 ms after saccade, whose activity peaked later than 100 ms after saccade, and were not otherwise categorized as movement-related.

6.2.6 Statistical Analyses

All t-tests presented are two-sided, unless otherwise stated. ANOVA were calculated on across-session mean response times and accuracy rates. To account for incidental variation across sessions while preserving relative relationships between conditions, we performed a repeated measures ANOVA with sessions accounting for the repeated measure. To avoid edge effects, accuracy rates were transformed using the logit transformation (Wharton & Hui, 2011).

6.3 RESULTS

6.3.1 Behavioral Sensitivity to Identifiability and Discriminability

To assess the effects of singleton identifiability and cue discriminability in the neural responses, we must first demonstrate that these effects are behaviorally significant. We found that both monkeys were significantly slower to respond to low identifiability trials with respect to high identifiability trials (Fig. 6.3A; Da: $F(1,61) = 2089.7$, $p < 0.001$; Le: $F(1,39) = 1608.9$, $p < 0.001$), and to low discriminability trials with respect to high discriminability trials (Da: $F(1,61) = 371.7$, $p < 0.001$; Le: ($F(1,39) = 275.1$, $p < 0.001$). These factors did not interact for either monkey (Da: $F(1,61) = 0.45$, $p = 0.5010$; Le: $F(1,39) = 1.03$, $p = 0.3170$).

We also assessed the effects of singleton identifiability and cue discriminability on the response accuracy. Both monkeys were significantly more accurate on high identifiability trials with respect to low identifiability trials (Fig. 6.3B; Da: $F(1,61) =$

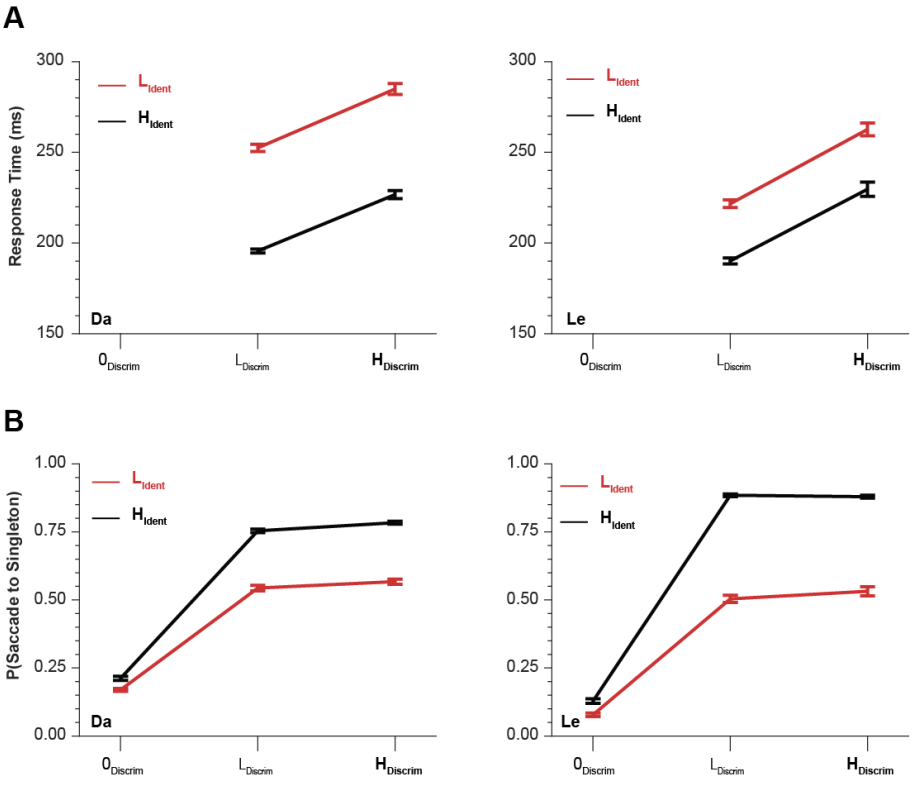

Figure 6.3. Behavioral results. (A) Mean ± SEM response times across sessions included in the neural analysis for monkey Da (left) and monkey Le (right). Response times were longer in the low discriminability condition ($H_{Discrim}$) and in the low identifiability condition (L_{Ident}). Response times for NO-GO trials, $0_{Discrim}$, are undefined. (B) Mean ± SEM probability of making a saccade toward the singleton for monkey Da (left) and monkey Le (right). For $L_{Discrim}$ and $H_{Discrim}$ conditions, these values correspond to behavioral accuracy. For the $0_{Discrim}$ condition, these correspond to failures to withhold response and are roughly equal to 1 – P(correct).

1209.4, $p < 0.001$; Le: $F(1,39) = 1466.7 < 0.001$). We also found that monkey Da was significantly more accurate on high discriminability trials with respect to low discriminability trials ($F(1,61) = 34.9$, $p < 0.001$) whereas the accuracy of monkey Le was not affected by discriminability ($F(1,39) = 0.96$, $p = 0.3339$). For Da, these factors did not interact ($F(1,61) = 2.31$, $p = 0.1337$). Whereas for monkey Le they did ($F(1,39)$ 6.70, $p = 0.0135$).

6.3.2 Neurometric Sensitivity to Identifiability and Discriminability

Movement-related neurons in FEF are considered to manifest an evidence accumulation process during decision-making tasks, ramping to a common threshold which triggers a saccade (Hanes et al., 1995; Hanes & Schall, 1995). This finding has been replicated in visual search, wherein the onset of movement activity is variable with respect to array presentation but not with respect to saccade initiation (Purcell, Schall, et al., 2012; Woodman et al., 2008). Because of this tight association between activity of movement-related neurons in FEF and saccade production, we expect that movement-related neurons should being ramping or discriminating a singleton in its RF at a time invariant with respect to the saccade on GO trials in the present task. This invariance should then manifest as being affected by both singleton identifiability and cue discriminability with respect to array onset.

We find this prediction to hold in the current sample of FEF movement neurons (Fig. 6.4). For Da, SST^{HH}_{Mov} was 134.0 ± 21.2 ms, SST^{HL}_{Mov} was 153.3 ± 29.2 ms,

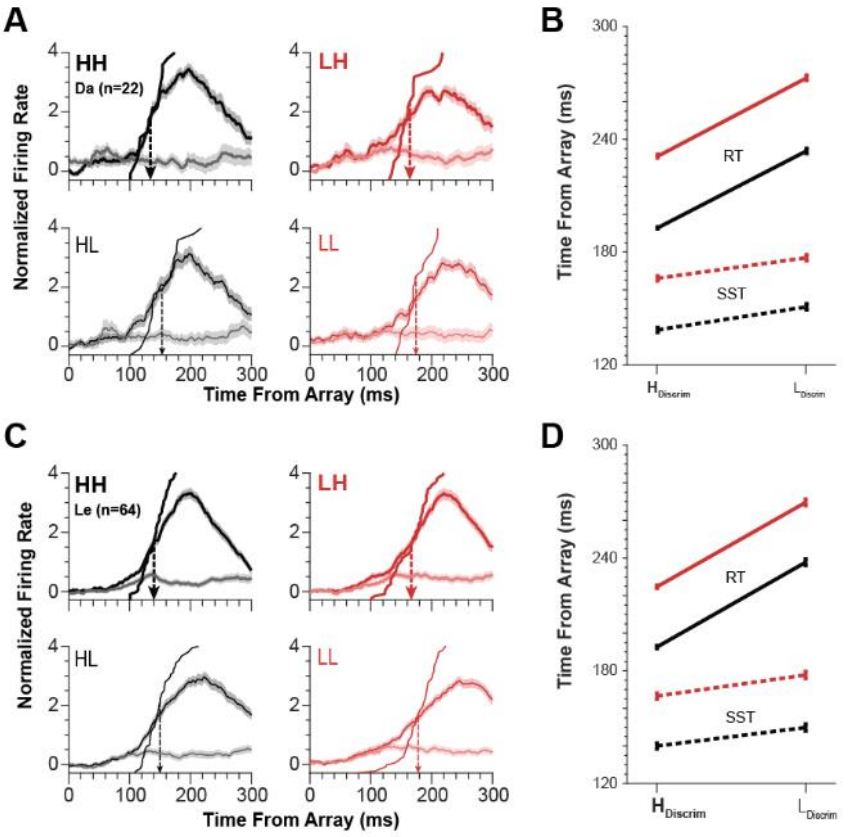

Figure 6.4: Movement-related responses. (A) Mean ± SEM normalized SDFs for movement neurons recorded from monkey Da in the HH, HL, LH, and LL conditions. Responses to singletons in the RF are shown in saturated colors, responses to singletons out of the RF are shown in desaturated colors. High and low singleton identifiability are shown in black and red, respectively. High and low cue discriminability are shown in thick and thin lines, respectively. Cumulative distrubutions of SST_{Mov} in each condition are shown, with the mean value indicated by the dashed arrow. (B) Mean ± SEM response times (solid) and SST_{Mov} (dashed lines) for the neurons whose responses are shown in (B). High and low singleton identifiability are shown in black and red, respectively. High and low cue discriminability are shown on the left and right, respectively. (C) Mean ± SEM normalized firing rates for movement neurons recorded from monkey Le. Conventions as in (A). (D) Mean ± SEM response times and SST_{Mov} for the neurons whose responses are shown in (C). Conventions as in (B).

SST^{LH}_{Mov} was 164.0 ± 26.1 ms, and SST^{LL}_{Mov} was 174.1 ± 22.4 ms. For Le, SST^{HH}_{Mov} was 139.9 ± 19.7 ms, SST^{HL}_{Mov} was 149.7 ± 23.9 ms, SST^{LH}_{Mov} was 166.4 ± 29.3 ms, and SST^{LL}_{Mov} was 177.7 ± 28.6 ms. The singleton selection time of movement related neurons (SST_{Mov}) was significantly longer for low identifiability trials than for high identifiability trials (Da: $F(1,21) = 76.9$, $p < 0.001$; Le: $F(1,63) = 111.0$, $p < 0.001$). SST_{Mov} was also significantly longer for low discriminability trials than for high discriminability trials (Da: $F(1,21) = 15.4$, $p < 0.001$; Le: $F(1,63) = 12.6$, $p < 0.001$). These two factors did not interact (Da: $F(1,21) = 1.1$, $p = 0.2975$; Le: $F(1,63) = 0.13$, $p = 0.716$). Thus, as predicted movement neurons are sensitive to the same factors as the RTs.

Visual neurons in FEF exhibit singleton selection (Schall, 2015; Schall & Hanes, 1993). This singleton selection tends to be locked to array onset (Thompson et al.,

1996), but can be modulated by search difficulty (Purcell et al., 2012b; Sato et al., 2001) or stimulus-response rule (Sato & Schall, 2003). Thus, these neurons are those for which the different processing architectures make differing predictions. Spike density functions of visual neurons for singletons in or out of the RF for each of the four GO conditions are shown in Fig 6.5A and Fig. 6.5C for monkey Da and Le, respectively. For Da, SST^{HH}_{Vis} was 131.5 ± 27.0 ms, SST^{HL}_{Vis} was 135.0 ± 28.4 ms, SST^{LH}_{Vis} was 146.9 ± 31.2 ms, and SST^{LL}_{Vis} was 150.4 ± 32.9 ms (Fig. 5B). Although RT was sensitive to both manipulations, SST_{Vis} was sensitive to singleton identifiability ($F(1,69) = 34.7$, $p < 0.001$) but not cue discriminability ($F(1,69) = 1.3$, $p = 0.257$), nor their interaction ($F(1,69) = 0.0$, $p = 0.999$). This distinction suggests that singleton identifiability and cue discriminability are separate operations that are selectively influenced by our manipulations, as predicted by all architectures except coactive.

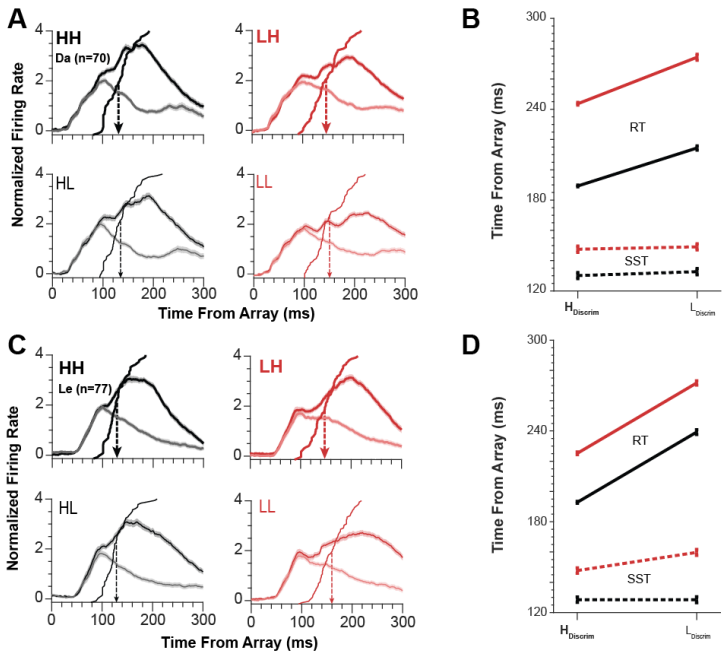

Figure 6.5: Visual responses. Mean ± SEM normalized SDFs from visually responsive neurons from monkey Da (A) and Le (C), and mean ± SEM and SST_{Vis} for these neurons from monkey Da (B) and Le (D). Conventions as in Fig. 6.4.

For Le, SST^{HH}_{Vis} was 128.5 ± 23.5 ms, SST^{HL}_{Vis} was 128.5 ± 26.0 ms, SST^{LH}_{Vis} was 147.7 ± 29.3 ms, and SST^{LL}_{Vis} was 159.8 ± 29.4 ms (Fig. 5D). SST_{Vis} was sensitive to both singleton identifiability ($F(1,76) = 114.4$, $p < 0.001$) and cue discriminability ($F(1,76) = 4.5$, $p = 0.0365$), as well as their interaction ($F(1,76) = 6.5$, $p =$

0.0129). This sensitivity to both manipulations and the interaction suggests that singleton identifiability and cue discriminability are integrated before a common decision point, as predicted by a coactive architecture.

Behaviorally, we have previously reported that monkey Da performs the task with a parallel exhaustive architecture and that monkey Le performs the task with a coactive architecture (Lowe et al., 2019). Thus, the sensitivity of the visual neurons to our manipulations is consistent with these architectures. However, we also reported variability in architectures between sessions. To test the hypothesis that these inter-monkey differences are due to the processing architectures used, and not simply differences between monkeys, we next examine processing architecture.

6.3.3 Effect of Processing Architecture

To determine which processing architecture was used by each monkey, we subjected the response time distributions to SFT analysis (Fig. 6.6A). On average, we found that both monkeys exhibited a serial exhaustive architecture as they both have negative deflections followed by positive deflections whose areas are approximately equal (Da: MIC = 1.90 ± 15.76; Le: MIC = 1.63 ± 9.00). Notably, these values are quite variable. To assess the extent of the heterogeneity in processing architecture, we performed a clustering analysis on the SIC curves. We found three clusters of SIC for monkey Da and two clusters for monkey Le (Fig. 6.6B). For both monkeys we found coactive and serial exhaustive clusters. Monkey Da also had a parallel exhaustive cluster.

For each neuron, we used SFT to classify the processing architecture used in the trials for which that neuron was isolated. An example schematic of a non-coactive architecture, specifically a parallel exhaustive architecture, is shown in Fig. 6.7A.

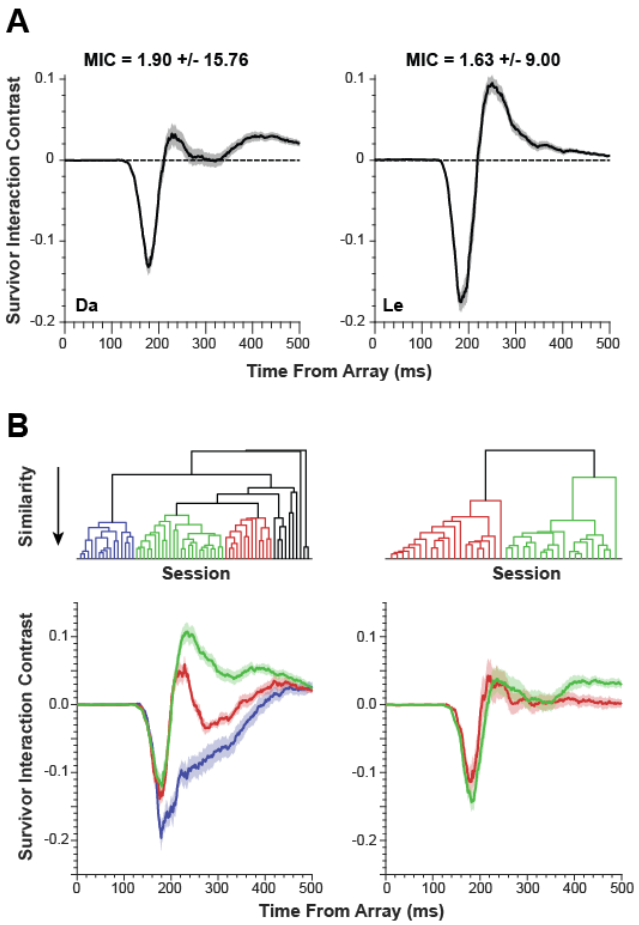

Figure 6.6: Survivor interaction contrasts. (A) Mean ± SEM survivor interaction contrast curve (SIC(t)) for sessions from monkey Da (left) and monkey Le (right). Mean ± SEM mean interaction contrast (MIC, the integral of SIC(t)) is also shown. (B) Given large SEM in the MIC, we examined heterogeneity of SIC curves across sessions using a cluster analysis. We identified three clusters of sessions for monkey Da (left) and two clusters of sessions for monkey Le. For both monkeys, coactive session clusters are shown in green, serial exhaustive session clusters are shown in red, and parallel exhaustive session clusters are shown in blue. The dendrogram for the clustering is shown on the top, and the mean ± SEM SIC curve for each cluster is shown on the bottom.

Normalized responses of visually responsive neurons from both monkeys during non-coactive architectures are shown in Fig. 6.7B, as are distributions of SST_{Vis}, mean ± SEM RT, and mean ± SEM SST_{Vis} for each condition. For these neurons, SST_{Vis} was sensitive to singleton identifiability (Da: $F(1,67) = 33.3$, $p < 0.001$; Le: $F(1,61) = 77.41$, $p < 0.001$; Both: $F(1,129) = 101.3$, $p < 0.001$) but not cue discriminability (Da: $F(1,67) = 1.1$, $p = 0.303$; Le: $F(1,66) = 1.70$, $p = 0.1974$); Both: $F(1,129) = 2.72$, $p = 0.101$) nor their interaction (Da: $F(1,67) = 0.0$, $p = 0.946$; Le: $F(1,66) = 2.44$, $p = 0.1233$; Both: $F(1,129) = 1.35$, $p = 0.248$). Similarly, responses for movement-related neurons are shown in Fig. 6.7C. SST_{Mov} was sensitive to both singleton identifiability (Da: $F(1,19) = 64.8$, $p < 0.001$; Le: $F(1,48) = 81.8$, $p < 0.001$; Both: $F(1,68) = 132.7$, $p < 0.001$) and cue discriminability (Da: $F(1,19) = 14.4$, $p = 0.001$; Le: $F(1,48) = 15.3$, $p < 0.001$; Both: $F(1,68) = 27.2$, $p < 0.001$).

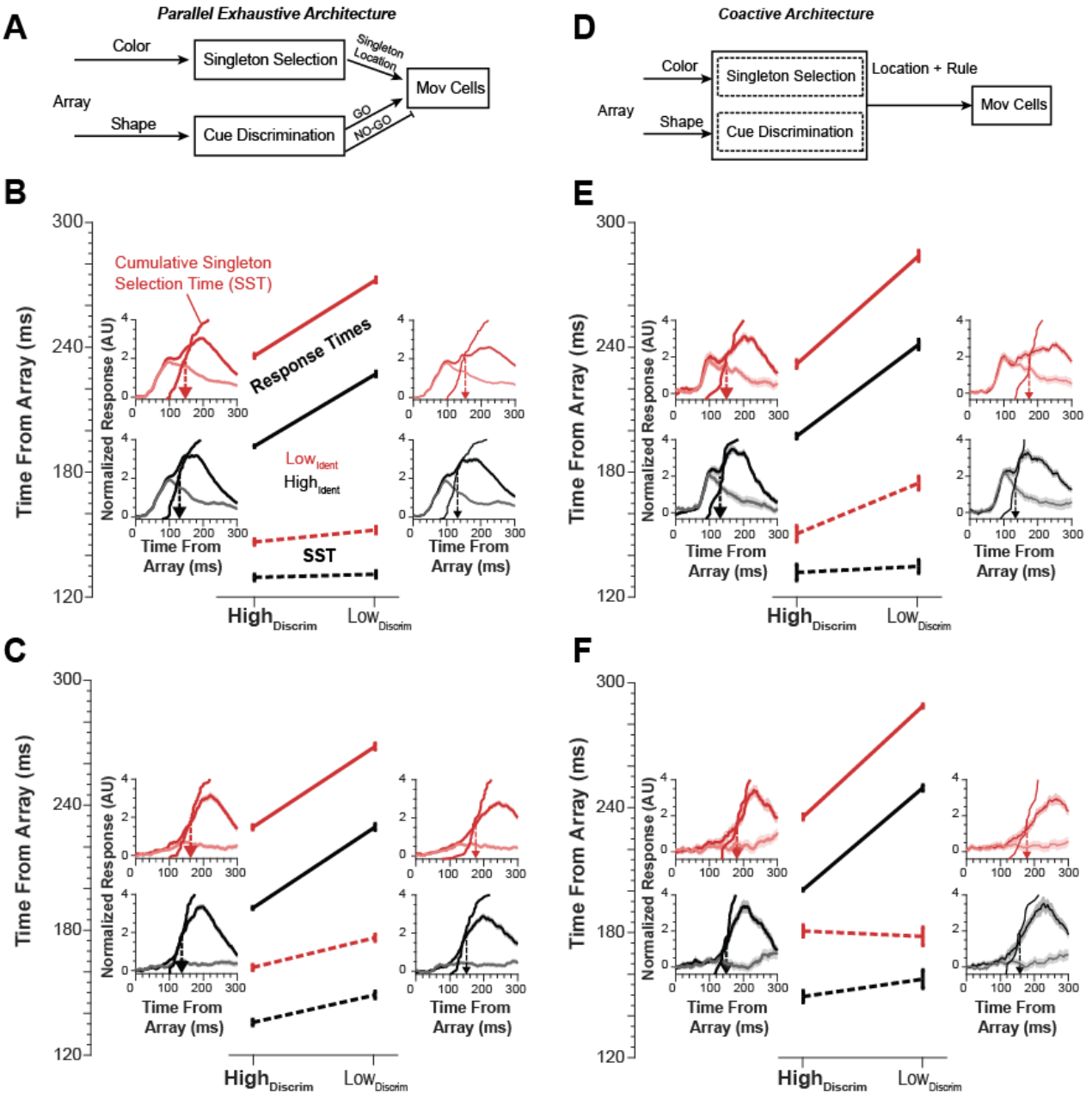

Figure 6.7: SST by architecture. (A) Schematic of an example non-coactive architecture, specifically parallel exhaustive. In this architecture, both manipulations affect different stages; color affects the singleton selection operation and shape affects the cue discrimination operation. Both operations drive or modulate movement-related neurons that drive the response. (B) Mean ± SEM RT (solid) and SST_{Vis} (dashed) for visually responsive neurons in non-coactive sessions. Mean ± SEM normalized SDFs for each condition, in four insets. Arrangement of conditions in the SDF plots follows the arrangement of RT conditions. Cumulative distributions and means are indicated as in Fig. 6.4. (C) Mean ± SEM RT and SST_{Mov} for movement-related neurons in non-coactive sessions. Conventions as in (B). (D) Schematic of a coactive architecture. In a coactive architecture, both manipulations affect a shared stage, which then drives movement neurons and the response. (E-F) RTs, SSTs, and SDFs as in (B) and (C) for visually responsive (E) and movement-related (F) neurons in a coactive architecture.

A schematic of a coactive architecture is shown in Fig. 6.7D. Responses of visually responsive neurons during coactive architectures are shown in Fig. 6.7E. For these neurons, SST_{Vis} was sensitive to singleton identifiability (Le: $F(1,14) = 49.21$, $p <$

0.001; Both: $F(1,16) = 44.0$, $p < 0.001$), cue discriminability (Le: $F(1,14) = 5.00$, $p = 0.0421$; Both: $F(1,16) = 6.2$, $p = 0.0244$), and their interaction (Le: $F(1,14) = 13.89$, $p = 0.0023$; Both: $F(1,16) = 9.3$, $p = 0.0076$). Responses of movement-related neurons during coactive architectures are shown in Fig. 6.7F. Interestingly, these neurons were only sensitive to singleton identifiability (Le: $F(1,14) = 28.30$, $p < 0.001$; Both: $F(1,16) = 35.54$, $p < 0.001$) but not cue discriminability (Le: $F(1,14) = 0.14$, $p = 0.7103$; Both: $F(1,16) = 0.28$, $p = 0.6041$) nor the interaction (Le: $F(1,14) = 3.37$, $p = 0.0875$; Both: $F(1,16) = 1.86$, $p = 0.1915$). This was surprising, but the lack of effect of cue discriminability is driven by the delay in $H_{Discrim}$ conditions, not a speeding of $L_{Discrim}$ conditions. Notably, monkey Da did not have enough neurons during performance with coactive architectures to analyze individually.

6.3.4 SST_{Mov} Accounts for More Change in RT Than SST_{Vis}

To assess whether the effects of singleton identifiability and cue discriminability on SST explain their effects on RT, we calculated the change in SST divided by change in RT, where we define the difference values as the average difference in one manipulation at fixed levels of the second manipulation. For example, ΔRT_{Ident} was the average of $RT^{LH} - RT^{HH}$ and $RT^{LL} - RT^{HL}$. For visually responsive neurons, we found that $\Delta SST_{Vis}/\Delta RT_{Ident}$ was 44.0 ± 77.8%, which was significantly above 0 ($t(129) = 6.45$, $p < 0.001$). Conversely, we found that $\Delta SST_{Vis}/\Delta RT_{Discrim}$ was 3.4 ± 156.1%, which was not significantly different than 0 ($t(129) = 0.28$, $p = 0.779$). Moreover, $\Delta SST_{Vis}/\Delta RT_{Ident}$ was significantly greater than $\Delta SST_{Vis}/\Delta RT_{Discrim}$ ($t(129) = 2.91$, $p = 0.004$). In contrast, for movement related neurons, we found that $\Delta SST_{Mov}/\Delta RT_{Ident}$ was 71.2 ± 68.6%, which was significantly above 0 ($t(68) = 8.62$, $p < 0.001$). $\Delta SST_{Mov}/\Delta RT_{Discrim}$ was 40.3 ±

107.5%, which was also significantly above 0 ($t(68) = 3.12$, $p = 0.003$). $\Delta SST_{Mov}/\Delta RT_{Ident}$ was also greater than $\Delta SST_{Mov}/\Delta RT_{Discrim}$ ($t(68) = 2.04$, $p = 0.046$). Comparing ΔSST_{Vis} to ΔSST_{Mov}, movement-related neurons account for more of the RT differences than visually responsive neurons, both in the effect of singleton identifiability (Wilcoxson rank sum: $Z = 2.30$, $p = 0.022$) and cue discriminability (Wilcoxson rank sum: $Z = 2.48$, $p = 0.013$).

Whereas these findings show that SST_{Vis} accounts for some of the RT differences due to identifiability, and SST_{Mov} accounts for some of the RT differences due to both identifiability and discriminability, these RT differences are all significantly less than 1. This suggests that while change in SST influences response production, it does not dictate it. There must exist some other influence preventing the execution of a saccade as soon as the correct location is discriminated. This influence likely arises from the subpopulation of neurons affected by cue discriminability but not singleton identifiability that we did not record in this sample. However, we can see evidence of the influence of this other subpopulation in the responses during NO-GO trials.

6.3.5 Visual Neurons Select Singletons During NO-GO Trials

One methodological consideration in the present study, with respect to processing architecture, is that all stimuli shared an aspect ratio. Thus, the GO/NO-GO rule could be determined by assessing the aspect ratio of any individual stimulus, not just that of the singleton. If the rule is decided upon via a distractor stimulus, the search for the singleton can be terminated in lieu of maintaining central fixation. To assess whether this self-termination of search after discrimination of the cue occurs, we analyzed the neural responses on the NO-GO trials.

Figure 6.8 shows the neural responses from visually responsive neurons during NO-GO trials. For monkey Da, a small separation between singleton in RF and singleton across from RF can be observed, but only in the high identifiability condition. In the low identifiability condition, the singleton in RF and singleton across from RF condition are nearly identical. However, this difference is transient and quickly collapses as the response returns to baseline; it does not continue to increase as it does in the GO trials (compare with Figs. 6.4, 6.5). For monkey Le, visually responsive neurons have differential responses when the singleton is in or across from RF on NO-GO trials, but the magnitude of this separation is different between the two conditions. Movement-related neurons demonstrate between monkey differences. For monkey Da, movement neurons do not activate on NO-GO trials. For monkey Le, movement neurons do activate on NO-GO trials, and to a larger magnitude on H_{Ident} trials than on L_{Ident} trials.

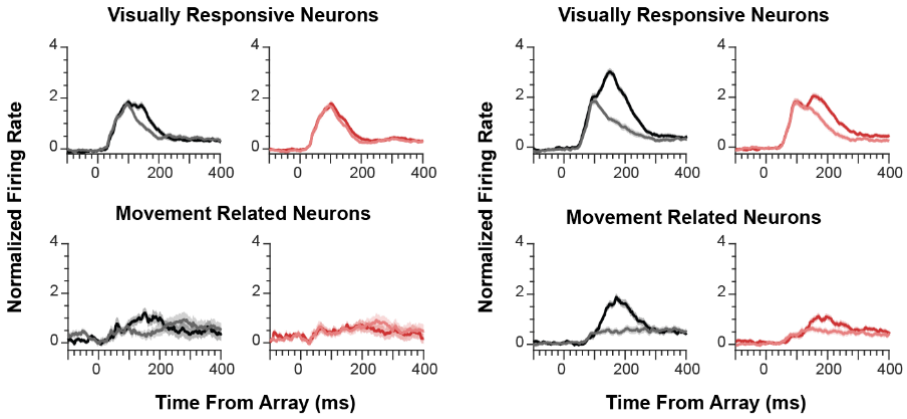

Figure 6.8: NO-GO responses. Responses of visually responsive neurons and movement-related neurons from monkey Da (left) and monkey Le (right) on NO-GO trials. Saturated lines indicate a NO-GO singleton in the RF, and desaturated lines indicate a NO-GO singleton out of the RF. High singleton identifiability NO-GO SDFs are shown in black, low singleton identifiability NO-GO SDFs are shown in red.

6.3.6 Visual and Movement Neurons Discriminate the Cue

The differential responses of both visual and movement neurons indicates that these neurons also discriminate the cue. The time at which the responses differ is the cue discrimination time (CDT). In a non-coactive architecture, CDT_{Vis} should complement

SST_{Vis} and be affected only by cue discriminability and not singleton identifiability. During performance with non-coactive architectures, we found that for the visually responsive neurons neurons that exhibited both singleton selection and cue discrimination, $CDT^{HH}{}_{Vis}$ was 133.1 ± 25.7 ms, $CDT^{HL}{}_{Vis}$ was 144.4 ± 28.9 ms, $CDT^{LH}{}_{Vis}$ was 130.0 ± 30.5 ms, and $CDT^{LL}{}_{Vis}$ was 149.9 ± 32.8 ms. These values were significantly modulated by cue discriminability (Fig. 6.9; Da: $F(1,55) = 33.4$, $p < 0.001$; Le: $F(1,20) = 19.7$, $p < 0.001$; Both: $F(1,76) = 52.5$, $p < 0.001$), but not singleton identifiability (Da: $F(1,55) = 0.2$, $p = 0.639$; Le: $F(1,20) = 0.1$, $p = 0.808$; Both: $F(1,76) = 0.26$, $p = 0.614$). For movement related neurons, $CDT^{HH}{}_{Vis}$ was 154.3 ± 20.9 ms, $CDT^{HL}{}_{Vis}$ was 169.8 ± 24.2 ms, $CDT^{LH}{}_{Vis}$ was 153.9 ± 25.1 ms, and $CDTLL_{Vis}$ was 172.6 ± 27.8 ms. These values were significantly modulated by cue discriminability (Da: $F(1,9) = 25.2$, $p < 0.001$; Le: $F(1,19) = 18.5$, $p < 0.001$; Both: $F(1,29) = 37.1$, $p < 0.001$), but

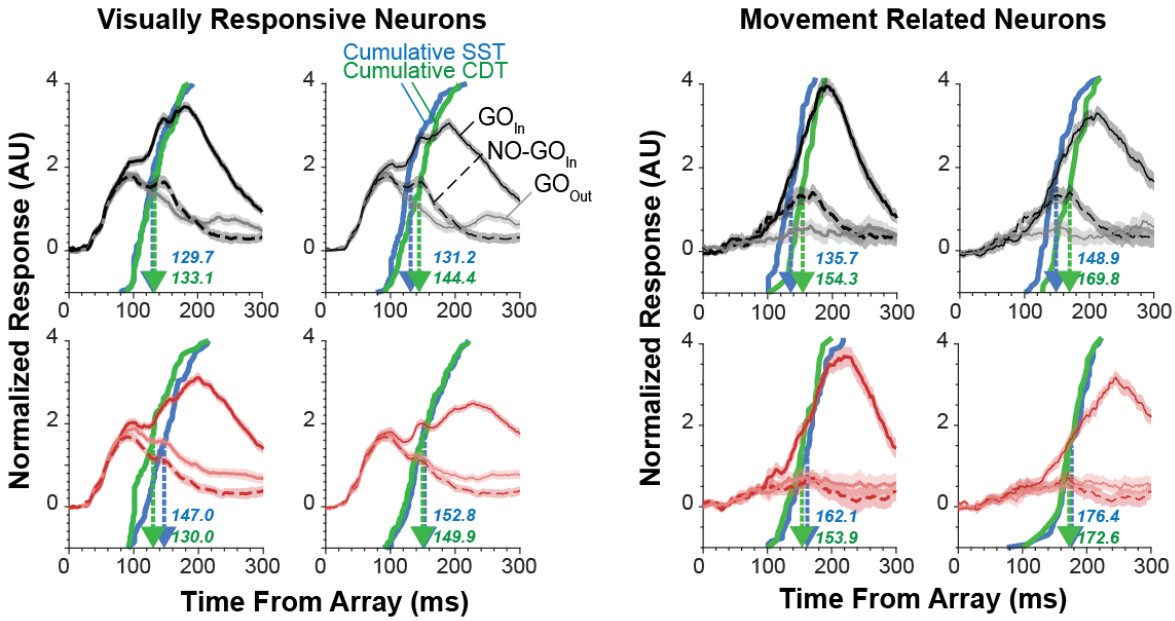

Figure 6.9: Cue discrimination compared to singleton selection. Mean ± SEM SDFs for visually responsive neurons (left) and movement-related neurons (right) combined across monkeys. Solid, saturated lines indicate GO trials with the singleton in the RF, solid desturated lines indicate GO trials with the singleton out of the RF. Dashed lines indicate NO-GO trials with the singleton in the RF. HH GO trials are compared with high identifiability NO-GO trials in the upper left, HL GO trials are compared with high identifiability NO-GO trials in the upper right. LH and LL trials are compared with low identifiability NO-GO trials in the bottom left and right, respectively. Singleton selection time for each condition is shown in blue as both cumulative distribution (solid) and mean (dashed arrow). Cue discrimination time (CDT) is similarly shown in green.

not singleton identifiability (Da: $F(1,9) = 0.2$, $p = 0.676$; Le: $F(1,19) = 0.0$, $p = 0.880$; Both: $F(1,29) = 0.1$, $p = 0.749$).

6.3.7 Simultaneous Analyses: Transmission Lag

The Gated Accumulator Model describes mechanisms by which visual neurons provide evidence regarding a singleton location to movement neurons, which accumulate to a threshold (Purcell et al., 2010, 2012b). However, this model was developed for a search task that did not include a GO/NO-GO manipulation. If this same model is applicable to the GO/NO-GO search task, it would predict that movement neuron accumulation should begin once the singleton is identified by the visual neurons. On the other hand, if instead there is an additional GO/NO-GO gate that prevents movement neuron accumulation until the GO cue is discriminated, then movement neuron accumulation should only begin when both operations are completed. That is, the delay between SST_{Vis} and SST_{Mov} should be affected by the level of cue discriminability.

To test these alternatives, we calculated the delay between SST_{Vis} and SST_{Mov} for each condition for simultaneously recorded neuron pairs. We focused on non-coactive architectures as the predictions rely on the existence of separate operations. In non-coactive architectures, we recorded 243 pairs of visually responsive and movement related neurons. To avoid the possibility of a small subset of neuron pairs skewing lag values, we randomly sampled half of the pairs and calculated the mean lag in each condition. We repeated this process 500 times to arrive at bootstrapped mean lags and

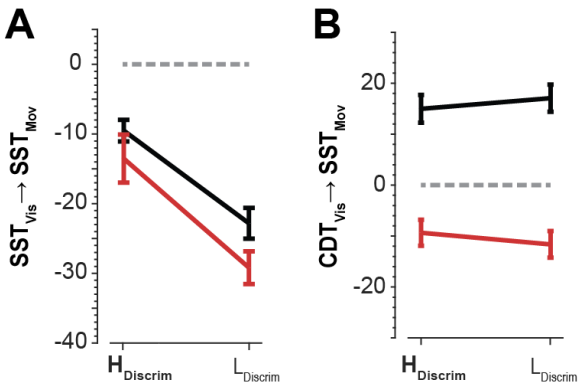

Figure 6.10. Simultaneous analysis. (A) For simultaneously recorded visually responsive and movement-related neurons, we calculated the difference between SST_{Vis} and SST_{Mov} to assess transmission lag between neuron subtypes for each condition. Lags are plotted such that negative values indicate that SST_{Vis} occurs before SST_{Mov}. Visuomotor transmission lag for high and low identifiability trials are shown in black and red, respectively. Lag for high and low cue discriminability are shown on the left and right, respectively. A dashed line at 0 indicates simultaneous SST_{Vis} and SST_{Mov}. (B) Similarly, we calculated the difference between CDT_{Vis} and SST_{Mov} for simultaneously recorded pairs. Conventions as in (A), with negative values indicating CDT_{Vis} occurring before SST_{Mov}.

sampling error. The lag between visual and movement related neurons was -5.8 ± 2.0 ms for the $H_{Ident}H_{Discrim}$ condition, -21.0 ± 2.3 ms for the $H_{Ident}L_{Discrim}$ condition, -12.6 ± 2.2 ms for the $L_{Ident}H_{Discrim}$ condition, and -25.2 ± 2.4 ms for the $L_{Ident}L_{Discrim}$ condition. These values were significantly affected by singleton identifiability (Fig. 6.10; $F(1,242) = 9.48$, $p = 0.002$) and cue discriminability (Both: $F(1,242) = 42.74$, $p < 0.001$). Importantly, these effects do not interact (Both: $F(1,242) = 0.56$, $p = 0.453$).

We also tested whether CDT_{Vis} is the instantiation of the cue discrimination operation or if it simply reflects interactions with the cue discrimination operation. For the simultaneously recorded neuron pairs, we similarly calculated transmission lag between CDT_{Vis} and SST_{Mov}. We found that the mean lag between visual and movement related neurons was 15.0 ± 2.7 ms for the $H_{Ident}H_{Discrim}$ condition, 17.1 ± 2.7 ms for the $H_{Ident}L_{Discrim}$ condition, -9.4 ± 2.6 ms for the $L_{Ident}H_{Discrim}$ condition, and -11.7 ± 2.6 ms for the $L_{Ident}L_{Discrim}$ condition. These values were significantly affected by singleton identifiability ($F(1,107) = 130.7$, $p < 0.001$) but not cue discriminability ($F(1,107) = 0.1$, $p = 0.777$).

6.4 DISCUSSION

For the first time, we recorded neural activity while monkeys performed a task with an explicit 2x2 factorial manipulation. To perform this task, monkeys were required to make a multidimensional decision: where is the singleton, and is this a GO or NO-GO trial. This explicit manipulation allows the inference of cognitive architecture from the response time distributions using systems factorial technology. In doing so, we can identify the neural correlates of the factorial manipulations and thus the neural instantiation of the constituent cognitive operations. This approach provides unprecedented leverage on the understanding of neural computations underlying complex behavior.

6.4.1 SST Conforms to SFT Predictions

The first important finding of this study is that the singleton selection time of visually responsive and movement related neurons conforms to the predictions made by SFT analysis (Lowe et al., 2019; Townsend & Nozawa, 1995). Specifically, when the architecture was coactive (i.e., the two manipulations influenced stages that drive a common decision operation), SST_{Vis} was modulated by both singleton identifiability and cue discriminability. Conversely, when the architecture was non-coactive (i.e., the two manipulations affected separate decision operations), SST_{Vis} was modulated only by singleton identifiability, but not cue discriminability. SST_{Mov}, on the other hand, was influenced by both operations. Thus, visual neurons instantiate the singleton identification operation and movement neurons instantiate the confluence of the singleton identification and cue discrimination operations and generation of the response. Interestingly, SST_{Mov} during performance with coactive architectures was

modulated only by singleton identifiability but not cue discriminability, counter to SFT predictions. However, it is notable that this lack of effect appears driven more by delaying SST^{*H}_{Mov} rather than a speeding of SST^{*L}_{Mov}.

This finding is not unexpected. SST_{Vis} has repeatedly been demonstrated to be linked to visual processing as opposed to movement selection (Kodaka et al., 1997; Sato & Schall, 2003; Thompson et al., 1996; Thompson et al., 2005b). Further, SST_{Vis} has already been shown to modulate with singleton-distractor similarity (Sato et al., 2001) and the set size effect (Cohen et al., 2009b). Similarly, SST_{Vis} has been shown to be invariant to response preparation (Sato et al., 2001; Sato & Schall, 2003). The mechanism by which SST_{Vis} is related to SST_{Mov} has also been demonstrated and quantitatively modeled using the Gated Accumulator Model (Purcell et al., 2010, 2012b). However, none of these studies explicitly manipulated both visual and motor processing simultaneously. Without simultaneous manipulations, the relationships between the manipulations are intangible; because SST_{Vis} relationships across conditions differ with cognitive architectures, guaranteeing constancy of architecture or inferring architecture at all is difficult or impossible. Therefore, we are uniquely able to demonstrate the cognitive architecture using behavioral means and confirm that SST is modulated as expected by manipulation and neuron type. Or rather, when SST relationships between visually responsive and movement-related neurons have a certain form, this generates behavior whose architecture is appropriately inferred.

6.4.2 Cue Discrimination Interacts with Singleton Identification

While SST_{Vis} is selectively influenced by singleton identifiability and not cue discriminability, the responses on NO-GO trials still indicate interactions with the cue

discrimination operation. Specifically, the magnitude of singleton identification is smaller on NO-GO trials than GO trials, if it occurs at all. If cue discriminability did not affect the singleton identification operation at all, the visually responsive neurons in FEF should still exhibit SST and to a comparable magnitude. Indeed, in other tasks FEF visual neurons do select singletons even in the absence of eye movements (Kodaka et al., 1997; Thompson et al., 2005b). The modulation of these neurons by the GO/NO-GO rule suggests that once the NO-GO rule is discriminated, the singleton identification process is cancelled. Further, the increase in activity of movement neurons for monkey Le, but not monkey Da, suggests that the cue discrimination operation has a different time course for the two monkeys; it is shorter for monkey Da than for monkey Le, and thus the singleton identification operation is cancelled earlier. It also suggests that movement neurons can be driven before cue discrimination is completed, so long as the visual neurons identify the singleton to a sufficient magnitude before being cancelled. Finally, these interactions and differences in time course between the two monkeys may explain the differences in overall architectures we have previously observed behaviorally (Lowe et al., 2019). In a parallel exhaustive system, interactions between operations result in a shift in the SIC curve from being entirely negative to being biphasic, and this shift is larger with larger degrees of interaction (Eidels et al., 2011).

The analysis of simultaneously recorded pairs of neurons further demonstrates the interactions between operations. Because CDT_{Vis} follows SST_{Mov} in H_{Ident} conditions, CDT_{Vis} cannot be instantiating the cue discrimination operation. Instead, it seems to reflect an interaction between the singleton identification and cue discrimination operations. There must be some other subpopulation of neurons that instantiates the

cue discrimination operation, and this operation in turn inhibits the singleton identification operation, resulting in the decreased magnitude of singleton selection and differential magnitude between identifiability conditions. This operation may also facilitate the singleton identification operation on GO trials, but without knowing the response properties of this cue discriminating subpopulation we can neither confirm nor rule out this possibility. Similarly, we can also not determine whether the cue discrimination operation drives movement neurons on GO trials beyond the drive from the singleton identification operation, nor can we determine whether the cue discrimination operation inhibits movement neurons on NO-GO trials directly or whether the cancellation of movement neuron response is inherited from the interactions between the cue discrimination operation and the singleton identification operation.

6.4.3 Architecture of the Visuomotor Transformation

Above, we demonstrate that the responses of visually responsive and movement-related neurons *per se* yield important insights into the cognitive architectures underlying the GO/NO-GO search task. However, because we used multicontact electrodes to perform these recordings, these architectures can be further understood by the lag between selection times in visually responsive and movement related neurons that were recorded simultaneously.

First, we consider the temporal lag between the visually responsive neurons selecting the singleton and the movement related neurons selecting the singleton. This lag between SST_{Vis} and SST_{Mov} depends on both cue discriminability and singleton identifiability. When cue discrimination is easy ($H_{Discrim}$ conditions), SST_{Vis} precedes SST_{Mov} by approximately 11 ms. When cue discrimination is difficult ($L_{Discrim}$ conditions),

SST_{Vis} precedes SST_{Mov} by approximately 23 ms. This dependence on cue discriminability is consistent with the existence of a GO/NO-GO gate preventing movement neuron accumulation until the GO cue is discriminated; that is, when cue discrimination becomes more difficult, there is additional time necessary to discriminate the GO cue before movement neurons are allowed to increase their response.

The dependence on singleton identifiability is curious, but can be explained by the visuomotor gate required by the GAM. This gate instantiates some level of visual activity that must be reached before movement neurons begin accumulating. At the time of SST^{HH}_{Mov}, 7 ms after SST^{HH}_{Vis}, the difference in visual response between singleton in and out of the RF is 1.49 ± 1.2 AU. At the time of SST^{LH}_{Mov}, 15 ms after SST^{LH}_{Vis}, the difference in visual response between singleton in and out of the RF is 1.27 ± 0.94 AU. These differences are not significantly different (Wilcoxson rank sum: $Z = 0.699$, $p = 0.485$), suggesting that while the difference in response in the LH condition is reliable at SST^{LH}_{Vis}, it is not large enough to exceed the visuomotor gate and begin driving movement neurons until later. Specifically, taking the lower of the two difference values, 1.27 AU, SST^{LH}_{Vis} occurs 15 ms before the difference exceeds the gating value whereas SST^{HH}_{Vis} occurs only 2 ms before the difference exceeds the gating value. This difference between SST_{Vis} and the time the gate is crossed can explain the greater transmission lag in the L_{Ident} conditions.

Given the above relationships between SST_{Vis} and SST_{Mov}, and interactions between the singleton identification and cue discrimination operations, we can propose a mechanistic architecture of the visuomotor transformation occurring during this task.

When the trial begins, an array of stimuli with color and feature dimensions appears on the screen. The relative color of the stimuli defines one stimulus as a color singleton. This singleton is identified by visually responsive neurons in FEF at a time that is modulated by the chromatic similarity of the singleton and distractors. These FEF neurons then partially drive the FEF movement-related neurons. This drive is partial because accumulation of movement-related neurons is only permitted once the GO/NO-GO cue is discriminated, as seen in the simultaneous recordings.

Alongside the singleton selection operation as instantiated by FEF visually responsive neurons, a separate latent subpopulation of neurons discriminates the shape of the singleton to discriminate whether it is a GO or NO-GO trial. The dynamics of this operation are unknown, but we can see that a GO discrimination permits accumulation in movement-related neurons and that a NO-GO discrimination inhibits the FEF visual neurons that instantiate the singleton identification operation. Whether this permission from a GO discrimination is active or passive is unknown, as is whether the NO-GO discrimination actively inhibits the FEF movement neurons, as discussed above. Nevertheless, FEF movement neurons begin activating when the FEF visual neurons identify the singleton to a particular magnitude and when the cue discrimination operation provides sufficient evidence that the trial is a GO trial, and can be cancelled if and when the cue discrimination operation determines that the trial is a NO-GO trial.

Finally, we should consider the meaning of a coactive architecture. In this case, the two manipulations are summed to drive a common decision operation. In other words, in a coactive architecture decisions regarding cue discriminability and singleton identifiability are made simultaneously. One way of conceptualizing this difference is

that in a non-coactive architecture, one identifies the singleton and discriminates the cue separately; one searches for the unique color and then determines whether the shape indicates a GO or NO-GO trial. In a coactive architecture, one instead searches directly for an elongated color singleton; the search is directed by both color and shape (or alternatively, there are extensive interactions between singleton identification and cue discrimination operations; see Eidels et al., 2011). In this case, the FEF visually responsive neurons, which instantiate the result of the search operation, will be modulated by both manipulations. The mechanism by which shape influences the responses of FEF visually responsive neurons is unclear, but will be discussed below.

6.4.4 Outstanding Issues

The present experiments provide unprecedented leverage on the organization of information processing by allowing comparisons of neural indices (e.g., SST_{Vis}, SST_{Mov}, CDT) across task conditions for the same individual neurons. However, this leverage still leaves many questions regarding the neural basis of complex visuomotor tasks.

The first major remaining question is whether there does, in fact, exist a subpopulation of neurons somewhere that instantiates the cue discrimination operation. One potential locus for this operation is the ventrolateral prefrontal cortex, *vlPFC*. In a conditional saccade countermanding task, this region has been implicated in mapping stimulus features to response rule regardless of which feature value defines the response rule (Xu et al., 2017). This was dissociated from response selection *per se* as FEF reflected the GO/NO-GO decision, correctly or not, whereas vlPFC reflected the GO/NO-GO rule whether the rule was followed or not. This area has also been implicated in rule discrimination in a delayed match-to-sample task (Miller et al., 1996).

This area may then be specifically involved in stimulus-rule associations to generate a stimulus-independent response. However, it is unclear whether this area would be spatially specific like FEF visually responsive neurons. In the present task this dissociation is difficult as all stimuli shared a shape and thus future work could implement a task where only the shape of the singleton is informative regarding the response rule. This may affect the cognitive architecture of the task, but if tested in the appropriate 2x2 manner proposed here, the influence of the cue discriminating neurons can be tested similarly to the singleton identifying neurons reported here.

The next outstanding question is the manner in which the feature dimensions affect the FEF visually responsive neurons or, more generally, what is the drive on the FEF visually responsive neurons. While FEF neurons generally form a salience or priority map (Bisley, 2011; Schall, 2015; Thompson & Bichot, 2005), the mechanisms by which these FEF neurons compute or reflect such a salience calculation are unclear. The inputs to FEF from visually responsive brain regions are diverse (Markov et al., 2014), but given the present task demands we focus on area V4. Neurons in area V4 are selective for both color (Schein & Desimone, 1990; Zeki, 1980) and shape (Desimone & Schein, 1987; Pasupathy & Connor, 1999), and are differentially active when their preferred stimulus has common features with a search target (Ogawa & Komatsu, 2004; Westerberg et al., 2020; Zhou & Desimone, 2011). The temporal relationship between this singleton selection and stimulus feature selection imply a directional relationship between the areas; specifically, feature selectivity in V4 precedes search target selection in FEF, which in turn precedes search target selection in V4 (Ogawa & Komatsu, 2006; Zhou & Desimone, 2011). That is, V4 neurons are

differentially responsive to preferred shape and color combinations earlier than FEF select singletons.

The direct connections between FEF and V4 suggest that this color and/or shape information is received by FEF neurons; however, these connections do not in and of themselves describe the mechanisms by which the singleton identification operation is performed. Because the features of the stimuli in the array are varied trial to trial, the color singleton is not defined by the specific shape and color features of the singleton *per se* as opposed to a search for a consistent feature (Bichot et al., 2001b; Purcell et al., 2012b; Sato et al., 2001), we see that the singleton identification in this task is, specifically, a singleton identification operation as opposed to a feature-matching operation. If FEF visual neurons are correctly identifying the singleton using color only, the pattern of SST_{Vis} would match that of the non-coactive architectures as the feature dimensions would affect separate operations. On the other hand, if FEF visual neurons are identifying the singleton using color and shape, where shape is an uninformative feature dimension for singleton identification but does cue the response rule, then the pattern of SST_{Vis} would match that of the coactive architecture. Thus, more work is necessary to understand how FEF visual neurons are driven, and how the weights of feature dimensions in the singleton identification operation can be dynamic.

The final remaining question from this experiment is the source of the remaining RT variation. Even the movement neurons, which instantiate the convergence of singleton identification and cue discrimination to generate a response, only account for 71.2% of the RT difference due to singleton identifiability and 40.3% of the RT difference due to cue discriminability. The visually responsive neurons account for an

even smaller proportion of the RT difference due to singleton identifiability (44.0%). In a similar search task without a simultaneous response interference component, SST differences due to an analog of singleton identifiability accounted for 87% of the RT differences, which was not significantly different than 100% (Sato et al., 2001). In other tasks, the SST within quantiles of the RT distribution also accounts for approximately 100% of RT variance (Bichot & Schall, 2002; Thompson et al., 1996). However, in a task with a stimulus-response component, SST_{Vis} did not vary with RT quantiles (Lowe & Schall, 2019) or RT differences across conditions, at least for Type I cells (Sato & Schall, 2003). In one of these studies, a different neurometric index, endpoint selection time, was found to account for approximately 25% of RT differences, similar to $\Delta SST_{Vis}/\Delta RT_{Ident}$ (Lowe & Schall, 2019). In the other, though, endpoint selection time across conditions in Type II cells did account for 100% of the RT variability (Sato & Schall, 2003). Together, these findings suggest that the added stimulus-response rule interferes with the direct transmission of saccade rule from visually responsive to movement-related neurons, suggesting additional gating mechanisms arising outside FEF. To fully understand the computations underlying this task, and the neural instantiation of those computations, the source of the remaining RT difference must be accounted for. Whether this can be accounted for by the drive on the visual units, the dynamics of the latent cue discriminating subpopulation, or a third unknown subpopulation is unknown and merits further quantitative modeling.

CHAPTER 7: GENERAL DISCUSSION

7.1 Summary of Results

In Chapter 2, I developed a consensus clustering algorithm to identify patterns of neural responses. This approach identified visually responsive, visuomotor, movement-related, post-saccadic, and fixation neurons; the traditional categories of FEF neural responses. However, it also identified additional variability within these categories that may be accounted for by anatomical diversity of inputs to FEF. In Chapter 3, I applied this clustering algorithm to a sample of neurons recorded in both FEF and dorsal premotor cortex (F2vr) during a more complex visuomotor task. This demonstrated the utility of the algorithm and its applicability to additional task conditions, and provided a mechanism for comparing the response profiles of neurons in different brain regions.

In Chapter 4, I applied an approach from cognitive psychology, *systems factorial technology (SFT)*, to behavior during a complex visual search task to infer the cognitive architecture of the task. This behavioral experiment was the first time that an explicit 2x2 factorial manipulation was performed in monkeys, let alone the first time the behavior was analyzed using SFT. I demonstrated that one monkey performed the task using a parallel exhaustive architecture, in which the two task manipulations affect separate decision operations, and the second monkey used a coactive architecture, one in which the two task manipulations affect the same decision operation. I also demonstrated that monkeys can use different architectures on different sessions.

In Chapter 5, I demonstrated that neural indices of cognitive operations are tractable using a similar complex visual search task. I demonstrated that by including two relevant feature dimensions, the feature dimension that does not define the search

singleton can still gain behavioral relevance when the monkey uses a behavioral shortcut. This induced feature selectivity allowed the separation of two cognitive operations: singleton selection and saccade selection. I demonstrated that the singleton selection operation occurs first and is invariant with respect to response time whereas the saccade selection operation occurs second and is modulated by response time. This approach can be extended to identify neural indices of other cognitive operations.

Finally, in Chapter 6 I defined such neural indices during the GO/NO-GO visual search task and related them to cognitive architectures. I demonstrated that when the task was performed using a coactive architecture, singleton selection in FEF was modulated by both task manipulations. However, when the task was performed using a non-coactive architecture, singleton selection in FEF was modulated only by the chromatic similarity of the search singleton and distractors but not by the discriminability of the response cue. Movement related neurons in FEF were modulated by both manipulations and are thus the confluence of the two individual operations, integrating them and generating a response. In doing so, I identified specific neural correlates of cognitive operations and architectures for the first time. This approach can be extended to additional manipulations and as such provides unique leverage for understanding the neurobiological mechanisms of information processing.

7.2 Levels of Explanation and Linking Propositions

Thus far, I have summarized the results of the experiments from this dissertation. Now, I assess the general scope of the experiments. First, I situate the findings in the level of analysis afforded, and assert and discuss resulting linking propositions.

7.2.1 Levels of Analysis

To most honestly discuss the present results, one must understand the level of analysis at which the present experiments operate. That is, at what level am I describing the neurobiological phenomena underlying the cognitive architectures I identified? I certainly am not describing them at their most fundamental level of ion flow across neurons' cell membranes (or more fundamental still, the electrochemistry of those ions). However, because the ionic nature of action potentials is well understood (Hodgkin & Huxley, 1952) and rate coding is generally accepted as a manner of understanding neural function (though spike timing is also argued to be critical; for review, see Brette, 2015), it is unlikely that these levels of understanding provide meaningful insights above and beyond the inferences I make from the rate code in these experiments (at least given our current knowledge; characterization of the phenomena in the rate code must be done first, and may later be updated using models at a more fine-grained scope). That being said, it is still difficult to understand the scope of these findings without explicitly defining the level of understanding achievable by the present experiments.

To define this level, one can invoke Marr's levels of analysis: the computational level, the algorithmic level, and the implementational level (Marr & Poggio, 1976; Marr, 1982). These levels correspond to the questions of what computations are performed by the system, what algorithms are used to perform those computations, and what is the physical realization of those algorithms. In the GO/NO-GO search task, the computations performed by the system are singleton identification, cue discrimination, and the integration of the two for response generation. This is exemplified by the response times, which are affected by our two task manipulations. The algorithms used to perform these computations are the cognitive architectures. That is, a representation

of stimulus color and stimulus shape are created, used to identify chromatic uniqueness and degree of elongation, respectively. These representations are integrated to generate (or withhold) a response. This level of explanation was accomplished in Chapter 4. However, my unique application of this framework to non-human primate research allows for the third level of explanation: the implementational level.

The physical instantiation of the algorithmic level of explanation was tested in Chapter 6. I found that when an algorithm was used in which singleton identification and cue discrimination were represented separately (i.e., a non-coactive cognitive architecture), the visually responsive neurons in FEF identified the singleton in accordance with the chromatic similarity of the stimuli, regardless of their elongation. The movement related neurons in FEF, on the other hand, identified the singleton and generated a response in accordance with both manipulations and in accordance with response times. This entails the existence of an additional latent subpopulation that discriminates the cue in accordance with the elongation of the stimuli but not the chromatic similarity. Together, these subpopulations comprise the implementation of the algorithms used to perform the computations necessary to complete this task.

An additional, complementary algorithmic level of explanation for the present findings is Bundesen's Theory of Visual Attention (Bundesen, 1990). This model describes response choice probabilities as a function of attentional weights and response biases. Specifically, a stimulus in an array is selected through feature values and the weighting of feature dimensions (the feature priority). Similarly, a response is selected by way of the weighting of response dimensions (the response bias). In the GO/NO-GO search task, the stimuli are selected by their color (i.e., the feature priority

for the color dimension is high, and for the shape dimension is low), whereas the responses are selected by their shape (i.e., the response bias for shape dimension is high, and for the color dimension is low). I demonstrated a segregation of operations for stimulus selection and response generation, embodied by the visually responsive and movement-related neurons in FEF respectively. This allows the physical instantiation of feature priority and response bias as the relative influence of feature dimensions on the response of visually responsive and movement-related neurons, respectively. It also allows the relative feature priorities to explain coactivity, as this architecture is defined by the use of both features in the selection of stimuli. Further understanding of the drive on visual neurons (see section 7.5.2) will provide additional an implementation level explanation of the mechanisms by which feature dimensions influence stimulus selection, and thereby will elaborate the implementational level of TVA.

While we can identify the levels of analysis afforded by these experiments, whether this final level of physical instantiation is truly satisfied requires comparisons to other quantitative models. Attractor models provide useful comparisons to the present results. These models have been used to explain neural activity in working memory tasks as well as search tasks (e.g., Standage et al., 2014; Wimmer et al., 2014). Importantly, these models also provide physical models of behavior, but as single stage models with explicit differentiation between excitation and inhibition. In the present experiments, we did not analyze differences between putative excitatory pyramidal neurons and putative inhibitory interneurons. Instead, I focused simply on the rate code. Thus, whether these experiments should be considered to describe the physical implementation of the cognitive algorithms or whether they provide a *neural algorithm*

whose biophysical basis still needs described is unclear. In any case, the different response properties of FEF neurons are associated with different biophysical properties (Cohen et al., 2009d; Lowe & Schall, 2018). Future work may bridge these levels and provide a more complete explanation of the implementational level of analysis.

7.2.2 Linking Propositions

Most generally, the goal of this work is to understand the neural basis of cognitive architectures used to perform complex behaviors. That is, when cognitive events occur, what are the neurobiological events associated with them? Or rather, what are the neurobiological events instantiating them? I focused on three cognitive events in these experiments: identification and selection of a stimulus, discriminating a rule cue and selecting a response, and response generation by way of integration of stimulus and response selection. Moreover, I also focused on the manner by which the information from the stimulus selection operation is transmitted to the movement-related neurons. Above, I discussed the level of analysis and scope afforded by these experiments. While there is still much to be learned, here I explore the extent of the relationship between the neurobiological and cognitive by describing linking propositions.

A linking proposition is “a claim that a particular mapping occurs, or particular mapping principle applies, between perceptual and physiological states” (Teller, 1984). This framework arises from the supposition that “… whenever two stimuli cause physically indistinguishable signals to be sent from the sense organs to the brain, the sensations produced by those stimuli, as reported by the subject in words, symbols or actions, must also be indistinguishable” (Brindley, 1970). As this formulation of the relationship between neurophysiological activity and cognitive function was derived from

visual science, it can be narrowly rephrased as: when visual neurons responsive to some feature or set of features X are responsive, an object with feature or set of features X is perceived (e.g., Teller, 1984). However, Brindley had a broader notion of sensation that includes reports by the subject with actions; for the below discussion, and because our task involves two response options of GO and NO-GO, I consider response option and percept to be the same.

This definition of a linking proposition entails a set of logical relationships between neural states and cognitive states that must hold (Teller, 1984):

(1) "The initial proposition states that identical neural states map onto identical cognitive states.

(2) The contrapositive of the initial proposition states that nonidentical cognitive states correspond to nonidentical neural states.

(3) The converse proposition states: identical cognitive states map onto identical neural states, and

(4) The contrapositive of the converse states: nonidentical neural states entail nonidentical cognitive states." (Schall, 2004a)

The brain regions that satisfy these propositions are known as *bridge loci*, so named because they form the bridge between the physical and psychical phenomena studied.

From the present set of experiments, I assert two linking propositions: (1) the visually responsive neurons in FEF constitute the bridge locus of stimulus selection, and (2) the movement-related neurons in FEF constitute the bridge locus of response selection. Because neural responses are directly accessible, I can evaluate the converse and contrapositive propositions.

Firstly, I assert that the activity of FEF visually responsive neurons is the selection of a stimulus. The converse proposition states that identical cognitive states map onto identical neural states. That is, when the same stimulus is selected, the same subpopulations of FEF visually responsive neurons have high levels of activity. I found this to be true in our data; when a response was made toward a given stimulus, FEF neurons with RFs at that location had high levels of activity. Moreover, this relatively higher level of activity was reached at a time dependent on the ease of selection, singleton identifiability, but not on response selection difficulty, cue discriminability, on GO trials. Similarly, in Chapter 5 I demonstrated that when responses were made to a stimulus in the RF, neural activity did not differentiate whether the response was correct or incorrect. The contrapositive proposition states that nonidentical responses correspond to nonidentical neural states. I also found this to be true as responses to a stimulus in the RF of a visual neuron, as opposed to out of the RF, were associated with different levels of activity in that visual neuron. Thus, FEF visually responsive neurons satisfy the requirements to be a bridge locus for stimulus selection.

Second, I assert that the activity of FEF movement-related neurons is the integration of singleton identifiability and cue discriminability for response generation. Similarly, the converse and contrapositive propositions can be evaluated. I found that when a saccade is generated to a stimulus in the movement field of our FEF movement-related neurons, activity in those neurons was high. This increased activity was dependent on both singleton identifiability and cue discriminability in contrast to visually responsive neurons. The contrapositive states that non-identical responses correspond to nonidentical neural states. I found that the activity of these movement-related

neurons was dependent on location, and responses made to or away from the movement field elicited high and low activity, respectively. As such, FEF movement-related neurons satisfy the requirements to be a bridge locus for response selection.

7.3 A Schematic Model of GO/NO-GO Visual Search

Having evaluated the scope of the results and the specifics of the linking propositions that can be asserted from this work, I now detail the model of GO/NO-GO visual search. This schematic model is shown in Figure 7.1. First, in architectures with selective influence, one subpopulation of neurons instantiates the cognitive operation of singleton identification, one subpopulation instantiates the cognitive operation of cue discrimination, and one subpopulation integrates these operations and generates a response. I identified the first and third subpopulations. Having done so, I formed the linking propositions that FEF visual neurons instantiate the singleton identification operation, and FEF movement neurons instantiate the integration and oculomotor response generation. The nature of information processing between these subpopulations has been studied previously and can be defined mathematically using the Gated Accumulator Model (Purcell et al., 2010, 2012b). Thus, the linking proposition that the Gated Accumulator Model is the visuomotor transformation occurring in FEF has been asserted. However, this model does not account for the increased delay between stimulus selection and response selection when cue discriminability is difficult, so a latent subpopulation that instantiates cue discrimination operation must exist.

Singleton identification and cue discrimination interact as seen in the cancelling of singleton selection on NO-GO trials. This suggests that on NO-GO trials, the cue discrimination neurons inhibit FEF visual neurons. These neurons may actively inhibit

FEF movement neurons, preventing or cancelling their response. Alternatively, these neurons may indirectly inhibit FEF movement neurons via their inhibition of FEF visual neurons, reducing the drive on the movement neurons.

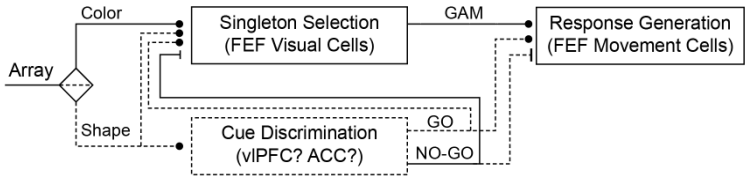

Figure 7.1. Schematic model of GO/NO-GO search. This search task is solved by selecting the singleton and discriminating the cue. These operations occur in parallel, with varying degrees of interactions. In this set of experiments, several components were identified empirically, shown in solid lines. Other components can be inferred but were not directly measured, shown in dashed lines. In this task, a feature filter (diamond) separates color and shape dimensions of the stimuli in the search array. The color information is used by the singleton selection operation, instantiated by FEF visual neurons, and the shape information is used by the cue discrimination operation, whose neural instantiation is unknown. This filtering may be imperfect as demonstrated by shape information driving the singleton selection operation. FEF visual neurons drive FEF movement neurons, which instantiate response selection and generation, via the Gated Accumulator Model (GAM; Purcell et al., 2010, 2012b).

Similarly, the cue discrimination neurons may actively drive FEF movement neurons on GO trials, or indirectly drive them through facilitating the FEF visual neurons.

Finally, the FEF visual neurons receive color information in order to identify the singleton. However, this color information may not be separated from shape information, as areas like V4 that are selective for color are also selective for shape (discussed below in section 7.5.2). In a non-coactive architecture, shape is fully and correctly filtered out of the singleton identification operation. But in a coactive architecture, shape is incompletely filtered and influences the singleton identification operation. Therefore, a mechanism for setting the degree of filtering of irrelevant feature dimensions must exist. This mechanism would then instantiate the degree of coactivity.

7.4 Importance of Cell Types

This set of experiments reinforces a notion that is often overlooked: neuron types are important. Specifically, in areas like FEF that have a remarkable diversity of response profiles, respecting this diversity provides more complete insights than lumping all neurons together. In Chapter 2, I identified 10 categories of response profiles,

discussed potential anatomical correlates of the subcategories of traditional neuron types, and developed an algorithm by which these categories can be determined in a less biased manner. In Chapter 5, by restricting analyses to those neurons that exhibited feature selectivity, I used this unexpected property to separate stimulus selection and saccade selection operations. In Chapter 6, separating neurons into visually responsive and movement-related allowed me to dissociate neurons that were modulated by only one task manipulation from those that were modulated by both. This dissociation then defined neural correlates of the two task operations as well as their integration. These inferences would have been impossible without separating neuron types, as the sample as a whole was modulated by both task conditions and FEF would have been ruled out as the locus of the singleton identification operation.

This identification of neuron types is contrasted by a wealth of studies analyzing *local field potentials, LFPs*. LFPs reflect neural activity pooled over many neurons, but are still finely localized (e.g., Katzner et al., 2009). Singleton selection in search is indexed by LFPs (Cohen et al., 2009a; Purcell et al., 2013) and measures of multiunit activity derived from them (Westerberg et al., 2020). LFPs can be used to assess coordination between areas, including FEF (Babapoor-Farrokhran et al., 2017; Fiebelkorn & Kastner, 2019; Gregoriou et al., 2009), as well as laminar compartmentalization of functions (Bastos et al., 2018; Johnston et al., 2019). However, such interactions are often cell-type specific, either functionally (Gregoriou et al., 2012) or anatomically (Voloh & Womelsdorf, 2018), and the pooling across neurons reflected in the LFP can obscure cell-type specific activity. Indeed, in a preliminary analysis I defined multiunit activity from the LFPs recorded in this task. I found that a nonspecific

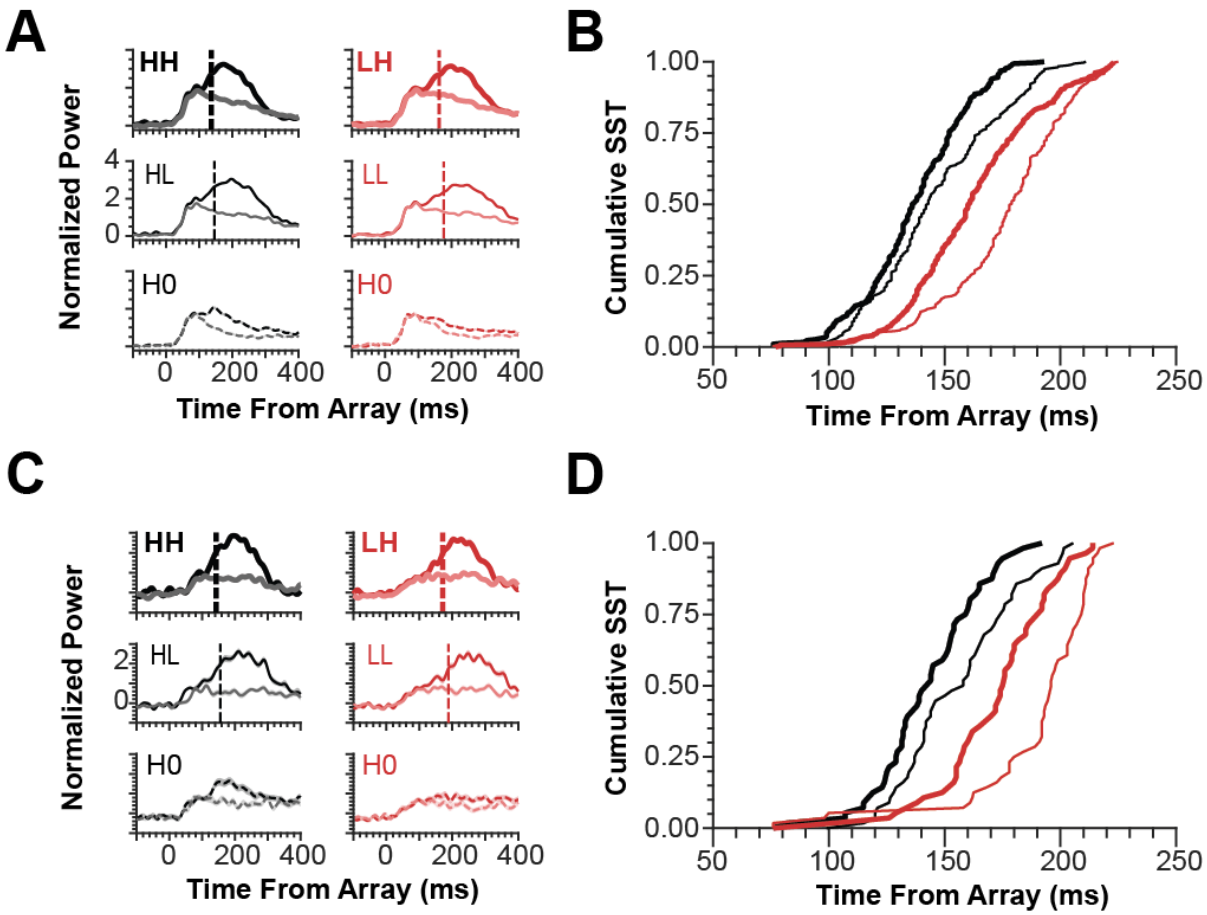

Figure 7.2. Multiunit acitivity. (A) Multiunit activity was defined from the local field potentials recorded in FEF during the GO/NO-GO search task by bandpass filtering between 80 and 150 Hz. Channels were defined as visually responsive, visuomovement, or movement-related using the same criteria as single units in Chapter 6. Responses from visually responsive channels are shown for each of the six task conditions, with vertical lines in the GO conditions indicating mean SST_{vis}. Responses are shown for singletons in the multiunit RF (saturated) and out of the multiunit RF (desaturated). (B) Cumulative SST for each of the four GO conditions is shown. High and low singleton identifiability are shown in black and red, respectively. High and low cue discriminability are shown in thick and thin lines, respectively. (C-D) Responses from movement-related channels and their cumulative SSTs are shown. Conventions as in (A-B).

visual transient was present on nearly all channels, and the separation between the singleton in and across from the RF is modulated by both task manipulations (Fig. 7.2). Thus, in order to achieve the level of description offered by these experiments, isolating single neurons and respecting the heterogeneity of their response profiles is necessary.

7.5 Outstanding Issues

While this set of experiments provides substantial leverage on an old problem in cognitive psychology, several remaining issues must be solved before fully

understanding the neural underpinnings of cognitive architectures. To conclude, I describe several prominent questions remaining and assert hypotheses regarding them, including the architectures of additional manipulations of visual search.

7.5.1 Bridge Locus of Cue Discrimination

The first and most task specific issue remaining is the identity of the neurons that instantiate the cue discrimination operation. One promising candidate for this task is the ventrolateral prefrontal cortex, *vlPFC*, the putative homologue of the human inferior frontal junction (Badre & Wagner, 2007; Chikazoe, 2010; Cieslik et al., 2015). This area has been implicated in representing task rules in delayed match-to-sample tasks (Bunge et al., 2003; Miller et al., 1996; Schwedhelm et al., 2020), strategy implementation (Baxter et al., 2009), and saccade countermanding (Xu et al., 2017). In the latter, vlPFC and FEF were specifically compared in a conditional saccade countermanding task. In this task, the shape of a fixation spot indicated whether a color cue indicated a GO or a NO-GO response. Neurons in vlPFC were found to encode the rule, regardless of which feature value indicated that rule, whereas neurons in FEF were found to encode the GO/NO-GO response, regardless of the correct rule. This area may then be specifically involved in generating stimulus-independent response rules.

It is also unclear whether these neurons would have spatially specific RFs like the FEF neurons. If vlPFC neurons are the loci of the cue discrimination operation, then this operation may not be spatially specific because they have RFs that are considerably larger than those in FEF (Suzuki & Azuma, 1983). However, GO/NO-GO neurons in this area in a simpler task have shown spatial selectivity (Hasegawa et al., 2004; Sakagami & Niki, 1994). Hasegawa and colleagues recorded neural activity in

FEF and preFEF, or area 8Ar on the convexity of the arcuate sulcus, and found two classes of spatially selective GO/NO-GO selective neurons: those that responded more for GO trials and those that responded more for NO-GO trials. While both classes of neurons were found in both areas, the NO-GO preferring neurons were more prevalent in preFEF than in FEF. Unfortunately, particulars of the anatomical localization of these neuron subtypes were not provided thus the discussion of these recordings are tentative. The recording area is consistent with caudal vlPFC and caudal dorsolateral prefrontal cortex, *dlPFC*. The latter has spatially restricted receptive fields (Hasegawa et al., 2000), which may be the source of the observed spatial selectivity, but vlPFC is more prominently involved in rule encoding than dlPFC (Wallis & Miller, 2003).

However, whether these classes of neurons should be taken as evidence that vlPFC is the bridge locus of cue discrimination is unclear, as FEF has similar GO/NO-GO selective neurons (e.g., Sommer & Wurtz, 2001). Our visually responsive neurons and movement-related neurons in FEF exhibited GO/NO-GO discrimination at a time modulated by cue discriminability, but temporal relationships of singleton identification and cue discrimination in these neurons are inconsistent with FEF being the bridge locus of cue discriminability (Chapter 6). Presence of these neurons is not sufficient for the proposition that these neurons instantiate cue discriminability. Moreover, none of the tasks above manipulated the difficulty of encoding the GO/NO-GO rule (perhaps with the exception of match/non-match tasks whose difficulty varies with delay period or sequence length (e.g., Wittig & Richmond, 2014), but other confounds prevent direct comparison). Without manipulating rule encoding difficulty, one cannot determine the relationships of neurometric indices of rule encoding to response times.

In any case, this dissociation is impossible in the present GO/NO-GO search task because all stimuli shared a shape. Thus, the shape of a stimulus in or out of a cue discriminating neuron's RF would never be different, nor would they be differentially informative about the rule on a given trial. In future work, the shape of all stimuli could be varied and the task rule defined only in terms of the shape of the color singleton. If tested in the appropriate 2x2 manner proposed here, the properties of cue discriminating neurons can be better understood.

An alternate candidate area for the bridge locus of cue discriminability is the anterior cingulate cortex, *ACC*. ACC contains an eye field that has been compared to other eye fields, FEF, LIP, and SEF specifically (Amiez & Petrides, 2009; Pouget et al., 2005). ACC and FEF are coordinated during task performance, with a failure of synchronization reflected as an increase in error rate in saccade tasks (Babapoor-Farrokhran et al., 2017). ACC is frequently compared to the dlPFC in studies of goal-directed behavior (e.g., Boschin et al., 2017; Johnston et al., 2007). Both of these areas are implicated in rule encoding in a pro-/anti-saccade task (Johnston et al., 2007). Whereas dlPFC activity is maintained throughout blocks sharing a response rule, ACC activity was most prominent on trials with a rule switch and decayed throughout the block. If ACC is involved in rule discrimination, it may be more prominently active during our task than prefrontal cortex (dlPFC or vlPFC) because there is no explicit blocking of stimulus-response rule, so rule switches are frequent and unpredictable. ACC has also been implicated in inhibition of movements (Bari & Robbins, 2013), a role which would be well suited for a GO/NO-GO discrimination.

Though ACC's involvement in rule encoding makes it a promising candidate for the bridge locus of cue discriminability, its role is more often considered in response monitoring than response generation (Boschin et al., 2017; Heilbronner & Hayden, 2016; Silvetti et al., 2014). Single neurons and local field potentials recorded from ACC during a saccade countermanding task are differentially responsive to correct and error trials, often signaling reward omission (Emeric et al., 2008; Ito et al., 2003). In other eye fields reward prediction is distinct from error monitoring (Sajad et al., 2019), but regardless both types of signals are considered as performance monitoring signals (Bissonette & Roesch, 2016; Botvinick, 2007), manifestations of high level abstract control (Heilbronner & Hayden, 2016), or the expected value of applying control (Shenhav et al., 2013), as opposed to signals generating behavior. Thus, in an actor-critic framework, in which an actor performs some function and a critic alters the actor's behavior for future behavior, ACC is generally considered a critic (e.g., Babapoor-Farrokhran et al., 2017; Silvetti et al., 2014). But for modeling of behavior within a trial, the bridge locus is the actor.

ACC may be more involved in behavior monitoring as compared to behavior production but the differences in perspectives of the two areas raises an important consideration for identifying the bridge locus of cue discrimination: does the bridge locus represent response rule *per se*, or does it represent the stimulus features cuing that response rule? In the GO/NO-GO search task, this distinction is subtle as feature dimensions are directly mapped to response dimensions. But consider a match/non-match task. As discussed above, there are subpopulations of neurons in vlPFC that respond more when a stimulus matches a sample stimulus (Miller et al., 1996). But is

this task modulation due to the correspondence of feature dimensions between the two stimuli, or due to the response cued by such a correspondence?

The question becomes whether the cue discrimination operation uses stimulus features or response option as the frame of reference. In the GO/NO-GO search task, a bottleneck could occur at a stage where stimuli are categorized as elongated or non-elongated, and these categories are subsequently mapped to GO or NO-GO rule. Alternatively, the bottleneck could occur at a stage where this mapping is carried out, and the degree of elongation may differentially drive GO or NO-GO units. Depending on the location of the bottleneck, differential responses to elongation and insensitivity to singleton identifiability are not sufficient to diagnose the bridge locus of cue discriminability. Instead, finding this bridge locus requires an understanding the mechanisms by which stimulus features are arbitrarily mapped to responses.

7.5.2 What Drives FEF Visual Cells?

The next open question is the nature of the visual input to FEF. While the responses of FEF visual neurons drive FEF movement neurons according to the Gated Accumulator Model, it is unknown how these visually responsive neurons are themselves driven. FEF receives input from numerous visual areas (Huerta et al., 1987; Markov et al., 2014; Schall et al., 1995b). Three of these merit specific discussion: V4, MT, and LIP.

Area V4 is a visual area with neurons selective for shape (Desimone & Schein, 1987; Pasupathy & Connor, 1999) and color (Schein & Desimone, 1990). Like FEF, V4 neurons have increased responses when a search target is in their receptive fields relative to a search target out of their receptive fields (Ogawa & Komatsu, 2004; Westerberg et al., 2020). Importantly, this target selection occurs later in V4 than in

FEF, but the feature selectivity in V4 precedes target selection in FEF (Ogawa & Komatsu, 2006; Zhou & Desimone, 2011). Thus, it seems likely that V4 is the source of the color and shape information required in the GO/NO-GO search task. Because these neurons are selective for color and shape, if retinotopically matched color selective and shape selective neurons both drive FEF visually responsive neurons, interactions between feature dimensions and thus coactivity could result. However, V4 neurons encode color and shape dimensions relatively independently (Bushnell & Pasupathy, 2012) so there may be a mechanism that allows color selective neurons to drive FEF visual neurons while preventing shape selective neurons from doing the same. This mechanism, then, may be instantiating the feature priorities and response biases that parameterize Bundesen's TVA (Bundesen, 1990).

Area MT is also densely interconnected with FEF. The connections between FEF and V4 are segregated from the connections between FEF and MT (Ninomiya et al., 2012). These areas are generally considered to belong to the ventral, or *what* pathway, and the dorsal, or *where* pathway, respectively (Mishkin et al., 1983; Ungerleider & Mishkin, 1982). In the present experiment, motion is not a relevant feature dimension in any way and thus the influence of MT on FEF visual neurons should be limited. However, FEF visual neurons can use motion information for selecting singletons, and singleton selection time in this domain is also modulated by singleton-distractor motion similarity (Sato et al., 2001).

A second alternative for the visual response driven by MT is that MT drives the transient visual neurons that do not select the singleton. As part of the dorsal stream, MT may be a part of a broad magnocellular pathway analogous to the retinal inputs to

the LGN and V1 (e.g., Callaway, 2005). This pathway is characterized by brisk, transient responses to visual stimulation with lower latencies than the sustained, longer latency parvocellular pathway. FEF visually responsive neurons that achieved color or shape selectivity due to a consistent target identity had latencies longer than those that did not achieve feature selectivity (Chapter 5; Bichot et al., 1996). This was taken as evidence that the neurons that received chromatic input were a different subpopulation than those that did not, and those that did not had faster latencies. Similarly, I identified two clusters of visually responsive neurons with different latencies and times of peak responses that could also reflect this pathway difference (Lowe & Schall, 2018).

The final visual area worth considering as providing drive to FEF visual neurons is area LIP. FEF and LIP are highly coordinated during spatial attention (Fiebelkorn et al., 2018, 2019). Neurons in area LIP, much like FEF, select salient stimuli that are in their RFs, regardless of specific feature values (Bisley, 2011; Bisley & Mirpour, 2019; Ipata et al., 2006a, b; Thomas & Paré, 2007). This selection takes place on a similar time course in both areas (Ibos et al., 2013; Sapountzis et al., 2018). Also like FEF, LIP has been described as an accumulator whose activity increases to a decision threshold (Schall, 2019; Shadlen & Kiani, 2013; Shadlen & Newsome, 2001). These two areas are broadly similar, but LIP has fewer motor signals than FEF (Ferraina et al., 2002; Sapountzis et al., 2018). Similarly, whereas singleton selection time in FEF increases with set size and explains RT differences (Cohen et al., 2009b), this is not the case in LIP (Balan et al., 2008; c.f. Cohen et al., 2009c). One additional difference is the nature of the salience of the stimuli; LIP selects a search singleton earlier than FEF if the search target is defined in terms of an intrinsic feature whereas FEF selects first if the

target is defined in terms of an extrinsic feature (Ibos et al., 2013). This largely similar, but subtly different, pattern of responses between the two areas may suggest that LIP operates in parallel to FEF as opposed to being a driving force.

While understanding the sources of the drive on FEF visual neurons is certainly important, to understand the system one must also understand the time course of those inputs. Connections between the discussed areas are largely reciprocal (Markov et al., 2014), suggesting a recursive pattern of activation. For example, responses of V4 neurons are modulated when covert attention is directed toward their RF (McAdams & Maunsell, 1999; Motter, 1993), and subthreshold microstimulation of FEF produces effects similar to deploying covert attention (Moore & Armstrong, 2003). Similarly, neurons in FEF and V4 are selectively synchronized during attention (Gregoriou et al., 2012). Similar behavioral attention manipulations have demonstrated comparable neural response differences in area MT (Treue & Martínez Trujillo, 1999), and presumably follow a similar mechanism. Thus if areas like V4 and MT are driving FEF visual neurons and FEF visual neurons in turn modulate responses in V4 and MT, modeling the responses of FEF visual neurons in terms of V4 and MT responses must also accommodate this feedback modulation.

The final consideration for inferring relationships between areas, and indeed neuron types within an area, is the difficulty of matching results across task demands. For example, Sato et al. (2001) found that singleton identifiability modulated singleton selection time in FEF, but not a response preparation manipulation. This formed my hypotheses that FEF visually responsive neurons would be selectively influenced by singleton identifiability and not cue discriminability in non-coactive architectures. Indeed,

this finding and its relationship to cognitive architectures may have been identified there if the two task manipulations were independently interleaved, as done here. In LIP, Cohen et al. (2009b) argue that the lack of a relationship between singleton selection time and response time across set sizes as reported by Balan et al. (2008) could have been due to differences in task conditions between their study and that of Cohen et al. (2009a), specifically the effector used for the response. Also studying LIP during visual search, Thomas & Paré (2007) note that "Perhaps the unconstrained nature of this visual search task does not allow visual and saccade selection processes to be dissociated…" Their task was a color singleton search task, as was mine. However, because I added a second relevant feature dimension, shape, I was able to dissociate singleton and saccade selection operations by exploiting unexpected feature selectivity (Chapter 5) and by adding an explicit GO/NO-GO rule (Chapter 6).

7.5.3 Additional Manipulations and Their Architecture

The results and inferences of this set of experiments, while informative, are restricted specifically to the relationship between a singleton selection operation and a stimulus-response rule mapping operation. However, there are multiple additional task manipulations that modulate search difficulty. One particular manipulation that I have referred to numerous times thus far is the set size effect, in which response times are longer when more distractors are presented (under certain conditions, e.g., Treisman & Gelade, 1980). In FEF, the set size effect is instantiated by visually responsive neurons (Cohen et al., 2009b; Purcell et al., 2012b). If the set size effect and singleton identification are indeed instantiated by the same pool of neurons, then they must necessarily affect the same cognitive operation. In this case, if set size and singleton

identifiability were simultaneously manipulated, this nexus of the two effects would be expected to produce a coactive architecture in the response times and SST_{Vis} would be modulated by both manipulations. If these operations are not in fact instantiated by these neurons, but the effects are instead inherited from other regions, they may produce non-coactive architectures and the true bridge locus of either manipulation may be sought elsewhere.

Another manipulation of response times in visual search is the priming effect, specifically priming of pop-out. When the feature defining a search target is repeated, response times are speeded (Maljkovic & Nakayama, 1994). At the neural level, this priming effect is reflected by visually responsive neurons in FEF (Bichot & Schall, 2002) and in area V4 (Westerberg et al., 2020). However, the origin of this priming effect is still debated as area V4 overpredicts RT effects (Westerberg et al., 2020). Thus, if the priming effect is in fact instantiated by FEF neurons and is fed back to V4 neurons, then testing priming of pop-out and singleton identifiability in tandem would again result in a coactive architecture that could be inferred behaviorally. However, if V4 neurons instantiate the priming effect, then it is possible (though not necessary) that the behaviorally inferred architecture could be non-coactive.

In the tasks described so far, the search target is defined by only one feature, with a secondary feature that defines the stimulus-response rule. However, when multiple features define a search target, response times are more sensitive to the set size effect (Bichot & Schall, 1999; Treisman & Gelade, 1980; Wolfe, 1994). Thus, it would be plausible to manipulate the difficulty of the individual conjunction features to determine the architecture by which the separate feature dimensions are combined. If

individual FEF visually responsive neurons select singletons based on both features together, a coactive architecture would be predicted. If instead separate subpopulations of visually responsive neurons are responsible for selecting the singleton based on the individual feature values, the relative contributions of these two subpopulations could be determined. For example, singleton selection time in visually responsive neurons in FEF is modulated by search difficulty when the selection feature is motion direction (Sato et al., 2001), but it is unknown whether these are the same neurons that select the singleton based on chromatic similarity. Above, I described reasons for thinking that the V4-recipient and MT-recipient FEF visual neurons may be separate subpopulations. Such a supposition could be empirically tested in a task where relevant feature dimensions are represented by different brain regions, as opposed to color and shape as in the present experiments which are both selectively encoded by V4 neurons.

Finally, additional manipulations may consider other response modalities; in particular, manual responses as opposed to oculomotor responses. FEF visually responsive neurons still select search targets during manual tasks (Neromyliotis & Moschovakis, 2017b; c.f. Mushiake et al., 1996), but movement-related neurons do not (Thompson & Bichot, 2005). Conversely, neurons in premotor cortex select search targets or saccade targets during oculomotor tasks (Neromyliotis & Moschovakis, 2018; Neromyliotis & Moschovakis, 2017b; Chapter 3), though they are generally considered to be related to manual movements (e.g., Cisek & Kalaska, 2005). It is presently unknown whether premotor cortex neurons are similarly affected by singleton identifiability or cue discriminability as defined in our task. Thus, the question remains whether the visually responsive neurons in FEF, which instantiate the singleton

identification operation in our task, similarly instantiate the singleton identification operation during manual tasks. This seems possible, even likely given the known similarities in responses between the two areas in oculomotor or manual tasks. Less likely is that the movement-related neurons in FEF instantiate the integration and response production operation in a manual task. However, it may be expected that the latent cue discriminating subpopulation of neurons would still be the bridge locus for cue discriminability regardless of effector. Such a supposition must be empirically tested but would ultimately describe modality-dependent and modality-independent operations that are coordinated for directed behavior. Using the research approach described and implemented here, specifically 2x2 factorial manipulations permit the application of SFT to infer the cognitive architecture, cognitive architectures can be related to neural indices of cognitive operations in a meaningful way. This research approach is well situated to address additional questions regarding the mimicry of multiple brain regions in similar tasks and their respective roles in the generation of directed behavior.

7.6 Conclusions

My goal with this dissertation was to increase neuroscientific understanding, defined as an understanding of the biological underpinnings of behavior. I have addressed this by approaching questions from both ends. In Chapters 2 and 3 I addressed the question of heterogeneity of functional neuron types and with my consensus clustering algorithm I developed a method by which this heterogeneity can be appreciated at a finer grain than has been done before. In Chapter 4 I addressed the question of cognitive operations and architectures and applied SFT, and even explicit 2x2 factorial manipulations, to non-human primate work for the first time, allowing the inference of

cognitive architectures in a model species where neural recordings are possible. In Chapter 6 I did just this by recording neural activity while monkeys performed a GO/NO-GO search task and, in conjunction with Chapter 5, identified neural indices of cognitive operations and their architectures. In sum, by respecting both the biology and psychology, I was able to relate these two domains to one another and describe the neural substrates of cognitive processing architectures.

BIBLIOGRAPHY

Abe, M., & Hanakawa, T. (2009). Functional coupling underlying motor and cognitive functions of the dorsal premotor cortex. *Behavioural Brain Research*, *198*(1), 13–23. https://doi.org/10.1016/j.bbr.2008.10.046

Adeli, H., Vitu, F., & Zelinsky, G. J. (2017). A Model of the Superior Colliculus Predicts Fixation Locations during Scene Viewing and Visual Search. *The Journal of Neuroscience: The Official Journal of the Society for Neuroscience*, *37*(6), 1453–1467. https://doi.org/10.1523/JNEUROSCI.0825-16.2016

Adeli, H., & Zelinsky, G. (2018). *Deep-BCN: Deep Networks Meet Biased Competition to Create a Brain-Inspired Model of Attention Control*. 1932–1942. http://openaccess.thecvf.com/content_cvpr_2018_workshops/w39/html/Adeli_Deep-BCN_Deep_Networks_CVPR_2018_paper.html

Adrian, E. D., & Zotterman, Y. (1926). The impulses produced by sensory nerve-endings. *The Journal of Physiology*, *61*(2), 151–171.

Amiez, C., & Petrides, M. (2009). Anatomical organization of the eye fields in the human and non-human primate frontal cortex. *Progress in Neurobiology*, *89*(2), 220–230. https://doi.org/10.1016/j.pneurobio.2009.07.010

Anderson, B. A. (2016). The attention habit: How reward learning shapes attentional selection. *Annals of the New York Academy of Sciences*, *1369*(1), 24–39. https://doi.org/10.1111/nyas.12957

Anderson, B. A., Laurent, P. A., & Yantis, S. (2011). Learned Value Magnifies Salience-Based Attentional Capture. *PLOS ONE*, *6*(11), e27926. https://doi.org/10.1371/journal.pone.0027926

Anderson, B. A., Laurent, P. A., & Yantis, S. (2014). Value-Driven Attentional Priority Signals in Human Basal Ganglia and Visual Cortex. *Brain Research*, *1587*, 88–96. https://doi.org/10.1016/j.brainres.2014.08.062

Arai, K., McPeek, R. M., & Keller, E. L. (2004). Properties of saccadic responses in monkey when multiple competing visual stimuli are present. *Journal of Neurophysiology*, *91*(2), 890–900. https://doi.org/10.1152/jn.00818.2003

Arcizet, F., Mirpour, K., Foster, D. J., & Bisley, J. W. (2018). Activity in LIP, But not V4, Matches Performance When Attention is Spread. *Cerebral Cortex (New York, N.Y.: 1991)*, *28*(12), 4195–4209. https://doi.org/10.1093/cercor/bhx274

Ardid, S., Vinck, M., Kaping, D., Marquez, S., Everling, S., & Womelsdorf, T. (2015). Mapping of functionally characterized cell classes onto canonical circuit operations in primate prefrontal cortex. *The Journal of Neuroscience: The Official*

Journal of the Society for Neuroscience, *35*(7), 2975–2991. https://doi.org/10.1523/JNEUROSCI.2700-14.2015

Ashby, F. G., & Townsend, J. T. (1980). Decomposing the reaction time distribution: Pure insertion and selective influence revisited. *Journal of Mathematical Psychology*, *21*(2), 93–123. https://doi.org/10.1016/0022-2496(80)90001-2

Audley, R. J., & Pike, A. R. (1965). Some alternative stochastic models of choice. *British Journal of Mathematical and Statistical Psychology*, *18*(2), 207–225. https://doi.org/10.1111/j.2044-8317.1965.tb00342.x

Awh, E., Belopolsky, A. V., & Theeuwes, J. (2012). Top-down versus bottom-up attentional control: A failed theoretical dichotomy. *Trends in Cognitive Sciences*, *16*(8), 437–443. https://doi.org/10.1016/j.tics.2012.06.010

Azzato, M. C., & Butter, C. M. (1984). Visual search in cynomolgus monkeys: Stimulus parameters affecting two stages of visual search. *Perception & Psychophysics*, *36*(2), 169–176. https://doi.org/10.3758/BF03202677

Babapoor-Farrokhran, S., Hutchison, R. M., Gati, J. S., Menon, R. S., & Everling, S. (2013). Functional connectivity patterns of medial and lateral macaque frontal eye fields reveal distinct visuomotor networks. *Journal of Neurophysiology*, *109*(10), 2560–2570. https://doi.org/10.1152/jn.01000.2012

Babapoor-Farrokhran, S., Vinck, M., Womelsdorf, T., & Everling, S. (2017). Theta and beta synchrony coordinate frontal eye fields and anterior cingulate cortex during sensorimotor mapping. *Nature Communications*, *8*. https://doi.org/10.1038/ncomms13967

Bacon, W. F., & Egeth, H. E. (1994). Overriding stimulus-driven attentional capture. *Perception & Psychophysics*, *55*(5), 485–496. https://doi.org/10.3758/bf03205306

Baddeley, A. (1986). *Working memory*. Clarendon Press/Oxford University Press.

Badre, D., & Wagner, A. D. (2007). Left ventrolateral prefrontal cortex and the cognitive control of memory. *Neuropsychologia*, *45*(13), 2883–2901. https://doi.org/10.1016/j.neuropsychologia.2007.06.015

Baker, J. T., Patel, G. H., Corbetta, M., & Snyder, L. H. (2006). Distribution of Activity Across the Monkey Cerebral Cortical Surface, Thalamus and Midbrain during Rapid, Visually Guided Saccades. *Cerebral Cortex*, *16*(4), 447–459. https://doi.org/10.1093/cercor/bhi124

Balan, P. F., Oristaglio, J., Schneider, D. M., & Gottlieb, J. (2008). Neuronal Correlates of the Set-Size Effect in Monkey Lateral Intraparietal Area. *PLOS Biology*, *6*(7), e158. https://doi.org/10.1371/journal.pbio.0060158

Bari, A., & Robbins, T. W. (2013). Inhibition and impulsivity: Behavioral and neural basis of response control. *Progress in Neurobiology*, *108*, 44–79. https://doi.org/10.1016/j.pneurobio.2013.06.005

Basso, M. A., & Wurtz, R. H. (2002). Neuronal activity in substantia nigra pars reticulata during target selection. *The Journal of Neuroscience: The Official Journal of the Society for Neuroscience*, *22*(5), 1883–1894.

Bastos, A. M., Loonis, R., Kornblith, S., Lundqvist, M., & Miller, E. K. (2018). Laminar recordings in frontal cortex suggest distinct layers for maintenance and control of working memory. *Proceedings of the National Academy of Sciences of the United States of America*, *115*(5), 1117–1122. https://doi.org/10.1073/pnas.1710323115

Bauer, R. H., & Fuster, J. M. (1976). Delayed-matching and delayed-response deficit from cooling dorsolateral prefrontal cortex in monkeys. *Journal of Comparative and Physiological Psychology*, *90*(3), 293–302. https://doi.org/10.1037/h0087996

Baxter, M. G., Gaffan, D., Kyriazis, D. A., & Mitchell, A. S. (2009). Ventrolateral prefrontal cortex is required for performance of a strategy implementation task but not reinforcer devaluation effects in rhesus monkeys. *The European Journal of Neuroscience*, *29*(10), 2049–2059. https://doi.org/10.1111/j.1460-9568.2009.06740.x

Bichot, N. P., Heard, M. T., DeGennaro, E. M., & Desimone, R. (2015). A Source for Feature-Based Attention in the Prefrontal Cortex. *Neuron*, *88*(4), 832–844. https://doi.org/10.1016/j.neuron.2015.10.001

Bichot, N. P., Rao, S. C., & Schall, J. D. (2001a). Continuous processing in macaque frontal cortex during visual search. *Neuropsychologia*, *39*(9), 972–982. https://doi.org/10.1016/S0028-3932(01)00022-7

Bichot, N. P., Rossi, A. F., & Desimone, R. (2005). Parallel and serial neural mechanisms for visual search in macaque area V4. *Science (New York, N.Y.)*, *308*(5721), 529–534. https://doi.org/10.1126/science.1109676

Bichot, N. P., & Schall, J. D. (1999). Saccade target selection in macaque during feature and conjunction visual search. *Visual Neuroscience*, *16*(1), 81–89. https://doi.org/10.1017/S0952523899161042

Bichot, N. P., & Schall, J. D. (2002). Priming in Macaque Frontal Cortex during Popout Visual Search: Feature-Based Facilitation and Location-Based Inhibition of Return. *Journal of Neuroscience*, *22*(11), 4675–4685. https://doi.org/10.1523/JNEUROSCI.22-11-04675.2002

Bichot, N. P., Schall, J. D., & Thompson, K. G. (1996). Visual feature selectivity in frontal eye fields induced by experience in mature macaques. *Nature*, *381*(6584), 697. https://doi.org/10.1038/381697a0

Bichot, N. P., Thompson, K. G., Rao, S. C., & Schall, J. D. (2001b). Reliability of Macaque Frontal Eye Field Neurons Signaling Saccade Targets during Visual Search. *Journal of Neuroscience*, *21*(2), 713–725. https://doi.org/10.1523/JNEUROSCI.21-02-00713.2001

Bichot, N. R., Cave, K. R., & Pashler, H. (1999). Visual selection mediated by location: Feature-based selection of noncontiguous locations. *Perception & Psychophysics*, *61*(3), 403–423. https://doi.org/10.3758/BF03211962

Bisley, J. W. (2011). The neural basis of visual attention. *The Journal of Physiology*, *589*(Pt 1), 49–57. https://doi.org/10.1113/jphysiol.2010.192666

Bisley, J. W., & Mirpour, K. (2019). The neural instantiation of a priority map. *Current Opinion in Psychology*, *29*, 108–112. https://doi.org/10.1016/j.copsyc.2019.01.002

Bissonette, G. B., & Roesch, M. R. (2016). Neurophysiology of Reward-Guided Behavior: Correlates Related to Predictions, Value, Motivation, Errors, Attention, and Action. *Current Topics in Behavioral Neurosciences*, *27*, 199–230. https://doi.org/10.1007/7854_2015_382

Bizzi, E., & Schiller, P. H. (1970). Single unit activity in the frontal eye fields of unanesthetized monkeys during eye and head movement. *Experimental Brain Research*, *10*(2), 150–158. https://doi.org/10.1007/bf00234728

Blake, R., & Logothetis, N. K. (2002). Visual competition. *Nature Reviews. Neuroscience*, *3*(1), 13–21. https://doi.org/10.1038/nrn701

Blanke, O., Spinelli, L., Thut, G., Michel, C., Perrig, S., Landis, T., & Seeck, M. (2000). Location of the human frontal eye field as defined by electrical cortical stimulation: Anatomical, functional and electrophysiological characteristics. *Neuroreport*, *11*(9), 1907–1913.

Blatt, G. J., Andersen, R. A., & Stoner, G. R. (1990). Visual receptive field organization and cortico-cortical connections of the lateral intraparietal area (area LIP) in the macaque. *Journal of Comparative Neurology*, *299*(4), 421–445. https://doi.org/10.1002/cne.902990404

Blurton, S. P., Kyllingsbæk, S., Nielsen, C. S., & Bundesen, C. (2020). A Poisson random walk model of response times. *Psychological Review*, *127*(3), 362–411. https://doi.org/10.1037/rev0000179

Boring, E. G. (1942). *Sensation and Perception in the History of Experimental Psychology*. D. Appleton Century Company.

Boschin, E. A., Brkic, M. M., Simons, J. S., & Buckley, M. J. (2017). Distinct Roles for the Anterior Cingulate and Dorsolateral Prefrontal Cortices During Conflict

Between Abstract Rules. *Cerebral Cortex (New York, NY)*, *27*(1), 34–45. https://doi.org/10.1093/cercor/bhw350

Botvinick, M. M. (2007). Conflict monitoring and decision making: Reconciling two perspectives on anterior cingulate function. *Cognitive, Affective & Behavioral Neuroscience*, *7*(4), 356–366. https://doi.org/10.3758/cabn.7.4.356

Boucher, L., Palmeri, T. J., Logan, G. D., & Schall, J. D. (2007). Inhibitory control in mind and brain: An interactive race model of countermanding saccades. *Psychological Review*, *114*(2), 376–397. https://doi.org/10.1037/0033-295X.114.2.376

Boussaoud, D. (1995). Primate premotor cortex: Modulation of preparatory neuronal activity by gaze angle. *Journal of Neurophysiology*, *73*(2), 886–890. https://doi.org/10.1152/jn.1995.73.2.886

Boussaoud, D., & Wise, S. P. (1993a). Primate frontal cortex: Effects of stimulus and movement. *Experimental Brain Research*, *95*(1), 28–40. https://doi.org/10.1007/bf00229651

Boussaoud, D., & Wise, S. P. (1993b). Primate frontal cortex: Neuronal activity following attentional versus intentional cues. *Experimental Brain Research*, *95*(1), 15–27. https://doi.org/10.1007/bf00229650

Boussaoud, D., Barth, T. M., & Wise, S. P. (1993). Effects of gaze on apparent visual responses of frontal cortex neurons. *Experimental Brain Research*, *93*(3). https://doi.org/10.1007/BF00229358

Boussaoud, D., Jouffrais, C., & Bremmer, F. (1998). Eye Position Effects on the Neuronal Activity of Dorsal Premotor Cortex in the Macaque Monkey. *Journal of Neurophysiology*, *80*(3), 1132–1150. https://doi.org/10.1152/jn.1998.80.3.1132

Bradley, P. S., & Fayyad, U. M. (1998). *Refining Initial Points for K-Means Clustering*. 91–99.

Brette, R. (2015). Philosophy of the Spike: Rate-Based vs. Spike-Based Theories of the Brain. *Frontiers in Systems Neuroscience*, *9*. https://doi.org/10.3389/fnsys.2015.00151

Brindley, G. S. (1970). *Physiology of the Retina and Visual Pathway*. Williams & Wilkins.

Britten, K. H., Shadlen, M. N., Newsome, W. T., & Movshon, J. A. (1992). The analysis of visual motion: A comparison of neuronal and psychophysical performance. *Journal of Neuroscience*, *12*(12), 4745–4765. https://doi.org/10.1523/JNEUROSCI.12-12-04745.1992

Britten, K. H., Shadlen, M. N., Newsome, W. T., & Movshon, J. A. (1993). Responses of neurons in macaque MT to stochastic motion signals. *Visual Neuroscience*, *10*(6), 1157–1169.

Broadbent, D. E. (1971). *Decision and stress.* Academic Press.

Brown, J. W., Bullock, D., & Grossberg, S. (2004). How laminar frontal cortex and basal ganglia circuits interact to control planned and reactive saccades. *Neural Networks: The Official Journal of the International Neural Network Society*, *17*(4), 471–510. https://doi.org/10.1016/j.neunet.2003.08.006

Brown, S. D., & Heathcote, A. (2008). The simplest complete model of choice response time: Linear ballistic accumulation. *Cognitive Psychology*, *57*(3), 153–178. https://doi.org/10.1016/j.cogpsych.2007.12.002

Bruce, C. J., & Goldberg, M. E. (1985). Primate frontal eye fields. I. Single neurons discharging before saccades. *Journal of Neurophysiology*, *53*(3), 603–635. https://doi.org/10.1152/jn.1985.53.3.603

Bruce, C. J., Goldberg, M. E., Bushnell, M. C., & Stanton, G. B. (1985). Primate frontal eye fields. II. Physiological and anatomical correlates of electrically evoked eye movements. *Journal of Neurophysiology*, *54*(3), 714–734. https://doi.org/10.1152/jn.1985.54.3.714

Bruce, N. D. B., Wloka, C., Frosst, N., Rahman, S., & Tsotsos, J. K. (2015). On computational modeling of visual saliency: Examining what's right, and what's left. *Vision Research*, *116*(Pt B), 95–112. https://doi.org/10.1016/j.visres.2015.01.010

Bundesen, C. (1990). A theory of visual attention. *Psychological Review*, *97*(4), 523–547. https://doi.org/10.1037/0033-295X.97.4.523

Bundesen, C., Habekost, T., & Kyllingsbæk, S. (2005). A Neural Theory of Visual Attention: Bridging Cognition and Neurophysiology. *Psychological Review*, *112*(2), 291–328. https://doi.org/10.1037/0033-295X.112.2.291

Bundesen, C., Habekost, T., & Kyllingsbæk, S. (2011). A neural theory of visual attention and short-term memory (NTVA). *Neuropsychologia*, *49*(6), 1446–1457. https://doi.org/10.1016/j.neuropsychologia.2010.12.006

Bunge, S. A., Kahn, I., Wallis, J. D., Miller, E. K., & Wagner, A. D. (2003). Neural circuits subserving the retrieval and maintenance of abstract rules. *Journal of Neurophysiology*, *90*(5), 3419–3428. https://doi.org/10.1152/jn.00910.2002

Buracas, G. T., & Albright, T. D. (1999). Gauging sensory representations in the brain. *Trends in Neurosciences*, *22*(7), 303–309. https://doi.org/10.1016/s0166-2236(98)01376-9

Buracas, Giedrius T., & Albright, T. D. (2009). Modulation of neuronal responses during covert search for visual feature conjunctions. *Proceedings of the National Academy of Sciences of the United States of America*, *106*(39), 16853–16858. https://doi.org/10.1073/pnas.0908455106

Buschman, T. J., & Miller, E. K. (2007). Top-Down Versus Bottom-Up Control of Attention in the Prefrontal and Posterior Parietal Cortices. *Science*, *315*(5820), 1860–1862. https://doi.org/10.1126/science.1138071

Bushnell, B. N., & Pasupathy, A. (2012). Shape encoding consistency across colors in primate V4. *Journal of Neurophysiology*, *108*(5), 1299–1308. https://doi.org/10.1152/jn.01063.2011

Callaway, E. M. (2005). Structure and function of parallel pathways in the primate early visual system. *The Journal of Physiology*, *566*(Pt 1), 13–19. https://doi.org/10.1113/jphysiol.2005.088047

Camalier, C. R., Gotler, A., Murthy, A., Thompson, K. G., Logan, G. D., Palmeri, T. J., & Schall, J. D. (2007). Dynamics of saccade target selection: Race model analysis of double step and search step saccade production in human and macaque. *Vision Research*, *47*(16), 2187–2211. https://doi.org/10.1016/j.visres.2007.04.021

Carpenter, R. H., & Williams, M. L. (1995). Neural computation of log likelihood in control of saccadic eye movements. *Nature*, *377*(6544), 59–62. https://doi.org/10.1038/377059a0

Casale, A. E., Foust, A. J., Bal, T., & McCormick, D. A. (2015). Cortical Interneuron Subtypes Vary in Their Axonal Action Potential Properties. *The Journal of Neuroscience: The Official Journal of the Society for Neuroscience*, *35*(47), 15555–15567. https://doi.org/10.1523/JNEUROSCI.1467-13.2015

Cave, K. R. (1999). The FeatureGate model of visual selection. *Psychological Research*, *62*(2–3), 182–194. https://doi.org/10.1007/s004260050050

Celebi, M. E., Kingravi, H. A., & Vela, P. A. (2013). A Comparative Study of Efficient Initialization Methods for the K-Means Clustering Algorithm. *Expert Systems with Applications*, *40*(1), 200–210. https://doi.org/10.1016/j.eswa.2012.07.021

Celebrini, S., & Newsome, W. T. (1994). Neuronal and psychophysical sensitivity to motion signals in extrastriate area MST of the macaque monkey. *The Journal of Neuroscience: The Official Journal of the Society for Neuroscience*, *14*(7), 4109–4124.

Cerkevich, C. M., Lyon, D. C., Balaram, P., & Kaas, J. H. (2014). Distribution of cortical neurons projecting to the superior colliculus in macaque monkeys. *Eye and Brain*, *2014*(6), 121–137. https://doi.org/10.2147/EB.S53613

Chelazzi, L., Duncan, J., Miller, E. K., & Desimone, R. (1998). Responses of neurons in inferior temporal cortex during memory-guided visual search. *Journal of Neurophysiology*, *80*(6), 2918–2940. https://doi.org/10.1152/jn.1998.80.6.2918

Chelazzi, L., Miller, E. K., Duncan, J., & Desimone, R. (1993). A neural basis for visual search in inferior temporal cortex. *Nature*, *363*(6427), 345–347. https://doi.org/10.1038/363345a0

Chelazzi, L., Miller, E. K., Duncan, J., & Desimone, R. (2001). Responses of neurons in macaque area V4 during memory-guided visual search. *Cerebral Cortex (New York, N.Y.: 1991)*, *11*(8), 761–772. https://doi.org/10.1093/cercor/11.8.761

Chen, X., Zirnsak, M., & Moore, T. (2018). Dissonant Representations of Visual Space in Prefrontal Cortex during Eye Movements. *Cell Reports*, *22*(8), 2039–2052. https://doi.org/10.1016/j.celrep.2018.01.078

Chikazoe, J. (2010). Localizing performance of go/no-go tasks to prefrontal cortical subregions. *Current Opinion in Psychiatry*, *23*(3), 267–272. https://doi.org/10.1097/YCO.0b013e3283387a9f

Cieslik, E. C., Mueller, V. I., Eickhoff, C. R., Langner, R., & Eickhoff, S. B. (2015). Three key regions for supervisory attentional control: Evidence from neuroimaging meta-analyses. *Neuroscience and Biobehavioral Reviews*, *48*, 22–34. https://doi.org/10.1016/j.neubiorev.2014.11.003

Cisek, P., & Kalaska, J. F. (2002). Modest Gaze-Related Discharge Modulation in Monkey Dorsal Premotor Cortex During a Reaching Task Performed With Free Fixation. *Journal of Neurophysiology*, *88*(2), 1064–1072. https://doi.org/10.1152/jn.00995.2001

Cisek, P., & Kalaska, J. F. (2005). Neural Correlates of Reaching Decisions in Dorsal Premotor Cortex: Specification of Multiple Direction Choices and Final Selection of Action. *Neuron*, *45*(5), 801–814. https://doi.org/10.1016/j.neuron.2005.01.027

Clark, K. L., Noudoost, B., & Moore, T. (2012). Persistent spatial information in the frontal eye field during object-based short-term memory. *The Journal of Neuroscience: The Official Journal of the Society for Neuroscience*, *32*(32), 10907–10914. https://doi.org/10.1523/JNEUROSCI.1450-12.2012

Cleland, B. G., Dubin, M. W., & Levick, W. R. (1971). Sustained and transient neurones in the cat's retina and lateral geniculate nucleus. *The Journal of Physiology*, *217*(2), 473–496. https://doi.org/10.1113/jphysiol.1971.sp009581

Coallier, É., Michelet, T., & Kalaska, J. F. (2015). Dorsal premotor cortex: Neural correlates of reach target decisions based on a color-location matching rule and conflicting sensory evidence. *Journal of Neurophysiology*, *113*(10), 3543–3573. https://doi.org/10.1152/jn.00166.2014

Cohen, J. Y., Heitz, R. P., Schall, J. D., & Woodman, G. F. (2009a). On the Origin of Event-Related Potentials Indexing Covert Attentional Selection During Visual Search. *Journal of Neurophysiology*, *102*(4), 2375–2386. https://doi.org/10.1152/jn.00680.2009

Cohen, J. Y., Heitz, R. P., Woodman, G. F., & Schall, J. D. (2009b). Neural Basis of the Set-Size Effect in Frontal Eye Field: Timing of Attention During Visual Search. *Journal of Neurophysiology*, *101*(4), 1699–1704. https://doi.org/10.1152/jn.00035.2009

Cohen, J. Y., Heitz, R. P., Woodman, G. F., & Schall, J. D. (2009c). Reply to Balan and Gottlieb. *Journal of Neurophysiology*, *102*(2), 1342–1343. https://doi.org/10.1152/jn.00403.2009

Cohen, J. Y., Pouget, P., Heitz, R. P., Woodman, G. F., & Schall, J. D. (2009d). Biophysical Support for Functionally Distinct Cell Types in the Frontal Eye Field. *Journal of Neurophysiology*, *101*(2), 912–916. https://doi.org/10.1152/jn.90272.2008

Cohen, J. Y., Pouget, P., Woodman, G. F., Subraveti, C. R., Schall, J. D., & Rossi, A. F. (2007). Difficulty of visual search modulates neuronal interactions and response variability in the frontal eye field. *Journal of Neurophysiology*, *98*(5), 2580–2587. https://doi.org/10.1152/jn.00522.2007

Connors, B. W., & Gutnick, M. J. (1990). Intrinsic firing patterns of diverse neocortical neurons. *Trends in Neurosciences*, *13*(3), 99–104. https://doi.org/10.1016/0166-2236(90)90185-d

Constantinidis, C., & Steinmetz, M. A. (2001). Neuronal responses in area 7a to multiple-stimulus displays: I. neurons encode the location of the salient stimulus. *Cerebral Cortex (New York, N.Y.: 1991)*, *11*(7), 581–591. https://doi.org/10.1093/cercor/11.7.581

Constantinidis, Christos, Funahashi, S., Lee, D., Murray, J. D., Qi, X.-L., Wang, M., & Arnsten, A. F. T. (2018). Persistent Spiking Activity Underlies Working Memory. *The Journal of Neuroscience: The Official Journal of the Society for Neuroscience*, *38*(32), 7020–7028. https://doi.org/10.1523/JNEUROSCI.2486-17.2018

Cosman, J. D., Lowe, K. A., Zinke, W., Woodman, G. F., & Schall, J. D. (2018). Prefrontal Control of Visual Distraction. *Current Biology*, *28*(3), 414-420.e3. https://doi.org/10.1016/j.cub.2017.12.023

Costello, M. G., Zhu, D., May, P. J., Salinas, E., & Stanford, T. R. (2016). Task dependence of decision- and choice-related activity in monkey oculomotor thalamus. *Journal of Neurophysiology*, *115*(1), 581–601. https://doi.org/10.1152/jn.00592.2015

Costello, M. G., Zhu, D., Salinas, E., & Stanford, T. R. (2013). Perceptual Modulation of Motor—But Not Visual—Responses in the Frontal Eye Field during an Urgent-Decision Task. *Journal of Neuroscience*, *33*(41), 16394–16408. https://doi.org/10.1523/JNEUROSCI.1899-13.2013

Crammond, D. J., & Kalaska, J. F. (1994). Modulation of preparatory neuronal activity in dorsal premotor cortex due to stimulus-response compatibility. *Journal of Neurophysiology*, *71*(3), 1281–1284. https://doi.org/10.1152/jn.1994.71.3.1281

Crapse, T. B., & Basso, M. A. (2015). Insights into decision making using choice probability. *Journal of Neurophysiology*, *114*(6), 3039–3049. https://doi.org/10.1152/jn.00335.2015

Crapse, T. B., Lau, H., & Basso, M. A. (2018). A Role for the Superior Colliculus in Decision Criteria. *Neuron*, *97*(1), 181-194.e6. https://doi.org/10.1016/j.neuron.2017.12.006

Crapse, T. B., & Sommer, M. A. (2008). The frontal eye field as a prediction map. *Progress in Brain Research*, *171*, 383–390. https://doi.org/10.1016/S0079-6123(08)00656-0

Crapse, T. B., & Sommer, M. A. (2012). Frontal Eye Field Neurons Assess Visual Stability Across Saccades. *Journal of Neuroscience*, *32*(8), 2835–2845. https://doi.org/10.1523/JNEUROSCI.1320-11.2012

Cromer, J. A., Roy, J. E., Buschman, T. J., & Miller, E. K. (2011). Comparison of Primate Prefrontal and Premotor Cortex Neuronal Activity during Visual Categorization. *Journal of Cognitive Neuroscience*, *23*(11), 3355–3365. https://doi.org/10.1162/jocn_a_00032

Davidson, D. (1970). *Mental Events* (L. Foster & J. W. Swanson, Eds.; pp. 207–224). Clarendon Press.

De Jaager, J. C. (1865). *De Physiologische Tijd bij Psychische Processen*. Medical Faculty of the University of Utrecht.

DeFelipe, J. (1997). Types of neurons, synaptic connections and chemical characteristics of cells immunoreactive for calbindin-D28K, parvalbumin and calretinin in the neocortex. *Journal of Chemical Neuroanatomy*, *14*(1), 1–19. https://doi.org/10.1016/s0891-0618(97)10013-8

Demb, J. B., & Singer, J. H. (2015). Functional Circuitry of the Retina. *Annual Review of Vision Science*, *1*(1), 263–289. https://doi.org/10.1146/annurev-vision-082114-035334

Desimone, R., & Schein, S. J. (1987). Visual properties of neurons in area V4 of the macaque: Sensitivity to stimulus form. *Journal of Neurophysiology*, *57*(3), 835–868. https://doi.org/10.1152/jn.1987.57.3.835

Desimone, Robert, & Duncan, J. (1995). Neural Mechanisms of Selective Visual Attention. *Annual Review of Neuroscience*, *18*(1), 193–222. https://doi.org/10.1146/annurev.ne.18.030195.001205

Dias, E. C., & Segraves, M. A. (1999). Muscimol-induced inactivation of monkey frontal eye field: Effects on visually and memory-guided saccades. *Journal of Neurophysiology*, *81*(5), 2191–2214. https://doi.org/10.1152/jn.1999.81.5.2191

Dibner, B. (1963). *Oersted and the discovery of electromagnetism*. Blaisdell Pub. Co.

Ding, L., & Gold, J. I. (2012). Neural correlates of perceptual decision making before, during, and after decision commitment in monkey frontal eye field. *Cerebral Cortex (New York, N.Y.: 1991)*, *22*(5), 1052–1067. https://doi.org/10.1093/cercor/bhr178

Ding, L., & Hikosaka, O. (2006). Comparison of Reward Modulation in the Frontal Eye Field and Caudate of the Macaque. *Journal of Neuroscience*, *26*(25), 6695–6703. https://doi.org/10.1523/JNEUROSCI.0836-06.2006

Distler, C., & Hoffmann, K.-P. (2015). Direct projections from the dorsal premotor cortex to the superior colliculus in the macaque (macaca mulatta). *Journal of Comparative Neurology*, *523*(16), 2390–2408. https://doi.org/10.1002/cne.23794

Donders, F. C. (1868). Over de snelheid van psychische processen. *Onderzoekingen gedaan in het Physiologisch Laboratorium der Utrechtsche Hoogeschool (1968–1869)*, *2*, 92–120.

Douglas, R. J., & Martin, K. A. (1991). A functional microcircuit for cat visual cortex. *The Journal of Physiology*, *440*, 735–769. https://doi.org/10.1113/jphysiol.1991.sp018733

Druckmann, S., Hill, S., Schürmann, F., Markram, H., & Segev, I. (2013). A hierarchical structure of cortical interneuron electrical diversity revealed by automated statistical analysis. *Cerebral Cortex (New York, N.Y.: 1991)*, *23*(12), 2994–3006. https://doi.org/10.1093/cercor/bhs290

Dubner, R., & Zeki, S. M. (1971). Response properties and receptive fields of cells in an anatomically defined region of the superior temporal sulcus in the monkey. *Brain Research*, *35*(2), 528–532. https://doi.org/10.1016/0006-8993(71)90494-X

Dubois, J., Hamker, F. H., & VanRullen, R. (2009). Attentional selection of noncontiguous locations: The spotlight is only transiently “split.” *Journal of Vision*, *9*(5), 3–3. https://doi.org/10.1167/9.5.3

Duncan, J., & Humphreys, G. W. (1989). Visual search and stimulus similarity. *Psychological Review*, *96*(3), 433–458. https://doi.org/10.1037/0033-295X.96.3.433

Eidels, A., Houpt, J. W., Altieri, N., Pei, L., & Townsend, J. T. (2011). Nice guys finish fast and bad guys finish last: Facilitatory vs. inhibitory interaction in parallel systems. *Journal of Mathematical Psychology*, *55*(2), 176–190. https://doi.org/10.1016/j.jmp.2010.11.003

Elsley, J. K., Nagy, B., Cushing, S. L., & Corneil, B. D. (2007). Widespread presaccadic recruitment of neck muscles by stimulation of the primate frontal eye fields. *Journal of Neurophysiology*, *98*(3), 1333–1354. https://doi.org/10.1152/jn.00386.2007

Emeric, E. E., Brown, J. W., Leslie, M., Pouget, P., Stuphorn, V., & Schall, J. D. (2008). Performance monitoring local field potentials in the medial frontal cortex of primates: Anterior cingulate cortex. *Journal of Neurophysiology*, *99*(2), 759–772. https://doi.org/10.1152/jn.00896.2006

Eriksen, B. A., & Eriksen, C. W. (1974). Effects of noise letters upon the identification of a target letter in a nonsearch task. *Perception & Psychophysics*, *16*(1), 143–149. https://doi.org/10.3758/BF03203267

Eriksen, C. W., & Schultz, D. W. (1979). Information processing in visual search: A continuous flow conception and experimental results. *Perception & Psychophysics*, *25*(4), 249–263. https://doi.org/10.3758/BF03198804

Everitt, B. S., Landau, S., Leese, M., & Stahl, D. (2011). *Cluster Analysis*. John Wiley & Sons.

Everling, S., & Munoz, D. P. (2000). Neuronal Correlates for Preparatory Set Associated with Pro-Saccades and Anti-Saccades in the Primate Frontal Eye Field. *Journal of Neuroscience*, *20*(1), 387–400. https://doi.org/10.1523/JNEUROSCI.20-01-00387.2000

Fechner, G. T. (1860). *Elemente der psychophysik*. Leipzig : Breitkopf und Härtel. http://archive.org/details/elementederpsych001fech

Fecteau, J. H., & Munoz, D. P. (2003). Exploring the consequences of the previous trial. *Nature Reviews. Neuroscience*, *4*(6), 435–443. https://doi.org/10.1038/nrn1114

Fernandes, H. L., Stevenson, I. H., Phillips, A. N., Segraves, M. A., & Kording, K. P. (2014). Saliency and Saccade Encoding in the Frontal Eye Field During Natural Scene Search. *Cerebral Cortex*, *24*(12), 3232–3245. https://doi.org/10.1093/cercor/bht179

Ferraina, S., Paré, M., & Wurtz, R. H. (2000). Disparity Sensitivity of Frontal Eye Field Neurons. *Journal of Neurophysiology*, *83*(1), 625–629. https://doi.org/10.1152/jn.2000.83.1.625

Ferraina, S., Paré, M., & Wurtz, R. H. (2002). Comparison of cortico-cortical and cortico-collicular signals for the generation of saccadic eye movements. *Journal of Neurophysiology*, *87*(2), 845–858. https://doi.org/10.1152/jn.00317.2001

Ferrera, V. P., Yanike, M., & Cassanello, C. (2009). Frontal eye field neurons signal changes in decision criteria. *Nature Neuroscience*, *12*(11), 1458–1462. https://doi.org/10.1038/nn.2434

Ferrier, D. (1875). XVI. The Croonian Lecture.—Experiments on the brain of monkeys (second series). *Philosophical Transactions of the Royal Society of London*, *165*, 433–488. https://doi.org/10.1098/rstl.1875.0016

Fiebelkorn, I. C., & Kastner, S. (2019). A rhythmic theory of attention. *Trends in Cognitive Sciences*, *23*(2), 87–101. https://doi.org/10.1016/j.tics.2018.11.009

Fiebelkorn, I. C., Pinsk, M. A., & Kastner, S. (2018). A dynamic interplay within the frontoparietal network underlies rhythmic spatial attention. *Neuron*, *99*(4), 842-853.e8. https://doi.org/10.1016/j.neuron.2018.07.038

Fiebelkorn, I. C., Pinsk, M. A., & Kastner, S. (2019). The mediodorsal pulvinar coordinates the macaque fronto-parietal network during rhythmic spatial attention. *Nature Communications*, *10*. https://doi.org/10.1038/s41467-018-08151-4

Fifić, M., Nosofsky, R. M., & Townsend, J. T. (2008a). Information-Processing Architectures in Multidimensional Classification: A Validation Test of the Systems Factorial Technology. *Journal of Experimental Psychology. Human Perception and Performance*, *34*(2), 356–375. https://doi.org/10.1037/0096-1523.34.2.356

Fifić, M., Townsend, J. T., & Eidels, A. (2008b). Studying visual search using systems factorial methodology with target–distractor similarity as the factor. *Perception & Psychophysics*, *70*(4), 583–603.

Findlay, J. M. (1997). Saccade target selection during visual search. *Vision Research*, *37*(5), 617–631. https://doi.org/10.1016/s0042-6989(96)00218-0

Finger, S., & Wade, N. J. (2002). The Neuroscience of Helmholtz and the Theories of Johannes Müller Part 1: Nerve Cell Structure, Vitalism, and the Nerve Impulse. *Journal of the History of the Neurosciences*, *11*(2), 136–155. https://doi.org/10.1076/jhin.11.2.136.15190

Finkelstein, G. (2015). Mechanical neuroscience: Emil du Bois-Reymond's innovations in theory and practice. *Frontiers in Systems Neuroscience*, *9*. https://doi.org/10.3389/fnsys.2015.00133

Fogassi, L., Raos, V., Franchi, G., Gallese, V., Luppino, G., & Matelli, M. (1999). Visual responses in the dorsal premotor area F2 of the macaque monkey. *Experimental Brain Research*, *128*(1–2), 194–199. https://doi.org/10.1007/s002210050835

Ford, K. A., Gati, J. S., Menon, R. S., & Everling, S. (2009). BOLD fMRI activation for anti-saccades in nonhuman primates. *NeuroImage*, *45*(2), 470–476. https://doi.org/10.1016/j.neuroimage.2008.12.009

Friedman, M. (2007). Kant—Naturphilosophie—Electromagnetism. In R. M. Brain, R. S. Cohen, & O. Knudsen (Eds.), *Hans Christian Ørsted And The Romantic Legacy In Science: Ideas, Disciplines, Practices* (pp. 135–158). Springer Netherlands. https://doi.org/10.1007/978-1-4020-2987-5_8

Fries, W. (1984). Cortical projections to the superior colliculus in the macaque monkey: A retrograde study using horseradish peroxidase. *The Journal of Comparative Neurology*, *230*(1), 55–76. https://doi.org/10.1002/cne.902300106

Fujii, N., Mushiake, H., & Tanji, J. (2000). Rostrocaudal Distinction of the Dorsal Premotor Area Based on Oculomotor Involvement. *Journal of Neurophysiology*, *83*(3), 1764–1769. https://doi.org/10.1152/jn.2000.83.3.1764

Fuster, J. M., Bauer, R. H., & Jervey, J. P. (1981). Effects of cooling inferotemporal cortex on performance of visual memory tasks. *Experimental Neurology*, *71*(2), 398–409. https://doi.org/10.1016/0014-4886(81)90098-4

Fuster, J. M., Bauer, R. H., & Jervey, J. P. (1982). Cellular discharge in the dorsolateral prefrontal cortex of the monkey in cognitive tasks. *Experimental Neurology*, *77*(3), 679–694. https://doi.org/10.1016/0014-4886(82)90238-2

Fuster, J. M., & Jervey, J. P. (1981). Inferotemporal neurons distinguish and retain behaviorally relevant features of visual stimuli. *Science (New York, N.Y.)*, *212*(4497), 952–955. https://doi.org/10.1126/science.7233192

Gee, A. L., Ipata, A. E., & Goldberg, M. E. (2010). Activity in V4 reflects the direction, but not the latency, of saccades during visual search. *Journal of Neurophysiology*, *104*(4), 2187–2193. https://doi.org/10.1152/jn.00898.2009

Geyer, S., Zilles, K., Luppino, G., & Matelli, M. (2000). Neurofilament protein distribution in the macaque monkey dorsolateral premotor cortex. *European Journal of Neuroscience*, *12*, 1554–1566.

Ghosh, S., & Gattera, R. (1995). A Comparison of the Ipsilateral Cortical Projections to the Dorsal and Ventral Subdivisions of the Macaque Premotor Cortex. *Somatosensory & Motor Research*, *12*(3–4), 359–378. https://doi.org/10.3109/08990229509093668

Glaser, J. I., Wood, D. K., Lawlor, P. N., Ramkumar, P., Kording, K. P., & Segraves, M. A. (2016). Role of expected reward in frontal eye field during natural scene search. *Journal of Neurophysiology*, *116*(2), 645–657. https://doi.org/10.1152/jn.00119.2016

Goder, A., & Filkov, V. (2008). Consensus clustering algorithms: Comparison and refinement. *Proceedings of the Meeting on Algorithm Engineering & Expermiments*, 109–117.

Gold, C., Girardin, C. C., Martin, K. A. C., & Koch, C. (2009). High-amplitude positive spikes recorded extracellularly in cat visual cortex. *Journal of Neurophysiology*, *102*(6), 3340–3351. https://doi.org/10.1152/jn.91365.2008

Goldberg, M. E., & Bruce, C. J. (1990). Primate frontal eye fields. III. Maintenance of a spatially accurate saccade signal. *Journal of Neurophysiology*, *64*(2), 489–508. https://doi.org/10.1152/jn.1990.64.2.489

Goldberg, M. E., & Bushnell, M. C. (1981). Behavioral enhancement of visual responses in monkey cerebral cortex. II. Modulation in frontal eye fields specifically related to saccades. *Journal of Neurophysiology*, *46*(4), 773–787. https://doi.org/10.1152/jn.1981.46.4.773

Goodale, M. A., & Milner, A. D. (1992). Separate visual pathways for perception and action. *Trends in Neurosciences*, *15*(1), 20–25.

Green, D. M., & Swets, J. A. (1966). *Signal detection theory and psychophysics* (pp. xi, 455). John Wiley.

Gregoriou, G. G., Gotts, S. J., & Desimone, R. (2012). Cell-Type-Specific Synchronization of Neural Activity in FEF with V4 during Attention. *Neuron*, *73*(3), 581–594. https://doi.org/10.1016/j.neuron.2011.12.019

Gregoriou, G. G., Gotts, S. J., Zhou, H., & Desimone, R. (2009). High-frequency, long-range coupling between prefrontal and visual cortex during attention. *Science (New York, N.Y.)*, *324*(5931), 1207–1210. https://doi.org/10.1126/science.1171402

Gries, S. T., & Stefanowitsch, A. (2010). Cluster analysis and the identification of collexeme classes. In S. Rice & J. Newman (Eds.), *Empirical and experimental methods in cognitive/functional research* (pp. 73–90).

Griggs, W. S., Amita, H., Gopal, A., & Hikosaka, O. (2018). Visual Neurons in the Superior Colliculus Discriminate Many Objects by Their Historical Values. *Frontiers in Neuroscience*, *12*. https://doi.org/10.3389/fnins.2018.00396

Hallett, P. E., & Adams, B. D. (1980). The predictability of saccadic latency in a novel voluntary oculomotor task. *Vision Research*, *20*(4), 329–339. https://doi.org/10.1016/0042-6989(80)90019-x

Hallett, P. E., & Lightstone, A. D. (1976). Saccadic eye movements towards stimuli triggered by prior saccades. *Vision Research*, *16*(1), 99–106. https://doi.org/10.1016/0042-6989(76)90083-3

Hamker, F. H. (2006). Modeling feature-based attention as an active top-down inference process. *Bio Systems*, *86*(1–3), 91–99. https://doi.org/10.1016/j.biosystems.2006.03.010

Hanes, D. P., Patterson II, W. F., & Schall, J. D. (1998). Role of frontal eye fields in countermanding saccades: Visual, movement, and fixation activity. *Journal of Neurophysiology*, *79*(2), 817–834.

Hanes, D. P., & Schall, J. D. (1995). Countermanding saccades in macaque. *Visual Neuroscience*, *12*(5), 929–937. https://doi.org/10.1017/S0952523800009482

Hanes, D. P., & Schall, J. D. (1996). Neural Control of Voluntary Movement Initiation. *Science*, *274*(5286), 427–430. https://doi.org/10.1126/science.274.5286.427

Hanes, D. P., Thompson, K. G., & Schall, J. D. (1995). Relationship of presaccadic activity in frontal eye field and supplementary eye field to saccade initiation in macaque: Poisson spike train analysis. *Experimental Brain Research*, *103*(1), 85–96. https://doi.org/10.1007/BF00241967

Harding, B., Goulet, M.-A., Jolin, S., Tremblay, C., Villeneuve, S.-P., & Durand, G. (2016). Systems Factorial Technology Explained to Humans. *The Quantitative Methods for Psychology*, *12*(1), 39–56. https://doi.org/10.20982/tqmp.12.1.p039

Hasegawa, R. P., Matsumoto, M., & Mikami, A. (2000). Search Target Selection in Monkey Prefrontal Cortex. *Journal of Neurophysiology*, *84*(3), 1692–1696. https://doi.org/10.1152/jn.2000.84.3.1692

Hasegawa, R. P., Peterson, B. W., & Goldberg, M. E. (2004). Prefrontal Neurons Coding Suppression of Specific Saccades. *Neuron*, *43*(3), 415–425. https://doi.org/10.1016/j.neuron.2004.07.013

Heilbronner, S. R., & Hayden, B. Y. (2016). Dorsal Anterior Cingulate Cortex: A Bottom-Up View. *Annual Review of Neuroscience*, *39*, 149–170. https://doi.org/10.1146/annurev-neuro-070815-013952

Heinzle, J., Hepp, K., & Martin, K. A. C. (2007). A microcircuit model of the frontal eye fields. *The Journal of Neuroscience: The Official Journal of the Society for Neuroscience*, *27*(35), 9341–9353. https://doi.org/10.1523/JNEUROSCI.0974-07.2007

Heitz, R. P., Cohen, J. Y., Woodman, G. F., & Schall, J. D. (2010). Neural Correlates of Correct and Errant Attentional Selection Revealed Through N2pc and Frontal Eye Field Activity. *Journal of Neurophysiology*, *104*(5), 2433–2441. https://doi.org/10.1152/jn.00604.2010

Heitz, R. P., & Schall, J. D. (2012). Neural mechanisms of speed-accuracy tradeoff. *Neuron*, *76*(3), 616–628. https://doi.org/10.1016/j.neuron.2012.08.030

Helmholtz, H. von. (1850). Vorläufiger Bericht über die Fortpflanzungs-Geschwindigkeit der Nervenreizung. *Archiv für Anatomie, Physiologie und wissenschaftliche Medicin*, 71–73.

Hickey, C., Di Lollo, V., & McDonald, J. J. (2008). Electrophysiological Indices of Target and Distractor Processing in Visual Search. *Journal of Cognitive Neuroscience*, *21*(4), 760–775. https://doi.org/10.1162/jocn.2009.21039

Hikosaka, O., & Wurtz, R. H. (1983). Visual and oculomotor functions of monkey substantia nigra pars reticulata. IV. Relation of substantia nigra to superior colliculus. *Journal of Neurophysiology*, *49*(5), 1285–1301. https://doi.org/10.1152/jn.1983.49.5.1285

Hodgkin, A. L., & Huxley, A. F. (1952). A quantitative description of membrane current and its application to conduction and excitation in nerve. *The Journal of Physiology*, *117*(4), 500–544. https://doi.org/10.1113/jphysiol.1952.sp004764

Hoffman, J. E. (1978). Search through a sequentially presented visual display. *Perception & Psychophysics*, *23*(1), 1–11. https://doi.org/10.3758/BF03214288

Holt, G. R., Softky, W. R., Koch, C., & Douglas, R. J. (1996). Comparison of discharge variability in vitro and in vivo in cat visual cortex neurons. *Journal of Neurophysiology*, *75*(5), 1806–1814. https://doi.org/10.1152/jn.1996.75.5.1806

Hopf, J. M., Luck, S. J., Girelli, M., Hagner, T., Mangun, G. R., Scheich, H., & Heinze, H. J. (2000). Neural sources of focused attention in visual search. *Cerebral Cortex (New York, N.Y.: 1991)*, *10*(12), 1233–1241. https://doi.org/10.1093/cercor/10.12.1233

Horwitz, G. D., Batista, A. P., & Newsome, W. T. (2004). Direction-selective visual responses in macaque superior colliculus induced by behavioral training. *Neuroscience Letters*, *366*(3), 315–319. https://doi.org/10.1016/j.neulet.2004.05.059

Hoshi, E., & Tanji, J. (2000). Integration of target and body-part information in the premotor cortex when planning action. *Nature*, *408*(6811), 466–470. https://doi.org/10.1038/35044075

Hoshi, E., & Tanji, J. (2004). Functional specialization in dorsal and ventral premotor areas. In *Progress in Brain Research* (Vol. 143, pp. 507–511). Elsevier. https://doi.org/10.1016/S0079-6123(03)43047-1

Hoshi, E., & Tanji, J. (2007). Distinctions between dorsal and ventral premotor areas: Anatomical connectivity and functional properties. *Current Opinion in Neurobiology*, *17*(2), 234–242. https://doi.org/10.1016/j.conb.2007.02.003

Houpt, J. W., Blaha, L. M., McIntire, J. P., Havig, P. R., & Townsend, J. T. (2014). Systems factorial technology with R. *Behavior Research Methods*, *46*(2), 307–330. https://doi.org/10.3758/s13428-013-0377-3

Houpt, J. W., & Townsend, J. T. (2010). The statistical properties of the Survivor Interaction Contrast. *Journal of Mathematical Psychology*, *54*(5), 446–453. https://doi.org/10.1016/j.jmp.2010.06.006

Hubel, D. H., & Wiesel, T. N. (1959). Receptive fields of single neurones in the cat's striate cortex. *The Journal of Physiology*, *148*(3), 574–591.

Hubel, D. H., & Wiesel, T. N. (1962). Receptive fields, binocular interaction and functional architecture in the cat's visual cortex. *The Journal of Physiology*, *160*(1), 106-154.2.

Hubel, D. H., & Wiesel, T. N. (1968). Receptive fields and functional architecture of monkey striate cortex. *The Journal of Physiology*, *195*(1), 215–243.

Hubel, David H., & Wiesel, T. N. (1974). Uniformity of monkey striate cortex: A parallel relationship between field size, scatter, and magnification factor. *Journal of Comparative Neurology*, *158*(3), 295–305. https://doi.org/10.1002/cne.901580305

Huerta, M. F., & Kaas, J. H. (1990). Supplementary eye field as defined by intracortical microstimulation: Connections in macaques. *Journal of Comparative Neurology*, *293*(2), 299–330. https://doi.org/10.1002/cne.902930211

Huerta, M. F., Krubitzer, L. A., & Kaas, J. H. (1986). Frontal eye field as defined by intracortical microstimulation in squirrel monkeys, owl monkeys, and macaque monkeys: I. Subcortical connections. *Journal of Comparative Neurology*, *253*(4), 415–439. https://doi.org/10.1002/cne.902530402

Huerta, M. F., Krubitzer, L. A., & Kaas, J. H. (1987). Frontal eye field as defined by intracortical microstimulation in squirrel monkeys, owl monkeys, and macaque monkeys II. cortical connections. *Journal of Comparative Neurology*, *265*(3), 332–361. https://doi.org/10.1002/cne.902650304

Huxley, A. F., & Stämpfli, R. (1949). Evidence for saltatory conduction in peripheral myelinated nerve fibres. *The Journal of Physiology*, *108*(3), 315–339.

Iba, M., & Sawaguchi, T. (2003). Involvement of the dorsolateral prefrontal cortex of monkeys in visuospatial target selection. *Journal of Neurophysiology*, *89*(1), 587–599. https://doi.org/10.1152/jn.00148.2002

Ibos, G., Duhamel, J.-R., & Hamed, S. B. (2013). A Functional Hierarchy within the Parietofrontal Network in Stimulus Selection and Attention Control. *Journal of Neuroscience*, *33*(19), 8359–8369. https://doi.org/10.1523/JNEUROSCI.4058-12.2013

Ichinohe, N., Watakabe, A., Miyashita, T., Yamamori, T., Hashikawa, T., & Rockland, K. S. (2004). A voltage-gated potassium channel, Kv3.1b, is expressed by a subpopulation of large pyramidal neurons in layer 5 of the macaque monkey cortex. *Neuroscience*, *129*(1), 179–185. https://doi.org/10.1016/j.neuroscience.2004.08.005

Ipata, A. E., Gee, A. L., & Goldberg, M. E. (2012). Feature attention evokes task-specific pattern selectivity in V4 neurons. *Proceedings of the National Academy of Sciences of the United States of America*, *109*(42), 16778–16785. https://doi.org/10.1073/pnas.1215402109

Ipata, A. E., Gee, A. L., Goldberg, M. E., & Bisley, J. W. (2006a). Activity in the lateral intraparietal area predicts the goal and latency of saccades in a free-viewing visual search task. *The Journal of Neuroscience: The Official Journal of the Society for Neuroscience*, *26*(14), 3656–3661. https://doi.org/10.1523/JNEUROSCI.5074-05.2006

Ipata, A. E., Gee, A. L., Gottlieb, J., Bisley, J. W., & Goldberg, M. E. (2006b). LIP responses to a popout stimulus are reduced if it is overtly ignored. *Nature Neuroscience*, *9*(8), 1071–1076. https://doi.org/10.1038/nn1734

Ito, S., Stuphorn, V., Brown, J. W., & Schall, J. D. (2003). Performance monitoring by the anterior cingulate cortex during saccade countermanding. *Science (New York, N.Y.)*, *302*(5642), 120–122. https://doi.org/10.1126/science.1087847

Itti, L., & Koch, C. (2000). A saliency-based search mechanism for overt and covert shifts of visual attention. *Vision Research*, *40*(10–12), 1489–1506. https://doi.org/10.1016/s0042-6989(99)00163-7

Izawa, Y., & Suzuki, H. (2014). Activity of fixation neurons in the monkey frontal eye field during smooth pursuit eye movements. *Journal of Neurophysiology*, *112*(2), 249–262. https://doi.org/10.1152/jn.00816.2013

Izawa, Y., & Suzuki, H. (2018). Motor action of the frontal eye field on the eyes and neck in the monkey. *Journal of Neurophysiology*, *119*(6), 2082–2090. https://doi.org/10.1152/jn.00577.2017

Johnston, K., Levin, H. M., Koval, M. J., & Everling, S. (2007). Top-down control-signal dynamics in anterior cingulate and prefrontal cortex neurons following task switching. *Neuron*, *53*(3), 453–462. https://doi.org/10.1016/j.neuron.2006.12.023

Johnston, K., Ma, L., Schaeffer, L., & Everling, S. (2019). Alpha Oscillations Modulate Preparatory Activity in Marmoset Area 8Ad. *The Journal of Neuroscience*, *39*(10), 1855–1866. https://doi.org/10.1523/JNEUROSCI.2703-18.2019

Joiner, W. M., Cavanaugh, J., & Wurtz, R. H. (2013). Compression and suppression of shifting receptive field activity in frontal eye field neurons. *The Journal of*

Neuroscience: The Official Journal of the Society for Neuroscience, *33*(46), 18259–18269. https://doi.org/10.1523/JNEUROSCI.2964-13.2013

Joshua, M., Elias, S., Levine, O., & Bergman, H. (2007). Quantifying the isolation quality of extracellularly recorded action potentials. *Journal of Neuroscience Methods*, *163*(2), 267–282. https://doi.org/10.1016/j.jneumeth.2007.03.012

Juan, C.-H., Muggleton, N. G., Tzeng, O. J. L., Hung, D. L., Cowey, A., & Walsh, V. (2008). Segregation of Visual Selection and Saccades in Human Frontal Eye Fields. *Cerebral Cortex*, *18*(10), 2410–2415. https://doi.org/10.1093/cercor/bhn001

Juan, Chi-Hung, Shorter-Jacobi, S. M., & Schall, J. D. (2004). Dissociation of spatial attention and saccade preparation. *Proceedings of the National Academy of Sciences*, *101*(43), 15541–15544. https://doi.org/10.1073/pnas.0403507101

Jun, J. J., Mitelut, C., Lai, C., Gratiy, S. L., Anastassiou, C. A., & Harris, T. D. (2017). Real-time spike sorting platform for high-density extracellular probes with ground-truth validation and drift correction. *BioRxiv*, 101030. https://doi.org/10.1101/101030

Kalaska, J. F., Sergio, L. E., & Cisek, P. (1998). Cortical control of whole-arm motor tasks. *Novartis Foundation Symposium*, *218*, 176–190; discussion 190-201.

Kalaska, John F, Scott, S. H., Cisek, P., & Sergio, L. E. (1997). Cortical control of reaching movements. *Current Opinion in Neurobiology*, *7*(6), 849–859. https://doi.org/10.1016/S0959-4388(97)80146-8

Katnani, H. A., & Gandhi, N. J. (2013). Time Course of Motor Preparation during Visual Search with Flexible Stimulus–Response Association. *Journal of Neuroscience*, *33*(24), 10057–10065. https://doi.org/10.1523/JNEUROSCI.0850-13.2013

Katzner, S., Nauhaus, I., Benucci, A., Bonin, V., Ringach, D. L., & Carandini, M. (2009). Local origin of field potentials in visual cortex. *Neuron*, *61*(1), 35–41. https://doi.org/10.1016/j.neuron.2008.11.016

Keller, E. L., Lee, B.-T., & Lee, K.-M. (2008). Chapter 2.4—Frontal eye field signals that may trigger the brainstem saccade generator. In C. Kennard & R. J. Leigh (Eds.), *Progress in Brain Research* (Vol. 171, pp. 107–114). Elsevier. https://doi.org/10.1016/S0079-6123(08)00614-6

Khayat, P. S., Pooresmaeili, A., & Roelfsema, P. R. (2009). Time course of attentional modulation in the frontal eye field during curve tracing. *Journal of Neurophysiology*, *101*(4), 1813–1822. https://doi.org/10.1152/jn.91050.2008

Kim, B., & Basso, M. A. (2008). Saccade target selection in the superior colliculus: A signal detection theory approach. *The Journal of Neuroscience: The Official*

Journal of the Society for Neuroscience, *28*(12), 2991–3007. https://doi.org/10.1523/JNEUROSCI.5424-07.2008

Kiss, M., Driver, J., & Eimer, M. (2009). Reward Priority of Visual Target Singletons Modulates Event-Related Potential Signatures of Attentional Selection. *Psychological Science*, *20*(2), 245–251. https://doi.org/10.1111/j.1467-9280.2009.02281.x

Kitcher, P. (1990). *Kant's Transcendental Psychology*. https://doi.org/10.2307/2185939

Klein, null. (2000). Inhibition of return. *Trends in Cognitive Sciences*, *4*(4), 138–147.

Knight, T. A. (2012). Contribution of the frontal eye field to gaze shifts in the head-unrestrained rhesus monkey: Neuronal activity. *Neuroscience*, *225*, 213–236. https://doi.org/10.1016/j.neuroscience.2012.08.050

Kodaka, Y., Mikami, A., & Kubota, K. (1997). Neuronal activity in the frontal eye field of the monkey is modulated while attention is focused on to a stimulus in the peripheral visual field, irrespective of eye movement. *Neuroscience Research*, *28*(4), 291–298. https://doi.org/10.1016/s0168-0102(97)00055-2

Koyama, M., Hasegawa, I., Osada, T., Adachi, Y., Nakahara, K., & Miyashita, Y. (2004). Functional magnetic resonance imaging of macaque monkeys performing visually guided saccade tasks: Comparison of cortical eye fields with humans. *Neuron*, *41*(5), 795–807. https://doi.org/10.1016/s0896-6273(04)00047-9

Krimer, L. S., Zaitsev, A. V., Czanner, G., Kröner, S., González-Burgos, G., Povysheva, N. V., Iyengar, S., Barrionuevo, G., & Lewis, D. A. (2005). Cluster analysis-based physiological classification and morphological properties of inhibitory neurons in layers 2-3 of monkey dorsolateral prefrontal cortex. *Journal of Neurophysiology*, *94*(5), 3009–3022. https://doi.org/10.1152/jn.00156.2005

Kristjánsson, Á., Sigurjónsdóttir, Ó., & Driver, J. (2010). Fortune and reversals of fortune in visual search: Reward contingencies for pop-out targets affect search efficiency and target repetition effects. *Attention, Perception, & Psychophysics*, *72*(5), 1229–1236. https://doi.org/10.3758/APP.72.5.1229

Krock, R. M., & Moore, T. (2016). Visual sensitivity of frontal eye field neurons during the preparation of saccadic eye movements. *Journal of Neurophysiology*, *116*(6), 2882–2891. https://doi.org/10.1152/jn.01140.2015

Lapointe, F.-J., & Legendre, P. (1994). A Classification of Pure Malt Scotch Whiskies. *Journal of the Royal Statistical Society. Series C (Applied Statistics)*, *43*(1), 237–257. JSTOR. https://doi.org/10.2307/2986124

Latimer, K. W., Yates, J. L., Meister, M. L. R., Huk, A. C., & Pillow, J. W. (2015). Single-trial spike trains in parietal cortex reveal discrete steps during decision-making. *Science*, *349*(6244), 184–187. https://doi.org/10.1126/science.aaa4056

Law, C.-T., & Gold, J. I. (2008). Neural correlates of perceptual learning in a sensory-motor but not a sensory cortical area. *Nature Neuroscience*, *11*(4), 505–513. https://doi.org/10.1038/nn2070

Lawrence, B. M., & Snyder, L. H. (2009). The Responses of Visual Neurons in the Frontal Eye Field Are Biased for Saccades. *Journal of Neuroscience*, *29*(44), 13815–13822. https://doi.org/10.1523/JNEUROSCI.2352-09.2009

Lawrence, B. M., White, R. L., & Snyder, L. H. (2005). Delay-period activity in visual, visuomovement, and movement neurons in the frontal eye field. *Journal of Neurophysiology*, *94*(2), 1498–1508. https://doi.org/10.1152/jn.00214.2005

Lebedev, M. A., & Wise, S. P. (2001). Tuning for the orientation of spatial attention in dorsal premotor cortex. *European Journal of Neuroscience*, *13*(5), 1002–1008. https://doi.org/10.1046/j.0953-816x.2001.01457.x

Lee, B.-T., & McPeek, R. M. (2013). The effects of distractors and spatial precues on covert visual search in macaque. *Vision Research*, *76*, 43–49. https://doi.org/10.1016/j.visres.2012.10.007

Lee, K.-M., & Keller, E. L. (2008). Neural Activity in the Frontal Eye Fields Modulated by the Number of Alternatives in Target Choice. *Journal of Neuroscience*, *28*(9), 2242–2251. https://doi.org/10.1523/JNEUROSCI.3596-07.2008

Lennert, T., & Martinez-Trujillo, J. C. (2013). Prefrontal neurons of opposite spatial preference display distinct target selection dynamics. *The Journal of Neuroscience: The Official Journal of the Society for Neuroscience*, *33*(22), 9520–9529. https://doi.org/10.1523/JNEUROSCI.5156-12.2013

Libera, C. D., & Chelazzi, L. (2006). Visual Selective Attention and the Effects of Monetary Rewards. *Psychological Science*, *17*(3), 222–227. https://doi.org/10.1111/j.1467-9280.2006.01689.x

Liesefeld, H. R. (2018). Estimating the Timing of Cognitive Operations With MEG/EEG Latency Measures: A Primer, a Brief Tutorial, and an Implementation of Various Methods. *Frontiers in Neuroscience*, *12*. https://doi.org/10.3389/fnins.2018.00765

Liesefeld, H. R., Liesefeld, A. M., Töllner, T., & Müller, H. J. (2017). Attentional capture in visual search: Capture and post-capture dynamics revealed by EEG. *NeuroImage*, *156*, 166–173. https://doi.org/10.1016/j.neuroimage.2017.05.016

Liesefeld, H. R., & Müller, H. J. (2020). A theoretical attempt to revive the serial/parallel-search dichotomy. *Attention, Perception, & Psychophysics*, *82*(1), 228–245. https://doi.org/10.3758/s13414-019-01819-z

Lochner, C., Hemmings, S. M. J., Kinnear, C. J., Niehaus, D. J. H., Nel, D. G., Corfield, V. A., Moolman-Smook, J. C., Seedat, S., & Stein, D. J. (2005). Cluster analysis of obsessive-compulsive spectrum disorders in patients with obsessive-

compulsive disorder: Clinical and genetic correlates. *Comprehensive Psychiatry*, *46*(1), 14–19. https://doi.org/10.1016/j.comppsych.2004.07.020

Logan, G. D. (1996). The CODE theory of visual attention: An integration of space-based and object-based attention. *Psychological Review*, *103*(4), 603–649. https://doi.org/10.1037/0033-295x.103.4.603

Logan, Gordon D. (2002). An instance theory of attention and memory. *Psychological Review*, *109*(2), 376–400. https://doi.org/10.1037/0033-295X.109.2.376

Logan, Gordon D., & Cowan, W. B. (1984). On the ability to inhibit thought and action: A theory of an act of control. *Psychological Review*, *91*(3), 295–327. https://doi.org/10.1037/0033-295X.91.3.295

Logan, Gordon D., Yamaguchi, M., Schall, J. D., & Palmeri, T. J. (2015). Inhibitory control in mind and brain 2.0: Blocked-input models of saccadic countermanding. *Psychological Review*, *122*(2), 115–147. https://doi.org/10.1037/a0038893

Logothetis, N. K., & Schall, J. D. (1989). Neuronal correlates of subjective visual perception. *Science (New York, N.Y.)*, *245*(4919), 761–763. https://doi.org/10.1126/science.2772635

Lovejoy, L. P., & Krauzlis, R. J. (2017). Changes in perceptual sensitivity related to spatial cues depends on subcortical activity. *Proceedings of the National Academy of Sciences of the United States of America*, *114*(23), 6122–6126. https://doi.org/10.1073/pnas.1609711114

Lowe, K. A., Reppert, T. R., & Schall, J. D. (2019). Selective influence and sequential operations: A research strategy for visual search. *Visual Cognition*, *27*(5–8), 387–415. https://doi.org/10.1080/13506285.2019.1659896

Lowe, K. A., & Schall, J. D. (2018). Functional Categories of Visuomotor Neurons in Macaque Frontal Eye Field. *ENeuro*, *5*(5), ENEURO.0131-18.2018. https://doi.org/10.1523/ENEURO.0131-18.2018

Lowe, K. A., & Schall, J. D. (2019). Sequential Operations Revealed by Serendipitous Feature Selectivity in Frontal Eye Field. *BioRxiv*, 683144. https://doi.org/10.1101/683144

Luce, R. D. (1959). *Individual choice behavior*. John Wiley.

Luce, R. D., & Marley, A. A. J. (1997). *Choice, decision, and measurement: Essays in honor of R. Duncan Luce*. https://doi.org/10.4324/9781315789408

Luck, S. J., & Hillyard, S. A. (1994). Spatial filtering during visual search: Evidence from human electrophysiology. *Journal of Experimental Psychology. Human Perception and Performance*, *20*(5), 1000–1014. https://doi.org/10.1037//0096-1523.20.5.1000

Lund, J. S., & Lewis, D. A. (1993). Local circuit neurons of developing and mature macaque prefrontal cortex: Golgi and immunocytochemical characteristics. *The Journal of Comparative Neurology*, *328*(2), 282–312. https://doi.org/10.1002/cne.903280209

Lundqvist, M., Herman, P., & Miller, E. K. (2018). Working Memory: Delay Activity, Yes! Persistent Activity? Maybe Not. *The Journal of Neuroscience: The Official Journal of the Society for Neuroscience*, *38*(32), 7013–7019. https://doi.org/10.1523/JNEUROSCI.2485-17.2018

Lundqvist, M., Rose, J., Herman, P., Brincat, S. L., Buschman, T. J., & Miller, E. K. (2016). Gamma and Beta Bursts Underlie Working Memory. *Neuron*, *90*(1), 152–164. https://doi.org/10.1016/j.neuron.2016.02.028

Luppino, G., Rozzi, S., Calzavara, R., & Matelli, M. (2003). Prefrontal and agranular cingulate projections to the dorsal premotor areas F2 and F7 in the macaque monkey. *European Journal of Neuroscience*, *17*(3), 559–578. https://doi.org/10.1046/j.1460-9568.2003.02476.x

Maljkovic, V., & Nakayama, K. (1994). Priming of pop-out: I. Role of features. *Memory & Cognition*, *22*(6), 657–672.

Mallet, N., Schmidt, R., Leventhal, D., Chen, F., Amer, N., Boraud, T., & Berke, J. D. (2016). Arkypallidal Cells Send a Stop Signal to Striatum. *Neuron*, *89*(2), 308–316. https://doi.org/10.1016/j.neuron.2015.12.017

Marcum, J. I. (1947). *A Statistical Theory of Target Detection by Pulsed Radar* [Product Page]. https://www.rand.org/pubs/research_memoranda/RM754.html

Markov, N. T., Vezoli, J., Chameau, P., Falchier, A., Quilodran, R., Huissoud, C., Lamy, C., Misery, P., Giroud, P., Ullman, S., Barone, P., Dehay, C., Knoblauch, K., & Kennedy, H. (2014). Anatomy of hierarchy: Feedforward and feedback pathways in macaque visual cortex. *The Journal of Comparative Neurology*, *522*(1), 225–259. https://doi.org/10.1002/cne.23458

Marr, D., & Poggio, T. (1976). *From Understanding Computation to Understanding Neural Circuitry*. https://dspace.mit.edu/handle/1721.1/5782

Marr, David. (1982). Vision: A Computational Investigation into the Human Representation and Processing of Visual Information. *New York, NY: W.H. Freeman and Company*. http://papers.cumincad.org/cgi-bin/works/_id=ecaade2013/Show?fafa

Matsushima, A., & Tanaka, M. (2014). Differential Neuronal Representation of Spatial Attention Dependent on Relative Target Locations during Multiple Object Tracking. *Journal of Neuroscience*, *34*(30), 9963–9969. https://doi.org/10.1523/JNEUROSCI.4354-13.2014

Mayo, J. P., DiTomasso, A. R., Sommer, M. A., & Smith, M. A. (2015). Dynamics of visual receptive fields in the macaque frontal eye field. *Journal of Neurophysiology*, *114*(6), 3201–3210. https://doi.org/10.1152/jn.00746.2015

Mazer, J. A., & Gallant, J. L. (2003). Goal-related activity in V4 during free viewing visual search. Evidence for a ventral stream visual salience map. *Neuron*, *40*(6), 1241–1250. https://doi.org/10.1016/s0896-6273(03)00764-5

McAdams, C. J., & Maunsell, J. H. R. (1999). Effects of Attention on Orientation-Tuning Functions of Single Neurons in Macaque Cortical Area V4. *The Journal of Neuroscience*, *19*(1), 431–441. https://doi.org/10.1523/JNEUROSCI.19-01-00431.1999

McCants, C. W., Berggren, N., & Eimer, M. (2018). The guidance of visual search by shape features and shape configurations. *Journal of Experimental Psychology. Human Perception and Performance*, *44*(7), 1072–1085. https://doi.org/10.1037/xhp0000514

McClelland, J. L. (1979). On the time relations of mental processes: An examination of systems of processes in cascade. *Psychological Review*, *86*(4), 287–330. https://doi.org/10.1037/0033-295X.86.4.287

McComas, A. (2011). Galvani's Spark: The Story of the Nerve Impulse. In *Galvani's Spark*. Oxford University Press. https://www.oxfordscholarship.com/view/10.1093/acprof:oso/9780199751754.001.0001/acprof-9780199751754

McCormick, D. A., Connors, B. W., Lighthall, J. W., & Prince, D. A. (1985). Comparative electrophysiology of pyramidal and sparsely spiny stellate neurons of the neocortex. *Journal of Neurophysiology*, *54*(4), 782–806. https://doi.org/10.1152/jn.1985.54.4.782

McPeek, R. M., & Keller, E. L. (2001). Short-term priming, concurrent processing, and saccade curvature during a target selection task in the monkey. *Vision Research*, *41*(6), 785–800. https://doi.org/10.1016/s0042-6989(00)00287-x

McPeek, Robert M. (2006). Incomplete Suppression of Distractor-Related Activity in the Frontal Eye Field Results in Curved Saccades. *Journal of Neurophysiology*, *96*(5), 2699–2711. https://doi.org/10.1152/jn.00564.2006

McPeek, Robert M., & Keller, E. L. (2002). Superior colliculus activity related to concurrent processing of saccade goals in a visual search task. *Journal of Neurophysiology*, *87*(4), 1805–1815. https://doi.org/10.1152/jn.00501.2001

Meyers, E. M., Liang, A., Katsuki, F., & Constantinidis, C. (2018). Differential Processing of Isolated Object and Multi-item Pop-Out Displays in LIP and PFC. *Cerebral Cortex (New York, N.Y.: 1991)*, *28*(11), 3816–3828. https://doi.org/10.1093/cercor/bhx243

Middlebrooks, P. G., & Sommer, M. A. (2012). Neuronal correlates of metacognition in primate frontal cortex. *Neuron*, *75*(3), 517–530. https://doi.org/10.1016/j.neuron.2012.05.028

Miller, E. K., Li, L., & Desimone, R. (1991). A neural mechanism for working and recognition memory in inferior temporal cortex. *Science (New York, N.Y.)*, *254*(5036), 1377–1379. https://doi.org/10.1126/science.1962197

Miller, E. K., Li, L., & Desimone, R. (1993). Activity of neurons in anterior inferior temporal cortex during a short- term memory task. *Journal of Neuroscience*, *13*(4), 1460–1478. https://doi.org/10.1523/JNEUROSCI.13-04-01460.1993

Miller, Earl K., & Buschman, T. J. (2013). Cortical circuits for the control of attention. *Current Opinion in Neurobiology*, *23*(2), 216–222. https://doi.org/10.1016/j.conb.2012.11.011

Miller, Earl K., & Desimone, R. (1994). Parallel Neuronal Mechanisms for Short-Term Memory. *Science*, *263*(5146), 520–522. JSTOR.

Miller, Earl K., Erickson, C. A., & Desimone, R. (1996). Neural Mechanisms of Visual Working Memory in Prefrontal Cortex of the Macaque. *Journal of Neuroscience*, *16*(16), 5154–5167. https://doi.org/10.1523/JNEUROSCI.16-16-05154.1996

Miller, J. (1982). Discrete versus continuous stage models of human information processing: In search of partial output. *Journal of Experimental Psychology: Human Perception and Performance*, *8*(2), 273–296. https://doi.org/10.1037/0096-1523.8.2.273

Miller, J. (1988). Discrete and continuous models of human information processing: Theoretical distinctions and empirical results. *Acta Psychologica*, *67*(3), 191–257. https://doi.org/10.1016/0001-6918(88)90013-3

Mirpour, K., Arcizet, F., Ong, W. S., & Bisley, J. W. (2009). Been there, seen that: A neural mechanism for performing efficient visual search. *Journal of Neurophysiology*, *102*(6), 3481–3491. https://doi.org/10.1152/jn.00688.2009

Mirpour, K., & Bisley, J. W. (2013). Evidence for differential top-down and bottom-up suppression in posterior parietal cortex. *Philosophical Transactions of the Royal Society of London. Series B, Biological Sciences*, *368*(1628), 20130069. https://doi.org/10.1098/rstb.2013.0069

Mirpour, K., Bolandnazar, Z., & Bisley, J. W. (2018). Suppression of frontal eye field neuronal responses with maintained fixation. *Proceedings of the National Academy of Sciences of the United States of America*, *115*(4), 804–809. https://doi.org/10.1073/pnas.1716315115

Mirpour, K., Bolandnazar, Z., & Bisley, J. W. (2019). Neurons in FEF Keep Track of Items That Have Been Previously Fixated in Free Viewing Visual Search. *Journal*

of Neuroscience, *39*(11), 2114–2124. https://doi.org/10.1523/JNEUROSCI.1767-18.2018

Mirpour, K., Ong, W. S., & Bisley, J. W. (2010). Microstimulation of posterior parietal cortex biases the selection of eye movement goals during search. *Journal of Neurophysiology*, *104*(6), 3021–3028. https://doi.org/10.1152/jn.00397.2010

Mishkin, M., Ungerleider, L. G., & Macko, K. A. (1983). Object vision and spatial vision: Two cortical pathways. *Trends in Neurosciences*, *6*, 414–417. https://doi.org/10.1016/0166-2236(83)90190-X

Mitchell, J. F., Sundberg, K. A., & Reynolds, J. H. (2007). Differential attention-dependent response modulation across cell classes in macaque visual area V4. *Neuron*, *55*(1), 131–141. https://doi.org/10.1016/j.neuron.2007.06.018

Mitchell, J. F., & Zipser, D. (2003). Sequential memory-guided saccades and target selection: A neural model of the frontal eye fields. *Vision Research*, *43*(25), 2669–2695. https://doi.org/10.1016/s0042-6989(03)00468-1

Mohler, C. W., & Wurtz, R. H. (1976). Organization of monkey superior colliculus: Intermediate layer cells discharging before eye movements. *Journal of Neurophysiology*, *39*(4), 722–744. https://doi.org/10.1152/jn.1976.39.4.722

Mohler, Charles W., Goldberg, M. E., & Wurtz, R. H. (1973). Visual receptive fields of frontal eye field neurons. *Brain Research*, *61*, 385–389. https://doi.org/10.1016/0006-8993(73)90543-X

Monosov, I. E., Sheinberg, D. L., & Thompson, K. G. (2010). Paired neuron recordings in the prefrontal and inferotemporal cortices reveal that spatial selection precedes object identification during visual search. *Proceedings of the National Academy of Sciences*, *107*(29), 13105–13110. https://doi.org/10.1073/pnas.1002870107

Monosov, I. E., & Thompson, K. G. (2009). Frontal Eye Field Activity Enhances Object Identification During Covert Visual Search. *Journal of Neurophysiology*, *102*(6), 3656–3672. https://doi.org/10.1152/jn.00750.2009

Monosov, I. E., Trageser, J. C., & Thompson, K. G. (2008). Measurements of Simultaneously Recorded Spiking Activity and Local Field Potentials Suggest that Spatial Selection Emerges in the Frontal Eye Field. *Neuron*, *57*(4), 614–625. https://doi.org/10.1016/j.neuron.2007.12.030

Moore, T., & Armstrong, K. M. (2003). Selective gating of visual signals by microstimulation of frontal cortex. *Nature*, *421*(6921), 370. https://doi.org/10.1038/nature01341

Moran, R., Zehetleitner, M., Liesefeld, H. R., Müller, H. J., & Usher, M. (2016). Serial vs. parallel models of attention in visual search: Accounting for benchmark RT-

distributions. *Psychonomic Bulletin & Review*, *23*(5), 1300–1315. https://doi.org/10.3758/s13423-015-0978-1

Motter, B. C. (1993). Focal attention produces spatially selective processing in visual cortical areas V1, V2, and V4 in the presence of competing stimuli. *Journal of Neurophysiology*, *70*(3), 909–919. https://doi.org/10.1152/jn.1993.70.3.909

Motter, B. C. (1994). Neural correlates of attentive selection for color or luminance in extrastriate area V4. *The Journal of Neuroscience: The Official Journal of the Society for Neuroscience*, *14*(4), 2178–2189.

Motter, B. C., & Holsapple, J. (2007). Saccades and covert shifts of attention during active visual search: Spatial distributions, memory, and items per fixation. *Vision Research*, *47*(10), 1261–1281. https://doi.org/10.1016/j.visres.2007.02.006

Motter, B. C., & Holsapple, J. W. (2000). Cortical image density determines the probability of target discovery during active search. *Vision Research*, *40*(10–12), 1311–1322. https://doi.org/10.1016/s0042-6989(99)00218-7

Motter, Brad C., & Belky, E. J. (1998). The guidance of eye movements during active visual search. *Vision Research*, *38*(12), 1805–1815. https://doi.org/10.1016/S0042-6989(97)00349-0

Mouret, I., & Hasbroucq, T. (2000). The chronometry of single neuron activity: Testing discrete and continuous models of information processing. *Journal of Experimental Psychology: Human Perception and Performance*, *26*(5), 1622–1638. https://doi.org/10.1037/0096-1523.26.5.1622

Mruczek, R. E. B., & Sheinberg, D. L. (2007a). Activity of inferior temporal cortical neurons predicts recognition choice behavior and recognition time during visual search. *The Journal of Neuroscience: The Official Journal of the Society for Neuroscience*, *27*(11), 2825–2836. https://doi.org/10.1523/JNEUROSCI.4102-06.2007

Mruczek, R. E. B., & Sheinberg, D. L. (2007b). Context familiarity enhances target processing by inferior temporal cortex neurons. *The Journal of Neuroscience: The Official Journal of the Society for Neuroscience*, *27*(32), 8533–8545. https://doi.org/10.1523/JNEUROSCI.2106-07.2007

Mruczek, R. E. B., & Sheinberg, D. L. (2012). Stimulus selectivity and response latency in putative inhibitory and excitatory neurons of the primate inferior temporal cortex. *Journal of Neurophysiology*, *108*(10), 2725–2736. https://doi.org/10.1152/jn.00618.2012

Müller, J. (1824). Über das Bedürfnis der Physiologie nach einer philosophischen Naturbetrachtung. In *Zur vergleichenden Physiologie des Gesichtssinnes des Menschen und der Thiere, nebst einem Versuch über die Bewegung der Augen und über den menschlichen Blick* (pp. 1–34). Knobloch.

Müller, J. (1835). *Handbuch der Physiologie des Menschen: Für Vorlesungen* / (2 Aufl. (des 1. Bd.), pp. 1–878). Hölscher,. https://doi.org/10.5962/bhl.title.128395

Müller, J. (1840). *Elements of Physiology*. Taylor and Walton.

Murray, J. D., Bernacchia, A., Roy, N. A., Constantinidis, C., Romo, R., & Wang, X.-J. (2017). Stable population coding for working memory coexists with heterogeneous neural dynamics in prefrontal cortex. *Proceedings of the National Academy of Sciences*, *114*(2), 394–399. https://doi.org/10.1073/pnas.1619449114

Murthy, A., Ray, S., Shorter, S. M., Priddy, E. G., Schall, J. D., & Thompson, K. G. (2007). Frontal eye field contributions to rapid corrective saccades. *Journal of Neurophysiology*, *97*(2), 1457–1469. https://doi.org/10.1152/jn.00433.2006

Murthy, A., Ray, S., Shorter, S. M., Schall, J. D., & Thompson, K. G. (2009). Neural control of visual search by frontal eye field: Effects of unexpected target displacement on visual selection and saccade preparation. *Journal of Neurophysiology*, *101*(5), 2485–2506. https://doi.org/10.1152/jn.90824.2008

Murthy, A., Thompson, K. G., & Schall, J. D. (2001). Dynamic Dissociation of Visual Selection From Saccade Programming in Frontal Eye Field. *Journal of Neurophysiology*, *86*(5), 2634–2637. https://doi.org/10.1152/jn.2001.86.5.2634

Mushiake, H., Fujii, N., & Tanji, J. (1996). Visually guided saccade versus eye-hand reach: Contrasting neuronal activity in the cortical supplementary and frontal eye fields. *Journal of Neurophysiology*, *75*(5), 2187–2191. https://doi.org/10.1152/jn.1996.75.5.2187

Mushiake, Hajime, Tanatsugu, Y., & Tanji, J. (1997). Neuronal Activity in the Ventral Part of Premotor Cortex During Target-Reach Movement is Modulated by Direction of Gaze. *Journal of Neurophysiology*, *78*(1), 567–571. https://doi.org/10.1152/jn.1997.78.1.567

Nakata, R., Eifuku, S., & Tamura, R. (2014). Effects of tilted orientations and face-like configurations on visual search asymmetry in macaques. *Animal Cognition*, *17*(1), 67–76. https://doi.org/10.1007/s10071-013-0638-7

Nakayama, Y., Yamagata, T., & Hoshi, E. (2016). Rostrocaudal functional gradient among the pre-dorsal premotor cortex, dorsal premotor cortex and primary motor cortex in goal-directed motor behaviour. *The European Journal of Neuroscience*, *43*(12), 1569–1589. https://doi.org/10.1111/ejn.13254

Nawrot, M. P., Boucsein, C., Rodriguez Molina, V., Riehle, A., Aertsen, A., & Rotter, S. (2008). Measurement of variability dynamics in cortical spike trains. *Journal of Neuroscience Methods*, *169*(2), 374–390. https://doi.org/10.1016/j.jneumeth.2007.10.013

Neggers, S. F. W., Diepen, R. M. van, Zandbelt, B. B., Vink, M., Mandl, R. C. W., & Gutteling, T. P. (2012). A functional and structural investigation of the human fronto-basal volitional saccade network. *PloS One*, *7*(1), e29517. https://doi.org/10.1371/journal.pone.0029517

Nelson, M. J., Murthy, A., & Schall, J. D. (2016). Neural control of visual search by frontal eye field: Chronometry of neural events and race model processes. *Journal of Neurophysiology*, *115*(4), 1954–1969. https://doi.org/10.1152/jn.01023.2014

Neromyliotis, E., & Moschovakis, A. K. (2017a). Saccades evoked in response to electrical stimulation of the posterior bank of the arcuate sulcus. *Experimental Brain Research*, *235*(9), 2797–2809. https://doi.org/10.1007/s00221-017-5012-6

Neromyliotis, E., & Moschovakis, A. K. (2017b). Response Properties of Motor Equivalence Neurons of the Primate Premotor Cortex. *Frontiers in Behavioral Neuroscience*, *11*, 61. https://doi.org/10.3389/fnbeh.2017.00061

Neromyliotis, E., & Moschovakis, A. K. (2018). Response properties of saccade-related neurons of the post-arcuate premotor cortex. *Journal of Neurophysiology*, *119*(6), 2291–2306. https://doi.org/10.1152/jn.00669.2017

Ninomiya, T., Sawamura, H., Inoue, K., & Takada, M. (2012). Segregated Pathways Carrying Frontally Derived Top-Down Signals to Visual Areas MT and V4 in Macaques. *Journal of Neuroscience*, *32*(20), 6851–6858. https://doi.org/10.1523/JNEUROSCI.6295-11.2012

Nishida, S., Tanaka, T., & Ogawa, T. (2013). Separate evaluation of target facilitation and distractor suppression in the activity of macaque lateral intraparietal neurons during visual search. *Journal of Neurophysiology*, *110*(12), 2773–2791. https://doi.org/10.1152/jn.00360.2013

Nishida, S., Tanaka, T., Shibata, T., Ikeda, K., Aso, T., & Ogawa, T. (2014). Discharge-rate persistence of baseline activity during fixation reflects maintenance of memory-period activity in the macaque posterior parietal cortex. *Cerebral Cortex (New York, N.Y.: 1991)*, *24*(6), 1671–1685. https://doi.org/10.1093/cercor/bht031

Nothdurft, H.-C., Pigarev, I. N., & Kastner, S. (2009). Overt and covert visual search in primates: Reaction times and gaze shift strategies. *Journal of Integrative Neuroscience*, *8*(2), 137–174. https://doi.org/10.1142/s0219635209002101

Noudoost, B., Clark, K. L., & Moore, T. (2014). A Distinct Contribution of the Frontal Eye Field to the Visual Representation of Saccadic Targets. *Journal of Neuroscience*, *34*(10), 3687–3698. https://doi.org/10.1523/JNEUROSCI.3824-13.2014

Noudoost, B., & Moore, T. (2011). The role of neuromodulators in selective attention. *Trends in Cognitive Sciences*, *15*(12), 585–591. https://doi.org/10.1016/j.tics.2011.10.006

Nowak, L., Azouz, R., Sanchez-Vives, M., Gray, C., & McCormick, D. (2003). Electrophysiological classes of cat primary visual cortical neurons. *Journal of Neurophysiology*, *89*, 1541–1566. https://doi.org/10.1152/jn.00580.2002

Ogawa, T., & Komatsu, H. (2004). Target Selection in Area V4 during a Multidimensional Visual Search Task. *Journal of Neuroscience*, *24*(28), 6371–6382. https://doi.org/10.1523/JNEUROSCI.0569-04.2004

Ogawa, T., & Komatsu, H. (2006). Neuronal dynamics of bottom-up and top-down processes in area V4 of macaque monkeys performing a visual search. *Experimental Brain Research*, *173*(1), 1–13. https://doi.org/10.1007/s00221-006-0362-5

Ogawa, T., & Komatsu, H. (2009). Condition-dependent and condition-independent target selection in the macaque posterior parietal cortex. *Journal of Neurophysiology*, *101*(2), 721–736. https://doi.org/10.1152/jn.90817.2008

Osman, A., Bashore, T. R., Coles, M. G. H., Donchin, E., & Meyer, D. E. (1992). On the transmission of partial information: Inferences from movement-related brain potentials. *Journal of Experimental Psychology: Human Perception and Performance*, *18*(1), 217–232. https://doi.org/10.1037/0096-1523.18.1.217

Paré, M., & Hanes, D. P. (2003). Controlled movement processing: Superior colliculus activity associated with countermanded saccades. *The Journal of Neuroscience: The Official Journal of the Society for Neuroscience*, *23*(16), 6480–6489.

Pasupathy, A., & Connor, C. E. (1999). Responses to Contour Features in Macaque Area V4. *Journal of Neurophysiology*, *82*(5), 2490–2502. https://doi.org/10.1152/jn.1999.82.5.2490

Paus, T. (1996). Location and function of the human frontal eye-field: A selective review. *Neuropsychologia*, *34*(6), 475–483. https://doi.org/10.1016/0028-3932(95)00134-4

Peel, T. R., Johnston, K., Lomber, S. G., & Corneil, B. D. (2014). Bilateral saccadic deficits following large and reversible inactivation of unilateral frontal eye field. *Journal of Neurophysiology*, *111*(2), 415–433. https://doi.org/10.1152/jn.00398.2013

Peña, J. M., Lozano, J. A., & Larrañaga, P. (1999). An empirical comparison of four initialization methods for the K-Means algorithm. *Pattern Recognition Letters*, *20*(10), 1027–1040. https://doi.org/10.1016/S0167-8655(99)00069-0

Peng, X., Sereno, M. E., Silva, A. K., Lehky, S. R., & Sereno, A. B. (2008). Shape Selectivity in Primate Frontal Eye Field. *Journal of Neurophysiology*, *100*(2), 796–814. https://doi.org/10.1152/jn.01188.2007

Petrides, M., & Pandya, D. N. (1984). Projections to the frontal cortex from the posterior parietal region in the rhesus monkey. *The Journal of Comparative Neurology*, *228*(1), 105–116. https://doi.org/10.1002/cne.902280110

Phillips, A. N., & Segraves, M. A. (2009). Predictive Activity in Macaque Frontal Eye Field Neurons During Natural Scene Searching. *Journal of Neurophysiology*, *103*(3), 1238–1252. https://doi.org/10.1152/jn.00776.2009

Phillips, A. N., & Segraves, M. A. (2010). Predictive activity in macaque frontal eye field neurons during natural scene searching. *Journal of Neurophysiology*, *103*(3), 1238–1252. https://doi.org/10.1152/jn.00776.2009

Platt, M. L., & Glimcher, P. W. (1999). Neural correlates of decision variables in parietal cortex. *Nature*, *400*(6741), 233. https://doi.org/10.1038/22268

Posner, M. I., & Cohen, Y. (1984). Components of Visual Orienting. *Attention and Performance X*, *32*, 531–556.

Pouget, P., Emeric, E. E., Stuphorn, V., Reis, K., & Schall, J. D. (2005). Chronometry of visual responses in frontal eye field, supplementary eye field, and anterior cingulate cortex. *Journal of Neurophysiology*, *94*(3), 2086–2092. https://doi.org/10.1152/jn.01097.2004

Pouget, P., Stepniewska, I., Crowder, E. A., Leslie, M. W., Emeric, E. E., Nelson, M. J., & Schall, J. D. (2009). Visual and motor connectivity and the distribution of calcium-binding proteins in macaque frontal eye field: Implications for saccade target selection. *Frontiers in Neuroanatomy*, *3*. https://doi.org/10.3389/neuro.05.002.2009

Purcell, B. A., Heitz, R. P., Cohen, J. Y., & Schall, J. D. (2012a). Response variability of frontal eye field neurons modulates with sensory input and saccade preparation but not visual search salience. *Journal of Neurophysiology*, *108*(10), 2737–2750. https://doi.org/10.1152/jn.00613.2012

Purcell, B. A., Heitz, R. P., Cohen, J. Y., Schall, J. D., Logan, G. D., & Palmeri, T. J. (2010). Neurally constrained modeling of perceptual decision making. *Psychological Review*, *117*(4), 1113–1143. https://doi.org/10.1037/a0020311

Purcell, B. A., Schall, J. D., Logan, G. D., & Palmeri, T. J. (2012b). From Salience to Saccades: Multiple-Alternative Gated Stochastic Accumulator Model of Visual Search. *Journal of Neuroscience*, *32*(10), 3433–3446. https://doi.org/10.1523/JNEUROSCI.4622-11.2012

Purcell, B. A., Schall, J. D., & Woodman, G. F. (2013). On the origin of event-related potentials indexing covert attentional selection during visual search: Timing of selection by macaque frontal eye field and event-related potentials during pop-out search. *Journal of Neurophysiology*, *109*(2), 557–569. https://doi.org/10.1152/jn.00549.2012

Ramkumar, P., Lawlor, P. N., Glaser, J. I., Wood, D. K., Phillips, A. N., Segraves, M. A., & Kording, K. P. (2016). Feature-based attention and spatial selection in frontal eye fields during natural scene search. *Journal of Neurophysiology*, *116*(3), 1328–1343. https://doi.org/10.1152/jn.01044.2015

Ratcliff, R. (1978). A theory of memory retrieval. *Psychological Review*, *85*(2), 59–108. https://doi.org/10.1037/0033-295X.85.2.59

Ratcliff, R., & McKoon, G. (2008). The Diffusion Decision Model: Theory and Data for Two-Choice Decision Tasks. *Neural Computation*, *20*(4), 873–922. https://doi.org/10.1162/neco.2008.12-06-420

Ratcliff, R., Smith, P. L., Brown, S. D., & McKoon, G. (2016). Diffusion Decision Model: Current Issues and History. *Trends in Cognitive Sciences*, *20*(4), 260–281. https://doi.org/10.1016/j.tics.2016.01.007

Ray, S., Pouget, P., & Schall, J. D. (2009). Functional Distinction Between Visuomovement and Movement Neurons in Macaque Frontal Eye Field During Saccade Countermanding. *Journal of Neurophysiology*, *102*(6), 3091–3100. https://doi.org/10.1152/jn.00270.2009

Reinhart, R. M. G., Heitz, R. P., Purcell, B. A., Weigand, P. K., Schall, J. D., & Woodman, G. F. (2012). Homologous Mechanisms of Visuospatial Working Memory Maintenance in Macaque and Human: Properties and Sources. *Journal of Neuroscience*, *32*(22), 7711–7722. https://doi.org/10.1523/JNEUROSCI.0215-12.2012

Reppert, T. R., Servant, M., Heitz, R. P., & Schall, J. D. (2018). Neural mechanisms of speed-accuracy tradeoff of visual search: Saccade vigor, the origin of targeting errors, and comparison of the superior colliculus and frontal eye field. *Journal of Neurophysiology*, *120*(1), 372–384. https://doi.org/10.1152/jn.00887.2017

Reynolds, J. H., & Heeger, D. J. (2009). The normalization model of attention. *Neuron*, *61*(2), 168–185. https://doi.org/10.1016/j.neuron.2009.01.002

Rheinberger, H. J. (1998). From the “originary phenomenon” to the “system of pelagic fishery”: Johannes Müller (1801-1858) and the relation between physiology and philosophy. *Clio Medica (Amsterdam, Netherlands)*, *48*, 133–152.

Riehle, A., & Requin, J. (1989). Monkey primary motor and premotor cortex: Single-cell activity related to prior information about direction and extent of an intended movement. *Journal of Neurophysiology*, *61*(3), 534–549. https://doi.org/10.1152/jn.1989.61.3.534

Riley, M. R., & Constantinidis, C. (2016). Role of Prefrontal Persistent Activity in Working Memory. *Frontiers in Systems Neuroscience*, *9*. https://doi.org/10.3389/fnsys.2015.00181

Robinson, D. A., & Fuchs, A. F. (1969). Eye movements evoked by stimulation of frontal eye fields. *Journal of Neurophysiology*, *32*(5), 637–648. https://doi.org/10.1152/jn.1969.32.5.637

Rocco, B. R., Sweet, R. A., Lewis, D. A., & Fish, K. N. (2016). GABA-Synthesizing Enzymes in Calbindin and Calretinin Neurons in Monkey Prefrontal Cortex. *Cerebral Cortex (New York, N.Y.: 1991)*, *26*(5), 2191–2204. https://doi.org/10.1093/cercor/bhv051

Roesch, M. R., & Olson, C. R. (2003). Impact of expected reward on neuronal activity in prefrontal cortex, frontal and supplementary eye fields and premotor cortex. *Journal of Neurophysiology*, *90*(3), 1766–1789. https://doi.org/10.1152/jn.00019.2003

Romo, R., Hernández, A., & Zainos, A. (2004). Neuronal Correlates of a Perceptual Decision in Ventral Premotor Cortex. *Neuron*, *41*(1), 165–173. https://doi.org/10.1016/S0896-6273(03)00817-1

Rouder, J. N., Speckman, P. L., Sun, D., Morey, R. D., & Iverson, G. (2009). Bayesian t tests for accepting and rejecting the null hypothesis. *Psychonomic Bulletin & Review*, *16*(2), 225–237. https://doi.org/10.3758/PBR.16.2.225

Sajad, A., Godlove, D. C., & Schall, J. D. (2019). Cortical microcircuitry of performance monitoring. *Nature Neuroscience*, *22*(2), 265–274. https://doi.org/10.1038/s41593-018-0309-8

Sajad, A., Sadeh, M., Keith, G. P., Yan, X., Wang, H., & Crawford, J. D. (2015). Visual-Motor Transformations Within Frontal Eye Fields During Head-Unrestrained Gaze Shifts in the Monkey. *Cerebral Cortex (New York, N.Y.: 1991)*, *25*(10), 3932–3952. https://doi.org/10.1093/cercor/bhu279

Sajad, A., Sadeh, M., Yan, X., Wang, H., & Crawford, J. D. (2016). Transition from Target to Gaze Coding in Primate Frontal Eye Field during Memory Delay and Memory–Motor Transformation. *ENeuro*, *3*(2). https://doi.org/10.1523/ENEURO.0040-16.2016

Sakagami, M., & Niki, H. (1994). Spatial selectivity of go/no-go neurons in monkey prefrontal cortex. *Experimental Brain Research*, *100*(1), 165–169. https://doi.org/10.1007/BF00227290

Sapountzis, P., Paneri, S., & Gregoriou, G. G. (2018). Distinct roles of prefrontal and parietal areas in the encoding of attentional priority. *Proceedings of the National Academy of Sciences*, *115*(37), E8755–E8764. https://doi.org/10.1073/pnas.1804643115

Sato, T., Murthy, A., Thompson, K. G., & Schall, J. D. (2001). Search Efficiency but Not Response Interference Affects Visual Selection in Frontal Eye Field. *Neuron*, *30*(2), 583–591. https://doi.org/10.1016/S0896-6273(01)00304-X

Sato, T. R., & Schall, J. D. (2003). Effects of Stimulus-Response Compatibility on Neural Selection in Frontal Eye Field. *Neuron*, *38*(4), 637–648. https://doi.org/10.1016/S0896-6273(03)00237-X

Sato, T. R., Watanabe, K., Thompson, K. G., & Schall, J. D. (2003). Effect of target-distractor similarity on FEF visual selection in the absence of the target. *Experimental Brain Research*, *151*(3), 356–363. https://doi.org/10.1007/s00221-003-1461-1

Sawaki, R., & Luck, S. J. (2010). Capture versus suppression of attention by salient singletons: Electrophysiological evidence for an automatic attend-to-me signal. *Attention, Perception, & Psychophysics*, *72*(6), 1455–1470. https://doi.org/10.3758/APP.72.6.1455

Scerra, V. E., Costello, M. G., Salinas, E., & Stanford, T. R. (2019). All-or-None Context Dependence Delineates Limits of FEF Visual Target Selection. *Current Biology*, *29*(2), 294-305.e3. https://doi.org/10.1016/j.cub.2018.12.013

Schafer, R. J., & Moore, T. (2011). Selective attention from voluntary control of neurons in prefrontal cortex. *Science (New York, N.Y.)*, *332*(6037), 1568–1571. https://doi.org/10.1126/science.1199892

Schall, J. D. (1991). Neuronal activity related to visually guided saccades in the frontal eye fields of rhesus monkeys: Comparison with supplementary eye fields. *Journal of Neurophysiology*, *66*(2), 559–579. https://doi.org/10.1152/jn.1991.66.2.559

Schall, J. D., Hanes, D. P., Thompson, K. G., & King, D. J. (1995a). Saccade target selection in frontal eye field of macaque. I. Visual and premovement activation. *Journal of Neuroscience*, *15*(10), 6905–6918. https://doi.org/10.1523/JNEUROSCI.15-10-06905.1995

Schall, J. D., Morel, A., & Kaas, J. H. (1993). Topography of supplementary eye field afferents to frontal eye field in macaque: Implications for mapping between saccade coordinate systems. *Visual Neuroscience*, *10*(2), 385–393. https://doi.org/10.1017/s0952523800003771

Schall, J. D., Morel, A., King, D. J., & Bullier, J. (1995b). Topography of visual cortex connections with frontal eye field in macaque: Convergence and segregation of processing streams. *Journal of Neuroscience*, *15*(6), 4464–4487. https://doi.org/10.1523/JNEUROSCI.15-06-04464.1995

Schall, Jeffrey D. (2001). Neural basis of deciding, choosing and acting. *Nature Reviews Neuroscience*, *2*(1), 33–42. https://doi.org/10.1038/35049054

Schall, Jeffrey D. (2003). Neural correlates of decision processes: Neural and mental chronometry. *Current Opinion in Neurobiology*, *13*(2), 182–186. https://doi.org/10.1016/S0959-4388(03)00039-4

Schall, Jeffrey D. (2004a). On Building a Bridge Between Brain and Behavior. *Annual Review of Psychology*, *55*(1), 23–50. https://doi.org/10.1146/annurev.psych.55.090902.141907

Schall, Jeffrey D. (2004b). On the role of frontal eye field in guiding attention and saccades. *Vision Research*, *44*(12), 1453–1467. https://doi.org/10.1016/j.visres.2003.10.025

Schall, Jeffrey D. (2015). Visuomotor Functions in the Frontal Lobe. *Annual Review of Vision Science*, *1*(1), 469–498. https://doi.org/10.1146/annurev-vision-082114-035317

Schall, Jeffrey D. (2019). Accumulators, Neurons, and Response Time. *Trends in Neurosciences*, *42*(12), 848–860. https://doi.org/10.1016/j.tins.2019.10.001

Schall, Jeffrey D., & Hanes, D. P. (1993). Neural basis of saccade target selection in frontal eye field during visual search. *Nature*, *366*(6454), 467. https://doi.org/10.1038/366467a0

Schall, Jeffrey D., Zinke, W., Cosman, J., Schall, M. S., Paré, M., & Pouget, P. (2017). *On the Evolution of the Frontal Eye Field: Comparisons of Monkeys, Apes, and Humans*. https://doi.org/10.1016/b978-0-12-804042-3.00130-5

Schein, S. J., & Desimone, R. (1990). Spectral properties of V4 neurons in the macaque. *Journal of Neuroscience*, *10*(10), 3369–3389. https://doi.org/10.1523/JNEUROSCI.10-10-03369.1990

Schiller, P. H., Sandell, J. H., & Maunsell, J. H. (1987). The effect of frontal eye field and superior colliculus lesions on saccadic latencies in the rhesus monkey. *Journal of Neurophysiology*, *57*(4), 1033–1049. https://doi.org/10.1152/jn.1987.57.4.1033

Schmolesky, M. T., Wang, Y., Hanes, D. P., Thompson, K. G., Leutgeb, S., Schall, J. D., & Leventhal, A. G. (1998). Signal Timing Across the Macaque Visual System. *Journal of Neurophysiology*, *79*(6), 3272–3278. https://doi.org/10.1152/jn.1998.79.6.3272

Schwedhelm, P., Baldauf, D., & Treue, S. (2020). The lateral prefrontal cortex of primates encodes stimulus colors and their behavioral relevance during a match-to-sample task. *Scientific Reports*, *10*(1), 1–12. https://doi.org/10.1038/s41598-020-61171-3

Schweickert, R. (1978). A critical path generalization of the additive factor method: Analysis of a Stroop task. *Journal of Mathematical Psychology*, *18*(2), 105–139. https://doi.org/10.1016/0022-2496(78)90059-7

Schwemmer, M. A., Feng, S. F., Holmes, P. J., Gottlieb, J., & Cohen, J. D. (2015). A Multi-Area Stochastic Model for a Covert Visual Search Task. *PloS One*, *10*(8), e0136097. https://doi.org/10.1371/journal.pone.0136097

Scudder, C. A., Kaneko, C. S., & Fuchs, A. F. (2002). The brainstem burst generator for saccadic eye movements: A modern synthesis. *Experimental Brain Research*, *142*(4), 439–462. https://doi.org/10.1007/s00221-001-0912-9

Segraves, M. A., & Goldberg, M. E. (1987). Functional properties of corticotectal neurons in the monkey's frontal eye field. *Journal of Neurophysiology*, *58*(6), 1387–1419. https://doi.org/10.1152/jn.1987.58.6.1387

Segraves, M. A., & Park, K. (1993). The relationship of monkey frontal eye field activity to saccade dynamics. *Journal of Neurophysiology*, *69*(6), 1880–1889. https://doi.org/10.1152/jn.1993.69.6.1880

Servant, M., Tillman, G., Schall, J. D., Logan, G. D., & Palmeri, T. J. (2019). Neurally constrained modeling of speed-accuracy tradeoff during visual search: Gated accumulation of modulated evidence. *Journal of Neurophysiology*, *121*(4), 1300–1314. https://doi.org/10.1152/jn.00507.2018

Servant, M., White, C., Montagnini, A., & Burle, B. (2015). Using Covert Response Activation to Test Latent Assumptions of Formal Decision-Making Models in Humans. *The Journal of Neuroscience: The Official Journal of the Society for Neuroscience*, *35*(28), 10371–10385. https://doi.org/10.1523/JNEUROSCI.0078-15.2015

Shadlen, M. N., Britten, K. H., Newsome, W. T., & Movshon, J. A. (1996). A computational analysis of the relationship between neuronal and behavioral responses to visual motion. *Journal of Neuroscience*, *16*(4), 1486–1510. https://doi.org/10.1523/JNEUROSCI.16-04-01486.1996

Shadlen, M. N., & Newsome, W. T. (1996). Motion perception: Seeing and deciding. *Proceedings of the National Academy of Sciences*, *93*(2), 628–633. https://doi.org/10.1073/pnas.93.2.628

Shadlen, Michael N., & Newsome, W. T. (2001). Neural Basis of a Perceptual Decision in the Parietal Cortex (Area LIP) of the Rhesus Monkey. *Journal of Neurophysiology*, *86*(4), 1916–1936. https://doi.org/10.1152/jn.2001.86.4.1916

Shadlen, Michael N., & Kiani, R. (2013). Decision Making as a Window on Cognition. *Neuron*, *80*(3), 791–806. https://doi.org/10.1016/j.neuron.2013.10.047

Shafi, M., Zhou, Y., Quintana, J., Chow, C., Fuster, J., & Bodner, M. (2007). Variability in neuronal activity in primate cortex during working memory tasks. *Neuroscience*, *146*(3), 1082–1108. https://doi.org/10.1016/j.neuroscience.2006.12.072

Shanahan, T. (1989). Kant, Naturphilosophie, and Oersted's Discovery of Electromagnetism: A Reassessment. *Studies in History and Philosophy of Science*, *20*, 287–305. https://doi.org/10.1016/0039-3681(89)90009-5

Shariat Torbaghan, S., Yazdi, D., Mirpour, K., & Bisley, J. W. (2012). Inhibition of return in a visual foraging task in non-human subjects. *Vision Research*, *74*, 2–9. https://doi.org/10.1016/j.visres.2012.03.022

Sharp, P. M., Tuohy, T. M., & Mosurski, K. R. (1986). Codon usage in yeast: Cluster analysis clearly differentiates highly and lowly expressed genes. *Nucleic Acids Research*, *14*(13), 5125–5143.

Shen, K., & Paré, M. (2006). Guidance of eye movements during visual conjunction search: Local and global contextual effects on target discriminability. *Journal of Neurophysiology*, *95*(5), 2845–2855. https://doi.org/10.1152/jn.00898.2005

Shen, K., & Paré, M. (2007). Neuronal activity in superior colliculus signals both stimulus identity and saccade goals during visual conjunction search. *Journal of Vision*, *7*(5), 15.1-13. https://doi.org/10.1167/7.5.15

Shen, K., & Paré, M. (2014). Predictive saccade target selection in superior colliculus during visual search. *The Journal of Neuroscience: The Official Journal of the Society for Neuroscience*, *34*(16), 5640–5648. https://doi.org/10.1523/JNEUROSCI.3880-13.2014

Shenhav, A., Botvinick, M. M., & Cohen, J. D. (2013). The expected value of control: An integrative theory of anterior cingulate cortex function. *Neuron*, *79*(2), 217–240. https://doi.org/10.1016/j.neuron.2013.07.007

Shin, S., & Sommer, M. A. (2012). Division of labor in frontal eye field neurons during presaccadic remapping of visual receptive fields. *Journal of Neurophysiology*, *108*(8), 2144–2159. https://doi.org/10.1152/jn.00204.2012

Shinomoto, S., Kim, H., Shimokawa, T., Matsuno, N., Funahashi, S., Shima, K., Fujita, I., Tamura, H., Doi, T., Kawano, K., Inaba, N., Fukushima, K., Kurkin, S., Kurata, K., Taira, M., Tsutsui, K.-I., Komatsu, H., Ogawa, T., Koida, K., … Toyama, K. (2009). Relating Neuronal Firing Patterns to Functional Differentiation of Cerebral Cortex. *PLOS Computational Biology*, *5*(7), e1000433. https://doi.org/10.1371/journal.pcbi.1000433

Shinomoto, S., Shima, K., & Tanji, J. (2003). Differences in spiking patterns among cortical neurons. *Neural Computation*, *15*(12), 2823–2842. https://doi.org/10.1162/089976603322518759

Silvetti, M., Alexander, W., Verguts, T., & Brown, J. W. (2014). From conflict management to reward-based decision making: Actors and critics in primate medial frontal cortex. *Neuroscience and Biobehavioral Reviews*, *46 Pt 1*, 44–57. https://doi.org/10.1016/j.neubiorev.2013.11.003

Smulders, F. T., Kok, A., Kenemans, J. L., & Bashore, T. R. (1995). The temporal selectivity of additive factor effects on the reaction process revealed in ERP

component latencies. *Acta Psychologica*, *90*(1–3), 97–109. https://doi.org/10.1016/0001-6918(95)00032-p

Sokal, R. R., & Michener, C. D. (1958). *A Statistical Method for Evaluating Systematic Relationships*. University of Kansas.

Soltani, A., Noudoost, B., & Moore, T. (2013). Dissociable dopaminergic control of saccadic target selection and its implications for reward modulation. *Proceedings of the National Academy of Sciences of the United States of America*, *110*(9), 3579–3584. https://doi.org/10.1073/pnas.1221236110

Sommer, M. A., & Wurtz, R. H. (1998). Frontal eye field neurons orthodromically activated from the superior colliculus. *Journal of Neurophysiology*, *80*(6), 3331–3335. https://doi.org/10.1152/jn.1998.80.6.3331

Sommer, Marc A., & Wurtz, R. H. (2000). Composition and Topographic Organization of Signals Sent From the Frontal Eye Field to the Superior Colliculus. *Journal of Neurophysiology*, *83*(4), 1979–2001. https://doi.org/10.1152/jn.2000.83.4.1979

Sommer, Marc A., & Wurtz, R. H. (2001). Frontal Eye Field Sends Delay Activity Related to Movement, Memory, and Vision to the Superior Colliculus. *Journal of Neurophysiology*, *85*(4), 1673–1685. https://doi.org/10.1152/jn.2001.85.4.1673

Song, J.-H., & McPeek, R. M. (2015). Neural correlates of target selection for reaching movements in superior colliculus. *Journal of Neurophysiology*, *113*(5), 1414–1422. https://doi.org/10.1152/jn.00417.2014

Song, J.-H., Takahashi, N., & McPeek, R. M. (2008). Target selection for visually guided reaching in macaque. *Journal of Neurophysiology*, *99*(1), 14–24. https://doi.org/10.1152/jn.01106.2007

Sperling, G. (1960). The information available in brief visual presentations. *Psychological Monographs: General and Applied*, *74*(11), 1–29. https://doi.org/10.1037/h0093759

Standage, D., Blohm, G., & Dorris, M. C. (2014). On the neural implementation of the speed-accuracy trade-off. *Frontiers in Neuroscience*, *8*. https://doi.org/10.3389/fnins.2014.00236

Stanford, T. R., Shankar, S., Massoglia, D. P., Costello, M. G., & Salinas, E. (2010). Perceptual decision making in less than 30 milliseconds. *Nature Neuroscience*, *13*(3), 379–385. https://doi.org/10.1038/nn.2485

Stanton, G. B., Bruce, C. J., & Goldberg, M. E. (1993). Topography of projections to the frontal lobe from the macaque frontal eye fields. *The Journal of Comparative Neurology*, *330*(2), 286–301. https://doi.org/10.1002/cne.903300209

Stanton, G. B., Bruce, C. J., & Goldberg, M. E. (1995). Topography of projections to posterior cortical areas from the macaque frontal eye fields. *The Journal of Comparative Neurology*, *353*(2), 291–305. https://doi.org/10.1002/cne.903530210

Stanton, G. B., Goldberg, M. E., & Bruce, C. J. (1988). Frontal eye field efferents in the macaque monkey: II. Topography of terminal fields in midbrain and pons. *Journal of Comparative Neurology*, *271*(4), 493–506. https://doi.org/10.1002/cne.902710403

Stauffer, R. C. (1953). Persistent Errors Regarding Oersted's Discovery of Electromagnetism. *Isis*, *44*(4), 307–310. https://doi.org/10.1086/348253

Steenrod, S. C., Phillips, M. H., & Goldberg, M. E. (2013). The lateral intraparietal area codes the location of saccade targets and not the dimension of the saccades that will be made to acquire them. *Journal of Neurophysiology*, *109*(10), 2596–2605. https://doi.org/10.1152/jn.00349.2012

Sternberg, S. (1969). The discovery of processing stages: Extensions of Donders' method. *Acta Psychologica*, *30*, 276–315.

Sternberg, S. (2001). Separate modifiability, mental modules, and the use of pure and composite measures to reveal them. *Acta Psychologica*, *106*(1–2), 147–246. https://doi.org/10.1016/S0001-6918(00)00045-7

Stone, M. (1960). Models for choice-reaction time. *Psychometrika*, *25*(3), 251–260. https://doi.org/10.1007/BF02289729

Strehl, A., & Ghosh, J. (2003). Cluster ensembles—A knowledge reuse framework for combining multiple partitions. *The Journal of Machine Learning Research*, *3*(null), 583–617. https://doi.org/10.1162/153244303321897735

Sugrue, L. P., Corrado, G. S., & Newsome, W. T. (2004). Matching Behavior and the Representation of Value in the Parietal Cortex. *Science*, *304*(5678), 1782–1787. https://doi.org/10.1126/science.1094765

Suzuki, H., & Azuma, M. (1983). Topographic studies on visual neurons in the dorsolateral prefrontal cortex of the monkey. *Experimental Brain Research*, *53*(1), 47–58. https://doi.org/10.1007/bf00239397

Tanaka, T., Nishida, S., & Ogawa, T. (2015). Different target-discrimination times can be followed by the same saccade-initiation timing in different stimulus conditions during visual searches. *Journal of Neurophysiology*, *114*(1), 366–380. https://doi.org/10.1152/jn.00043.2015

Tanné-Gariépy, J., Rouiller, E. M., & Boussaoud, D. (2002). Parietal inputs to dorsal versus ventral premotor areas in the macaque monkey: Evidence for largely

segregated visuomotor pathways. *Experimental Brain Research*, *145*(1), 91–103. https://doi.org/10.1007/s00221-002-1078-9

Taylor, D. A. (1976). Stage analysis of reaction time. *Psychological Bulletin*, *83*(2), 161–191. https://doi.org/10.1037/0033-2909.83.2.161

Tehovnik, E. J., Sommer, M. A., Chou, I.-H., Slocum, W. M., & Schiller, P. H. (2000). Eye fields in the frontal lobes of primates. *Brain Research Reviews*, *32*(2), 413–448. https://doi.org/10.1016/S0165-0173(99)00092-2

Teichert, T., Yu, D., & Ferrera, V. P. (2014). Performance monitoring in monkey frontal eye field. *The Journal of Neuroscience: The Official Journal of the Society for Neuroscience*, *34*(5), 1657–1671. https://doi.org/10.1523/JNEUROSCI.3694-13.2014

Teller, D. Y. (1984). Linking propositions. *Vision Research*, *24*(10), 1233–1246. https://doi.org/10.1016/0042-6989(84)90178-0

Teller, D. Y., & Pugh, E. N. Jr. (1983). Linking propositions in color vision. In J. D. Mollon & L. T. Sharpe (Eds.), *Colour Vision: Physiology and Psycho physics*. Academic Press.

Theeuwes, J. (1994). Stimulus-driven capture and attentional set: Selective search for color and visual abrupt onsets. *Journal of Experimental Psychology. Human Perception and Performance*, *20*(4), 799–806.

Theeuwes, Jan. (1991). Cross-dimensional perceptual selectivity. *Perception & Psychophysics*, *50*(2), 184–193. https://doi.org/10.3758/BF03212219

Theeuwes, Jan. (1992). Perceptual selectivity for color and form. *Perception & Psychophysics*, *51*(6), 599–606. https://doi.org/10.3758/BF03211656

Thiele, A., Brandt, C., Dasilva, M., Gotthardt, S., Chicharro, D., Panzeri, S., & Distler, C. (2016). Attention Induced Gain Stabilization in Broad and Narrow-Spiking Cells in the Frontal Eye-Field of Macaque Monkeys. *The Journal of Neuroscience: The Official Journal of the Society for Neuroscience*, *36*(29), 7601–7612. https://doi.org/10.1523/JNEUROSCI.0872-16.2016

Thomas, N. W. D., & Paré, M. (2007). Temporal Processing of Saccade Targets in Parietal Cortex Area LIP During Visual Search. *Journal of Neurophysiology*, *97*(1), 942–947. https://doi.org/10.1152/jn.00413.2006

Thompson, K. G., Hanes, D. P., Bichot, N. P., & Schall, J. D. (1996). Perceptual and motor processing stages identified in the activity of macaque frontal eye field neurons during visual search. *Journal of Neurophysiology*, *76*(6), 4040–4055. https://doi.org/10.1152/jn.1996.76.6.4040

Thompson, K. G., & Bichot, N. P. (2005). A visual salience map in the primate frontal eye field. In *Progress in Brain Research* (Vol. 147, pp. 249–262). Elsevier. https://doi.org/10.1016/S0079-6123(04)47019-8

Thompson, K. G., Bichot, N. P., & Sato, T. R. (2005a). Frontal Eye Field Activity Before Visual Search Errors Reveals the Integration of Bottom-Up and Top-Down Salience. *Journal of Neurophysiology*, *93*(1), 337–351. https://doi.org/10.1152/jn.00330.2004

Thompson, Kirk G., Bichot, N. P., & Schall, J. D. (1997). Dissociation of Visual Discrimination From Saccade Programming in Macaque Frontal Eye Field. *Journal of Neurophysiology*, *77*(2), 1046–1050. https://doi.org/10.1152/jn.1997.77.2.1046

Thompson, Kirk G., Biscoe, K. L., & Sato, T. R. (2005b). Neuronal basis of covert spatial attention in the frontal eye field. *The Journal of Neuroscience: The Official Journal of the Society for Neuroscience*, *25*(41), 9479–9487. https://doi.org/10.1523/JNEUROSCI.0741-05.2005

Thornton, T. L., & Gilden, D. L. (2007). Parallel and serial processes in visual search. *Psychological Review*, *114*(1), 71–103. https://doi.org/10.1037/0033-295X.114.1.71

Thura, D., & Cisek, P. (2014). Deliberation and commitment in the premotor and primary motor cortex during dynamic decision making. *Neuron*, *81*(6), 1401–1416. https://doi.org/10.1016/j.neuron.2014.01.031

Tibshirani, R., Walther, G., & Hastie, T. (2001). Estimating the number of clusters in a data set via the gap statistic. *Journal of the Royal Statistical Society: Series B (Statistical Methodology)*, *63*(2), 411–423. https://doi.org/10.1111/1467-9868.00293

Townsend, J. T. (1972). Some Results Concerning the Identifiability of Parallel and Serial Processes. *British Journal of Mathematical and Statistical Psychology*, *25*(2), 168–199. https://doi.org/10.1111/j.2044-8317.1972.tb00490.x

Townsend, James T. (1984). Uncovering mental processes with factorial experiments. *Journal of Mathematical Psychology*, *28*(4), 363–400. https://doi.org/10.1016/0022-2496(84)90007-5

Townsend, James T. (1990). Serial vs. parallel processing: Sometimes they look like Tweedledum and Tweedledee but they can (and should) be distinguished. *Psychological Science*, *1*(1), 46–54. https://doi.org/10.1111/j.1467-9280.1990.tb00067.x

Townsend, James T., & Ashby, F. G. (1983). *The stochastic modeling of elementary psychological processes*. Cambridge University Press.

Townsend, James T., & Nozawa, G. (1995). Spatio-temporal Properties of Elementary Perception: An Investigation of Parallel, Serial, and Coactive Theories. *Journal of Mathematical Psychology*, *39*(4), 321–359. https://doi.org/10.1006/jmps.1995.1033

Townsend, James T., & Wenger, M. J. (2004). A theory of interactive parallel processing: New capacity measures and predictions for a response time inequality series. *Psychological Review*, *111*(4), 1003–1035. https://doi.org/10.1037/0033-295X.111.4.1003

Trageser, J. C., Monosov, I. E., Zhou, Y., & Thompson, K. G. (2008). A perceptual representation in the frontal eye field during covert visual search that is more reliable than the behavioral report. *European Journal of Neuroscience*, *28*(12), 2542–2549. https://doi.org/10.1111/j.1460-9568.2008.06530.x

Treisman, A. (1988). Features and Objects: The Fourteenth Bartlett Memorial Lecture. *The Quarterly Journal of Experimental Psychology Section A*, *40*(2), 201–237. https://doi.org/10.1080/02724988843000104

Treisman, A. M., & Gelade, G. (1980). A feature-integration theory of attention. *Cognitive Psychology*, *12*(1), 97–136. https://doi.org/10.1016/0010-0285(80)90005-5

Treisman, M., & Faulkner, A. (1985). On the Choice between Choice Theory and Signal Detection Theory. *The Quarterly Journal of Experimental Psychology Section A*, *37*(3), 387–405. https://doi.org/10.1080/14640748508400941

Treue, S., & Martínez Trujillo, J. C. (1999). Feature-based attention influences motion processing gain in macaque visual cortex. *Nature*, *399*(6736), 575–579. https://doi.org/10.1038/21176

Umeno, M. M., & Goldberg, M. E. (1997). Spatial processing in the monkey frontal eye field. I. Predictive visual responses. *Journal of Neurophysiology*, *78*(3), 1373–1383. https://doi.org/10.1152/jn.1997.78.3.1373

Ungerleider, L. G., Galkin, T. W., Desimone, R., & Gattass, R. (2008). Cortical connections of area V4 in the macaque. *Cerebral Cortex (New York, N.Y.: 1991)*, *18*(3), 477–499. https://doi.org/10.1093/cercor/bhm061

Ungerleider, L. G., & Mishkin, M. (1982). Two cortical visual systems. In D. J. Ingle, M. A. Goodale, & R. J. W. Mansfield (Eds.), *Analysis of visual behavior* (pp. 549–586). MIT Press.

Vernet, M., Quentin, R., Chanes, L., Mitsumasu, A., & Valero-Cabré, A. (2014). Frontal eye field, where art thou? Anatomy, function, and non-invasive manipulation of frontal regions involved in eye movements and associated cognitive operations. *Frontiers in Integrative Neuroscience*, *8*. https://doi.org/10.3389/fnint.2014.00066

Vickers, D. (1970). Evidence for an accumulator model of psychophysical discrimination. *Ergonomics*, *13*(1), 37–58. https://doi.org/10.1080/00140137008931117

Vigneswaran, G., Kraskov, A., & Lemon, R. N. (2011). Large identified pyramidal cells in macaque motor and premotor cortex exhibit “thin spikes”: Implications for cell type classification. *The Journal of Neuroscience: The Official Journal of the Society for Neuroscience*, *31*(40), 14235–14242. https://doi.org/10.1523/JNEUROSCI.3142-11.2011

Voloh, B., & Womelsdorf, T. (2018). Cell-Type Specific Burst Firing Interacts with Theta and Beta Activity in Prefrontal Cortex During Attention States. *Cerebral Cortex (New York, NY)*, *28*(12), 4348–4364. https://doi.org/10.1093/cercor/bhx287

Waitzman, D. M., Ma, T. P., Optican, L. M., & Wurtz, R. H. (1991). Superior colliculus neurons mediate the dynamic characteristics of saccades. *Journal of Neurophysiology*, *66*(5), 1716–1737. https://doi.org/10.1152/jn.1991.66.5.1716

Wallis, J. D., & Miller, E. K. (2003). From Rule to Response: Neuronal Processes in the Premotor and Prefrontal Cortex. *Journal of Neurophysiology*, *90*(3), 1790–1806. https://doi.org/10.1152/jn.00086.2003

Wardak, C., Ibos, G., Duhamel, J.-R., & Olivier, E. (2006). Contribution of the Monkey Frontal Eye Field to Covert Visual Attention. *Journal of Neuroscience*, *26*(16), 4228–4235. https://doi.org/10.1523/JNEUROSCI.3336-05.2006

Wardak, C., Olivier, E., & Duhamel, J.-R. (2011). The relationship between spatial attention and saccades in the frontoparietal network of the monkey. *The European Journal of Neuroscience*, *33*(11), 1973–1981. https://doi.org/10.1111/j.1460-9568.2011.07710.x

Warton, D. I., & Hui, F. K. C. (2011). The arcsine is asinine: The analysis of proportions in ecology. *Ecology*, *92*(1), 3–10.

Westerberg, J. A., Maier, A., & Schall, J. D. (2020). Priming of attentional selection in macaque visual cortex: Feature-based facilitation and location-based inhibition of return. *ENeuro*. https://doi.org/10.1523/ENEURO.0466-19.2020

White, B. J., Boehnke, S. E., Marino, R. A., Itti, L., & Munoz, D. P. (2009). Color-related signals in the primate superior colliculus. *The Journal of Neuroscience: The Official Journal of the Society for Neuroscience*, *29*(39), 12159–12166. https://doi.org/10.1523/JNEUROSCI.1986-09.2009

White, B. J., Kan, J. Y., Levy, R., Itti, L., & Munoz, D. P. (2017). Superior colliculus encodes visual saliency before the primary visual cortex. *Proceedings of the National Academy of Sciences of the United States of America*, *114*(35), 9451–9456. https://doi.org/10.1073/pnas.1701003114

White, C. N., Ratcliff, R., & Starns, J. J. (2011). Diffusion models of the flanker task: Discrete versus gradual attentional selection. *Cognitive Psychology*, *63*(4), 210–238. https://doi.org/10.1016/j.cogpsych.2011.08.001

White, C. N., Servant, M., & Logan, G. D. (2018). Testing the validity of conflict drift-diffusion models for use in estimating cognitive processes: A parameter-recovery study. *Psychonomic Bulletin & Review*, *25*(1), 286–301. https://doi.org/10.3758/s13423-017-1271-2

Williams, L. P. (1980). *The Origins of Field Theory*. University Press of America.

Wimmer, K., Nykamp, D. Q., Constantinidis, C., & Compte, A. (2014). Bump attractor dynamics in prefrontal cortex explains behavioral precision in spatial working memory. *Nature Neuroscience*, *17*(3), 431–439. https://doi.org/10.1038/nn.3645

Wimmer, K., Spinelli, P., & Pasternak, T. (2016). Prefrontal Neurons Represent Motion Signals from Across the Visual Field But for Memory-Guided Comparisons Depend on Neurons Providing These Signals. *The Journal of Neuroscience: The Official Journal of the Society for Neuroscience*, *36*(36), 9351–9364. https://doi.org/10.1523/JNEUROSCI.0843-16.2016

Wise, S. P. (1985). The primate premotor cortex: Past, present, and preparatory. *Annual Review of Neuroscience*, *8*, 1–19. https://doi.org/10.1146/annurev.ne.08.030185.000245

Wise, S. P., Di Pellegrino, G., & Boussaoud, D. (1992). Primate premotor cortex: Dissociation of visuomotor from sensory signals. *Journal of Neurophysiology*, *68*(3), 969–972. https://doi.org/10.1152/jn.1992.68.3.969

Wise, S. P., di Pellegrino, G., & Boussaoud, D. (1996). The premotor cortex and nonstandard sensorimotor mapping. *Canadian Journal of Physiology and Pharmacology*, *74*(4), 469–482. https://doi.org/10.1139/cjpp-74-4-469

Wittig, J. H., & Richmond, B. J. (2014). Monkeys rely on recency of stimulus repetition when solving short-term memory tasks. *Learning & Memory*, *21*(6), 325–333. https://doi.org/10.1101/lm.034181.113

Wolfe, J., Cain, M., Ehinger, K., & Drew, T. (2015). Guided Search 5.0: Meeting the challenge of hybrid search and multiple-target foraging. *Journal of Vision*, *15*, 1106. https://doi.org/10.1167/15.12.1106

Wolfe, J. M., Cave, K. R., & Franzel, S. L. (1989). Guided search: An alternative to the feature integration model for visual search. *Journal of Experimental Psychology. Human Perception and Performance*, *15*(3), 419–433. https://doi.org/10.1037//0096-1523.15.3.419

Wolfe, Jeremy M. (1994). Guided Search 2.0 A revised model of visual search. *Psychonomic Bulletin & Review*, *1*(2), 202–238. https://doi.org/10.3758/BF03200774

Wolfe, Jeremy M. (2007). Guided Search 4.0: Current progress with a model of visual search. In *Integrated models of cognitive systems* (pp. 99–119). Oxford University Press. https://doi.org/10.1093/acprof:oso/9780195189193.003.0008

Wolfe, Jeremy M, & Utochkin, I. S. (2019). What is a preattentive feature? *Current Opinion in Psychology*, *29*, 19–26. https://doi.org/10.1016/j.copsyc.2018.11.005

Woodman, G. F., Kang, M.-S., Thompson, K., & Schall, J. D. (2008). The Effect of Visual Search Efficiency on Response Preparation: Neurophysiological Evidence for Discrete Flow. *Psychological Science*, *19*(2), 128–136. https://doi.org/10.1111/j.1467-9280.2008.02058.x

Woodman, G. F., Luck, S. J., & Schall, J. D. (2007). The role of working memory representations in the control of attention. *Cerebral Cortex (New York, N.Y.: 1991)*, *17 Suppl 1*, i118-124. https://doi.org/10.1093/cercor/bhm065

Woodworth, R. S., & Schlosberg, H. (1954). *Experimental psychology, Rev. Ed* (pp. xi, 948). Holt.

Xiao, Q., Barborica, A., & Ferrera, V. P. (2006). Radial motion bias in macaque frontal eye field. *Visual Neuroscience*, *23*(1), 49–60. https://doi.org/10.1017/S0952523806231055

Xu, K. Z., Anderson, B. A., Emeric, E. E., Sali, A. W., Stuphorn, V., Yantis, S., & Courtney, S. M. (2017). Neural Basis of Cognitive Control over Movement Inhibition: Human fMRI and Primate Electrophysiology Evidence. *Neuron*, *96*(6), 1447-1458.e6. https://doi.org/10.1016/j.neuron.2017.11.010

Yamagata, T., Nakayama, Y., Tanji, J., & Hoshi, E. (2012). Distinct Information Representation and Processing for Goal-Directed Behavior in the Dorsolateral and Ventrolateral Prefrontal Cortex and the Dorsal Premotor Cortex. *Journal of Neuroscience*, *32*(37), 12934–12949. https://doi.org/10.1523/JNEUROSCI.2398-12.2012

Yamamoto, S., Kim, H. F., & Hikosaka, O. (2013). Reward Value-Contingent Changes of Visual Responses in the Primate Caudate Tail Associated with a Visuomotor Skill. *The Journal of Neuroscience*, *33*(27), 11227–11238. https://doi.org/10.1523/JNEUROSCI.0318-13.2013

Yang, H., Fific, M., & Townsend, J. T. (2014). Survivor interaction contrast wiggle predictions of parallel and serial models for an arbitrary number of processes. *Journal of Mathematical Psychology*, *58*, 21–32. https://doi.org/10.1016/j.jmp.2013.12.001

Zaitsev, A. V., Povysheva, N. V., Gonzalez-Burgos, G., & Lewis, D. A. (2012). Electrophysiological classes of layer 2/3 pyramidal cells in monkey prefrontal cortex. *Journal of Neurophysiology*, *108*(2), 595–609. https://doi.org/10.1152/jn.00859.2011

Zeki, S. (1980). The representation of colours in the cerebral cortex. *Nature*, *284*(5755), 412. https://doi.org/10.1038/284412a0

Zeki, S. M. (1973). Colour coding in rhesus monkey prestriate cortex. *Brain Research*, *53*(2), 422–427. https://doi.org/10.1016/0006-8993(73)90227-8

Zhou, H., & Desimone, R. (2011). Feature-Based Attention in the Frontal Eye Field and Area V4 during Visual Search. *Neuron*, *70*(6), 1205–1217. https://doi.org/10.1016/j.neuron.2011.04.032

Zinke, W., Cosman, J., D., Woodman, G. F., & Schall, J. D. (2015, October). *A premotor eye field in the arcuate sulcus of macaque monkeys—Comparison with FEF*. 45th Annual Meeting of the Society for Neuroscience, Chicago, IL.